frontiers | Research Topics

Recent advancements in mycobacterial diseases research

Edited by
Vishwanath Venketaraman, Jotam G. Pasipanodya, Matt Johansen and Selvakumar Subbian

Published in
Frontiers in Microbiology

ISSN 1664-8714
ISBN 978-2-8325-5606-1
DOI 10.3389/978-2-8325-5606-1

About Frontiers

Frontiers is more than just an open access publisher of scholarly articles: it is a pioneering approach to the world of academia, radically improving the way scholarly research is managed. The grand vision of Frontiers is a world where all people have an equal opportunity to seek, share and generate knowledge. Frontiers provides immediate and permanent online open access to all its publications, but this alone is not enough to realize our grand goals.

Frontiers journal series

The Frontiers journal series is a multi-tier and interdisciplinary set of open-access, online journals, promising a paradigm shift from the current review, selection and dissemination processes in academic publishing. All Frontiers journals are driven by researchers for researchers; therefore, they constitute a service to the scholarly community. At the same time, the *Frontiers journal series* operates on a revolutionary invention, the tiered publishing system, initially addressing specific communities of scholars, and gradually climbing up to broader public understanding, thus serving the interests of the lay society, too.

Dedication to quality

Each Frontiers article is a landmark of the highest quality, thanks to genuinely collaborative interactions between authors and review editors, who include some of the world's best academicians. Research must be certified by peers before entering a stream of knowledge that may eventually reach the public - and shape society; therefore, Frontiers only applies the most rigorous and unbiased reviews. Frontiers revolutionizes research publishing by freely delivering the most outstanding research, evaluated with no bias from both the academic and social point of view. By applying the most advanced information technologies, Frontiers is catapulting scholarly publishing into a new generation.

What are Frontiers Research Topics?

Frontiers Research Topics are very popular trademarks of the *Frontiers journals series*: they are collections of at least ten articles, all centered on a particular subject. With their unique mix of varied contributions from Original Research to Review Articles, Frontiers Research Topics unify the most influential researchers, the latest key findings and historical advances in a hot research area.

Find out more on how to host your own Frontiers Research Topic or contribute to one as an author by contacting the Frontiers editorial office: frontiersin.org/about/contact

Recent advancements in mycobacterial diseases research

Topic editors

Vishwanath Venketaraman — Western University of Health Sciences, United States
Jotam G. Pasipanodya — Vanderbilt University Medical Center, United States
Matt Johansen — University of Technology Sydney, Australia
Selvakumar Subbian — Rutgers, The State University of New Jersey, United States

Citation

Venketaraman, V., Pasipanodya, J. G., Johansen, M., Subbian, S., eds. (2024). *Recent advancements in mycobacterial diseases research*. Lausanne: Frontiers Media SA. doi: 10.3389/978-2-8325-5606-1

Table of contents

frontiers | Frontiers in Microbiology

TYPE Editorial
PUBLISHED 16 October 2024
DOI 10.3389/fmicb.2024.1504449

OPEN ACCESS

EDITED AND REVIEWED BY
Axel Cloeckaert,
Institut National de recherche pour l'agriculture, l'alimentation et l'environnement (INRAE), France

*CORRESPONDENCE
Matt D. Johansen
✉ Matt.Johansen@uts.edu.au
Jotam G. Pasipanodya
✉ jotam.g.pasipanodya@vumc.org
Selvakumar Subbian
✉ subbiase@njms.rutgers.edu
Vishwanath Venketaraman
✉ vvenketaraman@westernu.edu

RECEIVED 30 September 2024
ACCEPTED 01 October 2024
PUBLISHED 16 October 2024

CITATION
Johansen MD, Pasipanodya JG, Subbian S and Venketaraman V (2024) Editorial: Recent advancements in mycobacterial diseases research. *Front. Microbiol.* 15:1504449. doi: 10.3389/fmicb.2024.1504449

Editorial: Recent advancements in mycobacterial diseases research

Matt D. Johansen[1]*, Jotam G. Pasipanodya[2]*, Selvakumar Subbian[3]* and Vishwanath Venketaraman[4]*

[1]Centre for Inflammation, Faculty of Science, School of Life Sciences, Centenary Institute and University of Technology Sydney, Sydney, NSW, Australia, [2]Department of Medicine, Vanderbilt University Medical Center, Nashville, TN, United States, [3]Public Health Research Institute, New Jersey Medical School, Rutgers University, Newark, NJ, United States, [4]Department of Basic Medical Sciences, Western University of Health Sciences, Pomona, CA, United States

KEYWORDS

mycobacterial diseases, TB, NTM diseases, *Mycobacterium tuberculosis*, non-tuberculous mycobacteria, drug resistance, diagnosis, therapies

Editorial on the Research Topic
Recent advancements in mycobacterial diseases research

Introduction

According to the World Health Organization, the number of global tuberculosis (TB) cases in 2021 reached 10.6 million, a 4.5% rise from the number of cases recorded in 2020 (*World Health Organization Global Tuberculosis Report-2022*). This indicates the urgent need to develop measures to curtail the disease. The diverse host immune response to *Mycobacterium tuberculosis* (Mtb), the causative agent of TB, is influenced by both host and bacterial factors and the immune response of the host to infection (Berrington and Hawn, 2007).

A pathologic hallmark of Mtb infection in humans is the formation of granulomas, a highly organized cellular structure at the site of infection (Kumar et al., 2024; Klever et al., 2023). Although granulomas are considered host-protective because they restrict Mtb into a confined space, the bacteria can utilize those granulomas to escape from killing by host immune cells. Thus, the fate of Mtb and the course of infection and disease progression is largely determined at the level of granulomas (Subbian et al., 2015; Warsinske et al., 2017; Gideon et al., 2022). Granulomas are heterogeneous, comprised of a variable mixture of immune and non-immune cells as shown in the spectrum of human TB disease and recapitulated in various animal models of Mtb infection. However, granulomas consistently evolve, undergoing caseous necrosis and cavitation in active pulmonary TB patients, however, this is only observed in non-human primates and rabbit models of Mtb infection (Kumar et al., 2024; Klever et al., 2023). While cavitary granulomas facilitate bacterial dissemination, highly cellular "solid" granulomas contain bacteria at the core. Importantly, the granulomas are encased by a layer of fibrotic material, comprised of various types of collagens and elastin secreted by the macrophages and fibroblasts surrounding the granulomas (Subbian et al., 2015; Warsinske et al., 2017; Gideon et al., 2022). These fibrotic cores leave residual parenchymal tissue damage, which hinders successful antibiotic penetration into the granuloma to kill Mtb. However, the mechanism

of collagen formation and the nature of collagen fibers that constitute the fibrotic zone of granulomas are not completely understood. Here, Song et al. describes an automated quantitative assay to determine fibrosis characteristics of various granuloma types using 16 tissue types of TB patients and lung sections from a Marmoset model of Mtb infection. The authors have used a conventional Masson trichrome staining method to visualize the extent of fibrosis in different types of lung granulomas. The authors used a novel, stain-free second harmonic generation (SHG) two-photon excited fluorescence (TPEF) microscopy to further characterize the nature of fibrosis in the granulomas. Results from these analyses show that in the fibrotic area, aggregated collagens, made of short and thick clusters of 200–620 nm in size were the predominant form, compared to the long and thick disseminated collagens of 200–300 nm size. Furthermore, MMP-9 which codes for matrix metalloproteinase-9, was found to be upregulated in the granulomas of various tissues. This study contributes a valuable quantitative imaging tool to gain insight into the fibrotic dynamics of TB granulomas. Further exploration and refinement of such tools to understand the mechanism of fibrosis in TB granulomas would facilitate the development of novel strategies to prevent TB sequelae and efficiently kill Mtb within those granulomas.

The host immune cell recognizes mycobacteria through various pattern recognition receptors (PRRs), such as the Toll-like receptor (TLR). TLR recognizes pathogen-associated molecular patterns (PAMPs), including lipoprotein and lipopolysaccharides that are present in bacteria (Jahantigh et al., 2013). TLR1 recognizes tri-acylated lipopeptide, and TLR6 recognizes di-acyl lipopeptide (Buwitt-Beckmann et al., 2005). TLR1 recognizes the 19 kD lipoprotein of Mtb (Takeuchi et al., 2002), and TLR2 recognizes 19 kD lipoproteins, lipoarabinomannan and other Mtb PAMPs (Brightbill et al., 1999). In this Research Topic, a study by Varshney et al. showed an association between *TLR2* deletion *(−196 to −174)* and *TLR1 743 A > G* gene polymorphism and drug-resistant pulmonary TB in a population from Agra, Uttar Pradesh, India. The findings from this study suggested that in the present population, the heterozygous (*Ins/Del*) genotype and deletion allele of *TLR2 deletion (−196 to −174)* polymorphism are associated with increased risk for the development of drug-resistant TB. Furthermore, for *TLR1 743 A > G* gene polymorphism, A/G genotype, and G allele are found associated with healthy controls, suggesting a protective role against TB which warrants further investigation.

The Research Topic also includes a study by Choreño-Parra et al. that aims to investigate the utility of the Systemic Immune-Inflammation Index (SII), Fibrinogen, and T-SPOT.TB in distinguishing between active pulmonary tuberculosis (PTB) and non-tuberculous lung diseases. This study concluded that SII and Fibrinogen are positively correlated with the degree of tuberculosis inflammation and the bacterial load. The combined detection of SII, Fibrinogen, and T-SPOT.TB is significant in distinguishing between active PTB with positive T-SPOT.TB results and non-tuberculous lung disease as described by Yu et al.. The proteolytic activity of A Disintegrin and Metalloproteinase 17 (ADAM17) regulates the release of tumor necrosis factor (TNF) and TNF receptors (TNFRs) from cell surfaces. These molecules play important roles in TB shaping innate immune reactions and granuloma formation. This Research Topic also includes study findings suggesting a role for SNPs of ADAM17 in genetic susceptibility to TB.

In addition to TB, non-tuberculous mycobacteria (NTM), also called "atypical mycobacteria" or "mycobacteria other than TB (MOTT) pose significant challenges to human health, particularly among vulnerable populations worldwide (Gopalaswamy et al., 2020). These ubiquitously present organisms were once considered environmental and opportunistic bacteria, however, recent clinical studies indicate that diseases due to NTMs are rising globally. Due to its overlapping characteristics with Mtb, such as acid-fastness and mechanism of pathogenesis, the diagnosis and transmission of NTM are underestimated in endemic populations (Gopalaswamy et al., 2021). Similarly, there are limited effective treatments currently available for NTM infections, although several drugs are in the process of being repurposed. However, most first-line anti-TB drugs are ineffective in clearing NTM infections. Thus, despite the continued emergence of NTM infections, currently available measures to diagnose or treat NTM infections are underdeveloped and require urgent attention. There are over 200 NTM species described to date whose prevalence varies significantly, depending on global geographic regions and populations. Importantly, only a small proportion of NTM species are opportunistic pathogens, mainly *Mycobacterium avium* complex (MAC), *Mycobacterium abscessus* complex (MABC), and *Mycobacterium kansasii* (*M. kansasii*), which collectively are known to account for the majority of human NTM infections. Furthermore, MAC, MABC, and *M. kansasii* account for >95% of NTM pulmonary disease (NTM-PD). In up to half of pulmonary NTM cases, the infecting bacteria do not cause invasive disease, rather, they just colonize the tissue. This ability to colonize host tissues without causing invasive disease ultimately complicates both the diagnosis and treatment of NTM infections. Furthermore, the clinical significance of NTM colonization, and in particular the risk factors predisposing individuals to NTM infection are poorly described and are still an enigma to healthcare providers in the clinic and researchers in laboratories. Indeed, even when NTM do cause pulmonary diseases, in ∼10% of such cases more than one NTM species is recovered from sputum samples, which is usually either MAC or MABC (Wallace Jr et al., 1998). Additionally, both organisms have been shown to form biofilms in lung lesions and to persist within diverse microbial communities, particularly in patients with pre-existing lung diseases such as bronchiectasis, previous TB, or chronic obstructive pulmonary disease (Yamazaki et al., 2006). These are significant knowledge gaps that pose challenges for NTM pharmacology and microbiology.

In the review article by Conyers and Saunders, the current challenges and prospects for the treatment of NTM were elaborately discussed. Various strategies adapted to determine the current treatment regimen and the challenges involved in such approaches to treat infections caused by different species of NTM were explained with relevant literature support from the late 1990s to the early 2000s. Importantly, this review summarizes five clinical trials conducted to evaluate the efficacy of inhaled liposomal amikacin with other adjunct antibiotics for the treatment of NTM infections and concludes that additional studies on drug optimization are needed to address potential

adverse effects due to drug-drug interactions in the combination therapy. Furthermore, this study analyzed 15 active clinical trials focused on the optimization of treatment regimens for NTM infection and highlights challenges such as antibiotic resistance, drug-susceptibility testing, and bacterial physiologic measures, including biofilm formation, colony morphology, and complications associated with bacterial cell wall for effective drug therapy. Finally, the review discusses novel therapeutic modalities such as phage therapy and newly approved antibacterials to combat NTM infections. These measures should help to effectively control NTM diseases worldwide.

A study by Meliefste et al. provided an extensive review of the literature surrounding *M. abscessus* biofilm characterization. In their review, they highlighted the significant differences in biofilm culture methods and techniques that exist and have been applied to *M. abscessus* biofilm studies. Furthermore, the authors also discuss the importance of *M. abscessus* strain selection and the role this plays in biofilm formation, with previous studies concluding that only the smooth morphotype forms biofilms, however subsequent studies have since demonstrated that the rough morphotype can indeed form biofilm and that these disparities between studies are largely due to differences in experimental conditions and strains. The authors also discussed the role of culture medium (Middlebrook 7H9, Synthetic Cystic Fibrosis Medium) and specific constituents such as Tween 80, Iron, and Magnesium. Finally, the authors also discussed drug activity testing on *M. abscessus* biofilms, with indications that traditional anti-mycobacterial drugs are relatively ineffective against *M. abscessus* biofilms, highlighting the significant global challenge in the treatment of chronic *M. abscessus* lung infections.

Another study by Narimisa et al. involved a systematic review and meta-analysis of the prevalence of *M. kansasii* in clinical and environmental isolates. Among 6,640 publications identified, only 134 (118 for clinical and 16 for environmental) met the criteria for inclusion for the analysis of *M. kansasii* prevalence. For the analysis of *M. kansasii* in environmental samples, two studies examining prevalence in soil found a prevalence rate of 0.5%, while 15 studies examined prevalence in water samples and found *M. kansasii* prevalence to be 6.4%. Overall, *M. kansasii* prevalence in environmental samples was found to be 5.8%. When examining geographical prevalence, *M. kansasii* prevalence was found to be highest in Europe at 12.1% and lowest in North America at 2.6%, while prevalence was shown to have significantly increased from 4.9% from 1990–2000 up to 8.9% in 2021–2022. Overall, this study highlighted that the prevalence of *M. kansasii* is significantly higher than originally thought and demonstrates the need for increased surveillance and effective management and infection control strategies.

Similarly, Nguyen et al. have provided a comprehensive review article summarizing antibiotic resistance mechanisms of *M. abscessus*. The authors emphasize the underpopulation of the *M. abscessus* drug pipeline, largely due to current drug discovery approaches that rely on anti-mycobacterial drug library screening which are largely ineffective due to intrinsic resistance mechanisms of *M. abscessus*. Further, the authors highlighted both the extensive intrinsic resistance traits of *M. abscessus*, as well as the novel acquired resistance traits occurring due to spontaneous mutations occurring at specific genes due to the presence of antibiotics following extensive exposure. In this review, the authors discuss antibiotic modifying/inactivating enzymes such as aminoglycosides, β-lactams, rifampicin, and active derivatives (such as rifabutin), as well as target-modifying enzymes such as macrolides, and the extensive repertoire of efflux pumps that *M. abscessus* possesses to extrude antimicrobials of different classes. Finally, the authors discuss acquired resistance traits of *M. abscessus* against newly discovered compounds such as MmpL3 inhibitors and emphasize the urgent need to expedite the discovery of new antimicrobial classes for the treatment of *M. abscessus* to overcome intrinsic and acquired resistance mechanisms.

Tan et al. performed comparative genomic and microbiological analyses to further our understanding of siderophore iron acquisition mechanisms in both environmental and respiratory isolates of NTMs from Hawai'i. Iron is a critical element required for many physiologic processes; hence it is tightly regulated by both the human host and mycobacterial pathogens. Therefore, the hypotheses put forward by Tan et al. are pertinent in explaining NTM diversity across geography and related virulence patterns, especially in the context of drug and immune tolerance, and the ability of the pathogen to persist within granulomatous lesions. In this study, the authors identified *M. abscessus*, *M. porcinum,* and *M. intracellulare* subsp. *chimaera* (hereafter referred to as *M. chimaera*) with a total of 51 isolates (28 respiratory and 23 environmental) used for further analysis. Overall, the authors found that respiratory NTM isolates showed a significantly higher mean number of mycobactin (*mbt*) compared to non-pathogenic environmental species. The exception was with *M. chimaera* from Hawai'i, which naturally had a higher number of *mbt* genes because of the higher iron content in the environment. Furthermore, ESX-3 is a Type VII secretion system possessed by mycobacteria with a known role in iron acquisition, and in this study, the authors showed that the number of *ESX-3* genes was significantly increased in environmental *M. chimaera* isolates as compared to respiratory isolates but remained unchanged for both *M. abscessus* and *M. porcinum*. Finally, the authors performed *in vitro* siderophore assays under low iron conditions and showed that both *M. abscessus* and *M. porcinum* grew better than *M. chimaera* which was in contradiction to the KEGG analysis. The authors concluded that further studies are required to understand the role of iron acquisition in NTM isolates and the contribution of the host respiratory conditions in driving iron siderophore utilization.

In summary, articles in this Research Topic have raised more questions than those answered by the data presented and have identified significant knowledge gaps that need to be addressed within the mycobacterial field. Specifically, and as pointed out by the authors, the role of iron acquisition in NTM clinical isolates raised questions as to whether dietary iron supplements would ameliorate or exacerbate infections. Further, are these observations restricted to NTM that grow on agar as well as those that only grow in liquid media? Would the expression of iron siderophore genes present an advantage to clinical isolates *in vivo*? In addition, correlating these physiological findings to clinical markers of NTM virulence such as bacterial growth rate, colony morphology, and phenotype, or drug minimum inhibitory

concentrations, would be critical for the application of these findings to combating NTM infections globally. The Research Topic of intrinsic resistance and drug tolerance to currently used chemotherapeutic agents is the focus of three reviews in the series. These are the "known unknowns" upending the recommendations for standardized treatments by the American Thoracic Society (ATS)/Infectious Disease Society of America (IDSA) and European Society for Clinical Microbiology and Infectious Disease (ESCMID). Although MABC is the focus for two of these reviews, the themes and lessons apply to MAC as well. Macrolides such as clarithromycin and azithromycin, and aminoglycosides like as amikacin form the backbone of chemotherapy for NTM infection treatment and management. Until recently, there had been no substantive pharmacokinetics (PK) and pharmacodynamics (PD) studies performed to inform drug doses and dosing schedules for these organisms. Most currently used therapy regimens and doses were developed from those used for Mtb, despite heterogeneous clinical phenotypes and the fact that many NTM species are highly drug-resistant. For that reason, optimal drug combinations are unknown, therapy durations are poorly defined, and therefore, clinical outcomes are universally poor (Pasipanodya et al., 2017a,b). The current clinical trial efforts targeting repurposed anti-tuberculosis drugs described by Conyers and Saunders in this series are notable developments. But they are stopgap efforts. The lasting solution is multiple regimens targeting each NTM organism. As mentioned earlier, each of these NTM species is distinct with variable minimum inhibitory concentrations and causes distinct clinical diseases (pulmonary vs. cutaneous vs. disseminated NTM disease). Therefore, PK/PD-informed and designed regimens with targeted drug doses that acknowledge the PK variability of the population and PD variability of mycobacteria represent the gold standard and should be adopted to rapidly accelerate drug discovery and the identification of next-generation antimicrobial therapies.

Author contributions

MDJ: Writing – original draft, Writing – review & editing. JGP: Writing – original draft, Writing – review & editing. SS: Writing – original draft, Writing – review & editing. VV: Writing – original draft, Writing – review & editing.

Acknowledgments

The editors would like to express gratitude to all the reviewers and authors of the manuscripts submitted to this Research Topic. Research effort and time for JGP was supported by the National Institute of General Medical Sciences of National Institutes of Health fellowship under award T32 GM007569.

Conflict of interest

The authors declare that the research was conducted in the absence of any commercial or financial relationships that could be construed as a potential conflict of interest.

The author(s) declared that they were an editorial board member of Frontiers, at the time of submission. This had no impact on the peer review process and the final decision.

Publisher's note

References

Berrington, W. R., and Hawn, T. R. (2007). Mycobacterium tuberculosis, macrophages, and the innate immune response: does common variation matter? *Immunol. Rev.* 219, 167–186. doi: 10.1111/j.1600-065X.2007.00545.x

Brightbill, H. D., Libraty, D. H., Krutzik, S. R., Yang, R. B., Belisle, J. T., Bleharski, J. R., et al. (1999). Host defense mechanisms triggered by microbial lipoproteins through toll-like receptors. *Science* 285, 732–736. doi: 10.1126/science.285.5428.732

Buwitt-Beckmann, U., Heine, H., Wiesmuller, K. H., Jung, G., Brock, R., Akira, S., et al. (2005). Toll-like receptor 6-independent signaling by diacylated lipopeptides. *Eur. J. Immunol.* 35, 282–289. doi: 10.1002/eji.200424955

Gideon, H. P., Hughes, T. K., Tzouanas, C. N., Wadsworth, M. H., Tu, A. A., Gierahn, T. M., et al. (2022). Multimodal profiling of lung granulomas in macaques reveals cellular correlates of tuberculosis control. *Immunity* 55, 827–846.e10. doi: 10.1016/j.immuni.2022.04.004

Gopalaswamy, R., Shanmugam, S., Mondal, R., and Subbian, S. (2020). Of tuberculosis and non-tuberculous mycobacterial infections - a comparative analysis of epidemiology, diagnosis and treatment. *J. Biomed. Sci.* 27, 74. doi: 10.1186/s12929-020-00667-6

Gopalaswamy, R., Subbian, S., Shanmugam, S., Mondal, R., and Padmapriyadarsini, C. (2021). Recent developments in the diagnosis and treatment of extrapulmonary non-tuberculous mycobacterial diseases. *Int. J. Tuberc. Lung Dis.* 25, 340–349. doi: 10.5588/ijtld.21.0002

Jahantigh, D., Salimi, S., Alavi-Naini, R., Emamdadi, A., Owaysee Osquee, H., Farajian Mashhadi, F., et al. (2013). Association between TLR4 and TLR9 gene polymorphisms with development of pulmonary tuberculosis in Zahedan, southeastern Iran. *Sci. World J.* 2013:534053. doi: 10.1155/2013/534053

Klever, A. M., Alexander, K. A., Almeida, D., Anderson, M. Z., Ball, R. L., Beamer, G., et al. (2023). The many hosts of mycobacteria 9 (MHM9): a conference report. *Tuberculosis* 142:102377. doi: 10.1016/j.tube.2023.102377

Kumar, R., Kolloli, A., Subbian, S., Kaushal, D., Shi, L., Tyagi, S., et al. (2024). Imaging the architecture of granulomas induced by *Mycobacterium tuberculosis* infection with single-molecule fluorescence in situ hybridization. *J. Immunol.* 213, 526–537. doi: 10.4049/jimmunol.2300068

Pasipanodya, J. G., Ogbonna, D., Deshpande, D., Srivastava, S., and Gumbo, T. (2017a). Meta-analyses and the evidence base for microbial outcomes in the treatment of pulmonary *Mycobacterium avium*-intracellulare complex disease. *J. Antimicrob. Chemother.* 72, i3–i19. doi: 10.1093/jac/dkx311

Pasipanodya, J. G., Ogbonna, D., Ferro, B. E., Magombedze, G., Srivastava, S., Deshpande, D., et al. (2017b). Systematic review and meta-analyses of the effect of chemotherapy on pulmonary Mycobacterium abscessus outcomes and disease recurrence. *Antimicrob. Agents Chemother.* 61, 10–1128. doi: 10.1128/AAC.01206-17

Subbian, S., Tsenova, L., Kim, M. J., Wainwright, H. C., Visser, A., Bandyopadhyay, N., et al. (2015). Lesion-specific immune response in granulomas of patients with pulmonary tuberculosis: a pilot study. *PLoS ONE* 10:e0132249. doi: 10.1371/journal.pone.0132249

Takeuchi, O., Sato, S., Horiuchi, T., Hoshino, K., Takeda, K., Dong, Z., et al. (2002). Cutting edge: role of Toll-like receptor 1 in mediating immune response to microbial lipoproteins. *J. Immunol.* 169, 10–14. doi: 10.4049/jimmunol.169.1.10

Wallace Jr, R. J., Zhang, Y., Brown, B. A., Dawson, D., Murphy, D. T., Wilson, R., et al. (1998). Polyclonal *Mycobacterium avium* complex infections in patients with nodular bronchiectasis. *Am. J. Respir. Crit. Care Med.* 158, 1235–1244. doi: 10.1164/ajrccm.158.4.9712098

Warsinske, H. C., DiFazio, R. M., Linderman, J. J., Flynn, J. L., and Kirschner, D. E. (2017). Identifying mechanisms driving formation of granuloma-associated fibrosis during *Mycobacterium tuberculosis* infection. *J. Theor. Biol.* 429, 1–17. doi: 10.1016/j.jtbi.2017.06.017

Yamazaki, Y., Danelishvili, L., Wu, M., Hidaka, E., Katsuyama, T., Stang, B., et al. (2006). The ability to form biofilm influences *Mycobacterium avium* invasion and translocation of bronchial epithelial cells. *Cell. Microbiol.* 8, 806–814. doi: 10.1111/j.1462-5822.2005.00667.x

frontiers | Frontiers in Microbiology

TYPE Original Research
PUBLISHED 10 November 2023
DOI 10.3389/fmicb.2023.1268963

OPEN ACCESS

EDITED BY
Matt Johansen,
University of Technology Sydney, Australia

REVIEWED BY
Avishek Mitra,
Oklahoma State University, United States
Andre Kipnis,
Universidade Federal de Goiás, Brazil

*CORRESPONDENCE
Jennifer R. Honda
✉ Jennifer.Honda@UTTyler.edu

†PRESENT ADDRESSES
Cara G. Tan,
Department of Economics, University of Hawai'i at Manoa, Honolulu, HI, United States
Nicole M. Oberlag,
Department of Biology, Claremont McKenna College, Claremont, CA, United States
Acelyn E. McGowan,
Krieger School of Arts and Sciences, Johns Hopkins University, Baltimore, MD, United States
Stephanie N. Dawrs,
Division of Pulmonary Science and Critical Care Medicine, University of Colorado Anschutz Medical Campus, Aurora, CO, United States

RECEIVED 01 August 2023
ACCEPTED 11 October 2023
PUBLISHED 10 November 2023

CITATION
Tan CG, Oberlag NM, McGowan AE, Dawrs SN, Chan YL, Strong M, Hasan NA and Honda JR (2023) Genomic and microbiological analyses of iron acquisition pathways among respiratory and environmental nontuberculous mycobacteria from Hawai'i.
Front. Microbiol. 14:1268963.
doi: 10.3389/fmicb.2023.1268963

Genomic and microbiological analyses of iron acquisition pathways among respiratory and environmental nontuberculous mycobacteria from Hawai'i

Cara G. Tan[1†], Nicole M. Oberlag[2†], Acelyn E. McGowan[3†], Stephanie N. Dawrs[2†], Yvonne L. Chan[1], Michael Strong[2], Nabeeh A. Hasan[2] and Jennifer R. Honda[2,4]*

[1]Iolani School, Honolulu, HI, United States, [2]Center for Genes, Environment and Health, National Jewish Health, Denver, CO, United States, [3]Rock Canyon High School, Highlands Ranch, CO, United States, [4]Department of Cellular and Molecular Biology, School of Medicine, The University of Texas Health Science Center at Tyler, Tyler, TX, United States

As environmental opportunistic pathogens, nontuberculous mycobacteria (NTM) can cause severe and difficult to treat pulmonary disease. In the United States, Hawai'i has the highest prevalence of infection. Rapid growing mycobacteria (RGM) such as *Mycobacterium abscessus* and *M. porcinum* and the slow growing mycobacteria (SGM) including *M. intracellulare* subspecies *chimaera* are common environmental NTM species and subspecies in Hawai'i. Although iron acquisition is an essential process of many microorganisms, iron acquisition via siderophores among the NTM is not well-characterized. In this study, we apply genomic and microbiological methodologies to better understand iron acquisition via siderophores for environmental and respiratory isolates of *M. abscessus*, *M. porcinum*, and *M. intracellulare* subspecies *chimaera* from Hawai'i. Siderophore synthesis and transport genes, including mycobactin *(mbt), mmpL/S*, and *esx-3* were compared among 47 reference isolates, 29 respiratory isolates, and 23 environmental Hawai'i isolates. Among all reference isolates examined, respiratory isolates showed significantly more siderophore pertinent genes compared to environmental isolates. Among the Hawai'i isolates, RGM *M. abscessus* and *M. porcinum* had significantly less *esx*-3 and *mbt* genes compared to SGM *M. chimaera* when stratified by growth classification. However, no significant differences were observed between the species when grown on low iron culture agar or siderophore production by the chrome azurol S (CAS) assay *in vitro*. These results indicate the complex mechanisms involved in iron sequestration and siderophore activity among diverse NTM species.

KEYWORDS

nontuberculous mycobacteria, Hawai'i, siderophores, bioinformatics, CAS assay

1. Introduction

Nontuberculous mycobacteria (NTM) are found in a variety of environmental habitats and biofilms including those collected from showerheads, water faucets, air conditioning units, hospital water faucets, and soil (Honda et al., 2018). There are more than 195 different species of rapid growing mycobacteria (RGM) and slow growing mycobacteria (SGM) that have been

identified to date (Parte et al., 2020), yet only a handful of these species are considered opportunistic pathogens that cause pulmonary disease (PD) particularly in susceptible individuals (Falkinham, 1996). NTM PD is becoming a mounting public health concern as the number of cases continue to increase globally (Adjemian et al., 2012).

In the United States (U.S.), Hawai'i had the highest period prevalence of NTM PD calculated at 396 cases/100,000 persons according to a Medicare Part B beneficiary analysis (Adjemian et al., 2012). In our prior research, we demonstrated frequent recovery of viable RGM including *Mycobacterium abscessus* and *Mycobacterium porcinum* from the Hawai'i environment. We also reported the preponderance of the SGM, *Mycobacterium intracellulare* subspecies *chimaera,* among both respiratory and environmental samples from this geographic NTM hot spot (Honda et al., 2016).

Iron is an essential element for microbial growth, used in various biological processes including electron transport, and iron plays a major role in metabolic and cellular pathways including energy generation, DNA replication, transcriptional regulation (Crosa, 1989; Skaar, 2010). In the human body, iron mainly exists in complex forms bound to protein (e.g., hemoprotein) as heme compounds (e.g., hemoglobin or myoglobin), heme enzymes, or nonheme compounds (e.g., flavin-iron enzymes, transferring, and ferritin) (McDowell, 1992; Abbaspour et al., 2014). Minute amounts, i.e., 10^{-18} M concentration of free iron are available or 0.4–0.9 mg Fe/g dry weight in blood or human lungs, respectively (Griffiths et al., 1980; Takemoto et al., 1991). Under this competitive iron-restricted environment, bacteria that have the capacity to sequester and use iron may be selectively advantaged. In contrast, iron is more readily available and in higher quantity in the exogenous environment. Hawai'i soil, for example, contains 95,550 mg/kg of iron on average but iron content varies with rock type as basaltic and mafic rocks range from 56,000–87,000 mg/kg (Hawai'i Department of Health Hazard Evaluation and Emergency Response, 2012).

To acquire exogenous iron, many bacteria exploit siderophores. For mycobacteria, intracellular and extracellular iron-chelating siderophores synergistically scavenge iron from the environment (Gobin et al., 1995) and are critical to pathogenicity (Braun and Winkelmann, 1988; De Voss et al., 2000). Mycobactin (*mbt*) is an intracellular siderophore produced by most mycobacteria, especially pathogenic species, under iron-limiting conditions and is restricted to the cell envelope (De Voss et al., 2000). Based on models for *Mycobacterium tuberculosis (Mtb)*, two gene complexes are needed to synthesize mycobactin: *mbt-1* and *mbt-2. Mbt-1* is comprised of ten genes, ranging from *mbtA* to *mbtJ*. *mbt-2* is comprised of four genes ranging from *mbtK* to *mbtN* (Sritharan, 2016). Exochelin is an extracellular peptide siderophore produced under iron-deficient conditions and exclusive to RGM. The mycobacterial membrane large/small proteins (*mmpL/S*) complex and the type VII secretion system, *esx*-3, are used to scavenge iron from the surroundings, facilitating acquisition of iron from mycobactin (Siegrist et al., 2009; Szekely and Cole, 2016). *esx*-3 involves a homologous gene system relating to protein production for iron acquisition. However, beyond confirmation of their existence, NTM siderophore biology is significantly understudied and most research in this area predates the current genomic era (Hall and Ratledge, 1982, 1984, 1985; Barclay et al., 1985).

The aim of the current study was to provide an updated assessment of mycobacterial iron acquisition via siderophores. This was achieved by leveraging genomic data from respiratory and environmental Hawai'i NTM isolates (Honda et al., 2016; Virdi et al., 2021) as well as NTM genomic data from the NCBI GenBank public database. Mycobacterial iron-acquisition gene comparisons among the RGM and SGM and between respiratory and environmental isolates from Hawai'i were assessed. To further confirm siderophore production, *in vitro* microbiological tests were performed using the same respiratory and environmental isolates from Hawai'i under low iron culture conditions.

2. Materials and methods

2.1. NTM isolates used in this study

We collected 51 Hawai'i NTM isolates, including 28 respiratory and 23 environmental NTM isolates (Tables 1, 2) for analysis. Respiratory isolates were from de-identified individuals living in Hawai'i with suspected mycobacterial infections whose sputum had been submitted for mycobacterial culture and processed by the Diagnostic Laboratory Services, Inc (Aiea, HI). Environmental NTM isolates were collected by our group from indoor household water biofilms including household shower heads and sink faucets. A minority of water biofilms were collected from outdoor sources in Hawai'i including beach showerheads and garden hoses (Honda et al., 2016; Virdi et al., 2021). A description of isolate collection processes and DNA extraction methods are published (Honda et al., 2016; Virdi et al., 2021). All environmental isolates tested in this study were recovered from O'ahu, Hawai'i. Respiratory and environmental isolates were stratified as RGM or SGM. For the Hawai'i isolate panel tested, *M. abscessus* and *M. porcinum* were included as representative RGM. *M. intracellulare* subspecies *chimaera* (referred herein as *M. chimaera*) was used as a representative SGM. Ethical review and approval were waived because the clinical isolates used in this study were de-identified patient residual isolates and not considered human subject research.

2.2. Whole-genome sequencing

DNA isolation for Illumina whole-genome sequencing (WGS) and genome assembly were performed as previously described (Epperson and Strong, 2020; Hasan et al., 2021). To contextualize the Hawai'i isolate data, DNA sequences for 47 additional non-Hawai'i respiratory and environmental NTM were downloaded from the publicly available National Center for Biotechnology Information (NCBI) GenBank database and are referred in this study as "NTM reference" isolates (Supplementary Tables 1A,B). Reference isolates used were *M. abscessus* subsp. *abscessus* ($n = 1$), *M. abscessus* subsp. *massiliense* ($n = 2$), *M. abscessus* subsp. *bolletii* ($n = 1$), *M. avium* ($n = 5$), *M. intracellulare* ($n = 4$), *M. paraintracellulare* ($n = 1$), *M. chimaera* ($n = 1$), *M. marseillense* ($n = 1$), *M. sinensis* ($n = 1$), *M. terrae* ($n = 1$), and *M. kansasii* ($n = 1$). There was no reference available for *M. porcinum*.

2.3. Siderophore gene analyses

The Kyoto Encyclopedia of Genes and Genomes (KEGG) database (Kanehisa et al., 2019) was used to interrogate NTM siderophore

TABLE 1 Respiratory NTM isolates used in this study.

	Isolate	ID used in phylogenetic trees	NCBI accession
1	248.MAB (MABS1)	MAB1	SAMN37352598
2	410.MAB (MAB2)	MAB2	SAMN37352599
3	423.MAB (MAB3)	MAB3	SAMN37352600
4	448.MAB (MAB4)	MAB4	SAMN37352601
5	528.MAB (MAB5)	MAB5	SAMN21208659
6	266.MAB (MAB6)	MAB6	SAMN21208657
7	311.MAB (MAB7)	MAB7	SAMN37352602
8	282.MPORC (MPORC1)	MPORC1	SAMN37352603
9	224.MPORC (MPORC2)	MPORC2	SAMN37352604
10	274.MPORC (MPORC3)	MPORC3	SAMN37352605
11	548.MPORC (MPORC4)	MPORC4	SAMN37352606
12	555.MPORC (MPORC5)	MPORC5	SAMN37352607
13	636.MPORC (MPORC6)	MPORC6	SAMN37352608
14	243.MPORC (MPORC7)	MPORC7	SAMN37352609
15	201.MCHIM (MCHIM1)	MCHIM1	SAMN37352610
16	202.MCHIM (MCHIM2)	MCHIM2	SAMN37352611
17	212.MCHIM (MCHIM3)	MCHIM3	SAMN37352612
18	225.MCHIM (MCHIM4)	MCHIM4	SAMN37352613
19	234.MCHIM (MCHIM5)	MCHIM5	SAMN37352614
20	242.MCHIM (MCHIM6)	MCHIM6	SAMN37352615
21	251.MCHIM (MCHIM7)	MCHIM7	SAMN37352616
22	252.MCHIM (MCHIM8)	MCHIM8	SAMN37352617
23	253.MCHIM (MCHIM9)	MCHIM9	SAMN37352618
24	254.MCHIM (MCHIM10)	MCHIM10	SAMN37352619
25	335.MCHIM (MCHIM11)	MCHIM11	SAMN37352620
26	406.MCHIM (MCHIM12)	MCHIM12	SAMN37352621
27	534.MCHIM (MCHIM13)	MCHIM13	SAMN37352622
28	733.MCHIM (MCHIM14)	MCHIM14	SAMN37352623

MAB, *Mycobacterium abscessus*; MPORC, *Mycobacterium porcinum*; MCHIM, *Mycobacterium chimaera*.

genes. Genes related to iron acquisition were identified by utilizing the KEGG pathway database to generate a list of each gene in the *mbt, mmpL/S*, and *esx*-3 gene pathways for each NTM species. All gene sequences with "*mbt*" in the gene name were acquired through the KEGG database.

Control metrics were performed to ensure the quality of the genome assemblies for each species: genome length (Supplementary Figure 1A), number of contigs (Supplementary Figure 1B), and the number of annotated genes (Supplementary Figure 1C). To assess the presence or absence of mycobactin (*mbt*), *mmpL/S*, and *esx-3* genes, WGS were annotated using Prokka (Seemann, 2014) and compiled into a pan-genome using Roary (Page et al., 2015). The genomes of respiratory and environmental Hawai'i NTM were parsed for *mbt*, *mmpL*, and *esx-3* genes, and the sequences of each gene for each isolate were aligned in a multiple sequence alignment using Geneious Prime (Version 2020.1).[1] For each gene, phylogenetic trees were created to investigate genetic variation between species and between respiratory and environmental isolates within each species as well.

2.4. *In vitro* siderophore screening

Siderophore assays were adapted from prior work by Hall and Ratledge (1982) and Louden et al. (2011). The NTM Hawai'i panel (Tables 1, 2) was streaked for isolation onto Middlebrook 7H10 OADC (oleic acid albumin dextrose catalase) plates and incubated at 37°C for 7 days for RGM and up to 21 days for *M. chimaera* to generate stock cultures. From stock cultures, isolates were picked and streaked for isolation onto low iron culture media (glycerol, L-asparagine, potassium phosphate monobasic, zinc chloride, manganese (II) chloride, magnesium sulfate heptahydrate) with agar. Low iron plates were incubated at 37°C for 9–16 days for RGM and up to 28 days for *M. chimaera*. Growth on low iron agar plates was indicative of viable bacteria and siderophore production. No growth on low iron plates was recorded as no siderophore production. In parallel, low iron culture broth was inoculated with the same panel of NTM isolates and incubated for 1 month. The chrome azurol S (CAS) assay was used to detect siderophore activity and adapted from Louden et al. (2011). 1 mL of low iron NTM cultures were dispensed into wells of a 24 well plate with 100 µL of CAS reagent per the Louden protocol. Samples were incubated at room temperature for 15 min. Siderophore activity was noted by an eye-visible color change from blue to yellow/orange 24 h post inoculation. The results of the CAS test and the low iron media plates were used to conclude which isolates produced siderophores in low iron environments. *Mycobacterium neoaurum* and *Mycobacterium fortuitum* were, respectively, used as positive and negative controls for the CAS assay.

2.5. Statistical analyses

Statistical tests were done in R Studio and Prism. The One Sample Student's t-test was used to compare the group with a higher or lesser number of genes between respiratory and environmental groups in the KEGG dataset. The Mann–Whitney-Wilcoxon test was used to determine whether the number of genes of respiratory and environmental groups for the Hawai'i data set were identical. The Kruskal-Wallis test was used to compare the number of genes in the comparison of respiratory/environmental and RGM/SGM from KEGG and to compare the number of genes between *M. abscessus, M. chimaera,* and *M. porcinum* from Hawai'i. The Games-Howell nonparametric post-hoc test was used to further compare the number of genes in the comparison of respiratory/environmental and RGM/SGM from different pairings of each group from KEGG. The Fisher's exact test was used to compare siderophore growth presence in RGM/SGM and respiratory/environmental samples for each *in vitro* analysis due to the small sample size.

1 https://www.geneious.com

TABLE 2 Environmental NTM isolates used in this study.

	Isolate	ID used in phylogenetic trees	Source	NCBI accession
1	12-39-Sw-B-1.MAB (MAB8)	MAB8	Kitchen-sink	SAMN21208626
2	12-39-SW-B-2.MAB (MAB9)	MAB9	Kitchen-sink	SAMN37352124
3	12-45-Sw-A-2.MAB (MAB10)	MAB10	Kitchen-sink	SAMN37352125
4	12-9-SW-B-2.MAB (MAB 11)	MAB11	Showerhead	SAMN21208670
5	17-15-Sw-A1-1-37.MAB (MAB12)	MAB12	Sink	SAMN37352126
6	17-17-Sw-A1-1-37.MAB (MAB13)	MAB13	Showerhead	SAMN37352127
7	17-51-Sw-B1-1-37.MAB (MAB14)	MAB14	Kitchen-sink	SAMN37352128
8	17 N-17-Sw-B1-1-37.MAB (MAB15)	MAB15	Showerhead	SAMN37352129
9	17-101-Sw-C1-1.MPORC (MPORC8)	MPORC8	Showerhead	SAMN37352130
10	17-17-Sw-B1-1-37.MPORC (MPORC9)	MPORC9	Garden-Hose	SAMN37352131
11	17 N-17-Sw-B1-2-37.MPORC (MPORC10)	MPORC10	Showerhead	SAMN37352132
12	18-204-Sw-A1-1-37.MPORC (MPORC11)	MPORC11	Sink	SAMN37352133
13	17-9-Sw-A1-1-37.MPORC (MPORC12)	MPORC12	Beach-Showerhead	SAMN37352134
14	17 N-17-Sw-E1-37.MPORC (MPORC13)	MPORC13	Garden-Hose	SAMN37352135
15	17-54-Sw-A-1-1-30.MCHIM (MCHIM16)	MCHIM16	Sink	SAMN37352136
16	17-65-Sw-A1-1-37.MCHIM (MCHIM17)	MCHIM17	Kitchen-sink	SAMN37352137
17	17-65-Sw-B1-1-37.MCHIM (MCHIM18)	MCHIM18	Showerhead	SAMN37352138
18	KM16-1-Sw-1-30.MCHIM (MCHIM19)	MCHIM19	NP *	SAMN37352139
19	KM16-15-Sw-2-30.MCHIM (MCHIM20)	MCHIM20	Toilet	SAMN37352140
20	KM16-16-Sw-1-37.MCHIM (MCHIM21)	MCHIM21	Sink	SAMN37352141
21	KM16-20-Sw-1-30.MCHIM (MCHIM22)	MCHIM22	Sink	SAMN37352142
22	KM16-33-Sw-2-30.MCHIM (MCHIM23)	MCHIM23	Sink	SAMN37352143
23	KM16-9-Sw-1-30.MCHIM (MCHIM24)	MCHIM24	Sink	SAMN37352144

MAB, *Mycobacterium abscessus*; MPORC, *Mycobacterium porcinum*; MCHIM, *Mycobacterium chimaera*.

3. Results

3.1. *mbt* genes are more abundant among respiratory NTM isolates compared to environmental NTM isolates

The *mbt* genes available through KEGG were identified from 47 NTM isolates including 20 respiratory NTM, 27 environmental NTM, and two species from the *Mtb* complex for comparison (*Mtb* H37Rv and *M. canetti*). Overall, respiratory NTM isolates showed significantly more *mbt* genes ($n = 10.7$ genes) compared to environmental NTM ($n = 8.3$ genes) ($p = 0.0002$) (Figure 1A). When the respiratory and environmental isolates were stratified by RGM and SGM, the mean number of *mbt* genes was statistically different between respiratory/RGM and environmental/RGM group ($p < 0.05$), the respiratory/SGM and environmental/RGM group ($p < 0.005$), and the environmental/RGM and environmental/SGM group ($p < 0.005$) (Figure 1B).

3.2. *Mycobacterium chimaera* shows more *mbt* genes compared to *M. abscessus* or *M. porcinum*

To study the differences between the number of *mbt* genes among NTM species that can cause respiratory disease, 51 isolates were compared including seven respiratory and eight environmental isolates of *M. abscessus,* seven respiratory and six environmental isolates of *M. porcinum*, and 14 respiratory and nine environmental isolates of *M. chimaera*. Comparing both respiratory and environmental isolates, gene duplications were observed for *mbtC*, *mbtD*, *mbtE*, and *mbtF*, generally located outside of the *mbt* locus (average: 888,213 bp; range: [1,328:2,671,854 bp]), and varied by gene and species. Among the RGM *M. abscessus* and *M. porcinum* isolates, only one *mbtD* gene was identified. *M. abscessus* showed an average number of 14 *mbt* genes while *M. porcinum* showed an average of 17 genes, which was significantly less than the 27 *mbt* genes for *M. chimaera* ($p = 0.005$) (Figure 2A). Of note, the *mbt-2* gene complex, *mbtL*, *mbtM*, and *mbtN* genes were absent from *M. abscessus* and *mbtI* and *mbtL* genes were missing from *M. porcinum*. All ten *mbt-1* and four *mbt-2* genes were detected in *M. chimaera* accounting for its significantly higher average number of *mbt* genes.

Similar numbers of *mbt* genes were observed between respiratory and environmental *M. abscessus* (Figure 2B) and respiratory and environmental *M. porcinum* (Figure 2C) isolates. However, respiratory *M. chimaera* isolates showed significantly lower numbers of *mbt* genes compared to environmental *M. chimaera* isolates ($p = 0.005$) (Figure 2D).

We constructed a phylogenetic tree to examine the genetic relatedness of *mbtA* genes among *M. abscessus, M. porcinum,* and *M. chimaera*. Each isolate contained one copy of the *mbtA* gene. *M. abscessus mbtA* is genetically similar to *M. porcinum mbtA* genes, as revealed by the close proximity in location on the phylogenetic tree

(Figure 3). All sequences from respiratory and environmental isolates of *M. porcinum* were identical. This was also observed for *M. abscessus,* except for one respiratory and two environmental isolates which shared a single nucleotide polymorphism (SNP). For *M. chimaera*, two environmental isolates showed the same 13 SNPs while the rest of the samples were identical in sequence. Similar results can be seen for the mbt synthase G, *mbtG* gene (Supplementary Figure 2), where respiratory and environmental isolates within *M. abscessus* and *M. porcinum* and had identical gene sequences compared to two sub-branches for the *M. chimaera* cluster.

For the mycobactin synthases *mbtM* gene, two copies of the gene were identified in *M. porcinum* and *M. chimaera*. All *M. porcinum* isolates had identical sequences for both *mbtM* copies. For one copy of *mbtM* in *M. chimaera,* the two environmental isolates sharing the *mbtA* variant also shared an *mbtM* copy variant with 18 SNPs. The other *mbtM* copy had the same relationships as within the *mbtG* gene of *M. chimaera*. This pattern of relationships was also observed in the *mbtM* and *mbtN* genes in *M. porcinum* and *M. chimaera*; however, these genes are single-copy in all isolates (Supplementary Figures 3A,B).

3.3. *mmpl*/S and *esx*-3 secretion system associated genes in NTM from Hawai'i

Because of their roles in siderophore and iron transport, we also investigated the number of *mmpL/S* and *esx*-3 secretion system associated genes in the same sample of Hawai'i NTM isolates. There were 13 *mmpL* proteins based on a model of *Mtb*, but we focused on *mmpL/S3, mmpL/S4,* and *mmpL/S5* for their roles in either siderophore or heme export (Szekely and Cole, 2016). While the number of *mmpL345* and *mmpS345* genes tended to follow the trend of *M. abscessus* > *M. porcinum* > *M. chimaera*, no significant differences were observed (Supplementary Figures 4A,B). When the number of *mmpL* genes were compared between respiratory or environmental isolates among the three different species, no significant differences were found (Supplementary Figures 5A–C).

The esx-3 secretion system is required for mycobacterial iron acquisition through *mbt* (Siegrist et al., 2009). The *esx*-3 locus contains the genes for the *esx*G and *esx*H proteins, and supporting genes identified as *ecc*A3, *ecc*B3, *ecc*C3, *ecc*D3, eccE3, *esp*G3, and *myc*P3 that are required for protein export and iron acquisition (Siegrist et al., 2014). While *esx*-3 gene numbers did not vary among the RGM isolates (Figures 4A,B), environmental *M. chimaera* isolates showed significantly more numbers of *esx*-3 genes compared to respiratory *M. chimaera* isolates ($p = 0.013$) which appear to be due to gene duplications of the *mycP3* gene (Figure 4C). Among Hawai'i *M. chimaera*, we found 1–3 copies of *esp*G3 or *mycP*3 per genome. The duplicate copies of *esp*G3 and *mycP*3 were inconsistently located throughout the genome. The average distance between *esp*G3 copies was 1,979,955 nt (range: 560,978–2,891,545 nt) and the average distance between *mycP*3 copies was 2,636,478 nt (range: 479,373 – 4,820,547 nt).

3.4. *In vitro* siderophore production is higher in RGM than in SGM

Next, two *in vitro* methodologies, including growth on low iron media plates and the CAS detection assay, were used to screen the isolates for siderophore production in low iron environments and results are summarized in Supplementary Tables 3, 4. Of the environmental *M. abscessus, M. porcinum,* and *M. chimaera* isolates tested, 88% ($n = 7/8$), 100% ($n = 6/6$), and 11% ($n = 1/9$), respectively showed visible colonies indicative of growth on low iron plates. Of the respiratory *M. abscessus*, *M. porcinum*, and *M. chimaera* isolates tested, 100% ($n = 7/7$), 86% ($n = 6/7$), and 29% ($n = 4/14$), respectively showed visible colonies indicative of growth on low iron plates.

No differences were observed between respiratory and environmental NTM growth on low iron plates ($p > 0.9999$) (data not shown). When these data were stratified by RGM (*M. abscessus* and *M. porcinum*) and SGM *(M. chimaera)* categories, growth on low iron agar was more frequently observed for the RGM compared to the SGM ($p < 0.0001$) (Figure 5A, left panel). This trend was also true when the isolates were stratified as respiratory RGM and SGM isolates ($p = 0.018$) (Figure 5A, middle panel) and environmental RGM and SGM isolates ($p = 0.0002$) (Figure 5A, right panel). No statistical differences were observed between the number of environmental and respiratory isolates that grew or did not grow on low iron agar.

The universal siderophore assay, CAS, was used as a second assay to assess siderophore production by NTM isolates. When a strong iron chelator such as a siderophore removes iron from the media a color change from green/blue to yellow/orange occurs. In Figure 5B, we show an example of CAS assay outcomes using 10 environmental *M. chimaera* isolates. Eight isolates (80%) showed a yellow/orange color change (positive) and two (20%) showed a green/blue color indicative of a negative test. *M. neoaurum* and *M. fortuitum* were used as positive and negative controls, respectively along with an uninoculated well. Finally, we tested the collection of environmental and respiratory NTM by the CAS assay. Among environmental *M. abscessus, M. porcinum,* and *M. chimaera* isolates, 88% ($n = 7/8$), 50% ($n = 3/6$), and 30% ($n = 3/10$), respectively showed positive color change for CAS. Of the respiratory *M. abscessus, M. porcinum,* and *M. chimaera* isolates tested, 100% ($n = 7/7$), 71% ($n = 5/7$), and 57% ($n = 8/14$), respectively showed positive color change for CAS (Supplementary Tables 3, 4). We did not observe any significant difference in CAS outcomes between environmental and respiratory isolate groups or when the isolates were sub-categorized by species. We observed more CAS positive tests in RGM versus SGM ($p < 0.05$) (Figure 5C, left panel) and among environmental isolates (e.g., environmental RGM vs. environmental SGM) ($p < 0.05$) (Figure 5C, middle panel), but not when comparing within respiratory isolates (e.g., respiratory RGM vs. respiratory SGM) (Figure 5C, right panel).

Because all isolates studied were tested for siderophore activity *via* growth on low iron plates and by the CAS assay, we determined the frequency at which the outcomes of the two assays matched or mismatched. We highlight in red font the between assay matches per isolate tested in Supplementary Tables 1A,B. Overall, among all 28 RGM isolates tested, 22 (79%) showed low iron assay outcomes matched CAS assay outcomes compared to 21% (6/28) mismatches (Supplementary Figure 6). When analyzed separately, assay concurrency was more often observed for respiratory isolates compared to environmental RGM isolates (93% vs. 64%) (Supplementary Figure 7). Taking an additional step, we separated the outcomes for *M. abscessus* and *M. porcinum.* Generally, low iron assay results aligned with CAS assay outcomes for respiratory *M. abscessus* (7/7) and *M. porcinum* (6/7) isolates, agreeing 100 and 86%,

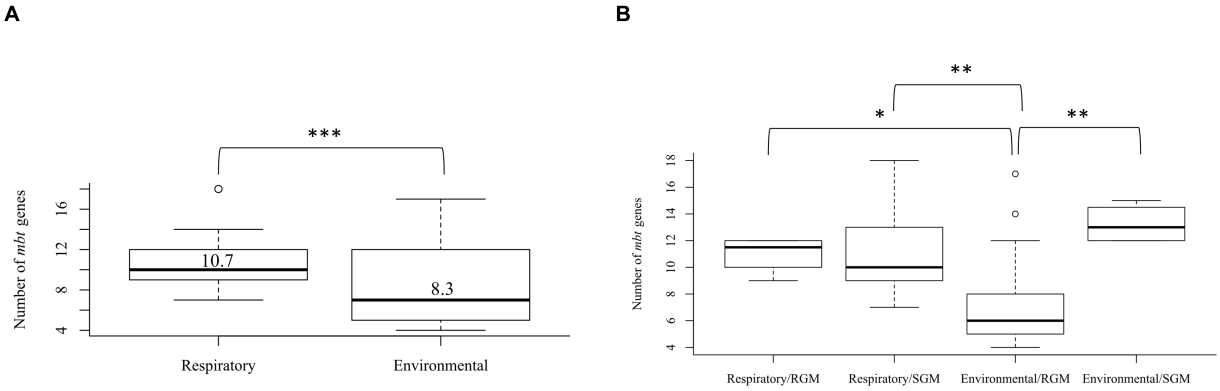

FIGURE 1
Varying number of mycobactin (*mbt*) genes between respiratory and environmental reference NTM isolates (Supplementary Tables 1A, B). Box plot showing **(A)** the number of *mbt* genes stratified by respiratory vs. environmental derived NTM; ***$p = 0.0001989$. **(B)** Number of *mbt* genes for respiratory vs. environmental NTM stratified by rapid growing mycobacteria (RGM) and slow growing mycobacteria (SGM). The central rectangle of the plot spans the interquartile range (IQR). The bar inside the rectangle represents the median, and the bars above and below show the location of the maximum and minimum, respectively. The small circle represents outliers. *$p < 0.05$; **$p < 0.005$.

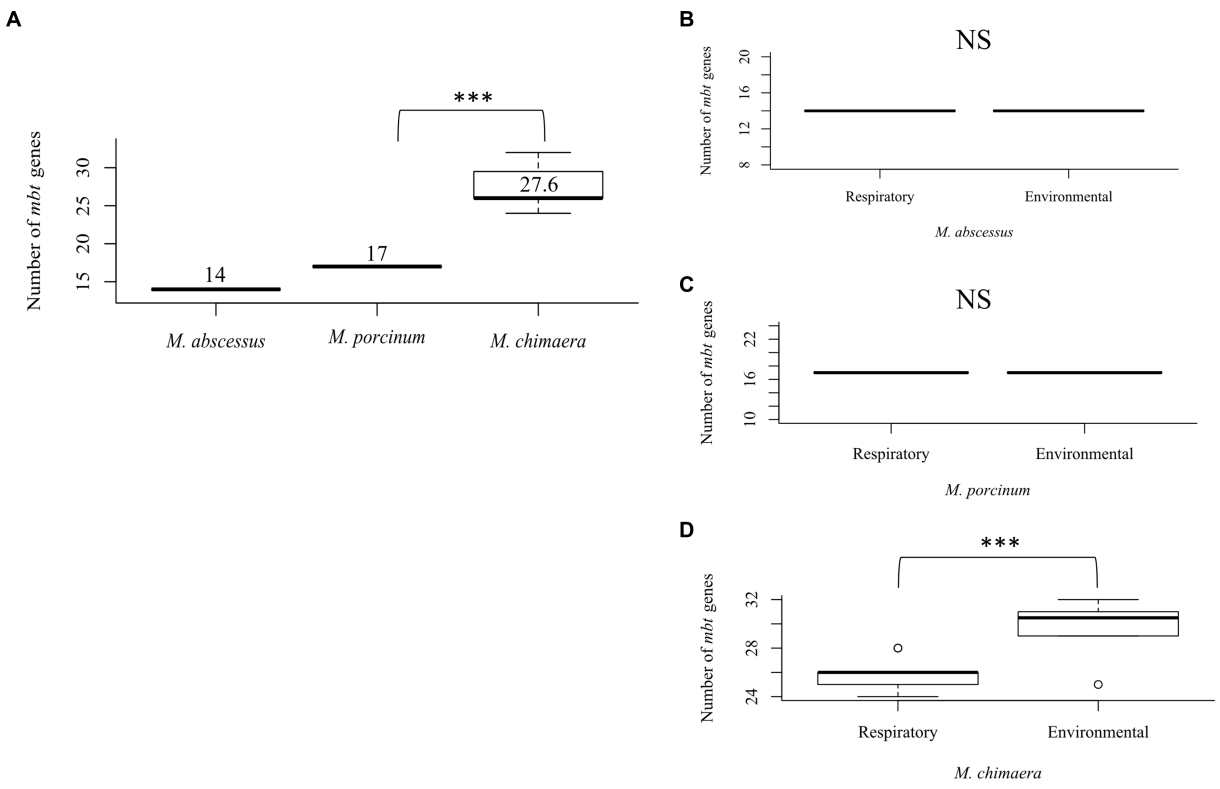

FIGURE 2
Mycobacterium chimaera shows more *mbt* genes compared to *M. abscessus* and *M. porcinum* **(A)** Distribution of the number of *mbt* genes among all *M. abscessus*, *M. chimaera*, and *M. porcinum* isolates from Hawai'i. ***$p = 0.0005097$. Number of *mbt* genes between respiratory or environmental **(B)** *M. abscessus*, **(C)** *M. porcinum*, **(D)** *M. chimaera*. ***$p = 0.0005097$. NS, not significant. Isolates studied in Figure 2 are listed in Tables 1, 2.

respectively, of the time. Among the environmental *M. abscessus* and *M. porcinum* isolates tested, the two assay outcomes agreed 75% (6/8) and 50% (3/6), respectively.

Similarly, for the SGM, 70% (16/23) *M. chimaera* isolates studied showed low iron assay outcomes matched CAS assay outcomes compared to 30% (7/23) mismatches (Supplementary Figure 6). By stratifying all *M. chimaera* isolates into respiratory and environmental categories, concurrency between the two tests was more often observed for environmental *M. chimaera* isolates compared to respiratory *M. chimaera* isolates (89% vs. 57%) (Supplementary Figure 7).

The combined outcomes from genomic analyses and *in vitro* assays for the three NTM species and subspecies tested in this study are summarized in a cartoon, Figure 6.

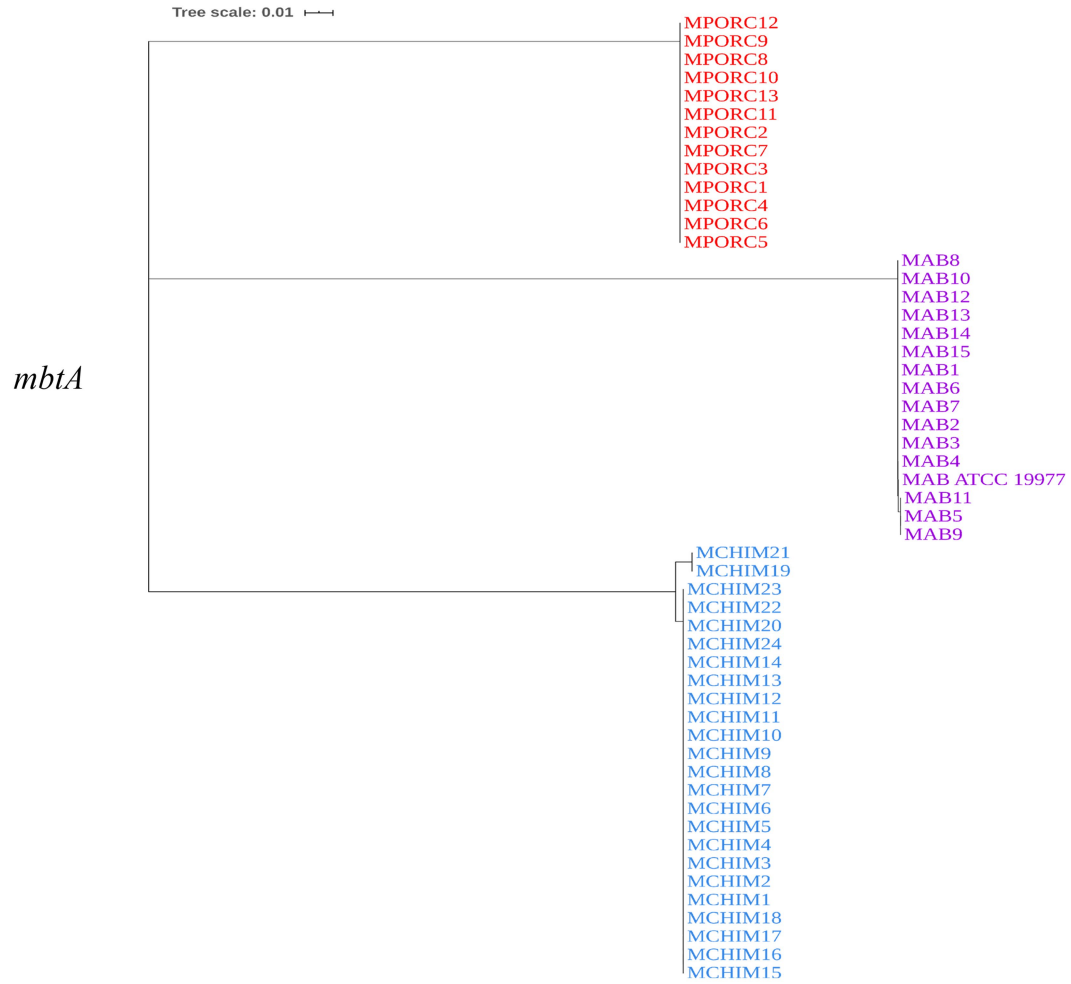

FIGURE 3
mbtA is genetically similar among the NTM. Neighbor-joining phylogenetic tree based on the *mbtA* gene. Scale bar indicates number of substitutions per site.

4. Discussion

NTM PD is a growing cause of concern as its prevalence has been increasing in Hawai'i, nationwide, and globally. A panel of NTM from Hawai'i comprised of environmental and respiratory isolates was used to examine differences, if any, between *M. abscessus, M. porcinum*, and *M. chimaera* isolates in terms of iron acquisition by siderophores when stratified by their (1) recovered niche and (2) growth type (i.e., RGM or SGM).

In the U.S., the mean amount of iron in surface soil (0–5 centimeters) is 214 μg/L or 0.214 mg/kg (Smith et al., 2013; Brittenham et al., 2018). For comparison, this is lower than the mean amount of iron in Hawaiian Island soils that is around 95,500 mg/kg (Hawai'i Department of Health Hazard Evaluation and Emergency Response, 2012). Drinking water in the U.S. seldom contains more than 300 μg/L (Services). The normal range for serum iron is 6 to 17 μg/L and iron is present in the cytoplasm of host cells at very low levels (Agoro and Mura, 2019). In prolonged iron starvation environments such as the granuloma, *Mtb* can show high expression of *mbt* genes and siderophore production (Agoro and Mura, 2019). Due to the limited amount of iron in the body compared to the overabundance of iron in the extracellular niches that environmental NTM inhabit, we hypothesized that respiratory NTM would be more likely to produce siderophores due to the limited access to iron in the lung, compared to environmental NTM isolates. To test this hypothesis, we performed complementary genomic and microbiological analyses to assess siderophore production.

Among the reference NTM gene sequences parsed through the KEGG database that we examined, respiratory NTM showed significantly higher mean number of *mbt* genes compared to environmentally isolated species (Figure 1A). On the other hand, the number of *mbt* genes were similar among the respiratory and environmental NTM isolates from Hawai'i based on the phylogenetic trees and multiple sequence alignments (Figure 3; Supplementary Figures 2, 3). For the Hawai'i isolates, we detected all ten *mbt-1* and four *mbt-2* genes in SGM *M. chimaera* compared to the RGM species (containing nine to ten *mbt-1* and one to three *mbt-2* genes) suggesting *M. chimaera* is selectively advantaged in iron acquisition from the environment compared to *M. abscessus* and *M. porcinum*. When we further analyzed for the presence of *mbt* genes where each species was stratified by their recovered niches, there was no statistical difference in *mbt* gene numbers between the respiratory

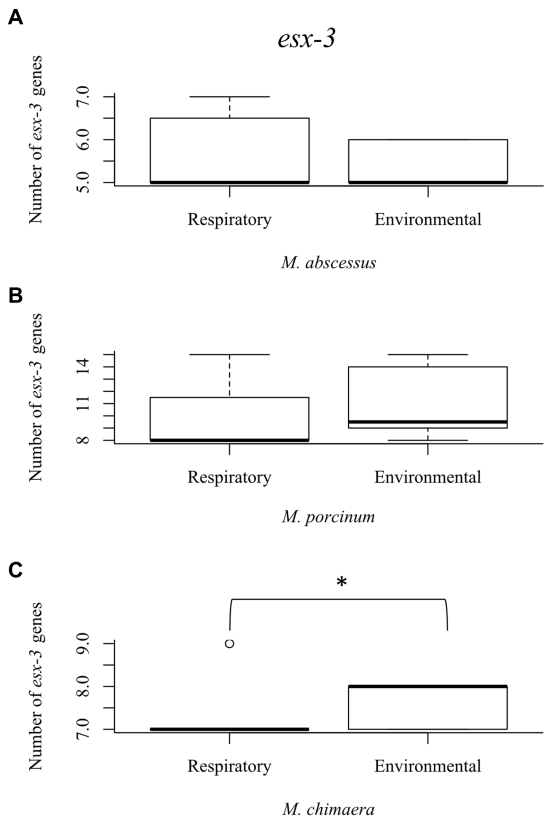

FIGURE 4
Mycobacterium chimaera shows significantly more *esx-3* genes compared to rapid growing mycobacteria. Box plot showing the number of *esx*-3 genes in respiratory and environmental **(A)** *M. abscessus;* **(B)** *M. porcinum;* and **(C)** *M. chimaera*. *$p = 0.01346$.

and environmental RGM isolates of *M. abscessus* and *M. porcinum* (Figures 2B,C). However, for SGM *M. chimaera* from Hawai'i, environmental isolates showed more *mbt* genes compared to respiratory isolates (Figure 2D). However, despite differences in the detection of siderophore genes among the isolates tested, we did not observe significant phenotypic differences in the *in vitro* assay outcomes.

Besides *mbt,* we also examined two other iron acquiring systems for mycobacteria, *mmpL*/S and *esx*-3. *mmpL3*, plays a key role in the acquisition of iron from heme (Tullius et al., 2011). *mmpL4* and *mmpL5* both have similar functions in iron acquisition *via* siderophores (Wells et al., 2013). In contrast to *mbt* genes of the SGM, the total number of *mmp*L proteins are more abundant in RGM compared to SGM, especially in the *M. abscessus* species (Viljoen et al., 2017). In our study, although not statistically significant, the number of *mmpL*/S genes tended to be higher in RGM compared to SGM (Supplementary Figure 4). The abundance of *mmpL* genes could allow the RGM to persist in various environments, and *M. abscessus* has been observed to evolve and acquire genetic material rapidly (Sapriel et al., 2016). Although, it is unknown how *esx*-3 plays a role in iron acquisition, it is essential for mycobacterial growth in iron-limited conditions. Similar to *mbt*, the environmental *M. chimaera* isolates showed significantly more esx-3 genes than respiratory *M. chimaera* isolates (Figure 4C).

These genetic results support siderophore producing advantages among Hawai'i *M. chimaera* environmental isolates that likely facilitate survival in exogenous niches. *M. chimaera* was the most common NTM recovered from the environment of Hawai'i (Honda et al., 2016); thus, this subspecies may have evolved methods to procure iron in nutrient limited environmental conditions. We have already shown that *M. chimaera*-derived from the Hawai'i environment grows better in the presence of iron oxide minerals such as hematite after 24 h in culture and binds to its surface (Glickman et al., 2020).

To complement our genomic analysis, we tested our NTM Hawai'i isolate panel for siderophore production by two microbiological assays, growth on low iron culture media and the CAS assay. Such assays have already been applied to study siderophore production in a variety of gram-negative and gram-positive bacteria (Hall and Ratledge, 1982; Louden et al., 2011; Ferreira et al., 2019). Based on the results from our genomic analyses, we posited that siderophore production would be more frequently observed *in vitro* for *M. chimaera* isolates compared to *M. abscessus* and *M. porcinum* isolates. However, iron scavenging from culture media containing low amounts of iron and production of siderophores was more frequently observed for the RGM *M. abscessus* and *M. porcinum* isolates compared to SGM *M. chimaera* categories (Figures 5A,C). We also observed discrepancies across the outcomes for the microbiological assays; that is, siderophore test outcomes did not match 100% of the time. For example, for 22 of the 28 RGM isolates tested and for 16 of 23 SGM isolates tested, low iron assay results matched CAS assay results 79 and 70% of the time, leaving mismatch outcomes for 21 and 30% of the isolates tested (Supplementary Figure 6). The reasons for the incongruency between the genomic analyses and *in vitro* outcomes and between the two microbiological tests used in our study are not known. Other studies have demonstrated SGM show significantly more inorganic ion transport gene clusters than RGM (Bachmann et al., 2019). Alternatively, discrepancies may be related to innate adaptation to exogenous iron or differences in siderophore secretion as our *in vitro* assays detect secreted siderophores. There may also be features of each culture media (e.g., dextrose, glycerol, or other components) that may influence siderophore activity which may also vary per isolate and between isolates of different growth rates (e.g., RGM and SGM). Future studies to reassess NTM siderophore production as supplemental iron is added to culture media, utilizing similar media components per assay, and repeating low iron tests using liquid culture would help to disentangle some of these outcomes.

This study has some limitations. For the gene sequences taken through the KEGG database, there was limited information on some of the genomes. For instance, there is a lack of clear information on isolation details. The data from those NTM isolates were excluded from the dataset; thus, reducing the sample size and variety of isolates analyzed. Secondly, the genomes from Hawai'i were from bacteria isolated from the island of O'ahu. While O'ahu is home to the majority of the state's population, it would be prudent to explore iron-acquisition mechanisms by NTM recovered from other islands and other geographic areas. In addition, the *in vitro* CAS assay analyses of extracellular siderophores was not included in the gene analysis of intracellular siderophores and other iron-acquisition processes. A follow up transcriptomic study would be helpful to explore other genes and proteins involved with iron metabolism

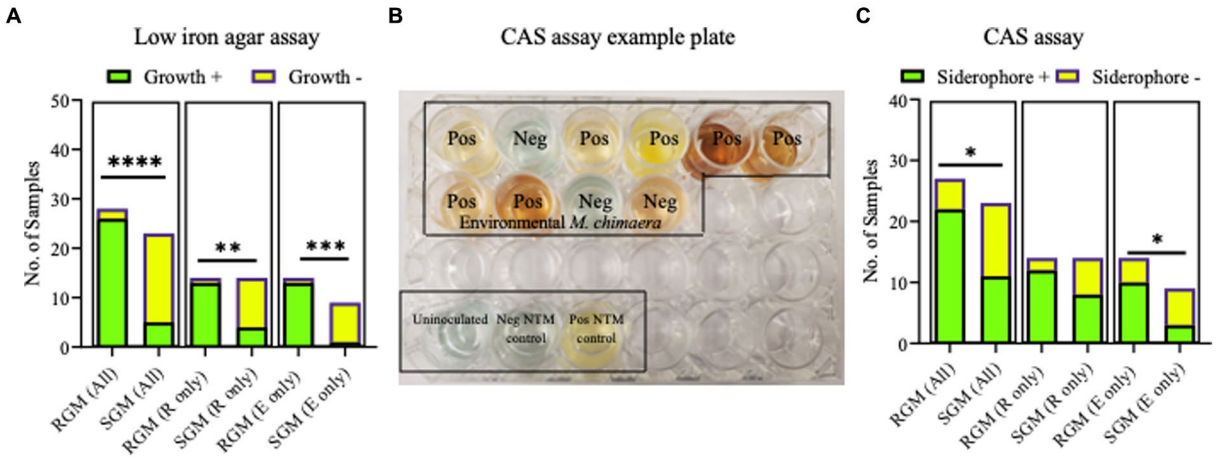

FIGURE 5
Growth on low iron agar and positive CAS assays are more often observed for rapid growing mycobacteria (RGM) compared to slow growing mycobacteria (SGM). **(A)** Stacked bar graphs showing +/− growth for RGM and SGM on low iron agar plates. R, respiratory derived isolates. E, environment derived isolates. Low iron RGM vs SGM ****p = <0.0001, ***p = 0.0002, *p = 0.0175. **(B)** To demonstrate CAS assay outcomes, we show an example of positive and negative media color change results for 10 environmental *M. chimaera* isolates, black box. *M. neoaurum* and *M. fortuitum* were used as positive and negative control isolates, respectively along with an uninoculated well (bottom of image, black box). **(C)** Outcomes for all CAS assays shown as stacked bar graphs. *R*, respiratory derived isolates. E, environment-derived isolates. *$p < 0.05$.

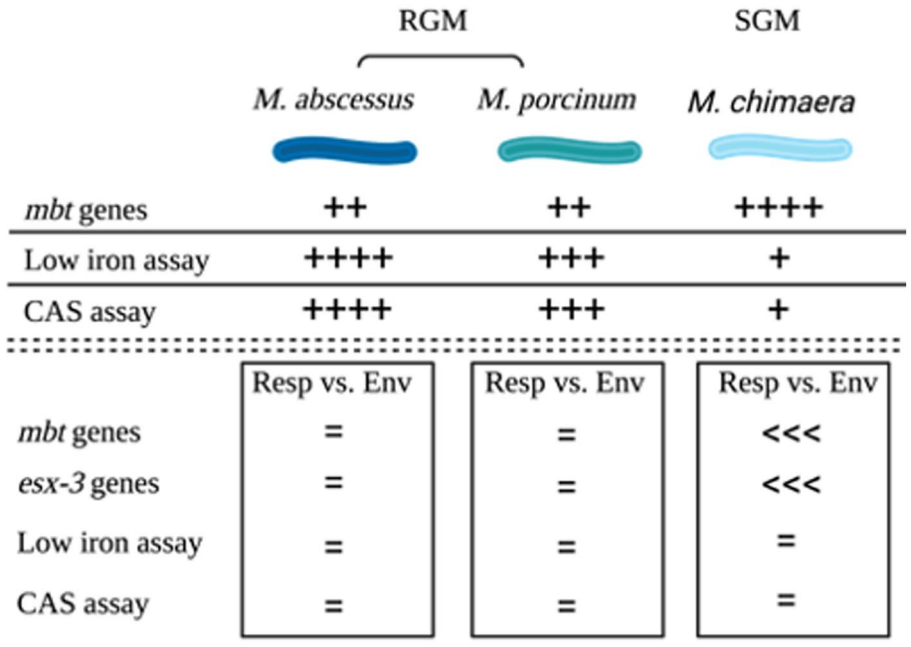

FIGURE 6
Summary. Cartoon summarizing the outcomes of genomic comparisons and applied microbiological assays to assess siderophores among *M. abscessus, M. porcinum*, and *M. chimaera* respiratory and environmental isolates. Image created using BioRender.

(e.g., transferrin, ferritin) and discern ones that are modulated with low iron exposure.

To expand upon this study, future studies may include similar experiments to analyze extracellular siderophore genes and siderophore activity using a more diversified panel of SGM and RGM species with larger numbers of environmental and respiratory isolates to further verify differences among NTM. In addition, other factors affecting iron acquisition such as competition could be analyzed through a combined analysis of other NTM and non-NTM isolates. More importantly, the roles of *mbt, mmpL/S,* and *esx-3* in iron acquisition for *M. abscessus*, *M. porcinum*, and *M. chimaera* should be further evaluated for their roles in virulence in the context of lung immune cell infections, as has been performed for *Mtb* and *Salmonella* (De Voss et al., 2000; Saha et al., 2019).

In summary, our data provide new insights into iron acquisition genes and the presence and activity of NTM siderophores. Clinical studies should be performed to understand the role of dietary iron in individuals with NTM PD. Outcomes of these studies may highlight NTM iron acquisition genes or siderophores as new targets for drug development.

Data availability statement

All relevant data is contained within the article. The original contributions presented in the study are included in the article/supplementary material, further inquiries can be directed to the corresponding author. Information for existing publicly accessible datasets is contained within the article. The datasets presented in this study can be found in online repositories. The names of the repository/repositories and accession number(s) can be found in the article/supplementary material. The data presented in this study are deposited in NCBI, accession numbers: SAMN37352598-SAMN37352623, SAMN21208657, SAMN21208659, SAMN37352124-SAMN37352144, SAMN21208626, SAMN212086270.

Author contributions

CT: Data curation, Investigation, Methodology, Visualization, Writing – review & editing, Formal analysis, Software, Validation, Writing – original draft. NO: Data curation, Formal analysis, Investigation, Methodology, Validation, Visualization, Writing – review & editing. AM: Data curation, Formal analysis, Investigation, Validation, Visualization, Writing – review & editing. SD: Formal analysis, Investigation, Validation, Visualization, Writing – review & editing. YC: Writing – review & editing, Funding acquisition, Methodology, Project administration, Resources, Software, Supervision, Writing – original draft. MS: Methodology, Software, Supervision, Writing – review & editing. NH: Methodology, Software, Supervision, Writing – review & editing, Data curation, Formal analysis, Investigation, Validation, Visualization, Writing – original draft. JH: Data curation, Formal analysis, Investigation, Methodology, Supervision, Visualization, Writing – original draft, Writing – review & editing, Conceptualization, Funding acquisition, Project administration, Resources.

Funding

The author(s) declare financial support was received for the research, authorship, and/or publication of this article. This research was funded, in part, by the National Science Foundation grant #1743587, Division of Environmental Biology, as part of the Ecology and Evolution of Infectious Diseases program. JH also acknowledges support from the Padosi Foundation.

Acknowledgments

The authors would like to acknowledge Diagnostic Laboratory Services, Inc. (Aiea, Hawai'i) at the time clinical NTM isolates were procured for their assistance and enthusiasm for this project.

Conflict of interest

The authors declare that the research was conducted in the absence of any commercial or financial relationships that could be construed as a potential conflict of interest.

Publisher's note

Supplementary material

The Supplementary material for this article can be found online at: https://www.frontiersin.org/articles/10.3389/fmicb.2023.1268963/full#supplementary-material

References

Abbaspour, N., Hurrell, R., and Kelishadi, R. (2014). Review on iron and its importance for human health. *J. Res. Med. Sci.* 19, 164–174. Available at: https://pubmed.ncbi.nlm.nih.gov/24778671/.

Adjemian, J., Olivier, K. N., Seitz, A. E., Holland, S. M., and Prevots, D. R. (2012). Prevalence of nontuberculous mycobacterial lung disease in U.S. Medicare beneficiaries. *Am. J. Respir. Crit. Care Med.* 185, 881–886. doi: 10.1164/rccm.201111-2016OC

Agoro, R., and Mura, C. (2019). Iron supplementation therapy, a friend and foe of mycobacterial infections? *Pharmaceuticals (Basel)* 12, 1–28. doi: 10.3390/ph12020075

Bachmann, N. L., Salamzade, R., Manson, A. L., Whittington, R., Sintchenko, V., Earl, A. M., et al. (2019). Key transitions in the evolution of rapid and slow growing *Mycobacteria* identified by comparative genomics. *Front. Microbiol.* 10:3019. doi: 10.3389/fmicb.2019.03019

Barclay, R., Ewing, D. F., and Ratledge, C. (1985). Isolation, identification, and structural analysis of the mycobactins of Mycobacterium avium, Mycobacterium intracellulare, Mycobacterium scrofulaceum, and Mycobacterium paratuberculosis. *J Bacteriol.* 164, 896–903. doi: 10.1128/JB.164.2.896-903.1985

Braun, V., and Winkelmann, G. (1988). "*Microbial iron transport structure and function of siderophores*": Springer Berlin/Heidelberg, 67–99.

Brittenham, G., Hoffman, R., Benz, E., and Silberstein, L. (2018). *Disorders of iron homeostasis: iron deficiency and overload*. Philadelphia, PA: Elsevier

Crosa, J. H. (1989). Genetics and molecular biology of siderophore-mediated iron transport in bacteria. *Microbiol. Rev.* 53, 517–530. doi: 10.1128/mr.53.4.517-530.1989

De Voss, J. J., Rutter, K., Schroeder, B. G., Su, H., Zhu, Y., and Barry, C. E. 3rd (2000). The salicylate-derived mycobactin siderophores of *Mycobacterium tuberculosis* are essential for growth in macrophages. *Proc. Natl. Acad. Sci. U. S. A.* 97, 1252–1257. doi: 10.1073/pnas.97.3.1252

Epperson, L. E., and Strong, M. (2020). A scalable, efficient, and safe method to prepare high quality DNA from mycobacteria and other challenging cells. *J. Clin. Tuberc. Other Mycobact. Dis.* 19:100150. doi: 10.1016/j.jctube.2020.100150

Falkinham, J. O. 3rd (1996). Epidemiology of infection by nontuberculous mycobacteria. *Clin. Microbiol. Rev.* 9, 177–215. doi: 10.1128/CMR.9.2.177

Ferreira, C. M. H., Vilas-Boas, A., Sousa, C. A., Soares, H., and Soares, E. V. (2019). Comparison of five bacterial strains producing siderophores with ability to chelate iron under alkaline conditions. *AMB Express* 9:78. doi: 10.1186/s13568-019-0796-3

Glickman, C. M., Virdi, R., Hasan, N. A., Epperson, L. E., Brown, L., Dawrs, S. N., et al. (2020). Assessment of soil features on the growth of environmental nontuberculous mycobacterial isolates from Hawai'i. *Appl. Environ. Microbiol.* 86:e00121-20. doi: 10.1128/AEM.00121-20

Gobin, J., Moore, C. H., Reeve, J. R. Jr., Wong, D. K., Gibson, B. W., and Horwitz, M. A. (1995). Iron acquisition by *Mycobacterium tuberculosis*: isolation and characterization of a family of iron-binding exochelins. *Proc. Natl. Acad. Sci. U. S. A.* 92, 5189–5193. doi: 10.1073/pnas.92.11.5189

Griffiths, E., Rogers, H. J., and Bullen, J. J. (1980). Iron, plasmids and infection. *Nature* 284, 508–509. doi: 10.1038/284508a0

Hall, R. M., and Ratledge, C. (1982). A simple method for the production of mycobactin, the lipid-soluble siderophore, from mycobacteria. *FEMS Microbiol. Lett.* 15, 133–136. doi: 10.1111/j.1574-6968.1982.tb00053.x

Hall, R. M., and Ratledge, C. (1984). Mycobactins as chemotaxonomic characters for some rapidly growing mycobacteria. *J Gen Microbiol.* 130, 1883–92. doi: 10.1099/00221287-130-8-1883

Hall, R. M., and Ratledge, C. (1985). Equivalence of mycobactins from Mycobacterium senegalense, Mycobacterium farcinogenes and Mycobacterium fortuitum. *J Gen Microbiol.* 131, 1691–6. doi: 10.1099/00221287-131-7-1691

Hasan, N. A., Davidson, R. M., Epperson, L. E., Kammlade, S. M., Beagle, S., Levin, A. R., et al. (2021). Population genomics and inference of *Mycobacterium avium* complex clusters in cystic fibrosis care centers, United States. *Emerg. Infect. Dis.* 27, 2836–2846. doi: 10.3201/eid2711.210124

Hawaii Department of Health Hazard Evaluation and Emergency Response. (2012). *Hawaiian Islands Soil Metal Background Evaluation Report*, May 2012 [Online]. Available at: https://health.hawaii.gov/heer/files/2012/05/Hawaiian-Islands-Soil-Metal-Background-Evaluation-Report-May-2012.pdf (Accessed October 26, 2023).

Honda, J. R., Hasan, N. A., Davidson, R. M., Williams, M. D., Epperson, L. E., Reynolds, P. R., et al. (2016). Environmental nontuberculous mycobacteria in the Hawaiian islands. *PLoS Negl. Trop. Dis.* 10:e0005068. doi: 10.1371/journal.pntd.0005068

Honda, J. R., Virdi, R., and Chan, E. D. (2018). Global environmental nontuberculous mycobacteria and their contemporaneous man-made and natural niches. *Front. Microbiol.* 9:2029. doi: 10.3389/fmicb.2018.02029

Kanehisa, M., Sato, Y., Furumichi, M., Morishima, K., and Tanabe, M. (2019). New approach for understanding genome variations in KEGG. *Nucleic Acids Res.* 147, D590–D595. doi: 10.1093/nar/gky962

Louden, B. C., Haarmann, D., and Lynne, A. M. (2011). Use of blue agar CAS assay for siderophore detection. *J. Microbiol. Biol. Educ.* 12, 51–53. doi: 10.1128/jmbe.v12i1.249

McDowell, L.R. (1992). *Minerals in animal and human nutrition*. San Diego, CA Academic Press Inc.

Page, A. J., Cummins, C. A., Hunt, M., Wong, V. K., Reuter, S., Holden, M. T., et al. (2015). Roary: rapid large-scale prokaryote pan genome analysis. *Bioinformatics* 31, 3691–3693. doi: 10.1093/bioinformatics/btv421

Parte, A. C., Sarda Carbasse, J., Meier-Kolthoff, J. P., Reimer, L. C., and Goker, M. (2020). List of prokaryotic names with standing in nomenclature (LPSN) moves to the DSMZ. *Int. J. Syst. Evol. Microbiol.* 70, 5607–5612. doi: 10.1099/ijsem.0.004332

Saha, P., Xiao, X., Yeoh, B. S., Chen, Q., Katkere, B., Kirimanjeswara, G. S., et al. (2019). The bacterial siderophore enterobactin confers survival advantage to Salmonella in macrophages. *Gut Microbes* 10, 412–423. doi: 10.1080/19490976.2018.1546519

Sapriel, G., Konjek, J., Orgeur, M., Bouri, L., Frezal, L., Roux, A. L., et al. (2016). Genome-wide mosaicism within *Mycobacterium abscessus*: evolutionary and epidemiological implications. *BMC Genomics* 17:118. doi: 10.1186/s12864-016-2448-1

Seemann, T. (2014). Prokka: rapid prokaryotic genome annotation. *Bioinformatics* 30, 2068–2069. doi: 10.1093/bioinformatics/btu153

Siegrist, M. S., Steigedal, M., Ahmad, R., Mehra, A., Dragset, M. S., Schuster, B. M., et al. (2014). Mycobacterial Esx-3 requires multiple components for iron acquisition. *MBio* 5, e01073–e01014. doi: 10.1128/mBio.01073-14

Siegrist, M. S., Unnikrishnan, M., Mcconnell, M. J., Borowsky, M., Cheng, T. Y., Siddiqi, N., et al. (2009). Mycobacterial Esx-3 is required for mycobactin-mediated iron acquisition. *Proc. Natl. Acad. Sci. U. S. A.* 106, 18792–18797. doi: 10.1073/pnas.0900589106

Skaar, E. P. (2010). The battle for iron between bacterial pathogens and their vertebrate hosts. *PLoS Pathog.* 6:e1000949. doi: 10.1371/journal.ppat.1000949

Smith, D.B., Cannon, W.F., Woodruff, L.G., Solano, F., Kilburn, J.E., and Fey, D.L. (2013). Geochemical and mineralogical data for soils of the conterminous United States. Data Series. (Reston, VA).

Sritharan, M. (2016). Iron Homeostasis in Mycobacterium tuberculosis: Mechanistic Insights into Siderophore-Mediated Iron Uptake. *J Bacteriol.* 198, 2399–409. doi: 10.1128/JB.00359-16

Szekely, R., and Cole, S. T. (2016). Mechanistic insight into mycobacterial MmpL protein function. *Mol. Microbiol.* 99, 831–834. doi: 10.1111/mmi.13306

Takemoto, K., Kawai, H., Kuwahara, T., Nishina, M., and Adachi, S. (1991). Metal concentrations in human lung tissue, with special reference to age, sex, cause of death, emphysema and contamination of lung tissue. *Int. Arch. Occup. Environ. Health* 62, 579–586. doi: 10.1007/BF00381111

Tullius, M. V., Harmston, C. A., Owens, C. P., Chim, N., Morse, R. P., Mcmath, L. M., et al. (2011). Discovery and characterization of a unique mycobacterial heme acquisition system. *Proc. Natl. Acad. Sci. U. S. A.* 108, 5051–5056. doi: 10.1073/pnas.1009516108

Viljoen, A., Dubois, V., Girard-Misguich, F., Blaise, M., Herrmann, J. L., and Kremer, L. (2017). The diverse family of MmpL transporters in mycobacteria: from regulation to antimicrobial developments. *Mol. Microbiol.* 104, 889–904. doi: 10.1111/mmi.13675

Virdi, R., Lowe, M. E., Norton, G. J., Dawrs, S. N., Hasan, N. A., Epperson, L. E., et al. (2021). Lower recovery of nontuberculous mycobacteria from outdoor Hawai'i environmental water biofilms compared to indoor samples. *Microorganisms* 9:224. doi: 10.3390/microorganisms9020224

Wells, R. M., Jones, C. M., Xi, Z., Speer, A., Danilchanka, O., Doornbos, K. S., et al. (2013). Discovery of a siderophore export system essential for virulence of *Mycobacterium tuberculosis*. *PLoS Pathog.* 9:e1003120. doi: 10.1371/journal.ppat.1003120

frontiers | Frontiers in Microbiology

TYPE Original Research
PUBLISHED 03 January 2024
DOI 10.3389/fmicb.2023.1301141

OPEN ACCESS

EDITED BY
Selvakumar Subbian,
Rutgers, The State University of New Jersey, United States

REVIEWED BY
Alfred Ankrah,
Korle Bu Teaching Hospital, Ghana
Jayne Hope,
University of Edinburgh, United Kingdom
Damien Portevin,
Swiss Tropical and Public Health Institute (Swiss TPH), Switzerland

*CORRESPONDENCE
Laura E. Via
✉ lvia@niaid.nih.gov
Decheng Wang
✉ dcwang99@163.com

†These authors have contributed equally to this work

‡Deceased

RECEIVED 24 September 2023
ACCEPTED 06 November 2023
PUBLISHED 03 January 2024

CITATION
Song L, Zhang D, Wang H, Xia X, Huang W, Gonzales J, Via LE and Wang D (2024) Automated quantitative assay of fibrosis characteristics in tuberculosis granulomas.
Front. Microbiol. 14:1301141.
doi: 10.3389/fmicb.2023.1301141

Automated quantitative assay of fibrosis characteristics in tuberculosis granulomas

Li Song[1,2,3,4†], Ding Zhang[1,2,3,4†], Hankun Wang[1,2,3,4†], Xuan Xia[1,2,3,4], Weifeng Huang[1,2,3,4‡], Jacqueline Gonzales[5], Laura E. Via[5,6*] and Decheng Wang[1,2,3,4*]

[1]The First College of Clinical Medical Science, China Three Gorges University, Yichang, China, [2]Yichang Central People's Hospital, Yichang, China, [3]Hubei Key Laboratory of Tumor Microenvironment and Immunotherapy, College of Basic Medical Sciences, China Three Gorges University, Yichang, China, [4]Institute of Infection and Inflammation, China Three Gorges University, Yichang, China, [5]Tuberculosis Research Section, Laboratory of Clinical Infectious Diseases, Division of Intramural Research, National Institute of Allergy and Infectious Diseases, National Institutes of Health, Bethesda, MD, United States, [6]Institute of Infectious Disease and Molecular Medicine, University of Cape Town, Cape Town, South Africa

Introduction: Granulomas, the pathological hallmark of *Mycobacterium tuberculosis* (*Mtb*) infection, are formed by different cell populations. Across various stages of tuberculosis conditions, most granulomas are classical caseous granulomas. They are composed of a necrotic center surrounded by multilayers of histocytes, with the outermost layer encircled by fibrosis. Although fibrosis characterizes the architecture of granulomas, little is known about the detailed parameters of fibrosis during this process.

Methods: In this study, samples were collected from patients with tuberculosis (spanning 16 organ types), and *Mtb*-infected marmosets and fibrotic collagen were characterized by second harmonic generation (SHG)/two-photon excited fluorescence (TPEF) microscopy using a stain-free, fully automated analysis program.

Results: Histopathological examination revealed that most granulomas share common features, including necrosis, solitary and compact structure, and especially the presence of multinuclear giant cells. Masson's trichrome staining showed that different granuloma types have varying degrees of fibrosis. SHG imaging uncovered a higher proportion (4%~13%) of aggregated collagens than of disseminated type collagens (2%~5%) in granulomas from matched tissues. Furthermore, most of the aggregated collagen presented as short and thick clusters (200~620 μm), unlike the long and thick (200~300 μm) disseminated collagens within the matched tissues. Matrix metalloproteinase-9, which is involved in fibrosis and granuloma formation, was strongly expressed in the granulomas in different tissues.

Discussion: Our data illustrated that different tuberculosis granulomas have some degree of fibrosis in which collagen strings are short and thick. Moreover, this study revealed that the SHG imaging program could contribute to uncovering the fibrosis characteristics of tuberculosis granulomas.

KEYWORDS

fibrosis, tuberculosis, granuloma, *Mycobacterium*, second harmonic generation (SHG)/two-photon excited fluorescence (TPEF)

1 Introduction

Granulomas, organized structures composed of various cells, are considered to be the hallmark lesion of tuberculosis (Adams, 1976; Barry et al., 2009; Silva Miranda et al., 2012; Shi et al., 2016). As physiologically isolated regions, granulomas were originally considered necessary for containing mycobacterial dissemination and infection (Adams, 1976); however,

understanding of the role of granulomas in mycobacterial infections has changed in light of accumulating reports with new views (Davis and Ramakrishnan, 2009; Russell et al., 2009; Gil et al., 2010; Ehlers and Schaible, 2012; Ramakrishnan, 2012; Cronan, 2022). Data from a *Mycobacterium marinum* (*Mm*)–larval zebrafish model system provided hints that granulomas may provide the mycobacteria with a nutrient microenvironment that "walls off" the bacteria from the host immune response, rather than simply containing them (Russell, 2007; Barry et al., 2009; Davis and Ramakrishnan, 2009; Ramakrishnan, 2012). To date, the full role of granulomas in the mycobacterial community remains enigmatic.

Three granuloma types can be found among humans and non-human primates (NHPs): classic caseous granulomas, fibrotic granulomas, and non-necrotizing granulomas (Barry et al., 2009). Conventional caseous granulomas, which have been extensively reported in active disease and latent conditions after mycobacterial infection, display a three-layered architecture: a necrotic center, viable cell areas, and an outer fibrotic rim (Adams, 1976; Russell, 2007; Barry et al., 2009; Silva Miranda et al., 2012). Because it is difficult to obtain biopsy samples from human lungs, animal models have been improved over the years to more closely duplicate the pathological progressions in humans, commonly applied in granuloma research. Mice are a practical animal model for the study of granuloma kinetics following infection with various mycobacterium species, even *Mm* (Carlsson et al., 2010). Importantly, although mice do not reproduce human tuberculosis pathology, especially the organized granulomas, mouse models have still been the most practical and widely used animal model for tuberculosis-related research, especially transgenic mouse models of chronic granulomatous disease that have normal granuloma formation and cytokine responses against *Mycobacterium avium* and *Schistosoma mansoni* eggs (North and Izzo, 1993; Iuvone et al., 1994; Kunkel et al., 1996; Segal et al., 1999; Jakubzick et al., 2002, 2004). By using an *Mm*–zebrafish infection system, Swaim et al. documented that zebrafish granulomas also undergo caseous necrosis, similar to human tuberculous granulomas, in which RD-defective *Mm*-induced granulomas are likely to be solitary, non-necrotizing, and loosely associated, unlike those in wildtype *Mm*-infected zebrafish (Swaim et al., 2006). To date, various animal models have been established and used to explore the mycobacterium–host interaction and the determinants of granuloma formation and development; these models have generated valuable information and improved our understanding of the host–pathogen relationship.

Fibrosis, a critical response to injury and/or inflammatory processes, is a pathophysiological consequence of chronic wound healing in which excess extracellular matrix is deposited (Diegelmann and Evans, 2004; Strieter, 2008). In an NHP model of *Mycobacterium tuberculosis* (*Mtb*) infection, granulomatous lesions were formed and surrounded by fibrillar collagens (DiFazio et al., 2016). Collagen, the most abundant mammalian protein, is not only the main component of connective tissues but it also provides the tensile strength of organs. This protein is extremely resistant to degradation but can be cleaved by matrix metalloproteinase (MMP). Interestingly, MMP-1 can degrade fibrillar collagens during *Mtb* infection, resulting in significant levels of collagen breakdown and alveolar destruction in lung granulomas (Elkington et al., 2011). MMP-9, which is homologous to MMP-1, can promote both the recruitment of macrophages to form nascent granulomas and bacterial growth (Volkman et al., 2010). Therefore, fibrosis and its associated factors play a crucial role in the immunopathology of granuloma formation.

There is an increasing need for the accurate assessment of fibrosis parameters in tuberculosis granulomas, such as the collagen content, geometric and textural features of collagen fibers, number of cross-linked collagen fibers, and physical appearance (thick or thin and short or long collagens). Unfortunately, there were few publications describing the fibrosis of tuberculosis granulomas in animal models by conventional Masson's trichrome staining (Swaim et al., 2006), until Warsinske et al. constructed a hybrid multi-scale model of fibrotic granuloma formation in 2017 and discovered the underlying mechanism that promoted fibrosis in *Mtb*-infected lungs (Warsinske et al., 2017). By combining the three-dimensional dynamics of molecular, cellular, and tissue scale data, Warsinske et al. described two types of fibrosis during granuloma formation: 1) peripherally fibrotic granuloma, with a cuff of collagen surrounding the granuloma, and 2) centrally fibrotic granuloma, with collagen throughout the granuloma. These findings inspired research to better understand the mechanisms of fibrosis dynamics and their clinical significance in granuloma formation following *Mtb* infection.

Stemming from the recent telecommunication boost, developments in highly sensitive optical lasers have made nonlinear optical microscopies, such as multiphoton excited fluorescence and multiharmonic generation, an affordable option for tissue imaging. Over the past decades, a new type of second harmonic generation/two-photon excited fluorescence (SHG/TPEF) microscopy, termed Genesis program, was initiated and developed to observe the morphological features of fibrosis-associated parameters in hepatitis and inflammation without staining (Tai et al., 2009; Xu et al., 2014; Wang et al., 2015, 2017; Liu et al., 2017). Second harmonic generation (SHG) microscopy is a novel tissue imaging system based on non-linear optical microscopy which enables observation of endogenous tissue signals such as Two-Photon Excitation Fluorescence (TPEF) and Second Harmonic Generation (SHG) in unstained tissue samples. TPEF provides visualization of the background tissue architecture while the SHG signal provides accurate identification of fibrillar collagen. Computerized algorithms based on SHG pattern recognition and logic modeling allow automated determination of the severity of fibrosis with the added advantage of objectivity, reproducibility and fast turnaround time. SHG exhibits intrinsic advantages over conventional staining and image capturing for collagen; as it is a nonlinear optical process that does not require staining, the image quality is more consistent than that of images obtained from stained slides, and this reproducibility is particularly useful for pathological assessment in multi-center clinical studies. SHG can be used for the quantitative measurement of collagen in various organs and tissues as an indication of fibrosis initiation and development during different conditions, including inflammation, infection, and cancer. Recently, the feasibility and effectiveness of using SHG microscopy for monitoring fibrosis in the liver has been established and demonstrated, particularly in patients with chronic hepatitis (Cox et al., 2003; Gorrell et al., 2003; Sun et al., 2008; Xu et al., 2014). Xu et al. demonstrated that SHG can improve fibrosis scoring accuracy in a hepatitis B virus-related animal model as well as in patients with hepatitis B; this allows for reproducible and reliable analyses of the efficacies of anti-fibrotic therapies in clinical research (Xu et al., 2014). Liu et al. employed an SHG evaluation system to assess the liver fibrosis induced by thioacetamide, carbon tetrachloride,

and bile duct ligation in rodent models and found that this system offers a reliable approach yielding impressive data for liver fibrosis studies that may be applicable for research of future anti-fibrotic drugs (Liu et al., 2017). Wang et al. used an SHG approach to assess hepatic fibrosis in nonalcoholic fatty liver disease (NAFLD) and demonstrated that SHG provides an accurate and reproducible method for evaluating fibrosis in NAFLD along a quantitative and continuous scale. However, although the application of SHG in liver fibrosis research is now common, the feasibility and effectiveness of applying the SHG system to the study of fibrosis of tuberculosis granulomas remain unknown.

In the present study, a set of 424 tissue samples from patients with tuberculosis, spanning 16 organ types, was collected and used to dissect the characteristics of granulomas from different organs. Masson's trichrome staining was performed to detect the distribution of collagen fibers in granulomatous lesions. Finally, an SHG automated system was applied in combination with SHG-associated parameters and mycobacterium-infected animal models, to evaluate the detailed characteristics of the collagen surrounding granulomas within granulomatous lesions. Our results may provide feasible approaches for improving the accuracy for quantitative analysis of the fibrotic setting surrounding granulomas during tuberculosis development, thus allowing for potentially reproducible and reliable research on anti-fibrotic therapies for tuberculosis.

2 Materials and methods

2.1 Sample collection

This study collected 1,070 samples from patients diagnosed with tuberculosis who came from The First People's Hospital of Yichang during the period from January 2012 to December 2017. After selection according to inclusion criteria and exclusion criteria, 424 samples with contact information from patients were chosen in this study (Figure 1). Inclusion criteria are as follows: patients who consented and were clinically stable for biopsies to be performed, and at least one tissue could be provided. This clinical patient must be diagnosed according to *WHO Treatment of tuberculosis: guidelines-4th* edition. WHO/HTM/TB/2009.420 (https://apps.who.int./iris/bitstream/handle/10665/44165/9789241547833_eng.pdf). Exclusion criteria are as follows: subjects had been negative according to pathological biopsy; comorbidity with carcinoma; repeated biopsy; unknown organ typing; basic information of patients is missing.

Clinical signs and pathological characteristics were obtained from the patient's medical records (Table 1). In total, samples spanning 16 types of tissues were collected from 424 cases (Table 2); 80 of these samples were selected randomly for continuous study according to tissue classification (Table 2).

The formalin-fixed, paraffin-embedded biopsy samples were acquired from the First People's Hospital of Yichang. This study was approved by the Ethical Review Committees of the First People's Hospital of Yichang and was conducted in accordance with the local legislation and institutional requirements. The paraffin-embedded lung tissues of *Mtb* aerosol-infected marmosets in this study were acquired from the Tuberculosis Research Section, National Institute of Allergy and Infectious Diseases (Via et al., 2015). The original animal experiment was approved by the NIAID Animal Care and Use Committee approved the experiments described herein under protocol LCID-9 (permit issued to NIH as A-4149-01) (Via et al., 2015). The study was conducted in accordance with the local legislation and institutional requirements. *Schistosoma japonicum*-infected specific pathogen-free C57BL/6 mice were established and their livers were sampled for subsequent study as previously described (Wan et al., 2017).

2.2 Masson's trichrome staining

Masson's trichrome staining was performed at the Department of Pathology, Yichang Central People's Hospital, as follows. First, 5-μm sections were prepared, deparaffinized, and hydrated in distilled water. Bouin's fixative was then used as a mordant at 56°C for 1 h. The formalin-fixed, paraffin-embedded sections were cooled and washed in running water until the yellow coloring disappeared. The samples were stained in Weigert's hematoxylin stain for 10 min, thoroughly washed in tap water for 10 min, stained again in an acid fuchsin solution for 15 min, and rinsed in distilled water for 3 min. After rinsing, the slides were treated with phosphomolybdic acid solution for 10 min and then rinsed in distilled water for 10 min. Finally, slides were stained with a light-green solution for 2 min and rinsed in distilled water. After thorough dehydration using alcohol, the slides were mounted, and coverslips were placed onto them. The intensity of fibrosis-positive staining in human and animal tissues was quantified in 25 microscopy fields of view (40× magnification), and the means were calculated. Images of all sections were unbiasedly captured under an Olympus BX63 microscope by a single investigator. The results are expressed as fibrosis area density (area of positives/area of whole field).

2.3 SHG image acquisition system and quantification analysis

Images of unstained sections of tissue samples were acquired automatically by using the Genesis system (Hangzhou HistoIndex Ltd., Hangzhou, China) in which SHG microscopy was applied for visualizing collagen, and other cell structures were visualized with TPEF microscopy. The images were acquired at a fixed magnification with 512 × 512-pixel resolution, and each image had a dimension of 200 μm^2 × 200 μm^2. Ten five-by-five images were acquired for each sample to image most of each sample area, with a final image size of 10 mm^2. Details of the optical parameters and settings were optimized based on established protocols (Tai et al., 2009; Xu et al., 2014; Wang et al., 2015; Liu et al., 2017).

The total content of collagen and previously described collagen features, including specific collagen strings and collagen connectivity-related measurements, were examined for correlations with the granuloma fibrosis scores. Nineteen morphological features were used in this study (detail seen in Supplementary Table 1). These variable parameters were divided into three groups, as follows:

Group 1: Collagen percentage of the total area (SHG), the aggregated collagen percentage of the total area (AGG), and the distributed collagen percentage of the total area (DIS). The total collagen level was detected by SHG and segmented from the raw images. The aggregated and distributed collagens were differentiated from one another with a low-pass filter.

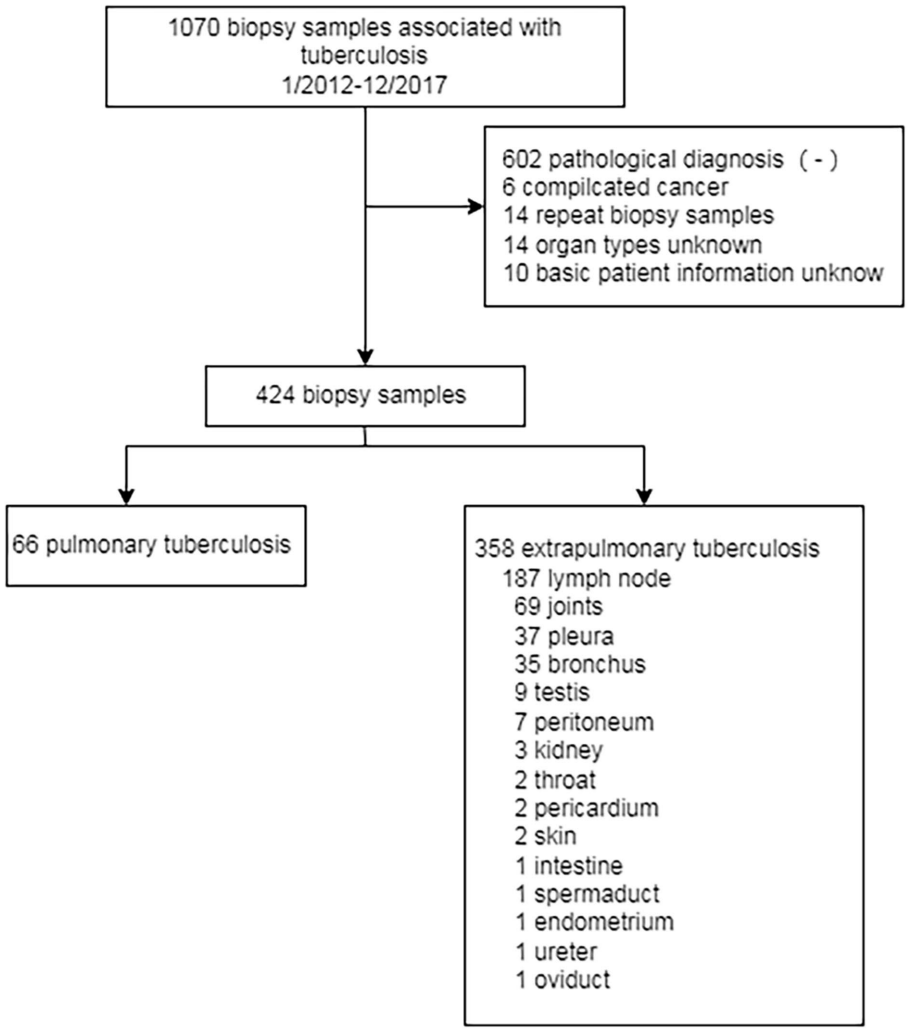

FIGURE 1
The flow chart of the designed study. 1,070 biospy have been collected from patient with clinical tuberculosis from 2012 to 2017. Only 424 samples have been chosen in this study. 66 samples belong to pulmonary tuberculosis while 358 sample belong to extrapulmonary tuberculosis.

Group 2: Collagen string number (NoStr), short collagen string number (NoShortStr), long collagen string number (NoLongStr), thin collagen string number (NoThinStr), thick collagen string number (NoThickStr), total string area (StrArea), total string length (StrLength), total string width (StrWidth), total string perimeter (StrPerimeter), and total crosslink number (NoXlink). The collagen strings were detected using a connected-component algorithm of binary images from previous image segmentation. Each connected component was fitted with an ellipse, and then the axes of the ellipses were used to divide the strings into long and short as well as thin and thick subgroups. The total lengths, widths, areas, and perimeters of the collagen strings were also measured. We used an image skeleton algorithm to detect branch points for determining the crosslink number.

Group 3: Ratio between the short string and total string numbers (NoShortStr/NoStr), ratio between the long string and total string numbers (NoLongStr/NoStr), ratio between the short string and long string numbers (NoShortStr/NoLongStr), ratio between the thin string and total string numbers (NoThinStr/NoStr), ratio between the thick string and total string numbers (NoThickStr/NoStr), and the ratio between the thin string and thick string numbers (NoThinStr/NoThickStr). We found that these relative ratios improved the system only when absolute (normalized) values were used for Group 2.

2.4 Immunohistochemistry staining

Measurement of MMP-9 levels in matched samples was performed by using immunohistochemistry staining and analysis based on established protocols (Wang et al., 2012). For all tissue samples, 5-μm serial paraffin sections were prepared by using the same protocol. First, the sections were immersed in xylol three times for 5 min each to remove paraffin, after which they were hydrated via five consecutive washings with alcohol (100, 100, 95, 80, and 70%, respectively). Second, the sections were immersed in citrate buffer solution (0.01 M, pH 6.0) and heated at 120°C in an autoclave sterilizer for 10 min,

TABLE 1 Demographical information of clinical TB patients.

Basic information	Classification	Amount (percentage, %)
Gender	Male	201(47.4%)
	Female	223(52.6%)
Age	<20	33(7.8%)
	20–39	161(38.0%)
	40–59	146(34.4%)
	60–79	78(18.4%)
	≥80	6(1.4%)
History of previous TB	Yes	24(5.6%)
	No	95(22.4%)
	Unkonwn	305(72%)
TB antibody test	Positive	4(1%)
	Negative	41(9.7%)
	Uncheck	68(16%)
	Unkonwn	311(73.3%)
TB protein chip	Positive	3(0.7%)
	Negative	13(3.1%)
	Uncheck	96(22.6%)
	Unkonwn	312(73.6%)
Interferon-γ release assays of A.TB test	Positive	3(0.7%)
	Negative	7(1.7%)
	Uncheck	101(23.8%)
	Unkonwn	313(73.8%)
Sputum smear	Positive	5(1.2%)
	Negative	32(7.5%)
	Uncheck	81(19.1%)
	Unkonwn	306(72.2%)
PPD test	Positive	6(1.4%)
	Negative	0(0)
	Uncheck	104(24.5%)
	Unkonwn	314(74.1%)

TB, tuberculosis.

naturally cooled for 30 min, then immersed in 3% aqueous hydrogen peroxide for endogenous peroxidase ablation at room temperature for 30 min. The following steps were performed in a moist chamber. The sections were incubated with blocking buffer (Zymed Laboratories Inc., San Diego, CA, USA) containing 20% normal donor bovine serum and 80% phosphate-buffered saline (0.01 M, pH 7.4) at room temperature for 30 min. The bovine serum was then discarded, and the sections were incubated with an optimized dilution of primary antibody anti-MMP-9 (ab38898) at 4°C overnight. The intensity of MMP-9-positive staining in human and animal tissues was quantified in 25 microscopy fields of view (40× magnification), and the means were calculated. Images of all sections were unbiasedly captured under an Olympus BX63 microscope by a single investigator. The area density of MMP-9 positives in the human and animal samples was measured by using an cellSens system (Olympus Co. Ltd., Japan) as previously described (Wang et al., 2012). The results are expressed as MMP-9 area density (area of positives/area of whole field).

TABLE 2 Demographical characterization of clinical TB patients.

Tissue category	Sample size (*n*, %)
Lymph node	187(44.1%)
Joints	69 (16.3%)
Lung	66 (15.6%)
Pleura	37 (8.7%)
Bronchus	35 (8.3%)
Testis	9 (2.1%)
Peritoneum	7 (1.7%)
Kidney	3 (0.7%)
Throat	2 (0.5%)
Pericardium	2 (0.5%)
Skin	2 (0.5%)
Intestine	1 (0.2%)
Spermaduct	1 (0.2%)
Endometrium	1 (0.2%)
Ureter	1 (0.2%)
Oviduct	1 (0.2%)

3 Results

3.1 Caseous necrosis and multinuclear giant cells were common features of human tuberculosis granulomas

The most common granuloma form observed in our human tuberculosis patient samples was caseous granuloma. Moreover, multinucleated giant cells in tuberculosis granulomas, also known as Langham giant cells, are typical cells in TB, and have a great significance for the development and diagnosis of TB (Silva Miranda et al., 2012; Brooks et al., 2019). For the 16 different tissue types examined, caseous necrosis was detected in all the human tuberculosis samples. Additionally, typical multinuclear giant cells were also observed in most clinical tuberculosis patient samples, excluding the oviduct, endometrium and bronchus samples (Figure 2); however, no multinuclear giant cells were seen in the samples from *Mtb*-infected marmosets (Figure 2). Moreover, the examined granulomas in both human and animal samples exhibited a variety of structures and morphologies, including compact and loose, necrotic and non-necrotic, multicentric and solitary (Figure 2). With Ziehl-Neelsen (ZN) staining, we observed red, rod bacteria distributed in some tuberculosis patient tissues, including the skin, bronchus, and throat. In samples from *Mtb*-infected animals, ZN-positive bacteria were detected in the lungs of marmosets (Supplementary Figure 1). In *S. japonicum*-infected mice, we found diffused necrosis of hepatocytes and egg-encased granulomatous lesions (Figure 2). This result demonstrates the special significance of multinuclear giant cells for clinical human tuberculosis granuloma formation and development, which should be further investigated in future studies.

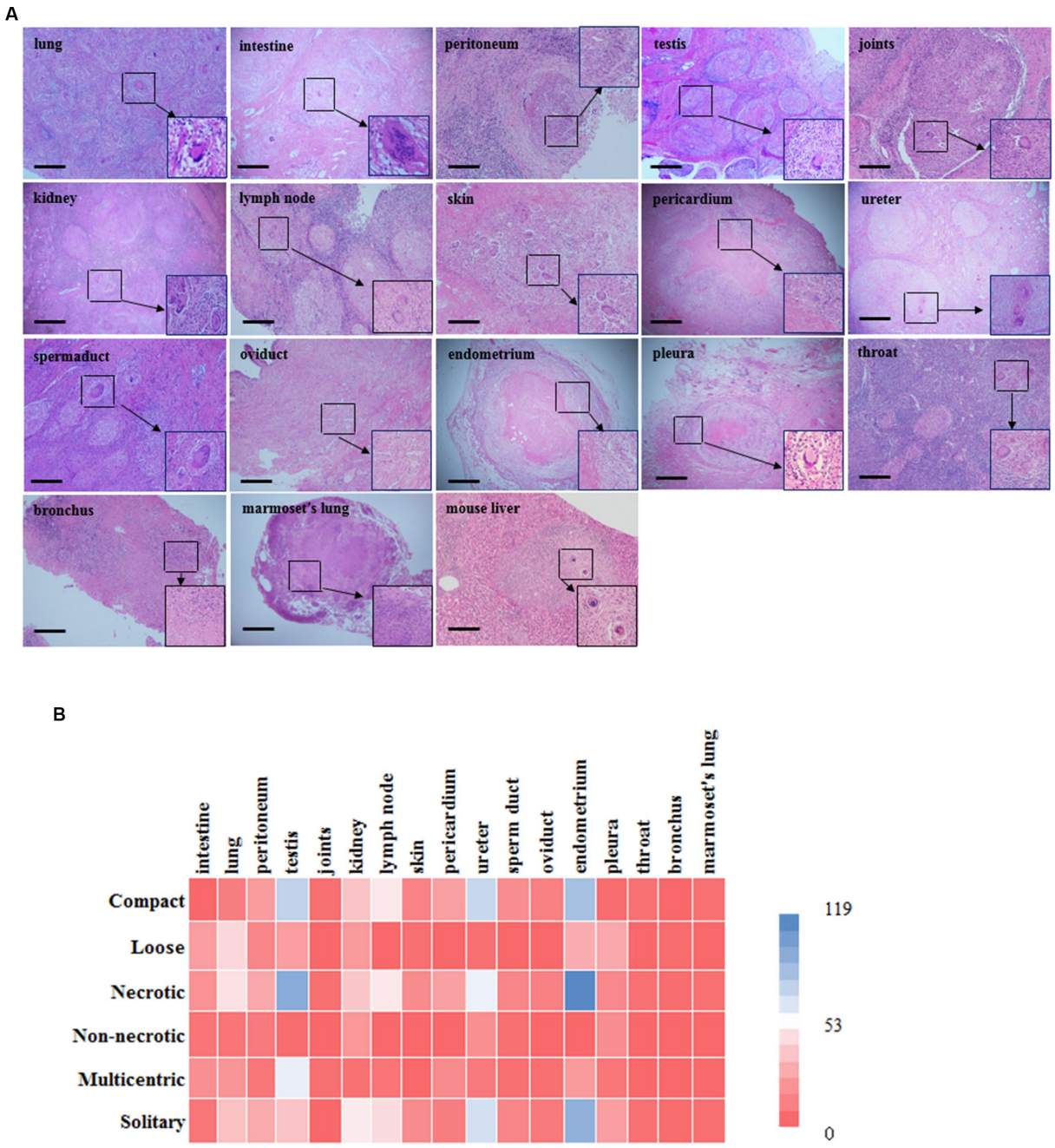

FIGURE 2
Histopathology examination and characteristics of granulomatous lesions among different organs. **(A)** There is morphology of different granulomas from tissues in human and marmoset by H & E staining. Typical multinuclear giant cells were formed in most human tuberculosis samples excluding the oviduct, endometrium and bronchus (scale bar = 500 μm). However, there were none of characterized multinuclear giant cells formed in *Mtb*-infected marmosets; **(B)** A heat map is shown in the figure. Color bar labelled with number (0 ~ 119) is granuloma counting under microscopy by pathologist. Overall, tuberculosis granulomas are mostly necrotic and solitary granulomas, and structurally they are mostly compact. Among them, necrotic granulomas are mainly seen in the testis and endometrium, while non-necrotic granulomas are mainly seen in the kidney and ureter; The main types of multicentric granulomas include the testis and intestine, while those solitary granulomas include the endometrium and ureter; Granuloma has a relatively compact structure in the testis and endometrium, while loose structures in the lung and pleura. Mouse: C57BL/6 J.

3.2 Masson's trichrome staining reveals fibrosis surrounding the granulomas

Masson's trichrome staining revealed the typical presence of blue fibers distributed within and surrounding the granulomas in tuberculosis patient tissues, especially in the intestine, lung, peritoneum, testis, joint, kidney, lymph node, skin, pericardium, ureter, sperm duct, oviduct, endometrium, pleura, throat and bronchus (Figure 3A). In *Mtb*-infected animal tissues, Masson's staining revealed that a fibrotic-ring surrounded the granulomas, with fibers clearly surrounding the granulomas in marmoset tissues (Figure 3A). In *S. japonicum*-infected murine livers, the blue-stained collagen mostly surrounded egg-encased granulomatous lesions (Figure 3A).

3.3 SHG image acquisition system

In the SHG image acquisition system, a green region shows the SHG labeling that indicates a fibrotic signal. In multiple tissues of patients with tuberculosis, higher levels of SHG labeling were observed in the intestine, lung, testis, joints, skin, kidney, skin, ureter, oviduct, throat, and pleura (Figure 4). Amazingly, most of the green-stained collagen were distributed directly around the granulomatous lesions (Figure 4). In *Mtb*-infected marmoset lungs, the positive SHG signals were concentrated in the area surrounding the granuloma (Figure 4). The shared parameters of the SHG system, including Agg, Dis, NoShortStr NoLongStr, NoThinStr, NoThickStr, were obtained automatically by the Genesis software system (Figure 5; Supplementary Table 1). Aggregated collagen formed the

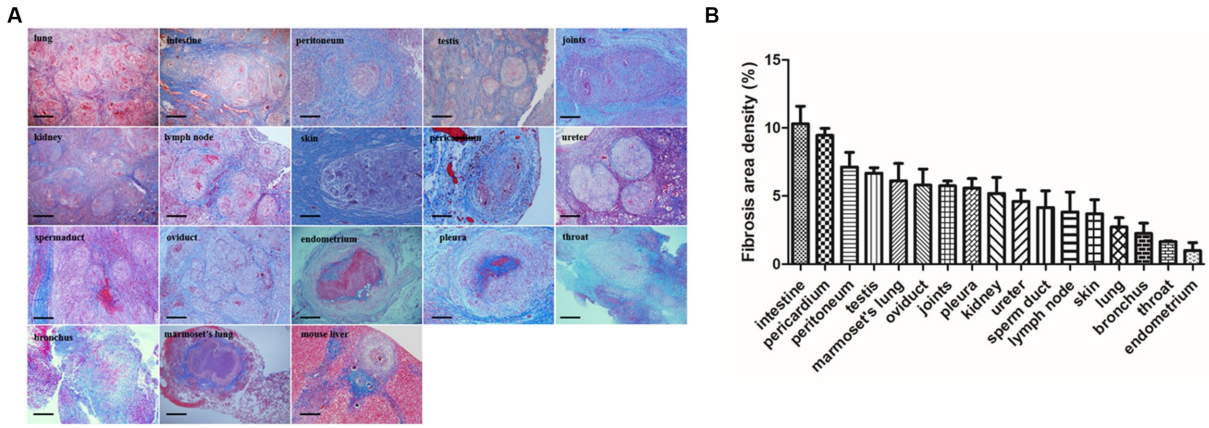

FIGURE 3
Fibrosis area of granulomas from tissure in clinical TB and MTB-infected marmoset's lung. **(A)** Masson's trichrome staining for fibrosis in clinical TB patients and animal tissues. Masson's trichrome staining revealed fibrosis surrounded the granulomas in most human TB patient tissues as well as in *Mtb*-infected marmoset lungs (scale bar bar = 500 μm). **(B)** The density of fibrosis-positive staining in human and animal tissues was quantified and the means were calculated. The results are expressed as fibrosis area density (area of positives/area of whole field).

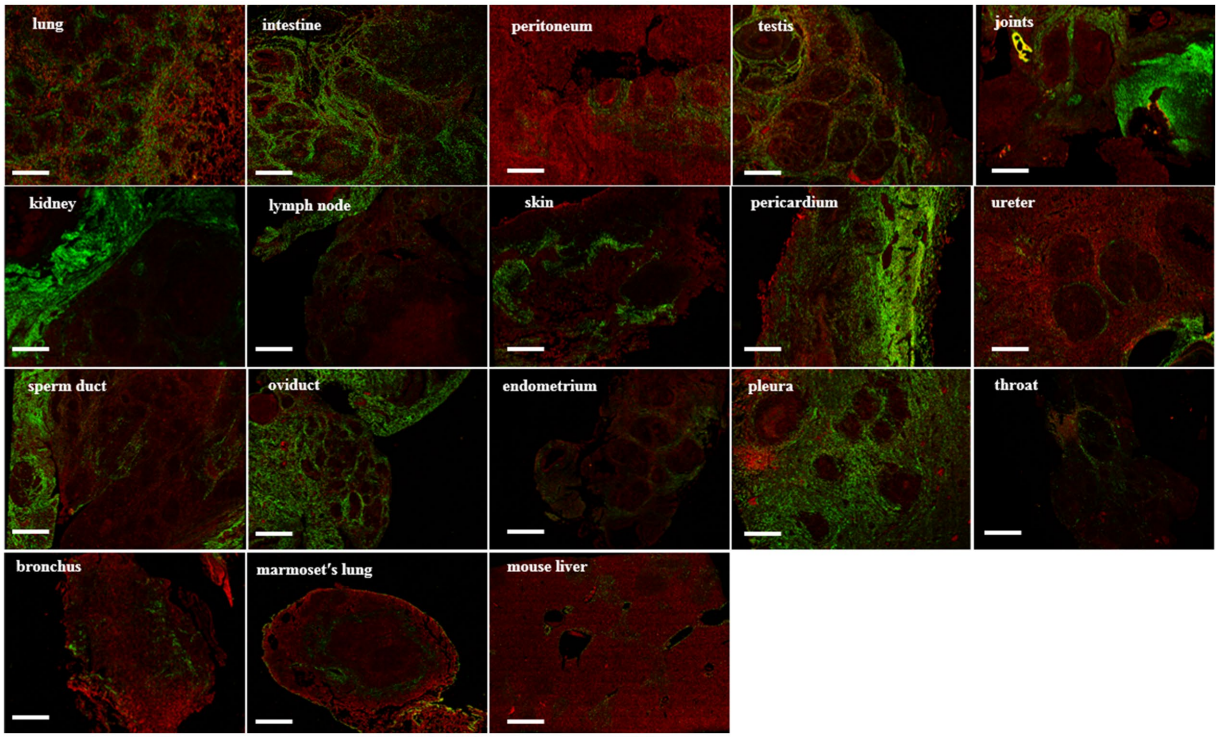

FIGURE 4
SHG image visualization for fibrosis in tuberculosis human and animal tissues. Green areas represent the collagen under SHG microscope system, while red areas represent the tissue under SHG detection. Scale bar = 500 μm.

major component of collagen in each tissue, with the Agg content being higher than that of distributed collagen within each sample (Figure 5). Moreover, the featured forms of collagenous fiber typically presented as short and thick in all examined tissues (Figure 5).

3.4 Comparison of fibrosis detection between Masson's trichrome staining and genesis SHG analysis

Data from the Genesis SHG automated image acquisition system indicate that the featured collagen was distributed peripherally around the granulomas in human tuberculosis tissues including the intestine, lung, peritoneum, and testis. This finding is not only in agreement with the fibrosis signal distribution detected by Masson's trichrome staining, but it also matches the known production and distribution of collagens among those tissues (Figure 6). Regarding validation of fibrosis detection in *Mtb*-infected marmoset lungs, the Genesis image analysis demonstrated that collagens directly surround the granuloma (Figure 6). Our results indicate that the SHG image system, an unstained approach, could improve the accuracy of collagen research and be used to describe the fibrosis surrounding granulomas induced by mycobacterial infection.

3.5 MMP-9 expression in various tissue-associated granulomas

MMP-9 is considered to be a critical factor involved in granuloma formation during mycobacterial infection (Ramakrishnan, 2012). Elevated MMP-9 expression is a featured characteristic in idiopathic pulmonary fibrosis, and MMP-9 inhibition was reported to ameliorate pulmonary fibrosis in a humanized immuno-deficient mouse model of idiopathic pulmonary fibrosis (Espindola et al., 2020). In a murine chronic pulmonary granulomatous fibrosis model combined elicited by multiwall carbon nanotube (MWCNT) and mycobacterial ESAT-6 (early secreted antigenic target protein 6), the mice showed exacerbated pulmonary fibrosis and granulomatous pathology and MMP-9 was sharply elevated during this process (Malur et al., 2019). MMP-9-deficiency mice led to reduced peribronchial fibrosis in an allergen-challenged fibrosis model and airway remodeling (Lim et al., 2006). Moreover, MMP-9 activity is actively involved in liver fibrosis (Lachowski et al., 2019) and bleomycin-induced pulmonary fibrosis (Li et al., 2019). In particular, a recent report revealed that MMP-1(-1607G), a member of MMP-9, and its polymorphism could act as a risk factor for fibrosis after pulmonary tuberculosis in Taiwan (Wang et al., 2010). Our results demonstrated that MMP-9 was extensively distributed in various tissue-associated granulomas (Figure 7), implying that MMP-9 was involved in the fibrosis of

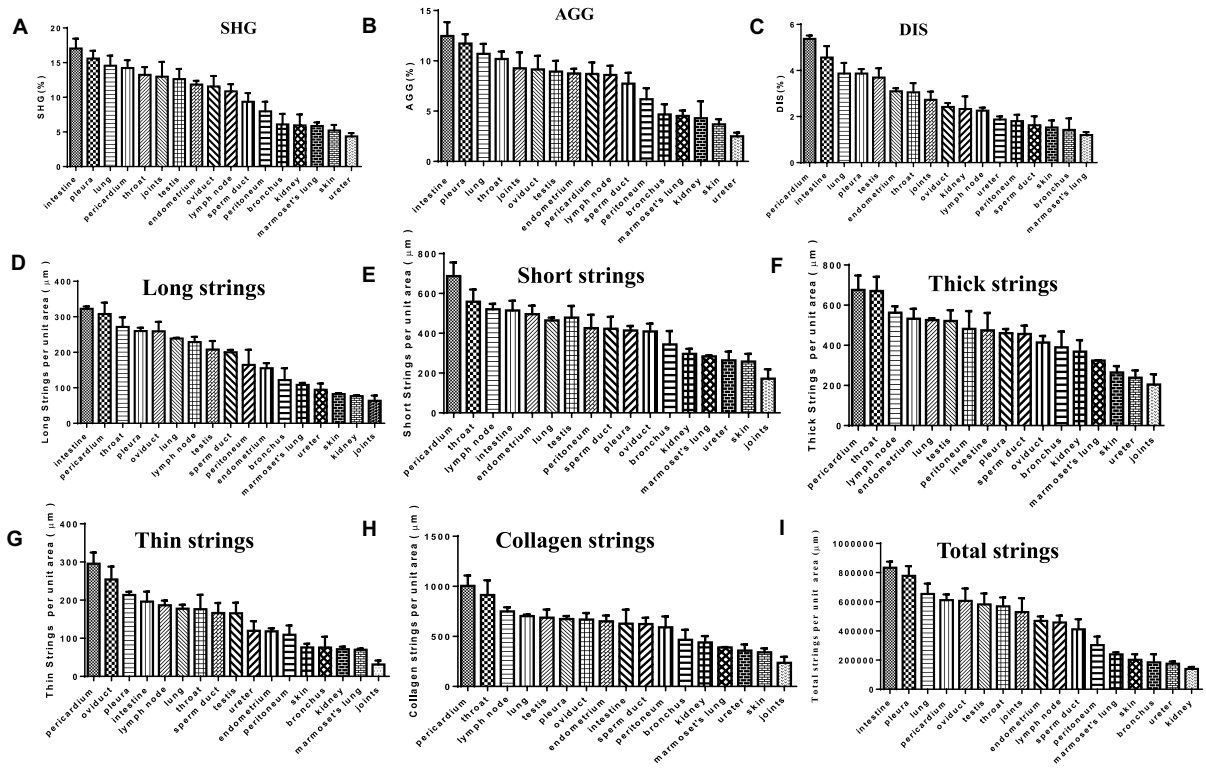

FIGURE 5
SHG image visualization for fibrosis in TB patients and animal tissues. **(A)** SHG (second harmonic generation): area percentage, indicating the proportion of collagen in the tissue; **(B)** AGG (aggregated Collagen Percentage): area percentage, indicating the proportion of aggregated collagen in the tissue; **(C)** DIS (Distributed Collagen): area percentage, indicating the proportion of aggregated distributed collagen in the tissue; **(D)** Long strings: number of long strings per unit tissue area; **(E)** Short strings: number of short strings per unit tissue area; **(F)** Thick strings: number of thick strings per unit tissue area; **(G)** Thin Strings: number of thin strings per unit tissue area; **(H)** Collagen strings: number of total strings above per unit tissue area; **(I)** Total strings: area of total strings per unit tissue area.

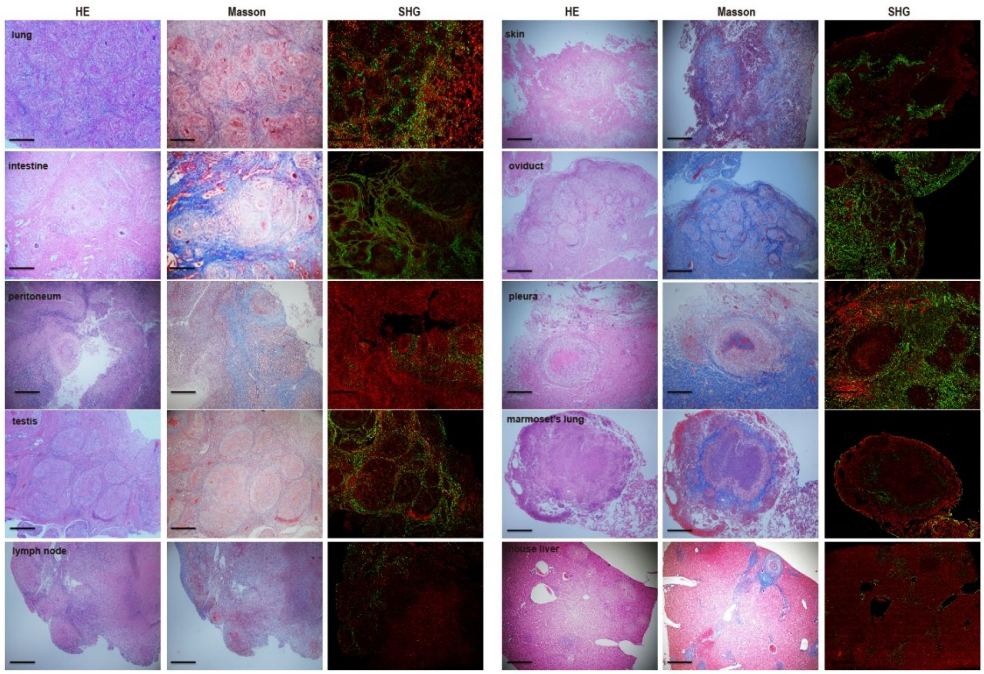

FIGURE 6
Comparison and consistency of fibrosis between Masson's trichrome staining and Genesis SHG analysis. Each set of samples are parallel sections of the same tissue. The SHG analysis is in agreement with the distribution of collagens detected by Masson's trichrome staining. There was a highly fitness for fibrosis detection of those two approaches and SHG analysis displayed powerful capacity for fibrosis examination in TB patients as well as *Mtb*-infected marmosets. Scale bar = 500 μm.

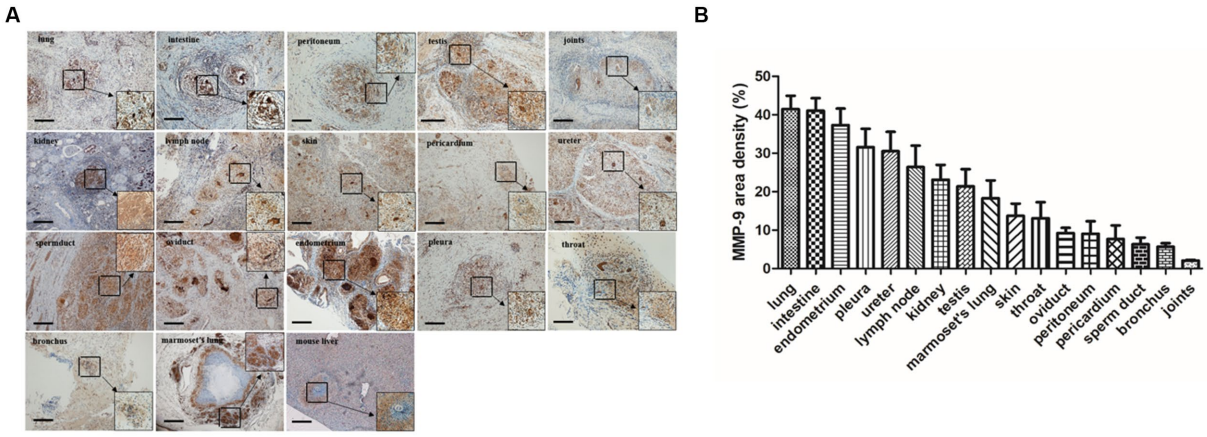

FIGURE 7
MMP-9 staining and distribution in granulomatous lesions from different tissues. **(A)** Immunohistochemistry staining demonstrated that MMP-9 was extensively distributed in various tuberculosis-associated granulomas including TB patients and marmoset tissues (scale bar = 500 μm). **(B)** The area density of MMP-9 positives in different tissues was quantified and the means were calculated. The results are expressed as MMP-9 area density (area of positives/area of whole field).

tuberculosis-associated granulomas including tuberculosis patient's tissues and marmoset model, which highlights the critical role of MMP-9 in the process of granulomatous fibrosis.

4 Discussion

In this study, we gathered samples spanning 16 organ types from a group of patients who presented with clinical tuberculosis and samples of *Mtb*-infected animal lung tissue to study granuloma characteristics and fibrosis-related parameters. We first applied Masson's trichrome staining to describe the collagen distribution and content. The SHG system was then employed and successfully used to acquire collagen images and quantitative indices of the 16 organ samples from clinical tuberculosis cases. This is the first time to apply SHG microscopy as an unstained and automated system of evaluation and detection of the collagen content and its related parameters in tuberculosis granuloma fibrosis.

When we checked the fibrosis in granulomas by using Masson's trichrome staining, we observed many collagen proteins distributed

around the granulomas in most tissues from human tuberculosis cases. We subsequently confirmed the feasibility of applying the SHG microscopy system to determine the fibrosis characteristics across 16 organ types sampled from patients with tuberculosis and *Mtb*-infected model animals. Finally, we analyzed the consistency between the SHG system and the conventional histopathological technique for studying fibrosis in tuberculosis granulomas and demonstrated that the use of the unstained approach could improve the visualization and digitalization of collagen within granulomatous areas.

In the 16 organ-type samples from human patients with tuberculosis, we found that caseous necrosis was observed overwhelmingly. Multinucleated giant cells, also termed Langham giant cells, are considered as an informative feature for tuberculosis especially have a important role in the TB processes (Silva Miranda et al., 2012; Brooks et al., 2019). In the present study, typical multinuclear giant cells were also observed in most samples, excluding the oviduct, endometrium and bronchus tissue. This finding suggests that multinuclear giant cells could have special significance for the pathological diagnosis of tuberculosis. Previous studies have demonstrated that *Mtb* infection stimulated the production of profibrotic mediators, including TGF-β and collagen, that subsequently mediated granuloma formation (Wang et al., 2011; Vanden Driessche et al., 2013). Additionally, fibrosis has been documented after *Mtb* infection and was shown to be involved in granuloma formation (Dye and Williams, 2010). Moreover, the granulomas from tuberculosis cases examined in the present study exhibited a variety of structures and morphologies, including compact and loose, necrotic and non-necrotic, multi-centric, and solitary. According to the conventional Masson's staining results, almost all the human tuberculosis samples displayed blue collagen surrounding the granuloma, as did the *Mtb*-infected marmoset lung samples; these findings suggest that fibrosis is involved in the formation of granulomas during tuberculosis development.

To analyze the dynamics and parameters of the collagen involved in granuloma formation, we applied an innovative imaging system that was previously developed and has been widely used as a liver fibrosis assay in animal models and chronic hepatitis patients. SHG and TPEF microscopy, a computer-assisted, fully automated, staining-free method for fibrosis assessment, was employed to assess fibrillar collagen development by using eleven shared parameters for both the early and later stages of liver fibrosis. This method has been previously used to provide quantitative scores incorporating histopathological features of liver fibrosis and facilitate the staging and evaluation of clinical research and management of liver-associated diseases (Denk et al., 1990; Cox et al., 2003; Gorrell et al., 2003; Sun et al., 2008; Tai et al., 2009; Xu et al., 2014; Wang et al., 2015, 2017; Liu et al., 2017). Little is known regarding the fibrosis in tuberculosis granulomas, and data obtained from *Mtb*-infected animals is just beginning to reveal some details. Recently, Warsinske's group developed a hybrid multi-scale agent-based model to uncover novel critical players and mechanisms driving the formation and development of granuloma-associated fibrosis in *Mtb*-infected animals (Warsinske et al., 2017). Although their findings demonstrate the presence of multiphase mediators in the formation of complicated granuloma structures and morphologies, additional detailed information about fibrosis and its critical parameters still needs to be determined.

With the application of the Genesis program, eleven shared parameters were captured by an automated system, and they revealed that aggregated collagen was the major component in all examined tissue of patients with tuberculosis and *Mtb*-infected marmoset's lung. Aggregated collagen was reported to surround the granulomatous lesions in severe pulmonary acariasis in a Japanese macaque model (Hiraoka et al., 2001). Although collagen has been reported to play a role in tissue remodeling and granuloma formation during *Mtb* infection (Dye and Williams, 2010; Vanden Driessche et al., 2013), the type of collagen involved in granulomatous lesions was unclear. Our data reveal that aggregated collagen plays an essential role in granuloma formation in both clinical tuberculosis and *Mtb*-infected animals. Furthermore, during granuloma formation, the fasciculus of those aggregated collagens was short and thick in shape.

Several cytokines, such as TNF-α, TGF-β, and MMP-9, are critical for granuloma formation following *Mtb* infection (Iliopoulos et al., 2006; Taylor et al., 2006; Barry et al., 2009; Mootoo et al., 2009; Beham et al., 2011; Fallahi-Sichani et al., 2011; Ramakrishnan, 2012; Roh et al., 2013; Shmarina et al., 2013; Al Shammari et al., 2015; Datta et al., 2015; Ordonez et al., 2016; Warsinske et al., 2017; Walton et al., 2018). Here, we further characterized the profile of those cytokines in clinical tuberculosis human and *Mtb*-infected model animal tissues and found that MMP-9 was highly expressed. MMP-9 is upregulated in the pleural fluid of tuberculous cases and correlated with granulomatous development (Sheen et al., 2009). Furthermore, this cytokine, which is produced by epithelial cells that neighbor *Mtb*-infected macrophages to facilitate macrophage recruitment to the nascent granuloma, also promotes bacterial growth (Volkman et al., 2010). Our data found extensive up-regulation of MMP-9 in various tuberculosis-associated granulomas and demonstrated the significance of MMP-9 in granulomatous fibrosis. Understanding the complicated architecture of all granuloma aspects is critical for developing innovative immunotherapy and medications. Fibrosis aids granuloma formation and contributes to the isolated architecture that is seen in many clinical tuberculosis cases and *Mtb*-infected animal models. Our research reveals that aggregated collagen is the major player involved in granulomatous fibrosis and that most of those aggregated collagens were short and thick in shape.

In summary, the present study first provided insight into the fibrosis dynamics of tuberculosis granulomas by applying an automated quantitative approach, and its results may provide useful insight for developing effective strategies to improve the treatment strategies of tuberculosis and patient outcomes. To the best of our knowledge, although it is the first report that second harmonic generation (SHG)/two-photon excited fluorescence (TPEF) microscopy to determine the fibrosis of tuberculosis-associated granulomas, there are also some limitations in this study. Firstly, due to the influence of anti-tuberculosis treatment, clinical specimen collection time, tissue preservation mode, specimen number and other factors, the results of the study may have certain limitations. Secondly, this study has a preliminary understanding of the fibrotic components of tuberculosis granuloma, but how to

use the obtained fibrosis characteristic parameters to provide a basis for the clinical diagnosis and treatment of tuberculosis still needs a lot of clinical research in the future. Finally, due to the complex pathophysiology and functional state of tuberculosis granuloma, the role of various cytokines in the development of tuberculosis is also very complex, and its specific role and mechanism need to be further studied.

Data availability statement

The raw data supporting the conclusions of this article will be made available by the authors, without undue reservation.

Ethics statement

The studies involving humans were approved by the Ethical Review Committees of the First People's Hospital of Yichang. The studies were conducted in accordance with the local legislation and institutional requirements. The human samples used in this study were acquired from the formalin-fixed, paraffin-embedded samples were acquired from the First People's Hospital of Yichang. Written informed consent for participation was not required from the participants or the participants' legal guardians/next of kin in accordance with the national legislation and institutional requirements. The animal study was approved by paraffin-embedded lung tissues of *Mtb* aerosol-infected marmosets in this study were acquired from the Tuberculosis Research Section, National Institute of Allergy and Infectious Diseases (Via et al., 2015). The original animal experiment was approved by the NIAID Animal Care and Use Committee approved the experiments described herein under protocol LCID-9 (permit issued to NIH as A-4149-01). The study was conducted in accordance with the local legislation and institutional requirements.

Author contributions

LS: Data curation, Formal analysis, Methodology, Project administration, Resources, Software, Writing – original draft. DZ: Writing – original draft, Methodology, Data curation, Investigation. HW: Data curation, Formal analysis, Investigation, Project administration, Software, Writing – original draft. XX: Data curation, Formal analysis, Investigation, Visualization, Writing – original draft. WH: Conceptualization, Data curation, Investigation, Methodology, Writing – original draft. JG: Project administration, Resources, Writing – original draft. LV: Conceptualization, Investigation, Project administration, Resources, Writing – original draft. DW: Conceptualization, Formal analysis, Funding acquisition, Investigation, Resources, Supervision, Validation, Visualization, Writing – original draft.

In Memoriam

This article is dedicated to the memory of our beloved Dr. Weifeng Huang who passed away during the preparation and writing of this manuscript.

Funding

The author(s) declare financial support was received for the research, authorship, and/or publication of this article. This work was supported in part by the National Natural Science Foundation of China (Grant nos. 31772709 and 31572485 to DW), the Construction and Clinical Practice of Standardized Nursing Plan for Spinal Tuberculosis during Perioperative Period, Yichang Medical and Health Science and Technology Project (A21-2-023 to LS), the new faculty startup research fund of China Three Gorges University (KJ2014B023 to DW), and in part by the intramural research program of NIAID, NIH (Bethesda MD, United States).

Acknowledgments

DW is a special volunteer trainee of the Tuberculosis Research Section, LCIM, NIAID of National Institutes of Health (USA). We thank Katie Oakley, PhD, from Liwen Bianji, Edanz Editing China (www.liwenbianji.cn/ac), for editing the English text of a draft of this manuscript.

Conflict of interest

The authors declare that the research was conducted in the absence of any commercial or financial relationships that could be construed as a potential conflict of interest.

Publisher's note

Supplementary material

The Supplementary material for this article can be found online at: https://www.frontiersin.org/articles/10.3389/fmicb.2023.1301141/full#supplementary-material

References

Adams, D. O. (1976). The granulomatous inflammatory response. A review. *Am. J. Pathol.* 84, 164–192.

Al Shammari, B., Shiomi, T., Tezera, L., Bielecka, M. K., Workman, V., Sathyamoorthy, T., et al. (2015). The extracellular matrix regulates granuloma necrosis in tuberculosis. *J. Infect. Dis.* 212, 463–473. doi: 10.1093/infdis/jiv076

Barry, C. E. 3rd, Boshoff, H. I., Dartois, V., Dick, T., Ehrt, S., Flynn, J., et al. (2009). The spectrum of latent tuberculosis: rethinking the biology and intervention strategies. *Nat. Rev. Microbiol.* 7, 845–855. doi: 10.1038/nrmicro2236

Beham, A. W., Puellmann, K., Laird, R., Fuchs, T., Streich, R., Breysach, C., et al. (2011). A TNF-regulated recombinatorial macrophage immune receptor implicated in

granuloma formation in tuberculosis. *PLoS Pathog.* 7:e1002375. doi: 10.1371/journal.ppat.1002375

Brooks, P. J., Glogauer, M., and McCulloch, C. A. (2019). An overview of the derivation and function of multinucleated giant cells and their role in pathologic processes. *Am. J. Pathol.* 189, 1145–1158. doi: 10.1016/j.ajpath.2019.02.006

Carlsson, F., Kim, J., Dumitru, C., Barck, K. H., Carano, R. A., Sun, M., et al. (2010). Host-detrimental role of Esx-1-mediated inflammasome activation in mycobacterial infection. *PLoS Pathog.* 6:e1000895. doi: 10.1371/journal.ppat.1000895

Cox, G., Kable, E., Jones, A., Fraser, I., Manconi, F., and Gorrell, M. D. (2003). 3-dimensional imaging of collagen using second harmonic generation. *J. Struct. Biol.* 141, 53–62. doi: 10.1016/S1047-8477(02)00576-2

Cronan, M. R. (2022). In the thick of it: formation of the tuberculous granuloma and its effects on host and therapeutic responses. *Front. Immunol.* 13:820134. doi: 10.3389/fimmu.2022.820134

Datta, M., Via, L. E., Kamoun, W. S., Liu, C., Chen, W., Seano, G., et al. (2015). Anti-vascular endothelial growth factor treatment normalizes tuberculosis granuloma vasculature and improves small molecule delivery. *Proc. Natl. Acad. Sci. U. S. A.* 112, 1827–1832. doi: 10.1073/pnas.1424563112

Davis, J. M., and Ramakrishnan, L. (2009). The role of the granuloma in expansion and dissemination of early tuberculous infection. *Cells* 136, 37–49. doi: 10.1016/j.cell.2008.11.014

Denk, W., Strickler, J. H., and Webb, W. W. (1990). Two-photon laser scanning fluorescence microscopy. *Science* 248, 73–76. doi: 10.1126/science.2321027

Diegelmann, R. F., and Evans, M. C. (2004). Wound healing: an overview of acute, fibrotic and delayed healing. *Front. Biosci.* 9, 283–289. doi: 10.2741/1184

DiFazio, R. M., Mattila, J. T., Klein, E. C., Cirrincione, L. R., Howard, M., Wong, E. A., et al. (2016). Active transforming growth factor-beta is associated with phenotypic changes in granulomas after drug treatment in pulmonary tuberculosis. *Fibrogenesis Tissue Repair* 9:6. doi: 10.1186/s13069-016-0043-3

Dye, C., and Williams, B. G. (2010). The population dynamics and control of tuberculosis. *Science* 328, 856–861. doi: 10.1126/science.1185449

Ehlers, S., and Schaible, U. E. (2012). The granuloma in tuberculosis: dynamics of a host-pathogen collusion. *Front. Immunol.* 3:411. doi: 10.3389/fimmu.2012.00411

Elkington, P., Shiomi, T., Breen, R., Nuttall, R. K., Ugarte-Gil, C. A., Walker, N. F., et al. (2011). MMP-1 drives immunopathology in human tuberculosis and transgenic mice. *J. Clin. Invest.* 121, 1827–1833. doi: 10.1172/JCI45666

Espindola, M. S., Habiel, D. M., Coelho, A. L., Stripp, B., Parks, W. C., Oldham, J., et al. (2020). Differential responses to targeting matrix metalloproteinase 9 in idiopathic pulmonary fibrosis. *Am. J. Respir. Crit. Care Med.* 203, 458–470. doi: 10.1164/rccm.201910-1977OC

Fallahi-Sichani, M., El-Kebir, M., Marino, S., Kirschner, D. E., and Linderman, J. J. (2011). Multiscale computational modeling reveals a critical role for TNF-alpha receptor 1 dynamics in tuberculosis granuloma formation. *J. Immunol.* 186, 3472–3483. doi: 10.4049/jimmunol.1003299

Gil, O., Diaz, I., Vilaplana, C., Tapia, G., Diaz, J., Fort, M., et al. (2010). Granuloma encapsulation is a key factor for containing tuberculosis infection in minipigs. *PLoS One* 5:e10030. doi: 10.1371/journal.pone.0010030

Gorrell, M. D., Wang, X. M., Levy, M. T., Kable, E., Marinos, G., Cox, G., et al. (2003). Intrahepatic expression of collagen and fibroblast activation protein (FAP) in hepatitis C virus infection. *Adv. Exp. Med. Biol.* 524, 235–243. doi: 10.1007/0-306-47920-6_28

Hiraoka, E., Sato, T., Shirai, W., Kimura, J., Nogami, S., Itou, M., et al. (2001). A case of pulmonary acariasis in lung of Japanese macaque. *J. Vet. Med. Sci.* 63, 87–89. doi: 10.1292/jvms.63.87

Iliopoulos, A., Psathakis, K., Aslanidis, S., Skagias, L., and Sfikakis, P. P. (2006). Tuberculosis and granuloma formation in patients receiving anti-TNF therapy. *Int. J. Tuberc. Lung Dis.* 10, 588–590.

Iuvone, T., Carnuccio, R., and Di Rosa, M. (1994). Modulation of granuloma formation by endogenous nitric oxide. *Eur. J. Pharmacol.* 265, 89–92. doi: 10.1016/0014-2999(94)90227-5

Jakubzick, C., Kunkel, S. L., Joshi, B. H., Puri, R. K., and Hogaboam, C. M. (2002). Interleukin-13 fusion cytotoxin arrests *Schistosoma mansoni* egg-induced pulmonary granuloma formation in mice. *Am. J. Pathol.* 161, 1283–1297. doi: 10.1016/S0002-9440(10)64405-7

Jakubzick, C., Wen, H., Matsukawa, A., Keller, M., Kunkel, S. L., and Hogaboam, C. M. (2004). Role of CCR4 ligands, CCL17 and CCL22, during *Schistosoma mansoni* egg-induced pulmonary granuloma formation in mice. *Am. J. Pathol.* 165, 1211–1221. doi: 10.1016/S0002-9440(10)63381-0

Kunkel, S. L., Lukacs, N. W., Strieter, R. M., and Chensue, S. W. (1996). Th1 and Th2 responses regulate experimental lung granuloma development. *Sarcoidosis Vasc. Diffuse Lung Dis.* 13, 120–128.

Lachowski, D., Cortes, E., Rice, A., Pinato, D., Rombouts, K., and Del Rio Hernandez, A. (2019). Matrix stiffness modulates the activity of MMP-9 and TIMP-1 in hepatic stellate cells to perpetuate fibrosis. *Sci. Rep.* 9:7299. doi: 10.1038/s41598-019-43759-6

Li, G., Jin, F., Du, J., He, Q., Yang, B., and Luo, P. (2019). Macrophage-secreted TSLP and MMP9 promote bleomycin-induced pulmonary fibrosis. *Toxicol. Appl. Pharmacol.* 366, 10–16. doi: 10.1016/j.taap.2019.01.011

Lim, D. H., Cho, J. Y., Miller, M., McElwain, K., McElwain, S., and Broide, D. H. (2006). Reduced peribronchial fibrosis in allergen-challenged MMP-9-deficient mice. *Am. J. Physiol. Lung Cell. Mol. Physiol.* 291, L265–L271. doi: 10.1152/ajplung.00305.2005

Liu, F., Chen, L., Rao, H. Y., Teng, X., Ren, Y. Y., Lu, Y. Q., et al. (2017). Automated evaluation of liver fibrosis in thioacetamide, carbon tetrachloride, and bile duct ligation rodent models using second-harmonic generation/two-photon excited fluorescence microscopy. *Lab. Investig.* 97, 84–92. doi: 10.1038/labinvest.2016.128

Malur, A., Mohan, A., Barrington, R. A., Leffler, N., Malur, A., Muller-Borer, B., et al. (2019). Peroxisome proliferator-activated receptor-γ deficiency exacerbates fibrotic response to mycobacteria peptide in murine sarcoidosis model. *Am. J. Respir. Cell Mol. Biol.* 61, 198–208. doi: 10.1165/rcmb.2018-0346OC

Mootoo, A., Stylianou, E., Arias, M. A., and Reljic, R. (2009). TNF-alpha in tuberculosis: a cytokine with a split personality. *Inflamm. Allergy Drug Targets* 8, 53–62. doi: 10.2174/187152809787582543

North, R. J., and Izzo, A. A. (1993). Granuloma formation in severe combined immunodeficient (SCID) mice in response to progressive BCG infection. Tendency not to form granulomas in the lung is associated with faster bacterial growth in this organ. *Am. J. Pathol.* 142, 1959–1966.

Ordonez, A. A., Tasneen, R., Pokkali, S., Xu, Z., Converse, P. J., Klunk, M. H., et al. (2016). Mouse model of pulmonary cavitary tuberculosis and expression of matrix metalloproteinase-9. *Dis. Model. Mech.* 9, 779–788. doi: 10.1242/dmm.025643

Ramakrishnan, L. (2012). Revisiting the role of the granuloma in tuberculosis. *Nat. Rev. Immunol.* 12, 352–366. doi: 10.1038/nri3211

Roh, I. S., Cho, S., Eum, S. Y., and Cho, S. N. (2013). Kinetics of IFN-gamma and TNF-alpha gene expression and their relationship with disease progression after infection with *Mycobacterium tuberculosis* in guinea pigs. *Yonsei Med. J.* 54, 707–714. doi: 10.3349/ymj.2013.54.3.707

Russell, D. G. (2007). Who puts the tubercle in tuberculosis? *Nat. Rev. Microbiol.* 5, 39–47. doi: 10.1038/nrmicro1538

Russell, D. G., Cardona, P. J., Kim, M. J., Allain, S., and Altare, F. (2009). Foamy macrophages and the progression of the human tuberculosis granuloma. *Nat. Immunol.* 10, 943–948. doi: 10.1038/ni.1781

Segal, B. H., Doherty, T. M., Wynn, T. A., Cheever, A. W., Sher, A., and Holland, S. M. (1999). The p47 (phox−/−) mouse model of chronic granulomatous disease has normal granuloma formation and cytokine responses to *Mycobacterium avium* and *Schistosoma mansoni* eggs. *Infect. Immun.* 67, 1659–1665. doi: 10.1128/IAI.67.4.1659-1665.1999

Sheen, P., O'Kane, C. M., Chaudhary, K., Tovar, M., Santillan, C., Sosa, J., et al. (2009). High MMP-9 activity characterises pleural tuberculosis correlating with granuloma formation. *Eur. Respir. J.* 33, 134–141. doi: 10.1183/09031936.00127807

Shi, L., Eugenin, E. A., and Subbian, S. (2016). Immunometabolism in tuberculosis. *Front. Immunol.* 7:150. doi: 10.3389/fimmu.2016.00150

Shmarina, G., Pukhalsky, A., Petrova, N., Zakharova, E., Avakian, L., Kapranov, N., et al. (2013). TNF gene polymorphisms in cystic fibrosis patients: contribution to the disease progression. *J. Transl. Med.* 11:19. doi: 10.1186/1479-5876-11-19

Silva Miranda, M., Breiman, A., Allain, S., Deknuydt, F., and Altare, F. (2012). The tuberculous granuloma: an unsuccessful host defence mechanism providing a safety shelter for the bacteria? *Clin. Dev. Immunol.* 2012, 1–14. doi: 10.1155/2012/139127

Strieter, R. M. (2008). What differentiates normal lung repair and fibrosis? Inflammation, resolution of repair, and fibrosis. *Proc. Am. Thorac. Soc.* 5, 305–310. doi: 10.1513/pats.200710-160DR

Sun, W., Chang, S., Tai, D. C., Tan, N., Xiao, G., Tang, H., et al. (2008). Nonlinear optical microscopy: use of second harmonic generation and two-photon microscopy for automated quantitative liver fibrosis studies. *J. Biomed. Opt.* 13:064010. doi: 10.1117/1.3041159

Swaim, L. E., Connolly, L. E., Volkman, H. E., Humbert, O., Born, D. E., and Ramakrishnan, L. (2006). *Mycobacterium marinum* infection of adult zebrafish causes caseating granulomatous tuberculosis and is moderated by adaptive immunity. *Infect. Immun.* 74, 6108–6117. doi: 10.1128/iai.00887-06

Tai, D. C., Tan, N., Xu, S., Kang, C. H., Chia, S. M., Cheng, C. L., et al. (2009). Fibro-C-Index: comprehensive, morphology-based quantification of liver fibrosis using second harmonic generation and two-photon microscopy. *J. Biomed. Opt.* 14:044013. doi: 10.1117/1.3183811

Taylor, J. L., Hattle, J. M., Dreitz, S. A., Troudt, J. M., Izzo, L. S., Basaraba, R. J., et al. (2006). Role for matrix metalloproteinase 9 in granuloma formation during pulmonary *Mycobacterium tuberculosis* infection. *Infect. Immun.* 74, 6135–6144. doi: 10.1128/iai.02048-05

Vanden Driessche, K., Persson, A., Marais, B. J., Fink, P. J., and Urdahl, K. B. (2013). Immune vulnerability of infants to tuberculosis. *Clin. Dev. Immunol.* 2013, 1–16. doi: 10.1155/2013/781320

Via, L. E., England, K., Weiner, D. M., Schimel, D., Zimmerman, M. D., Dayao, E., et al. (2015). A sterilizing tuberculosis treatment regimen is associated with faster clearance of bacteria in cavitary lesions in marmosets. *Antimicrob. Agents Chemother.* 59, 4181–4189. doi: 10.1128/aac.00115-15

Volkman, H. E., Pozos, T. C., Zheng, J., Davis, J. M., Rawls, J. F., and Ramakrishnan, L. (2010). Tuberculous granuloma induction via interaction of a bacterial secreted protein with host epithelium. *Science* 327, 466–469. doi: 10.1126/science.1179663

Walton, E. M., Cronan, M. R., Cambier, C. J., Rossi, A., Marass, M., Foglia, M. D., et al. (2018). Cyclopropane modification of trehalose dimycolate drives granuloma angiogenesis and mycobacterial growth through Vegf signaling. *Cell Host Microbe* 24, 514–525.e6. doi: 10.1016/j.chom.2018.09.004

Wan, C., Jin, F., Du, Y., Yang, K., Yao, L., Mei, Z., et al. (2017). Genistein improves schistosomiasis liver granuloma and fibrosis via dampening NF-kB signaling in mice. *Parasitol. Res.* 116, 1165–1174. doi: 10.1007/s00436-017-5392-3

Wang, T. H., Chen, T. C., Teng, X., Liang, K. H., and Yeh, C. T. (2015). Automated biphasic morphological assessment of hepatitis B-related liver fibrosis using second harmonic generation microscopy. *Sci. Rep.* 5:12962. doi: 10.1038/srep12962

Wang, C. H., Lin, H. C., Lin, S. M., Huang, C. D., Liu, C. Y., Huang, K. H., et al. (2010). MMP-1(-1607G) polymorphism as a risk factor for fibrosis after pulmonary tuberculosis in Taiwan. *Int. J. Tuberc. Lung Dis.* 14, 627–634.

Wang, Q., Usinger, W., Nichols, B., Gray, J., Xu, L., Seeley, T. W., et al. (2011). Cooperative interaction of CTGF and TGF-beta in animal models of fibrotic disease. *Fibrogenesis Tissue Repair* 4:4. doi: 10.1186/1755-1536-4-4

Wang, Y., Vincent, R., Yang, J., Asgharpour, A., Liang, X., Idowu, M. O., et al. (2017). Dual-photon microscopy-based quantitation of fibrosis-related parameters (q-FP) to model disease progression in steatohepatitis. *Hepatology* 65, 1891–1903. doi: 10.1002/hep.29090

Wang, D., Zhou, W., Lu, S., Wang, Q., Feng, Y., Zhu, G., et al. (2012). Increased density of macrophage migration inhibitory factor (MIF) in tuberculosis granuloma. *Exp. Mol. Pathol.* 93, 207–212. doi: 10.1016/j.yexmp.2012.05.004

Warsinske, H. C., DiFazio, R. M., Linderman, J. J., Flynn, J. L., and Kirschner, D. E. (2017). Identifying mechanisms driving formation of granuloma-associated fibrosis during *Mycobacterium tuberculosis* infection. *J. Theor. Biol.* 429, 1–17. doi: 10.1016/j.jtbi.2017.06.017

Warsinske, H. C., Pienaar, E., Linderman, J. J., Mattila, J. T., and Kirschner, D. E. (2017). Deletion of TGF-beta 1 increases bacterial clearance by cytotoxic T cells in a tuberculosis granuloma model. *Front. Immunol.* 8:1843. doi: 10.3389/fimmu.2017.01843

Xu, S., Wang, Y., Tai, D. C. S., Wang, S., Cheng, C. L., Peng, Q., et al. (2014). qFibrosis: a fully-quantitative innovative method incorporating histological features to facilitate accurate fibrosis scoring in animal model and chronic hepatitis B patients. *J. Hepatol.* 61, 260–269. doi: 10.1016/j.jhep.2014.02.015

frontiers | Frontiers in Microbiology

TYPE Original Research
PUBLISHED 24 January 2024
DOI 10.3389/fmicb.2023.1305974

OPEN ACCESS

EDITED BY
Vishwanath Venketaraman,
Western University of Health Sciences,
United States

REVIEWED BY
Shibali Das,
Washington University in St. Louis,
United States
Luis Horacio Gutiérrez-González,
National Institute of Respiratory Diseases-Mexico (INER), Mexico

*CORRESPONDENCE
Keshar Kunja Mohanty
✉ keshar63@yahoo.com;
✉ mohanty.kk@icmr.gov.in

†PRESENT ADDRESS
Sushanta Kumar Barik,
Institute of Biosciences and Technology, MGM University, Chhatrapati Sambhajinagar, Aurangabad, Maharashtra, India

RECEIVED 02 October 2023
ACCEPTED 26 December 2023
PUBLISHED 24 January 2024

CITATION
Varshney D, Singh SV, Mohanty KK, Kumar S, Varshney N, Sinha E and Barik SK (2024) *Toll-like receptor 2 (–196 to –174) del* and *TLR1 743 A > G* gene polymorphism—a possible association with drug-resistant tuberculosis in the north Indian population.
Front. Microbiol. 14:1305974.
doi: 10.3389/fmicb.2023.1305974

Toll-like receptor 2 (–196 to –174) del and *TLR1 743 A > G* gene polymorphism—a possible association with drug-resistant tuberculosis in the north Indian population

Deepika Varshney[1], Shoor Vir Singh[2], Keshar Kunja Mohanty[1]*, Santosh Kumar[3], Nitin Varshney[4], Ekata Sinha[1] and Sushanta Kumar Barik[1†]

[1]ICMR-National JALMA Institute for Leprosy and Other Mycobacterial Diseases, Agra, Uttar Pradesh, India, [2]Department of Biotechnology, Institute of Applied Sciences & Humanities, GLA University, Mathura, Uttar Pradesh, India, [3]Department of Chest and Tuberculosis, S. N. Medical College & Hospital, Agra, Uttar Pradesh, India, [4]Department of Agricultural Statistics and Computer Centre, N. M. College of Agriculture, Navsari Agricultural University, Navsari, Gujarat, India

Objectives: The objective of this study is to analyze the association between *TLR2 deletion (–196 to –174)* and *TLR1 743 A > G* gene polymorphism with drug resistant tuberculosis (PTB, MDR-TB, and XDR-TB) in a population from Agra, Uttar Pradesh.

Methods: The present case–control study included 101 pulmonary TB patients, 104 multidrug-resistant TB patients, 48 extremely drug-resistant TB patients, and 130 healthy and unrelated controls residing in the same locality. The genotyping method for *TLR2 deletion (–196 to –174)* was carried out by allele-specific polymerase chain reaction (PCR), and *TLR1 743 A > G* gene polymorphism was performed by hybridization probe chemistry in Roche Real-Time PCR. Genotype and allele frequencies were analyzed by the chi-square test. Cytokine levels were measured by ELISA and compared using Mann–Whitney and Kruskal–Wallis tests.

Results: The frequency of heterozygous (*Ins/del*) genotypes for *TLR2 (–196 to –174)* polymorphism was predominant in XDR-TB patients (0.57), whereas heterozygous A/G genotype for *TLR1 743 A > G* single nucleotide polymorphism (SNP) was predominant in healthy controls (0.57) for *TLR1 743 A > G* gene polymorphism. The heterozygous genotype of *TLR2 deletion* polymorphism was found to be significantly higher in XDR-TB ($p = 0.0001$). *TLR1 743 A > G* SNP, AG genotypes were found to be significantly associated with healthy controls than PTB ($p = 0.047$). The level of serum cytokines (IL-6, TNF-α, and IFN-γ) was also found to be significantly different among TB patients and healthy controls.

Conclusion: The findings suggested that in the present population, the heterozygous (*Ins/Del*) genotype and deletion allele of *TLR2 deletion (–196 to –174)* polymorphism are associated with the risk for the development of drug-resistant TB. Furthermore, for *TLR1 743 A>G* gene polymorphism, A/G genotype, and G allele are found associated with healthy controls, suggesting the protective role against TB.

KEYWORDS

Toll-like receptors, drug-resistant tuberculosis, genotyping, TNF-α, IL-6, IFN-γ

1 Introduction

According to epidemiological data provided by the World Health Organization, the global count of newly reported Tuberculosis (TB) cases in 2021 reached 10.6 million cases, reflecting a 4.5% rise from the 10.1 million cases recorded in 2020. Between 2020 and 2021, there is an estimated 3.6% rise in the Tuberculosis (TB) incidence rate. In 2021, an estimated rate of DR-TB was observed to be 450,000 cases, which is reported to have increased 3.1% from 437,000 in 2020 (World Health Organization, 2022). The diverse host immune response to *Mycobacterium tuberculosis* infection is influenced by both host genetic factors and the reaction of the host to the infection (Berrington and Hawn, 2007). The host cell recognizes Mycobacteria through various receptors, and one of them is Toll-like receptor (TLR). TLR recognizes molecules such as lipoprotein and lipopolysaccharides known as PAMPs that are present in bacteria and bind to host pattern recognition receptors (PRRs) (Jahantigh et al., 2013). TLR1 recognizes tri-acylated lipopeptide, and TLR6 recognizes di-acyl lipopeptide (Buwitt-Beckmann et al., 2005; Omueti et al., 2005). TLR1 recognizes 19 kD lipoprotein of *M.tb* (Takeuchi et al., 2002), and TLR2 recognizes 19 kD lipoproteins and lipoarabinomann and other PAMPs molecule of *M.tb* (Brightbill et al., 1999). Dendritic cells, macrophages, natural killer cells, and T and B lymphocytes express TLRs (Vidya et al., 2018). The human *TLR2* gene is situated on chromosome 4q32, and TLR2 molecules consist of two non-coding exons and one coding exon (Haehnel et al., 2002). Toll-like receptors involved in recognizing *M.tb* include TLR1, TLR2, TLR4, TLR6, TLR8, and TLR9 (Thada et al., 2013). The initial defense of our immune system is the innate immune response (Chen et al., 2010). In the previous study by Mittal et al., the frequency of −196 to −174 del polymorphism of the *TLR2* gene was compared between PTB cases and healthy controls in population of Agra (Uttar Pradesh), and the similar allele frequencies were reported in both cases and controls; no significant difference was observed in genotype frequencies of TB patients and healthy controls (Mittal et al., 2018). In addition, the previous study by Sinha et al., where they examined the frequency of the *743 A > G* gene polymorphism in the *TLR1* gene, compared the cases of pulmonary tuberculosis (PTB) with healthy controls from the Agra region. The study revealed that AG genotypes were significantly more prevalent in healthy controls than in PTB cases. Additionally, the research indicated that the heterozygous condition at the *743 A > G* locus conferred a degree of resistance to the disease by restricting bacterial growth (Sinha et al., 2014).

TLR2 (−196 to −174) del polymorphism is studied in various populations, suggesting the role in susceptibility toward TB. Khan et al. in their study has reported the higher allele frequency of the deletion allele of *TLR2 (−196 to −174) (Ins/del)* polymorphism in TB-infected patients in the Pakistani population (Khan et al., 2014). The study conducted by Ma et al. revealed an association between alleles encoding the *743 A > G* variant and cases of pulmonary tuberculosis (PTB) in the African-American population (Ma et al., 2007). Uciechowski et al. discovered that the *743A > G* variant was linked to susceptibility to tuberculosis (TB) in a low-endemic country, and at the same time, they did not observe any association in the Ghanaian population (Uciechowski et al., 2011). The role of these polymorphisms is unexplored in drug-resistant tuberculosis. Drug resistance develops due to some possible causes such as (1) drug compliance, (2) bacterial genotype, and (3) host genetic factors (Ben-Kahla and Sahal, 2016). The prevalence of DR-TB is high in India and is listed as one of the 30 high burden countries for DR-TB (World Health Organization, 2022). Observing the prevalence rate and the severity of the disease, it becomes imperative to conduct such studies which look into the cause of the disease.

2 Materials and methods

2.1 Ethics statement

The study protocol was approved by the Institute Human Ethics Committee and established following the guidelines outlined by the Indian Council of Medical Research (2017).

2.2 Study population

The tuberculosis patients were recruited from the Outpatient Department (OPD) of the Department of Chest and Tuberculosis, Sarojini Naidu Medical College, Agra, and ICMR-National JALMA Institute for Leprosy and Other Mycobacterial Diseases (NJIL & OMD), who were registered in the OPD from Monday to Friday from 2019 to 2021. Informed consent was obtained from all participants. Only those patients were included who consented to participate in the study. Most of these patients were inhabitants of Agra or neighboring areas within the state of Uttar Pradesh. The patients were clinically examined by the chest physician and evaluated following the guidelines of TB India (2017). Based on the findings of AFB smear positivity in sputum, CBNAAT, radiography, LPA and DST, the participants were categorized as follows.

2.2.1 Pulmonary tuberculosis (PTB) patients

PTB patients were those who were diagnosed based on smear positivity for AFB, CBNAAT (rifampicin resistance not detected), and clinical manifestations, following the guidelines of NTEP. A new TB patient is defined as someone with pulmonary tuberculosis (PTB) has never undergone treatment for TB or has taken anti-TB drugs for less than 1 month. Patients with seropositive HIV infection or suffering from diabetes or any other immunosuppressive disorders were excluded from the study.

2.2.2 Multi drug-resistant tuberculosis (MDR-TB) patients

Patients classified as MDR are those whose biological specimen demonstrates resistance to both isoniazid and rifampicin, with or without resistance to other first-line anti-TB drugs. Diagnosis of MDR-TB patients was confirmed based on the CBNAAT test (resistant to rifampicin) and FL-LPA, SL-LPA, and LC DST, following the guidelines (Guidelines on Programmatic Management of

Abbreviations: *M.tb*, *Mycobacterium tuberculosis*; TLR, Toll-like receptor; PTB, Pulmonary Tuberculosis; MDR-TB, Multi-drug resistant-TB; XDR-TB, Extensively drug resistant tuberculosis; PAMP, Pathogen associated molecular pattern; AFB, Acid fast bacteria; CBNAAT, Cartridge-based nucleic acid amplification test; LPA, Line probe assay; LC DST, Liquid culture Drug susceptibility testing; FL-LPA, First line-line probe assay; SL-LPA, Second line-line probe assay; TNF-α, Tumour necrosis factor-alpha; IL-6, Interleukin-6; IFN-γ, Interferon-gamma.

Drug-Resistant Tuberculosis in India, 2017). Patients who were showing co-infection with HIV or any other immunosuppressive disease were excluded from the study.

2.2.3 Extensively drug-resistant tuberculosis (XDR-TB) patients

XDR patients meet the criteria for MDR/RR-TB and additionally showed resistance to any fluoroquinolone (levofloxacin or moxifloxacin) and at least one additional Group A drug (either bedaquiline or linezolid or both). XDR patients were diagnosed based on FL-LPA, SL-LPA, and LC DST following the guidelines (Guidelines on Programmatic Management of Drug-Resistant Tuberculosis in India, 2017).

2.2.4 Healthy controls

Healthy unrelated individuals from the same socioeconomic background, including those accompanying patients to hospitals and students visiting our institute for training and project work, were enlisted as healthy controls. Schedules containing subject details were filled, and individuals with a recent history of fever, viral infection, other illnesses, or any immunological diseases, as well as those who had received treatment for tuberculosis or leprosy in the past or had a family history of tuberculosis, were excluded from the study. The current study included individuals aged 18–60 years who were in overall good health.

2.3 Selection of gene polymorphism

TLR2 (−196 to −174) del polymorphism is reported to alter the function of TLR2 promoter and decrease transcription-responsive promoters (Tahara et al., 2008). The *TLR1* gene polymorphism *743 A > G* located in the extracellular domain is associated with ligand-binding activity (Ma et al., 2007). Meta-analysis revealed that *TLR2 (−196 to −174) del* polymorphism and *TLR1 743 A > G* gene polymorphism were significantly associated with TB disease (Varshney et al., 2022). Although there are reports related to frequencies and association between *TLR2 (−196 to −174) del* polymorphism (Mittal et al., 2018) and *TLR1 743 A > G* gene polymorphism (Sinha et al., 2014), from Agra population, no information is available about the host gene polymorphism among the drug-resistant tuberculosis. The present study will be the first report on the frequencies of *TLR2 (−196 to −174) del* and *TLR1 743 A > G* gene polymorphisms in drug-resistant tuberculosis patients. Hence, *TLR2 (−196 to −174) del* polymorphism and *TLR1 743 A > G* gene polymorphism were selected.

2.4 Genotyping for the *TLR2* gene

DNA extraction was performed using the salting out procedure from 1 mL of blood collected in tubes containing acid citrate dextrose from each subject (Miller et al., 1988) or promega genomic DNA isolation kit. Genotyping of this polymorphism at *TLR2 (−196 to −174) del* was performed by allele-specific polymerase chain reaction (PCR). The sequence of forward and reverse primers was adopted from the study by Tahara et al. (2008). The details of sequence of primers are presented in Table 1. The PCR products were observed through electrophoresis on a 3% agarose gel and stained with ethidium bromide for visualization. The observation was finally recorded after assessment of three independent observers. The amplified product of a single band of 286 bp was judged as wild type (insertion/insertion), and a single band of 264 bp was judged as homozygous mutant (deletion/deletion), whereas two bands of 284 and 264 bp were judged as heterozygous (insertion/deletion) for *TLR2 (−196 to −174) del* polymorphism.

TABLE 1 Sequence of primers used for genotyping experiments.

TLR polymorphism	Sequence of primers
TLR2 (−196 to-174) del polymorphism	Forward Primer 5′-CACGGAGGCAGCGAGAAA-3′ Reverse Primers 5′-CTGGGCCGTGCAAAGAAG-3
TLR1 743 A > G gene polymorphism	Forward Primer 5′-TTGGATGTGTCAGTCAAGACTGTAG-3′ Reverse Primer 5′-GCTTCACGTTTGAAATTGAG-3′ Sensor Probe 5′-TTAAGGTAAGACTTGATAACTTTGG-FL-3′ Anchor probe 5'LCRed640- GTTTGAAGTTTCGCCAGAATACTTAGG

2.5 Genotyping for the *TLR1* gene

DNA extraction was performed as described above in section 2.4. Genotyping of *TLR1 743 A > G* gene polymorphism was performed by hybridization probe chemistry in Roche real-time PCR machine. The sequence of *TLR1 gene* (*743 A > G, rs 4833095*), forward primer, reverse primer, sensor probe, and anchor probe was adopted from the study by Sinha et al. (2014). Primers and probes were synthesized from TIB Mol biol, Berlin, Germany. The LightCycler 480 genotyping master mix was procured from Roche Company. The primer and probe sequences used for amplification and the FRET mechanism in detecting *TLR1 743 A > G* gene polymorphism are presented in Table 1. Real-time PCR was performed using 1.5 µL DNA, 2.5 Mm Mgcl2, TLR1 primers at 1.25 pmol, and 250 nm of the *TLR1 743 A > G* sensor probe and anchor probe. The sensor probe was labeled with fluorescein at the 3'end. The anchor probe was labeled with LightCycler red 640 at the 5'end. The amplification was conducted in the LightCycler 480 system (Roche Diagnostics) with the following parameters: initial denaturation at 95°C for 10 min, followed by 40 cycles of amplification with denaturation at 95°C for 10 s, annealing at 60°C for 20 s, and extension at 72°C for 15 s. Subsequently, a melting curve analysis was performed with 1 cycle at 95°C for 1 min, 40°C for 30 s, followed by a temperature increase to 80°C, and final cooling at 40°C.

2.6 Stimulation of the peripheral blood mononuclear cells (PBMCs)

Heparin-containing tubes were used to collect eight milliliters of blood samples from eleven PTB, ten MDR-TB, and eleven

TABLE 2 *TLR2 gene (–196 to –174)* del polymorphism and *TLR1 743 A > G* genotype and allele frequencies among drug resistant TB patients (PTB, MDR and XDR).

TLR2 (–196 to-174) del polymorphism	PTB (*N* = 101)	MDR (*N* = 104)	XDR (*N* = 48)	Genotype frequency Chi, *p*, DF	Allele frequency Chi, *p*, DF
I/I	74 (0.73)	73 (0.70)	16 (0.33)	27.58, 0.0001, 4	21.79, 0.0001, 2
I/D	23 (0.23)	22 (0.21)	27 (0.57)		
D/D	4 (0.04)	9 (0.09)	5 (0.10)		
I	171 (0.85)	168 (0.81)	59 (0.61)		
D	31 (0.15)	40 (0.19)	37 (0.38)		
TLR1 743 A > G					
A/A	29 (0.29)	31 (0.29)	15 (0.31)	0.22, 0.99, 4	0.018, 0.99, 2
A/G	50 (0.49)	49 (0.48)	22 (0.46)		
G/G	22 (0.22)	24 (0.23)	11 (0.23)		
A	108 (0.54)	111 (0.53)	52 (0.54)		
G	94 (0.46)	97 (0.47)	44 (0.46)		

healthy controls. Density gradient centrifugation was used to isolate PBMCs. One million cells were stimulated with 1 μg/mL of Pam3CSK4 molecule, which is a ligand of TLR2/TLR1 agonist (Hook et al., 2020) of *M.tb* for 24, 48, and 72 h and incubated at 37°C in 5% CO_2 in a water-jacketed CO_2 incubator (Thermo Electron Corporation). At each time point, the supernatant was collected and stored at −20°C for cytokine assay.

2.7 Measurement of TNF-α, IL-6, and IFN-γ in sera samples and culture supernatant of patients and healthy controls

Cytokines were estimated by sandwich ELISA system using the commercially available reagents from R&D System, United States, following the instructions of the manufacturer. Initially, standardization of PBMC culture was carried out to find out the optimum duration for the production of TNF-α and IL-6 in culture supernatant, which was observed to be highest in 24 h. Cytokines were estimated in culture supernatant of PBMCs and sera samples. The analysis of cytokines in sera samples was performed in 97 PTB, 98 MDR, 45 XDR, and 98 healthy controls.

2.8 Statistical analysis

Frequency of genotypes and alleles was counted. Hardy–Weinberg Equilibrium of genotype and allelic frequencies were checked by the chi-square test. Genotype and allele frequencies were compared among the participants by the chi-square test. All statistical analyses were performed by STATA/MP 16.1 software. Comparison of level of cytokine in sera samples and production in culture supernatant was performed by non-parametric analyses (Mann–Whitney test) using GraphPad Prism version 8.01 for Windows (GraphPad software, San Diego, CA) and STATA. The results are depicted in the form of a scattered plots. Comparisons of groups were performed using Kruskal–Wallis equality of proportion rank test. Data were expressed as Mean+_SD or median. $p < 0.05$ was considered as significant.

3 Results

3.1 Analysis of demographic parameters

A total of 101 PTB, 104 MDR, 48 XDR patients, and 130 healthy controls were included in the study. The mean age of TB patients and healthy controls was found to be significantly different ($p = 0.007$). The male-to-female ratio was similar ($p = 0.49$) among drug-resistant TB patients. On the analysis of various risk factors (smoking and alcoholic habits), among PTB, MDR and XDR cases, no significant difference was observed for smoking ($p = 0.49$) and alcoholic habits ($p = 0.52$), although a significant difference was observed related to consumption ($p = 0.02$) of tobacco among TB patients and healthy controls. A detailed analysis of demographic factors is shown in Supplementary Table S1.

3.2 *TLR2 del* polymorphism genotypic analysis

In the present study, genetic polymorphism of the *TLR2* gene was analyzed by allele-specific polymerase chain reaction. The frequencies of genotypes for *TLR2 del* polymorphism did not deviate from Hardy–Weinberg equilibrium in PTB and XDR patients ($p > 0.05$) but were found to have deviated in healthy controls ($p < 0.05$) and MDR cases ($p < 0.05$). The wild-type genotype (Ins/Ins) was observed to be predominant in healthy controls (0.71), PTB (0.73), and MDR-TB participants (0.70), and heterozygous genotypes (Ins/del) were predominant in XDR TB patients (0.57). Table 2 displays the genotype and allele frequency distributions among the different TB patient categories. A pairwise comparison was made between PTB versus MDR, MDR versus XDR, and XDR versus PTB and is presented in Table 3, and TB patients with healthy controls are presented in Table 4. A significant difference was observed in allele and genotypic frequencies of PTB, MDR, and XDR patients for *TLR2 deletion* polymorphism ($p = 0.0001$), and no significant difference was observed in *TLR1 743 A > G* gene polymorphism (Table 2). On analyzing genotype and allele frequencies between MDR-TB and XDR and PTB and XDR-TB, a significant difference was observed between the groups of dominant and over-dominant models ($p = 0.0001$), as shown in

TABLE 3 *TLR2 gene (–196 to –174) del* polymorphism and *TLR1 743 A > G* genotype and allele frequencies among PTB and MDR, MDR and XDR, PTB and XDR.

	PTB (*N* = 101)	MDR (*N* = 104)	XDR (*N* = 48)	Chi, (DF) & *p* value			OR (95% CI)		
				PTB vs. MDR	MDR vs. XDR	PTB vs. XDR	PTB vs. MDR	MDR vs. XDR	PTB vs. XDR
TLR2 (–196 to –174) del polymorphism									
I/I	74 (0.73)	73 (0.70)	16 (0.33)	1.90, (2) & 0.38	20.27 (2) & 0.0001	21.70 (2) & 0.0001			
I/D	23 (0.23)	22 (0.21)	27 (0.57)						
D/D	4 (0.04)	9 (0.09)	5 (0.10)						
I	171 (0.85)	168 (0.81)	59 (0.61)	1.07 (1) & 0.29	12.95 (1) & 0.0001	19.87 (1) & 0.0001	1.31 (0.78–2.19)	2.63 (1.54–4.49)	3.45 (1.97–6.04)
D	31 (0.15)	40 (0.19)	37 (0.38)						
Dominant									
II	74 (0.73)	73 (0.70)	16 (0.34)	0.23 (1) & 0.62	18.38 (1) & 0.0001	21.69 (1) & 0.0001	1.16 (0.63–2.13)	4.70 (2.27–9.74)	5.48 (2.61–11.47)
ID+DD	27 (0.27)	31 (0.29)	32 (0.66)						
Over-dominant									
II + DD	78 (0.77)	82 (0.78)	21 (0.44)	0.07 (1) & 0.78	18.51 (1) & 0.0001	16.35 (1) & 0.0001	0.90 (0.47–1.75)	4.79 (2.29–9.99)	4.36 (2.09–9.05)
ID	23 (0.23)	22 (0.21)	27 (0.56)						
Recessive									
ID+II	97 (0.96)	95 (0.91)	43 (0.90)	1.90 (1) & 0.168	0.122 & 0.72	2.38 (1) & 0.12	2.29 (0.72–7.26)	1.22 (0.40–3.72)	2.18 (0.77–10.2)
DD	4 (0.04)	9 (0.09)	5 (0.10)						
TLR1 743 A>G									
A/A	29 (0.29)	31 (0.29)	15 (0.31)	0.11 (2) & 0.94	0.034 (2) & 0.98	0.18 (2) & 0.91			
A/G	50 (0.49)	49 (0.48)	22 (0.46)						
G/G	22 (0.22)	24 (0.23)	11 (0.23)						
A	108 (0.54)	111 (0.53)	52 (0.54)	0.0004 (1) & 0.98	0.017 (1) & 0.89	0.01 (1) & 0.91	1.00 (0.68–1.47)	0.96 (0.59–1.57)	0.97 (0.59–1.5 8)
G	94 (0.46)	97 (0.47)	44 (0.46)						
Dominant									
AA	29 (0.28)	31 (0.30)	15 (0.32)	0.02 (1) & 0.86	0.032 & 0.85	0.106 (1) & 0.75	0.94 (0.52–1.75)	0.93 (0.44–1.94)	0.88 (0.42–1.85)
AG + GG	72 (0.72)	73 (0.70)	33 (0.68)						
Over dominant									
AA+GG	51 (0.51)	55 (0.52)	26 (0.54)	0.11 (1) & 0.73	0.021 (1) & 0.88	0.17 (1) & 0.67	0.90 (0.52–1.56)	0.94 (0.48–1.87)	0.86 (0.43–1.71)
AG	50 (0.49)	49 (0.48)	22 (0.46)						
Recessive									
AG + AA	79 (0.78)	80 (0.77)	37 (0.77)	0.04 (1) & 0.82	0.0005 (1) & 0.98	0.02 (1) & 0.87	1.07 (0.56–2.06)	0.99 (0.44–2.21)	1.06 (0.47–2.40)
GG	22 (0.22)	24 (0.23)	11 (0.23)						

Table 3, whereas no significant difference was observed between PTB and MDR-TB with healthy controls (Table 4).

3.3 *TLR1 743 (A > G)* gene polymorphism genotypic analysis

In the present study, *TLR1 743 A > G* allele and genotype frequencies were analyzed by hybridization probe chemistry. *TLR1 743 A > G* gene polymorphism was analyzed in 101 PTB, 104 MDR, and 48 XDR patients and 130 healthy controls. The genotypic and allele frequencies did not deviate from Hardy–Weinberg equilibrium in any of the studied groups. The heterozygous genotype was observed to be predominant in healthy controls (0.57). Furthermore, analyses of genotype frequencies were carried out among the drug-resistant TB patients (PTB, MDR-TB, and XDR-TB). There was no significant difference in frequencies of alleles and genotypes ($p = 0.99$), as shown in Table 2. A significant difference in the frequencies of alleles and genotypes was observed between healthy controls and PTB patients, as well as between healthy controls and MDR-TB patients ($p = 0.047$), ($p = 0.007$) and also in the dominant model ($p = 0.01$), ($p = 0.007$), respectively, as shown in Table 4.

3.4 Estimation of TNF-α in relation to severity of tuberculosis disease (PTB, MDR-TB, XDR-TB, and HC) in sera samples and culture supernatant

The TNF-α level in sera samples among all categories is graphically presented in Figure 1A. The median level of TNF-α in sera samples was observed to be higher in PTB cases (97) ($p < 0.0001$) as compared with healthy controls (98), MDR-TB (98), and XDR cases (45). The level was higher in healthy controls compared with MDR ($p < 0.0001$) and XDR ($p = 0.0006$). There was no significant difference in TNF-α level between MDR and XDR TB patients, as shown in Figure 1A. The participants were

TABLE 4 *TLR2 gene (–196 to –174) del* polymorphism and *TLR1 743 A>G* genotype and allele frequencies between healthy controls and PTB, healthy controls and MDR, and healthy controls and XDR patients.

	Healthy (*N* = 130)	PTB (*N* = 101)	MDR (*N* = 104)	XDR (*N* = 48)	Chi (DF) & *p* value			OR (95% CI)		
					Healthy vs. PTB	Healthy vs. MDR	Healthy vs. XDR	Healthy vs. PTB	Healthy vs. MDR	Healthy vs. XDR
TLR2 (–196 to –174) del polymorphism										
I/I	92 (0.71)	74 (0.73)	73 (0.70)	16 (0.33)	1.39 (2) & 0.49	0.07 (2) & 0.96	22.07 (2) & 0.0001	0.88 (0.49–1.57)	1.02 (0.58–1.80)	4.84 (2.39–9.77)
I/D	28 (0.21)	23 (0.23)	22 (0.21)	27 (0.57)						
D/D	10 (0.08)	4 (0.04)	9 (0.09)	5 (0.10)						
I	212 (0.82)	171 (0.85)	168 (0.81)	59 (0.61)	0.77 (1) & 0.37	0.04 (1) & 0.83	15.55 (1) & 0.0001	0.80 (0.48–1.30)	1.05 (0.66–1.67)	2.76 (1.65–4.63)
D	48 (0.18)	31 (0.15)	40 (0.19)	37 (0.38)						
Dominant										
II	92 (0.71)	74 (0.73)	73 (0.70)	16 (0.34)	0.17 (1) & 0.67	0.009 (1) & 0.92	20.59 (1) & 0.0001	0.88 (0.49–1.57)	1.02 (0.58–1.80)	4.84 (2.39–9.77)
ID+DD	38 (0.29)	27 (0.27)	31 (0.29)	32 (0.66)						
Over-dominant										
II + DD	102 (0.78)	78 (0.77)	82 (0.78)	21 (0.44)	0.05 (1) & 0.82	0.005 (1) & 0.94	19.78 (1) & 0.0001	1.04 (0.57–1.99)	0.97 (0.52–1.82)	4.68 (2.32–9.45)
ID	28 (0.22)	23 (0.23)	22 (0.21)	27 (0.56)						
Recessive										
ID+II	120 (0.92)	97 (0.96)	95 (0.91)	43 (0.89)	1.39 (1) & 0.23	0.07 (1) & 0.78	0.33 (1) & 0.56	0.49 (0.15–1.54)	1.13 (0.45–2.83)	1.39 (0.47–4.14)
DD	10 (0.08)	4 (0.04)	9 (0.09)	5 (0.10)						
TLR1 743 A>G										
A/A	20 (0.15)	29 (0.29)	31 (0.29)	15 (0.31)	6.133 (2) & 0.047	7.05 (2) & 0.007	5.58 (2) & 0.06	0.45 (0.23–0.85)	0.42 (0.22–0.80)	0.4 (0.18–0.85)
A/G	74 (0.57)	50 (0.49)	49 (0.48)	22 (0.46)						
G/G	36 (0.28)	22 (0.22)	24 (0.23)	11 (0.23)						
A	114 (0.44)	108 (0.54)	111 (0.53)	52 (0.54)	4.21 (1) & 0.04	4.19 (1) & 0.04	3.00 (1) & 0.08	0.67 (0.46–0.98)	0.68 (0.47–0.98)	0.66 (0.41–1.05)
G	146 (0.56)	94 (0.46)	97 (0.47)	44 (0.46)						
Dominant										
AA	20 (0.15)	29 (0.28)	31 (0.30)	15 (0.32)	6.041 (1) & 0.014	7.05 (1) & 0.007	5.58 (1) & 0.018	0.45 (0.23–0.85)	0.42 (0.22–0.80)	0.4 (0.18–0.85)
AG + GG	110 (0.85)	72 (0.72)	73 (0.70)	33 (0.68)						
Over-dominant										
AA+GG	56 (0.44)	51 (0.51)	55 (0.52)	26 (0.54)	1.25 (1) & 0.26	2.22 (1) & 0.135	1.73 (1) & 0.18	0.74 (0.44–1.24)	0.67 (0.40–1.13)	0.64 (0.33–1.23)
AG	74 (0.56)	50 (0.49)	49 (0.48)	22 (0.46)						
Recessive										
AA+AG	94 (0.72)	79 (0.78)	80 (0.77)	37 (0.77)	1.05 (1) & 0.304	0.64 (1) & 0.42	0.41 (1) & 0.52	0.72 (0.39–1.33)	0.78 (0.43–1.41)	0.77 (0.36–1.66)
GG	36 (0.28)	22 (0.22)	24 (0.23)	11 (0.23)						

stratified as per their TLR2 and TLR1 genotypes, and the level of TNF-α was compared among them. No significant difference was observed in the median level of cytokine among persons having various TLR2 genotypes within healthy controls and all disease types (PTB, MDR, and XDR cases). However, the level of serum TNF-α was higher in healthy controls having Ins/Ins and Ins/Del genotypes compared to XDR TB patients having similar genotypes. The observations are presented in Supplementary Figure S1. When the TNF-α level was analyzed in healthy controls and PTB cases having various TLR1 genotypes, a significant difference was observed in *A/A* ($p = 0.003$), *A/G* genotypes ($p = 0.011$), and *G/G* genotype ($p = 0.003$). There was no difference in the level of TNF-α among three TLR1 genotypes within the group (healthy controls, PTB cases, MDR cases, and XDR cases). The observations are presented in Supplementary Figure S2. The median level of TNF-α in culture supernatant was not significantly different in PTB cases and healthy controls in unstimulated samples as well as in samples stimulated with Pam3CSK4. When the level was compared in MDR and PTB cases, the median level was detected to be higher in MDR cases in unstimulated as well as in stimulated samples. The observations are presented in Supplementary Figure S3.

3.5 Estimation of IL-6 with the severity of tuberculosis disease (PTB, MDR-TB, XDR-TB, and HC) in sera samples and culture supernatant

The median level of IL-6 was detected to be higher in PTB cases as compared with healthy controls ($p < 0.0001$) and MDR-TB and XDR-TB cases. The level was higher in healthy controls compared with MDR ($p < 0.0001$) and XDR cases ($p = 0.0005$). The graphical representation of IL-6 level in sera samples is shown in Figure 1B. The participants were stratified as per their *TLR1* and *TLR2* genotypes, and the level of IL-6 was compared among them. No significant difference was observed in the mean level of cytokine among various genotypes within healthy controls and all disease types (PTB, MDR, and XDR cases). However, the level of serum IL-6 was higher in healthy controls having Ins/Ins and Ins/Del genotypes compared to XDR TB patients having similar genotypes. The observations are presented in Supplementary Figure S4. In the *TLR1* gene, a significant difference was observed between healthy controls and PTB cases having *A/A* (0.006) and *A/G* (0.01) genotypes. The observations are presented in Supplementary Figure S5. The median level of IL-6 in culture supernatant was detected to be higher in PTB cases as compared with healthy controls in unstimulated and stimulated

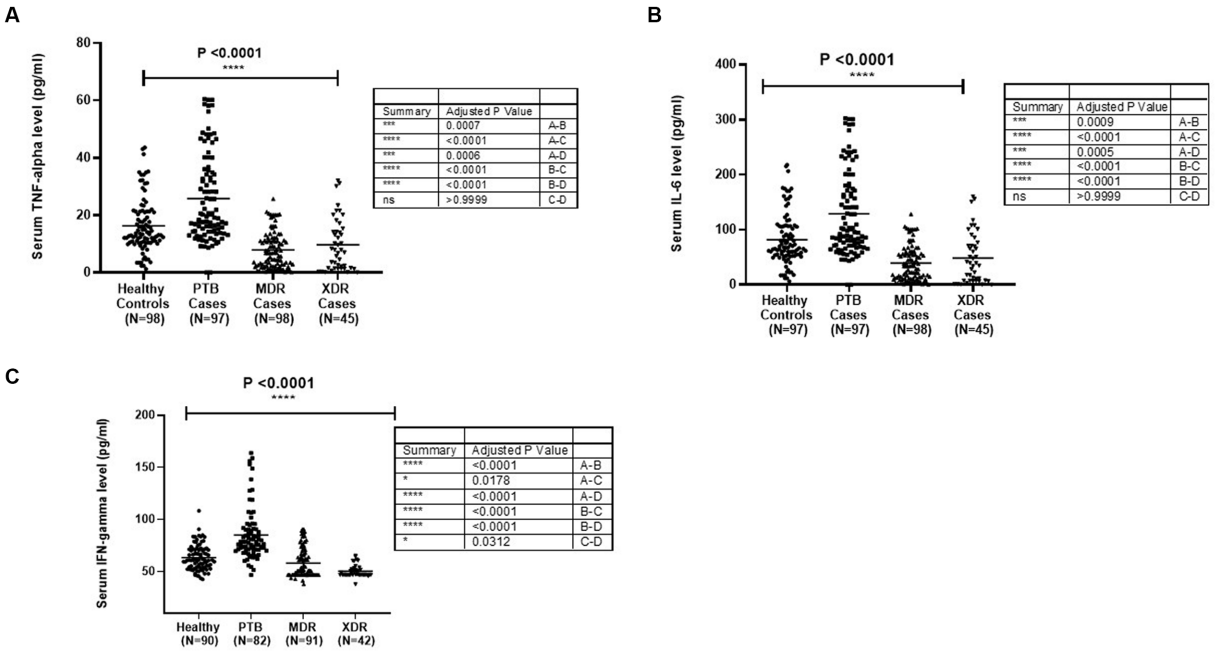

FIGURE 1
Cytokines [**(A)** TNF-α, **(B)** IL6 and **(C)** IFNγ] level in sera samples of healthy controls PTB, MDR-TB and XDR-TB patients. Each dot represents the level in pg/mL in the serum of one individual. The horizontal bar represents the median level. The level was compared among groups using the Kruskal-Wallis and Mann–Whitney test for pairwise comparison.

(Pam3CSK4) samples. The observations are presented in Supplementary Figure S6.

3.6 Estimation of IFN-γ in relation to severity of tuberculosis disease (PTB, MDR-TB, XDR-TB, and HC) in sera samples and culture supernatant

The graphical representation of IFN-γ level in sera samples is shown in Figure 1C. The median level of IFN-γ was detected to be higher in PTB cases as compared with healthy controls ($p < 0.0001$). The level was higher in healthy controls as compared with MDR ($p = 0.0178$) and XDR cases ($p < 0.0001$), as shown in Figure 1C. The participants were stratified as per their *TLR1* and *TLR2* genotypes, and the level of IFN-γ was compared among them. No significant difference was observed in the mean level of IFN-γ level among various genotypes within healthy controls and all disease types (PTB, MDR, and XDR cases). The observations are presented in Supplementary Figure S7. When the IFN-γ level was analyzed in healthy controls and PTB cases having various TLR1 genotypes, significantly higher level was observed in PTB patients *A/A* ($p = 0.0021$), *A/G* genotypes ($p < 0.0001$), and *G/G* genotype ($p < 0.0001$) as compared with healthy controls. No significant difference was observed in the median level of cytokine among various genotypes within healthy controls and all disease types (PTB, MDR, and XDR cases). The observations are presented in Supplementary Figure S8.

4 Discussion

TLRs play a crucial role in both innate and adaptive immune responses (Wu et al., 2015). The interaction between TLRs and their corresponding ligands initiates the recruitment of TIR domain-containing adaptor proteins, initiating signaling pathways that protect the host from microbial infections (Ogus et al., 2004). Human TLRs are a family of 10 proteins that selectively recognize microbes and initiate signaling pathways, resulting in the activation of the innate immune response, cytokine production, and the formation of an adaptive immune response (Guan et al., 2010).

The present study addressed the *TLR2 (−196 to −174) del* polymorphism and *TLR1 743 A > G* gene polymorphism among PTB, MDR, XDR, and healthy controls. The frequency of *TLR2 (−196 to −174) ins/del* genotype is observed to be higher among XDR-TB cases (0.57), whereas the frequency of *TLR2 (−196 to −174) ins/del* genotype in MDR-TB and PTB cases is almost equal (0.21 and 0.23, respectively). As a result, a significant difference is observed between XDR-TB and MDR-TB. The allele frequency of *del* allele of *TLR2 (−196 to −174) polymorphism* was observed to be higher among XDR-TB cases (0.38). When the genotypes carrying all *del allele (ins/del + del/del)* were compared against the *ins allele (ins/ins),* a significant difference was observed in both XDR-TB and MDR-TB ($p = 0.0001$) and XDR-TB and PTB ($p = 0.0001$), pointing toward the role of del polymorphism in developing XDR-TB. Velez et al. have reported the most robust association in *TLR2 del* polymorphism with TB in both Caucasian and African populations. This study indicated that *TLR2 del* is the susceptible gene for TB (Velez et al., 2010). According to the report by Khan et al., del polymorphism *TLR2 (−196 to −174)* increased the chance of TB in the Pakistani population (Khan et al., 2014). Tahara et al. identified the effect of this *TLR2 (−196 to −174)* del polymorphism on the severity of *H. pylori*-induced gastritis (Tahara et al., 2008). Noguchi et al. reported that the *ins/ins* and *ins/del* genotypes of this *TLR2 (−196 to −174) del* polymorphism were associated with highly transcriptional activity (Noguchi et al., 2004).

All research studies conducted up to this point has revealed information regarding the susceptibility of a gene polymorphism to either extrapulmonary or pulmonary tuberculosis. *TLR2 (−196 to −174) del* polymorphism may contribute to drug resistance in tuberculosis given that it is associated with disease severity and is found in a higher proportion of drug-resistant cases of the disease. This study represents the first attempt to comprehend the impact of this polymorphism.

The heterozygous genotype (AG) of the *TLR1 743 A > G* polymorphism is predominant in all tuberculosis cases, including PTB (49%), MDR-TB (48%), and XDR-TB cases (46%) and healthy controls (57%). When tuberculosis cases were compared with healthy controls, there was a significant difference found in PTB ($p = 0.047$) and MDR-TB cases ($p = 0.007$). The AG genotype may have a protective role against tuberculosis (TB) since it was more common in healthy controls than in PTB, MDR-TB, or XDR-TB cases.

According to Dittrich et al., the *TLR1 743 A > G* gene is linked to TB protection (Dittrich et al., 2015). According to Salie et al., TLR1 rs 4833095 was found to be significantly associated with tuberculosis diseases (Salie et al., 2015). Moreover, after being stimulated with *M. tuberculosis,* transfected HEK cells carrying the rs 4833095 genotype showed an increased NF-kβ induction (Dittrich et al., 2015). In the meta-analysis conducted by Schurz et al. and Zhou et al., the AG heterozygous genotype of TLR1 rs 4833095 was found to be associated with resistance to tuberculosis in various ethnic groups (Schurz et al., 2015; Zhou and Zhang, 2020). TLR2 plays a significant role in recognizing gram-positive bacteria and other microbial components, such as peptidoglycan and lipopolysaccharides (Akira et al., 2006). TLR1 is a 786 residue type I transmembrane protein having an extracellular domain that is 581 amino acids long and leucine-rich, a transmembrane domain that is 23 amino acids long, and a cytoplasmic toll homology signaling protein that is 181 amino acids long (Zarember and Godowski, 2002). Certain studies have suggested that mutations in the *TLR1* gene, which change the amount of IL-10 and tumor necrosis factor in macrophages, raise the risk of leprosy in Brazil and India (Schuring et al., 2009). The rs 4833095 mutation changes the DNA sequence to replace an adenine with a guanine. It is a missense mutation that causes the asparagine to turn into serine at amino acid position 248 of the protein, lowering TLR1 receptor expression in immune system cells (Uciechowski et al., 2011).

All these studies provide information about the susceptibility of gene polymorphisms with pulmonary TB or extrapulmonary TB. Our observations suggested that a significant difference in frequencies of genotypes among TB patients and heterozygous genotype (Ins/del) of *TLR2 (−196 to −174) del* polymorphism was more prevalent in drug-resistant patients. When the allele was considered, the del allele was predominant in drug-resistant patients (XDR-TB). *TLR2 (−196 to −174) del* polymorphism may have a role in contributing to drug resistance in tuberculosis, though the exact mechanism is still unknown, given its correlation with disease severity and the higher frequency in drug-resistant tuberculosis cases. The present study is the maiden effort to understand the effect of this polymorphism.

We have analyzed various demographic and environmental factors that may contribute to the severity of the disease. A significant difference was observed among various tuberculosis cases related to age, so it was adjusted in all the analyses. No significant difference was observed related to smoking and alcoholism, but a significant difference was observed in relation to tobacco chewing ($p = 0.02$). In the study by Yu et al., they found a positive association of smoking with pulmonary TB (Yu et al., 1988). According to Ghasemian et al., smokers were 2.9 times more susceptible to suffering from pulmonary TB (Ghasemian et al., 2009). The inhalation of smoke activates the alveolar macrophage and produces an inflammatory response, and the longer use of these risk factors diminishes the expression of surface proteins related to antigen presentation by these macrophages (Pankow et al., 1991).

Cytokines play a pivotal role in the host defense mechanism against *M.tb* infection (Anoosheh et al., 2009). Multifunctional cytokines are responsible for the activation, shaping, and response of host body functions. However, a proper balance of cytokines is essential for the right protective responses (Cicchese et al., 2018), since hypo-reactions or hyper-reactions can be harmful and worsen the illness. TNF-α is a proinflammatory cytokine that showed multiple biological effects (Barnes et al., 1993). TNF-α stimulates apoptosis of macrophages, resulting in cell death and subsequent presentation of mycobacterial infection by dendritic cells (Keane et al., 2000). Nakya et al. studied that serum level of TNF-α in pulmonary tuberculosis patients is greater than the control group (Nakaya et al., 1995). The cytokine level is likely to be lower in MDR TB patients (Donnelly et al., 1995). Many investigators have documented that TNF-α level is higher in newly diagnosed TB patients (Juffermans et al., 1998). The result of our study showed that TNF-α level in sera, IL-6, and IFN-γ in PTB patients was greater than the healthy controls, MDR patients, and XDR patients.

Cytokines work in a cascade fashion during TB, where IL-12 controls T1 cytokine (IL-2/IFN-γ) production (Cooper and Khader, 2008; Cooper, 2009; Kumar et al., 2019). The IFN-γ, in turn, activates macrophages (Tötemeyer et al., 2006; Basingnaa et al., 2018) that induce TNF-α secretion for infection containment and mycobacterial growth restriction (Mattos et al., 2010; Nemeth et al., 2011; Basingnaa et al., 2018). TNF-α and IL-1α are the predominant contributors of granuloma formation (Hernandez-Pando et al., 1997; Yao et al., 2017). However, their protective effect was downregulated by the high IL-6/IL-10 levels in association with pSTAT3/SOCS3 expression, which ultimately led to immune suppression and impaired T-cell function (Harling et al., 2019). Moreover, type 1 cytokines (TNF-α and IFN-γ) change their protective nature to promote the spread of disease and use their distinct association with bacterial density to indicate the severity of an infection (Kumar et al., 2019). A significant difference was observed between PTB and MDR cases for TNF-α and healthy and PTB cases for IL-6 cytokine in stimulated samples in culture supernatant samples. It can be deduced that the increased cytokine levels in cases (TNF-α, IL-6 and IFN-γ) by *M. tuberculosis* components are the effect of the defense mechanism mediated through *TLR2 del* and *TLR1 743 A > G* gene polymorphism.

There was a significant difference observed between healthy controls and PTB cases having A/G genotypes for *TLR1 743 A > G* gene polymorphism and healthy controls and XDR cases having Ins/del genotypes for *TLR2 del* polymorphism. So it could be suggested that TLR genotypes may be just one of several factors controlling the cytokine level as TLR2 signaling is known to regulate the activation of various transcription factors (Grassin-Delyle et al., 2020) which in turn regulates the cytokine levels in sera. A variety of factors, in addition to specific genotypes or mutations, may modulate host responses in a way that affects the host's ability to fight off the continuously multiplying drug-resistant tuberculosis bacteria by up-regulating or down-regulating immunity-related genes and

pathways (Ben-Kahla and Sahal, 2016). TLRs, which are a component of the immune system's physiological barrier, are responsible for identifying mycobacteria and determining which ligands, such as PAM, are linked to them. Any mutation in the TLR gene would prevent it from recognizing the ligand and, as a result, prevent the signaling mechanism from being triggered (Basu et al., 2012). Altered TLR function might lead to reduced recognition of bacteria, contributing to a host environment that is more permissive to the growth of a resistant *M. tuberculosis* stain. It is the complex interplay between host genetics and the pathogen's ability to evade the immune system (Vijay, 2018; Sia and Rengarajan, 2019). However, further study is required to establish the essential role of *TLR2 del* and *TLR1 743 A > G* gene polymorphism in the recognition of *M.tb* and induction of TNF-α and other cytokines. This may be the first study to analyze the immune response to drug-resistant tuberculosis patients by analyzing *TLR2 (−196 to −174) del* and *TLR1 743 A > G* gene polymorphism.

Data availability statement

The original contributions presented in the study are included in the article/Supplementary material, further inquiries can be directed to the corresponding author.

Ethics statement

The studies involving humans were approved by Institute Human Ethics Committee, ICMR-National JALMA Institute for Leprosy and Other Mycobacterial Diseases, Agra. The studies were conducted in accordance with the local legislation and institutional requirements. The participants provided their written informed consent to participate in this study.

Author contributions

DV: Formal analysis, Methodology, Writing – original draft, Writing – review & editing, Data curation, Software. SS: Writing – review & editing. KM: Conceptualization, Supervision, Funding acquisition, Formal analysis, Writing – review & editing, Software, Project administration. SK: Writing – review & editing, Investigation, Methodology, Validation. NV: Formal analysis, Writing – review & editing. ES: Writing – review & editing. SKB: Writing – review & editing.

Funding

The author(s) declare financial support was received for the research, authorship, and/or publication of this article. This study is funded by intramural research funding of ICMR-National JALMA Institute for Leprosy and Other Mycobacterial Diseases, Agra. Raj Pal Suman is acknowledged for technical help. DV was financially supported as PhD scholar by the Department of Science and Technology (DST), New Delhi (Award letter code. IF180309).

Conflict of interest

The authors declare that the research was conducted in the absence of any commercial or financial relationships that could be construed as a potential conflict of interest.

Publisher's note

All claims expressed in this article are solely those of the authors and do not necessarily represent those of their affiliated organizations, or those of the publisher, the editors and the reviewers. Any product that may be evaluated in this article, or claim that may be made by its manufacturer, is not guaranteed or endorsed by the publisher.

Supplementary material

The Supplementary material for this article can be found online at: https://www.frontiersin.org/articles/10.3389/fmicb.2023.1305974/full#supplementary-material

References

Akira, S., Uematsu, S., and Takeuchi, O. (2006). Pathogen recognition and innate immunity. *Cells* 124, 783–801. doi: 10.1016/j.cell.2006.02.015

Anoosheh, S., Farnia, P., Kargar, M., Kazem Poor, M., Seif, S., Noroozi, J., et al. (2009). Relationship between TNF-αGene polymorphisms and susceptibility to pulmonary tuberculosis. *J. Adv. Med. Biomed. Res.* 17, 45–54.

Barnes, P. F., Lu, S., Abrams, J. S., Wang, E., Yamamura, M., and Modlin, R. (1993). Cytokine production at the site of disease in human tuberculosis. *Infect. Immun.* 61, 3482–3489. doi: 10.1128/iai.61.8.3482-3489.1993

Basingnaa, A., Antwi-Bafour, S., Nkansah, D. O., Afutu, E., and Owusu, E. (2018). Plasma levels of cytokines (IL-10, IFN-γ and TNF-α) in multidrug resistant tuberculosis and drug responsive tuberculosis patients in Ghana. *Diseases* 7:2. doi: 10.3390/diseases7010002

Basu, J., Shin, D. M., and Jo, E. K. (2012). Mycobacterial signaling through toll-like receptors. *Front. Cell. Infect. Microbiol.* 2, 301–747. doi: 10.3389/fcimb.2012.00145

Ben-Kahla, I., and Sahal, A. H. (2016). Drug-resistant tuberculosis viewed from bacterial and host genomes. *Int. J. Antimicrob. Agents* 48, 353–360. doi: 10.1016/j.ijantimicag.2016.07.010

Berrington, W. R., and Hawn, T. R. (2007). *Mycobacterium tuberculosis*, macrophages, and the innate immune response: does common variation matter. *Immunol. Rev.* 219, 167–186. doi: 10.1111/j.1600-065X.2007.00545.x

Brightbill, H. D., Libraty, D. H., Krutzik, S. R., Yang, R. B., Belisle, J. T., Bleharski, J. R., et al. (1999). Host defense mechanisms triggered by microbial lipoproteins through toll-like receptors. *Science* 285, 732–736. doi: 10.1126/science.285.5428.732

Buwitt-Beckmann, U., Heine, H., Wiesmüller, K. H., Jung, G., Brock, R., Akira, S., et al. (2005). Toll-like receptor 6-independent signaling by diacylated lipopeptides. *Eur. J. Immunol.* 35, 282–289. doi: 10.1002/eji.200424955

Chen, Y. C., Hsiao, C. C., Chen, C. J., Chin, C. H., Liu, S. F., Wu, C. C., et al. (2010). Toll-like receptor 2 gene polymorphisms, pulmonary tuberculosis, and natural killer cell counts. *BMC Med. Genet.* 11, 1–10. doi: 10.1186/1471-2350-11-17

Cicchese, J. M., Evans, S., Hult, C., Joslyn, L. R., Wessler, T., Millar, J. A., et al. (2018). Dynamic balance of pro- and anti-inflammatory signals controls disease and limits pathology. *Immunol. Rev.* 285, 147–167. doi: 10.1111/imr.12671

Cooper, A. M. (2009). Cell-mediated immune responses in tuberculosis. *Annu. Rev. Immunol.* 27, 393–422. doi: 10.1146/annurev.immunol.021908.132703

Cooper, A. M., and Khader, S. A. (2008). The role of cytokines in the initiation, expansion, and control of cellular immunity to tuberculosis. *Immunol. Rev.* 226, 191–204. doi: 10.1111/j.1600-065X.2008.00702.x

Dittrich, N., Berrocal-Almanza, L. C., Thada, S., Goyal, S., Slevogt, H., Sumanlatha, G., et al. (2015). Toll-like receptor 1 variations influence susceptibility and immune response to Mycobacterium-tuberculosis. *Tuberculosis* 95, 328–335. doi: 10.1016/j.tube.2015.02.045

Donnelly, R. P., Freeman, S. L., and Hayes, M. P. (1995). Inhibition of IL-10 expression by IFN-gamma up-regulates transcription of TNF-alpha in human monocytes. *J. Immunol.* 155, 1420–1427. doi: 10.4049/jimmunol.155.3.1420

Ghasemian, R., Najafi, N., Yadgarinia, D., and Alian, S. (2009). Association between cigarette smoking and pulmonary tuberculosis in men: a case-control study in Mazandaran, Iran. *Iran. J. Clin. Infect. Dis.* 4, 135–141.

Grassin-Delyle, S., Abrial, C., Salvator, H., Brollo, M., Naline, E., and Devillier, P. (2020). The role of toll-like receptors in the production of cytokines by human lung macrophages. *J. Innate Immun.* 12, 63–73. doi: 10.1159/000494463

Guan, Y., Ranoa, D. R. E., Jiang, S., Mutha, S. K., Li, X., Baudry, J., et al. (2010). Human TLRs 10 and 1 share common mechanisms of innate immune sensing but not signaling. *J. Immunol.* 184, 5094–5103. doi: 10.4049/jimmunol.0901888

Haehnel, V., Schwarz Fischer, L., Fenton, M. J., and Rehli, M. (2002). Transcriptional regulation of the human toll-like receptor 2 gene in monocytes and macrophages. *J. Immunol.* 168, 5629–5637. doi: 10.4049/jimmunol.168.11.5629

Harling, K., Adankwah, E., Güler, A., Afum-Adjei Awuah, A., Adu-Amoah, L., Mayatepek, E., et al. (2019). Constitutive STAT3 phosphorylation and IL-6/IL-10 co-expression are associated with impaired T-cell function in tuberculosis patients. *Cell. Mol. Immunol.* 16, 275–287. doi: 10.1038/cmi.2018.5

Hernandez-Pando, R., Orozco, H., Arriaga, K., Sampieri, A., Larriva-Sahd, J., and Madrid-Marina, V. (1997). Analysis of the local kinetics and localization of interleukin-1 alpha, tumour necrosis factor-alpha and transforming growth factor-beta, during the course of experimental pulmonary tuberculosis. *Immunology* 90, 607–617. doi: 10.1046/j.1365-2567.1997.00193.x

Hook, J. S., Cao, M., Weng, K., Kinnare, N., and Moreland, J. G. (2020). *Mycobacterium tuberculosis* lipoarabinomannan activates human neutrophils via a TLR2/1 mechanism distinct from Pam3CSK4. *J. Immunol.* 204, 671–681. doi: 10.4049/jimmunol.1900919

Indian Council of Medical Research. *Ethical guidelines for biomedical research on human subjects*. New Delhi: Indian Council of Medical Research; (2017).

Jahantigh, D., Salimi, S., Alavi-Naini, R., Emamdadi, A., Owaysee Osquee, H., and Farajian Mashhadi, F. (2013). Association between TLR4 and TLR9 gene polymorphisms with development of pulmonary tuberculosis in Zahedan, southeastern Iran. *Sci. World J.* 2013:534053. doi: 10.1155/2013/534053

Juffermans, N. P., Verbon, A., Van Deventer, S. J., Van Deutekom, H. E. N. K., Speelman, P., and Van Der Poll, T. O. M. (1998). Tumor necrosis factor and interleukin-1 inhibitors as markers of disease activity of tuberculosis. *Am. J. Respir. Crit. Care Med.* 157, 1328–1331. doi: 10.1164/ajrccm.157.4.9709126

Keane, J., Remold, H. G., and Kornfeld, H. (2000). Virulent *Mycobacterium tuberculosis* strains evade apoptosis of infected alveolar macrophages. *J. Immunol.* 164, 2016–2020. doi: 10.4049/jimmunol.164.4.2016

Khan, A. U. H., Aslam, M. A., Hussain, I., Naz, A. G., Rana, I. A., Ahmad, M. M., et al. (2014). Role of toll-like receptor 2 (−196 to −174) polymorphism in susceptibility to pulmonary tuberculosis in Pakistani population. *Int. J. Immunogenet.* 41, 105–111. doi: 10.1111/iji.12086

Kumar, N. P., Moideen, K., Banurekha, V. V., Nair, D., and Babu, S. (2019). Plasma proinflammatory cytokines are markers of disease severity and bacterial burden in pulmonary tuberculosis. *Open Forum Infect. Dis.* 6:257. doi: 10.1093/ofid/ofz257

Ma, X., Liu, Y., Gowen, B. B., Graviss, E. A., Clark, A. G., and Musser, J. M. (2007). Full-exon resequencing reveals toll-like receptor variants contribute to human susceptibility to tuberculosis disease. *PLoS One* 2, 1–9. doi: 10.1371/journal.pone.0001318

Mattos, A. M. M., Almeida, C. S., Franken, K. L. M. C., Alves, C. C. S., Abramo, C., de Souza, M. A., et al. (2010). Increased IgG1, IFN-gamma, TNF-alpha and IL-6 responses to *Mycobacterium tuberculosis* antigens in patients with tuberculosis are lower after chemotherapy. *Int. Immunol.* 22, 775–782. doi: 10.1093/intimm/dxq429

Miller, S. A., Dykes, D., and Polesky, H. (1988). A simple salting out procedure for extracting DNA from human nucleated cells. *Nucleic Acids Res.* 16:1215. doi: 10.1093/nar/16.3.1215

Mittal, M., Biswas, S. K., Singh, V., Arela, N., Katoch, V. M., Das, R., et al. (2018). Association of Toll like receptor 2 and 9 gene variants with pulmonary tuberculosis: exploration in a northern Indian population. *Mol. Biol. Rep.* 45, 469–476. doi: 10.1007/s11033-018-4182-z

Nakaya, M., Yoneda, T., Yoshikawa, M., Tsukaguchi, K., Tokuyama, T., Fu, A., et al. (1995). The evaluation of interleukin-8 (IL-8) and tumor necrosis factor-α(TNF-α) level in peripheral blood of patients with active pulmonary tuberculosis. *Kekkaku (Tuberculosis)* 70, 461–466. doi: 10.11400/kekkaku1923.70.461

Guidelines on Programmatic Management of Drug-Resistant Tuberculosis in India. (2017). Revised National Tuberculosis Control Programme. Central TB Division, Directorate General of Health Services.

Nemeth, J., Winkler, H. M., Boeck, L., Adegnika, A. A., Clement, E., Mve, T. M., et al. (2011). Specific cytokine patterns of pulmonary tuberculosis in Central Africa. *Clin. Immunol.* 138, 50–59. doi: 10.1016/j.clim.2010.09.005

Noguchi, E., Nishimura, F., Fukai, H., Kim, J., Ichikawa, K., Shibasaki, M., et al. (2004). An association study of asthma and total serum immunoglobin E levels for toll-like receptor polymorphisms in a Japanese population. *Clin Exp Allergy* 34, 177–183. doi: 10.1111/j.1365-2222.2004.01839.x

Ogus, A. C., Yoldas, B., Ozdemir, T., Uguz, A., Olcen, S., Keser, I., et al. (2004). The Arg753GLn polymorphism of the human toll-like receptor 2 gene in tuberculosis disease. *Eur. Respir. J.* 23, 219–223. doi: 10.1183/09031936.03.00061703

Omueti, K. O., Beyer, J. M., Johnson, C. M., Lyle, E. A., and Tapping, R. I. (2005). Domain exchange between human toll-like receptors 1 and 6 reveals a region required for lipopeptide discrimination. *J. Biol. Chem.* 280, 36616–36625. doi: 10.1074/jbc.M504320200

Pankow, W., Neumann, K., Rüschoff, J., Schröder, R., and von Wichert, P. (1991). Reduction in HLA-DR antigen density on alveolar macrophages of smokers. *Lung* 169, 255–262. doi: 10.1007/BF02714161

Salie, M., Daya, M., Lucas, L. A., Warren, R. M., van der Spuy, G. D., van Helden, P. D., et al. (2015). Association of toll-like receptors with susceptibility to tuberculosis suggests sex-specific effects of TLR8 polymorphisms. *Infect. Genet. Evol.* 34, 221–229. doi: 10.1016/j.meegid.2015.07.004

Schuring, R. P., Hamann, L., Faber, W. R., Pahan, D., Richardus, J. H., Schumann, R. R., et al. (2009). Polymorphism N248S in the human toll-like receptor 1 gene is related to leprosy and leprosy reactions. *J. Infect. Dis.* 199, 1816–1819. doi: 10.1086/599121

Schurz, H., Daya, M., Möller, M., Hoal, E. G., and Salie, M. (2015). TLR1, 2, 4, 6 and 9 variants associated with tuberculosis susceptibility: a systematic review and meta-analysis. *PLoS One* 10:e0139711. doi: 10.1371/journal.pone.0139711

Sia, J. K., and Rengarajan, J. (2019). Immunology of *Mycobacterium tuberculosis* infections. *Microbiol. Spectr.* 7, 10–1128. doi: 10.1128/microbiolspec.gpp3-0022-2018

Sinha, E., Biswas, S. K., Mittal, M., Bajaj, B., Singh, V., Arela, N., et al. (2014). Toll-like receptor 1 743 A>G, 1805 T>G & Toll-like Receptor 6 745 C>T gene polymorphism and tuberculosis: a case control study of north Indian population from Agra (India). *Hum. Immunol.* 75, 880–886. doi: 10.1016/j.humimm.2014.06.014

Tahara, T., Arisawa, T., Wang, F., Shibata, T., Nakamura, M., Sakata, M., et al. (2008). Toll-like receptor 2 (TLR) -196 to -174 del polymorphism in gastro-duodenal diseases in Japanese population. *Dig. Dis. Sci.* 53, 919–924. doi: 10.1007/s10620-007-9950-x

Takeuchi, O., Sato, S., Horiuchi, T., Hoshino, K., Takeda, K., Dong, Z., et al. (2002). Cutting edge: role of toll-like receptor 1 in mediating immune response to microbial lipoproteins. *J. Immunol.* 169, 10–14. doi: 10.4049/jimmunol.169.1.10

TB India. (2017). Revised National Tuberculosis Control Programme, Annual Status Report. *Central TB Division, Director General of Health Services, Ministry of Health and Family Welfare,* New Delhi. www.tbcindia.gov.in

Thada, S., Valluri, V. L., and Gaddam, S. L. (2013). Influence of toll-like receptor gene polymorphisms to tuberculosis susceptibility in humans. *Scand. J. Immunol.* 78, 221–229. doi: 10.1111/sji.12066

Tötemeyer, S., Sheppard, M., Lloyd, A., Roper, D., Dowson, C., Underhill, D., et al. (2006). IFN-gamma enhances production of nitric oxide from macrophages via a mechanism that depends on nucleo-tide oligomerization domain-2. *J. Immunol.* 176, 4804–4810. doi: 10.4049/jimmunol.176.8.4804

Uciechowski, P., Imhoff, H., Lange, C., Meyer, C. G., Browne, E. N., Kirsten, D. K., et al. (2011). Susceptibility to tuberculosis is associated with TLR1 polymorphisms resulting in a lack of TLR1 cell surface expression. *J. Leukoc. Biol.* 90, 377–388. doi: 10.1189/jlb.0409233

Varshney, D., Singh, S., Sinha, E., Mohanty, K. K., Kumar, S., Barik, S. K., et al. (2022). Systematic review and meta-analysis of human toll-like receptors genetic polymorphisms for susceptibility to tuberculosis infection. *Cytokine* 152:155791. doi: 10.1016/j.cyto.2021.155791

Velez, D. R., Wejse, C., Stryjewski, M. E., Abbate, E., Hulme, W. F., Myers, J. L., et al. (2010). Variants in toll-like receptors 2 and 9 influence susceptibility to pulmonary tuberculosis in Caucasians, African-Americans, and west Africans. *Hum. Genet.* 127, 65–73. doi: 10.1007/s00439-009-0741-7

Vidya, M. K., Kumar, V. G., Sejian, V., Bagath, M., Krishnan, G., and Bhatta, R. (2018). Toll-like receptors: significance, ligands, signaling pathways, and functions in mammals. *Int. Rev. Immunol.* 37, 20–36. doi: 10.1080/08830185.2017.1380200

Vijay, K. (2018). Toll-like receptors in immunity and inflammatory diseases: past, present, and future. *Int. Immunopharmacol.* 59, 391–412. doi: 10.1016/j.intimp.2018.03.00

World Health Organization. (2022) Global tuberculosis report.

Wu, L., Hu, Y., Li, D., Jiang, W., and Xu, B. (2015). Screening toll-like receptor markers to predict latent tuberculosis infection and subsequent tuberculosis disease in a Chinese population. *BMC Med. Genet.* 16, 19–11. doi: 10.1186/s12881-015-0166-1

Yao, X., Liu, Y., Liu, Y., Liu, W., Ye, Z., Zheng, C., et al. (2017). Multiplex analysis of plasma cytokines/chemokines showing different immune responses in active TB patients, latent TB infection and healthy participants. *Tuberculosis (Edinb)* 107, 88–94. doi: 10.1016/j.tube.2017.07.013

Yu, G. P., Hsieht, C. C., and Peng, J. (1988). Risk factors associated with the prevalence of pulmonary tuberculosis among sanitary workers in Shanghai. *Tubercle* 69, 105–112. doi: 10.1016/0041-3879(88)90072-4

Zarember, K. A., and Godowski, P. J. (2002). Tissue expression of human toll-like receptors and differential regulation of toll-like receptor mRNAs in leukocytes in response to microbes, their products, and cytokines. *J. Immunol.* 168, 554–561. doi: 10.4049/jimmunol.168.2.554

Zhou, Y., and Zhang, M. (2020). Associations between genetic polymorphisms of TLRs and susceptibility to tuberculosis: a meta-analysis. *Innate Immun.* 26, 75–83. doi: 10.1177/1753425919862354

frontiers | Frontiers in Microbiology

TYPE Review
PUBLISHED 06 February 2024
DOI 10.3389/fmicb.2024.1331508

OPEN ACCESS

EDITED BY
Matt Johansen,
University of Technology Sydney, Australia

REVIEWED BY
Peter Sander,
University of Zurich, Switzerland
Shabir A. Bhat,
University of California, Los Angeles,
United States

*CORRESPONDENCE
Jichan Jang
✉ jichanjang@gnu.ac.kr

RECEIVED 01 November 2023
ACCEPTED 17 January 2024
PUBLISHED 06 February 2024

CITATION
Nguyen TQ, Heo BE, Jeon S, Ash A, Lee H, Moon C and Jang J (2024) Exploring antibiotic resistance mechanisms in *Mycobacterium abscessus* for enhanced therapeutic approaches.
Front. Microbiol. 15:1331508.
doi: 10.3389/fmicb.2024.1331508

Exploring antibiotic resistance mechanisms in *Mycobacterium abscessus* for enhanced therapeutic approaches

Thanh Quang Nguyen[1], Bo Eun Heo[1], Seunghyeon Jeon[1], Anwesha Ash[1], Heehyun Lee[1], Cheol Moon[2] and Jichan Jang[1]*

[1]Division of Life Science, Department of Bio & Medical Big Data (BK21 Four Program), Research Institute of Life Science, Gyeongsang National University, Jinju, Republic of Korea, [2]Department of Clinical Laboratory Science, Semyung University, Jecheon, Republic of Korea

Mycobacterium abscessus, a leading cause of severe lung infections in immunocompromised individuals, poses significant challenges for current therapeutic strategies due to resistance mechanisms. Therefore, understanding the intrinsic and acquired antibiotic resistance of *M. abscessus* is crucial for effective treatment. This review highlights the mechanisms employed by *M. abscessus* to sustain antibiotic resistance, encompassing not only conventional drugs but also newly discovered drug candidates. This comprehensive analysis aims to identify novel entities capable of overcoming the notorious resistance exhibited by *M. abscessus*, providing insights for the development of more effective therapeutic interventions.

KEYWORDS

***Mycobacterium abscessus*, mycobacterium drug efficacy, drug resistance, efflux pump, intrinsic-extrinsic drug resistance**

1 Introduction

Non-tuberculous mycobacteria (referred to as NTMs hereafter) have emerged as a significant public health concern, with steadily increasing morbidity and mortality rates worldwide, eventually surpassing those of tuberculosis (Howard et al., 2006; Wassilew et al., 2016). NTM infections are opportunistic diseases primarily affecting individuals with compromised immune systems, such as patients with cystic fibrosis (*CF*), chronic obstructive pulmonary disease, renal failure, transplant recipients with chronic corticosteroid use, TNF-α, and leukemia (Faria et al., 2015). While NTM infections most commonly occur in the lungs, they can also develop in other organs. Importantly, NTM infections are rarely contagious, signifying that they do not spread from person to person, distinguishing them from other types of respiratory infections (Swenson et al., 2018; Lipman et al., 2021).

Mycobacterium abscessus (referred to as *Mab* hereafter) is the second most significant pathogen in NTM-induced pulmonary disease, and it is increasingly emerging as the most prominent and concerning pathogen in hospitals and *CF* centers worldwide (Degiacomi et al., 2019). *Mab* was firstly isolated in 1952 by Moore and Frerichs from a 63-year-old woman's knee abscess and it was classified as *Mycobacterium chelonae* subsp. *abscessus* (MOORE and FRERICHS Moore and Frerichs, 1953; Victoria et al., 2021). However, *Mab* was recognized as an independent species from *M. chelonae* based on DNA hybridization and two new species *Mycobacterium massiliense* and *Mycobacterium bolletii* were described as novel and closely

related to *Mab* based on the *rpoB* gene sequence (Lee et al., 2015; Lopeman et al., 2019; Victoria et al., 2021). However, since all these thee species share more than 70% relatedness based on DNA–DNA hybridization, *M. massiliense*, *M. bolletii*, and *M. abscessus* were presented as subspecies such as *Mab* subsp. *abscessus*, *Mab* subsp. *bolletti*, and *Mab* subsp. *massiliense* (hereafter referred to as *M. abscessus*, *M. bolletii*, and *M. massiliense*) and the combinations of the three subspecies were known as *Mab* complex (Lopeman et al., 2019; Victoria et al., 2021). The genome of *Mab* (CIP 104536T) comprise 5,067,172-bp circular chromosome including 4,920 predicted coding sequences (CDS), an 81-kb full-length prophage and 5 IS elements, and a 23-kb mercury resistance plasmid almost identical to pMM23 from *Mycobacterium marinum* (Ripoll et al., 2009). *Mab* complex is responsible for 2.6–13.0% of all NTM pulmonary infections (Dedrick et al., 2023). The natural habitat of *Mab* is in soil and water sources, leading to a high rate of human-pathogen contact. Furthermore, nosocomial outbreaks and the transmission of *Mab* have been continuously occurring in clinics that conduct cosmetic surgery, liposuction, mesotherapy, or intravenous infusion of cell therapy (Lee et al., 2015; Desai and Hurtado, 2018). Nosocomial outbreaks of *Mab* through *Mab* contaminated surgical materials and hospital tap water, have also been reported as well in patients without *CF* (Baker et al., 2017; Fernandes Garcia de Carvalho et al., 2018). While it was previously believed that a significant portion of *Mab* infections in *CF* patients originated from exposure to sources such as soil, household dust, or water, potentially through contact with contaminated objects (fomites) or airborne particles (aerosols) (Falkinham, 2011), recent studies indicate that individuals with *CF* can also be infected through person-to-person transmission through hospital-based (Bryant et al., 2016). Additionally, a study by Ruis et al. suggests that dominant *Mab* circulating clones initially emerged within non-*CF* populations and were later amplified and spread within the *CF* community. Consequently, individuals with *CF* might be more permissible hosts, while non-*CF* individuals play a crucial role in transmission networks, potentially facilitating long-distance spread. This conclusion was drawn from an evolutionary phylogenetic analysis employing whole-genome sequences of clinical isolates from 1,178 *CF* and non-*CF* individuals across five continents (Ruis et al., 2021).

For the aspect of *Mab* diagnosis, there is frequent misdiagnosis of *Mab* as *M. tuberculosis* (referred to as *Mtb*), primarily due to the visual similarities observed in sputum samples under microscopic analysis (Wu et al., 2018). These circumstances not only lead to incorrect treatments but also have significant consequences, including the underestimation of NTM incidence and the inefficient allocation of budgetary resources dedicated to combating the disease. Moreover, it's crucial to recognize that monotherapies alone are insufficient to fully eradicate the microbiological infection. According to the latest 2020 ATS/ERS/ESCMID/IDSA clinical practice guidelines, the treatment for *Mab* pulmonary disease is categorized based on macrolide susceptibility. For macrolide-susceptible cases, the guidelines recommend an initial phase with 1–2 parenteral drugs (amikacin; AMK, imipenem; IMP, cefoxitin; CFX, and tigecycline; TGC) and two oral drugs (azithromycin; AZM, clofazimine; CFZ, and linezolid; LZ), along with inhaled AMK. In the case of macrolide-resistant organisms, the recommendations include an initial phase with 2–3 parenteral drugs (AMK, IMP, CFX, and TGC) and 2–3 oral drugs (AZM, CFZ, and LZ), supplemented with inhaled AMK. The addition of AZM is for its immunomodulatory effect, although adherence to these guidelines may have adverse effects on NTM patients (Moguillansky et al., 2023). However, *Mab* has demonstrated resistance to a broad spectrum of antibiotics, including the aforementioned treatment regimen, and patients experience multiple relapses with low cure rates, making it challenging to achieve a complete cure (Victoria et al., 2021). This discouraging success rate primarily stems from the rapid development of drug resistance, which can be attributed to both intrinsic and acquired multidrug resistance to antibiotics. Notably, even first-line anti-TB medications, such as isoniazid (INH) and rifampicin (RFP), lack efficacy against *Mab* (Zheng et al., 2023). As a result, the majority of *Mab* treatment protocols involve extended multi-antibiotic regimens that can last up to 24 months (Wu et al., 2018; Ratnatunga et al., 2020). However, the effectiveness of these treatments remains limited, with disease remission rates reaching only 30% (Wu et al., 2018; Ratnatunga et al., 2020). Additionally, in cases of pulmonary infections, no class of antibiotics has demonstrated the ability to achieve long-term sputum smear conversion (Wu et al., 2018; Ratnatunga et al., 2020).

The three subspecies of *Mab* shows distinct clinical outcomes (Blauwendraat et al., 2012; Harada et al., 2012; Shin et al., 2013; Jeong et al., 2017; Abate et al., 2019). Firstly, *M. abscessus* exhibits resistance to macrolides such as AZM and clarithromycin (CLR) due to an adaptive resistance mechanism involving the inducible erythromycin ribosomal methyltransferase, *erm(41)* (Stout and Floto, 2012; Rubio et al., 2015; Christianson et al., 2016; Abate et al., 2019). Consequently, the use of macrolides in treating *M. abscessus* infections should be approached with great caution (Maurer et al., 2014). Secondly, *M. massiliense* is the most recent subspecies within this group and has a broader geographical distribution compared to the other subspecies. Notably, this subspecies tends to yield more favorable clinical outcomes than the other two, primarily because it lacks the functional *erm* gene. Lastly, *M. bolletii* represents the rarest among the three subspecies and is also resistant to CLR.

However, our understanding of the intrinsic or acquired antibiotic resistance of *Mab* remains limited. Therefore, alongside the ongoing efforts to discover novel alternative compounds for *Mab* treatment, it is crucial to elucidate the resistance mechanisms employed by *Mab* against existing antibiotics. This endeavor not only aids in enhancing the effectiveness of current antibiotics to overcome these resistance barriers but also provides valuable insights for the development of new compounds. This review aims to offer a comprehensive overview of the current knowledge of antibiotic resistance mechanisms in *Mab*, with the goal of clarifying the molecular components contributing to its significant resistance to chemotherapy and facilitating the development of a drug pipeline for *Mab*.

1.1 Drug discovery and limitations

The quantity of initiatives in antimicrobial drug development has significantly diminished since the remarkable era of antibiotic discovery, and several factors contribute to this decline. Firstly, the increasing prevalence of drug-resistant bacteria limits the effectiveness of new antibiotics, making it challenging to recoup investments in antibiotic development. Secondly, antibiotics are typically prescribed for short durations, in contrast to drugs for chronic conditions like hypertension or diabetes, which may render antibiotics less financially

appealing to pharmaceutical companies. Thirdly, novel effective drugs are often preserved as last-resort treatments for highly-resistant bacterial infections. The goal is to mitigate the development of further resistance by limiting their widespread use. Overuse or misuse of these potent drugs can accelerate the emergence of resistant strains, making them ineffective sooner. Overexposure can diminish their efficacy over time, making it crucial to reserve them for cases where no other options are viable (Baker et al., 2017). Lastly, the discovery of new antibiotics presents scientific challenges (Ventola, 2015; Quang and Jang, 2021). Finding compounds that are both effective against bacteria and safe for humans is a complex process, and success is not guaranteed (Chopra et al., 2011). The identification and development of innovative and potent medications for combating NTMs are of paramount importance in the medical field. In comparison to the tuberculosis drug pipeline, which features a significant number of compounds undergoing clinical trials, the NTMs drug pipeline lags considerably (Wu et al., 2018). Notably, there is a critical need for the development of new treatments targeting *Mab* as there are currently no antibiotics approved by the Food and Drug Administration (FDA) for *Mab* infection.

Two primary strategies exist to bolster the development of effective *Mab*-targeting medicines. The first strategy follows the conventional drug development process, which encompasses the identification of novel chemical compounds. This process commences with drug screening using chemical and natural product libraries, progressing through hit identification, lead optimization, target identification, comprehensive preclinical investigations, and ultimately clinical trials (Egorova et al., 2021). Various screening methods have been employed in this pursuit for *Mab* drug discovery, including reporter-based assays, resazurin-based microplate assays, and image-based phenotypic screens (Gupta et al., 2017; Jeong et al., 2018; Richter et al., 2018; Kim et al., 2019; Malin et al., 2019; Hanh et al., 2020a,b). Nevertheless, despite these efforts, promising new chemical leads ready for clinical trials and market release remain scarce (Hanh et al., 2020a). This challenge may be attributed to the intrinsic drug-resistant mechanisms of *Mab*, resulting in a low hit rate for compounds targeting this bacterium (Malin et al., 2019). It's noteworthy that the hit rate achieved in *Mab* screens is significantly lower than what is typically observed in screens targeting *Mtb* (Malin et al., 2019; Hanh et al., 2020a). Moreover, recent *Mab* drug screens have relied on conventional libraries composed of known antimycobacterial or antibacterial agents (Malin et al., 2019), diminishing the likelihood of identifying novel compounds targeting new mechanisms of action. Hence, there is an urgent need to develop new libraries with expanded chemical diversity to discover unique compounds. Additionally, reliable cell-based or *in vivo* assessment/screening methods that accurately mimic the host environment infected with *Mab* are imperative to advance our understanding and discovery of effective treatments for *Mab*-induced human infections (Carvalho et al., 2011; Bernut et al., 2014, 2015). The second strategy involves repurposing or repositioning existing medications for novel therapeutic indications. Most contemporary antibiotics and potential prospects against *Mab* have origins in the repurposing of pre-existing drugs or the cross-testing of compounds with activity and various mechanism of action against *Mtb* (Egorova et al., 2021). This method is particularly intriguing in the field of antibacterials, as the rapid evolution of resistance often outpaces the pace of medication development (Egorova et al., 2021). Repurposing previously approved pharmaceuticals can expedite the development process and reduce expenses (Egorova et al., 2021). Regrettably, the *Mab* drug pipeline remains underpopulated (Ganapathy and Dick, 2022). Currently, there are four recruiting, four completed, one terminated, and two non-recruiting clinical trials evaluating drug efficacy in *Mab* infection (NIH ClinicalTrials, 2023). However, these clinical trials have primarily utilized existing antibiotics through various drug delivery methods, including inhalation, novel drug encapsulation using biocompatible liposomes, and the exploration of new drug combinations (Quang and Jang, 2021). The primary reason for the limited success in anti-*Mab* drug discovery is the remarkable intrinsic resistance capabilities of *Mab* and its rapid acquired resistance against currently available active drugs (Wu et al., 2018).

2 Mechanisms of *Mab* resistance to current antibiotics

Inherent drug resistance in NTMs is responsible for their limited susceptibility to a wide range of medicines and chemicals (Wu et al., 2018). This inherent resistance in *Mab* and other mycobacterial species can be attributed to several factors, including the presence of a waxy impermeable cell wall that acts as both a physical (size exclusion) and a chemical (hydrophobic) barrier, drug export systems, enzymes capable of modifying drugs or target enzymes, and genetic polymorphisms in target genes (Nessar et al., 2012) (Figure 1). In addition to harboring numerous intrinsic resistance mechanisms, *Mab* possesses the ability to acquire novel resistance through genetic changes that can be passed down to subsequent generations. Acquired resistance is not linked to genes introduced by transmissible genetic elements like plasmids and transposons (Martin et al., 1990). Instead, resistance arises due to spontaneous mutations occurring at specific genes in response to the presence of antibiotics following extended courses of treatment (Johansen et al., 2020b). This allows bacteria to undergo genetic changes in the target gene or other associated genes, resulting in the acquisition of significant levels of resistance, rendering the medicine ineffective. However, species or subspecies may exhibit variations in their antibiotic resistance phenotype and genotype, emphasizing the need for research on accurately identified strains (Nessar et al., 2012). In this section, we focus on intrinsic and acquired resistance to essential drugs and new drug candidates that have demonstrated efficacy against *Mab*.

2.1 Mycobacterial cell envelope

Mycobacteria's cell wall is primarily composed of lipids, specifically mycolic acids, constituting a significant portion (up to 60%) of the bacteria's overall dry mass (Brennan and Nikaido, 1995). This cell wall features a waxy composition that serves as a physical barrier (Nessar et al., 2012), rendering mycobacteria less permeable than the outer membranes of gram-negative bacteria. In more detail, the mycobacterial envelope consists of three distinct layers: a typical plasma membrane, a complex cell wall, and an outer layer. The cell wall, notably, comprises a thick peptidoglycan layer covalently linked to arabinogalactan, which is esterified by mycolic acids, forming the inner leaflet of the mycomembrane (Figure 2). This unique structure inherently makes mycobacteria resistant to many antimicrobials.

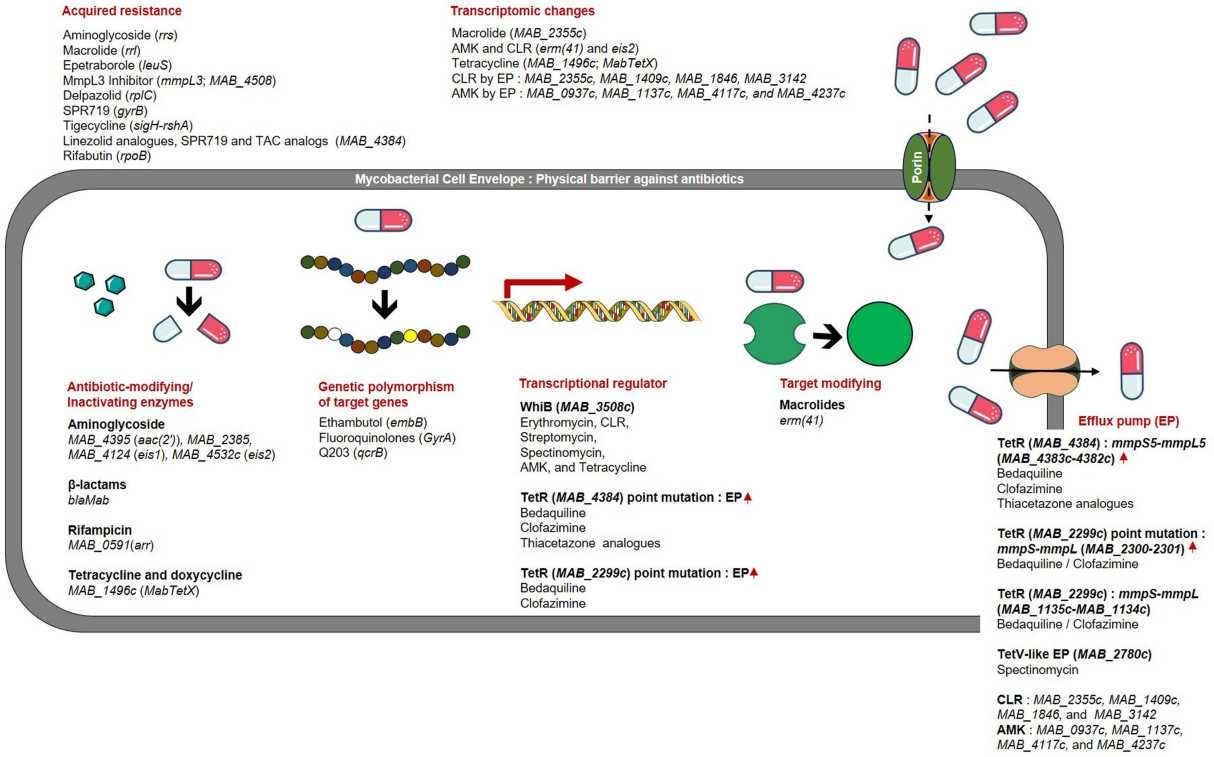

FIGURE 1
Drug resistance mechanisms and related genes in *Mab*.

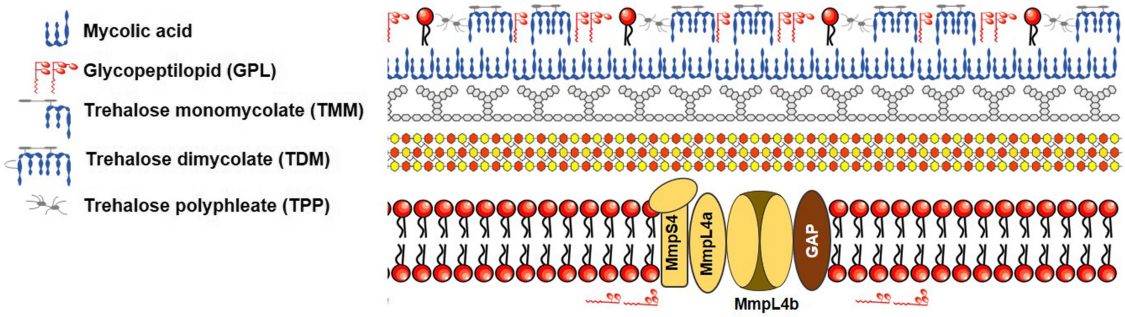

FIGURE 2
Schematic representation of mycobacterial cell envelope based on the figure of Gutiérrez et al.

Hydrophilic drugs penetrate the mycobacterial cell wall slowly due to the inefficiency of mycobacterial porin in allowing antibiotic permeation, resulting in low antibiotic concentrations within the bacteria. The dense mycobacterial cell wall not only shields the bacterium from stressors but also poses challenges in nutrient uptake from the environment. To address this, mycobacteria often produce porins, proteins that create limited pathways for nutrient absorption. The expression of these porins is closely tied to the growth rate of NTMs, and they provide a conduit for certain antimicrobial agents to enter the mycobacterial cell (Saxena et al., 2021). Lipophilic agents may be hindered by the lipid bilayer, which has unusually low fluidity and thickness (Jarlier and Nikaido, 1994; Gutiérrez et al., 2018).

Intriguingly, *Mycobacterium chelonae*, a species closely related to *Mab* due to its nearly identical biochemical features, has a cell envelope that is about 10–20 times less permeable than that of *Mtb* (Jarlier and Nikaido, 1994). Similar to *Mtb*, *Mab* possesses a mycobacterial cell wall with low permeability, which contributes to its drug resistance. Notably, like *Mtb*, *Mab* is thought to regulate cell wall structure and homeostasis through lipoprotein glycosylation. For example, the absence of protein-O-mannosyltransferase Pmt (*MAB_1122c*) in *Mab* leads to increased cell wall permeability and greater susceptibility to antibiotics such as RFP (Ganapathy et al., 2019). Furthermore, glycosylation of lipoproteins limits cell wall permeability to antibiotics like β-lactam agents that inhibit peptidoglycan synthesis. In β-lactam

drug resistance, mycobacterial porins also play a role by facilitating the transport of small hydrophilic drugs across the membrane. Once antibiotics are internalized, they can reach their target in the cytoplasm and activate potential internal drug resistance mechanisms, collectively known as the "intrinsic resistome." This resistome includes efflux pumps, antibiotic-modifying/inactivating enzymes, target-modifying enzymes, and genes conferring metal resistance (Nguyen and Thompson, 2006; Nessar et al., 2012).

Remarkably, unlike *Mtb*, *Mab* exhibits two distinct colony morphotypes: smooth non-cording (S) and rough cording morphotype (R). These differences in morphotypes depend on the presence or absence of cell surface-associated glycopeptidolipids (GPL), respectively (Howard et al., 2006). This distinctive property, associated with GPL status, affects sliding motility, biofilm formation, and drug susceptibility. For example, S morphotype strains that contain GPL, such as *M. abscessus* and *M. bolletii*, facilitate sliding across the surface and biofilm formation. Indeed, the *Mab* growing inside biofilms become tolerant to antibiotics due to physical barrier that can prevent the intracellular penetration of compounds. In fact, *in vitro* biofilm models of *Mab* have been exhibited to have decreased susceptibility to several first-line antibiotics, such as cefoxitin, amikacin, and clarithromycin (Greendyke and Byrd, 2008; Marrakchi et al., 2014). Conversely, R morphotype strains exhibit aggregation and cording. Recent studies suggest that *Mab* R strains are capable of growing in biofilm-like structures, which, similar to S biofilms, show greater tolerance than planktonic cultures to acidic pH, hydrogen peroxide, and treatment with antibiotics like AMK, AZM, and β-lactams (Gutiérrez et al., 2018; Story-Roller et al., 2018; Daher et al., 2022; López-Roa et al., 2022). Furthermore, biofilms formed by R colony types display higher mechanical resistance compared to those formed by S colony types (López-Roa et al., 2022). Biofilms also inhibit oxygen and nutrients from entering the cell, which causes a reduction *Mab* metabolism and, consequently, an increased tolerance to a harsh environment such as antibiotics treatment. Therefore, compounds that specifically target biofilm formation during antibiotic therapy are a new therapeutic strategy for clearance of *Mab.*

In invasive infections causing pulmonary colonization, *Mab* R strains are accountable for producing higher levels of trehalose dimycolate, consequently leading to the formation of massive bacterial cords. With the rough variant, the entire phagosome quickly merges with the lysosome, inducing phagosomal acidification and activating apoptosis and autophagy (Roux et al., 2016; López-Roa et al., 2022). This robust apoptosis-driven cell-death activity facilitates the extracellular replication of the R variant through rapid cord formation, preventing the engulfment of bacilli by neutrophils and macrophages. This process leads to abscess formation, tissue destruction, and acute infection (Jönsson et al., 2013; Bernut et al., 2016; López-Roa et al., 2022).

2.2 Antibiotic-modifying/inactivating enzymes and acquired drug resistance

2.2.1 Aminoglycosides (AGs)

Mab produces enzymes capable of modifying antibiotics by cleaving, altering their structure, and adding or removing chemical groups (Luthra et al., 2018). These modifications can render antibiotics ineffective by either preventing their binding to their target or increasing their susceptibility to hydrolysis by the bacteria (Luthra et al., 2018). The efficacy of antibiotics was restored when these modifying genes were knocked down (Nessar et al., 2012). AG antibiotics are composed of amino carbohydrates linked by glycoside bonds (Mingeot-Leclercq et al., 1999). Among antibacterial drugs, AMK has shown the most efficacy against *Mab* (Tsai et al., 2015). AGs can diffuse through porins and interact with 30S ribosomes (e.g., streptomycin), 50S ribosomes (others), or both 30S and 50S ribosomes (Chulluncuy et al., 2016). This interaction prevents the initiation of protein synthesis, the continuation of translation, or the incorporation of incorrect proteins (Bhattacharjee, 2016). Unfortunately, *Mab* has developed resistance to aminoglycosides. *Mab's* genome annotation suggests the presence of various AG-modifying enzymes, including AG phosphotransferases, AG nucleotidyltransferases, and AG acetyltransferases (AACs). Among these, AG AAC (2′-N-acetyltransferase) and AG phosphotransferases render AG antibiotics inactive by transferring acetyl or phosphate residues to crucial positions within the antibiotic (Nessar et al., 2012) (Supplementary Figures S1, S2). *Mab*'s genome analysis and AG drug susceptibility testing indicate the presence of several putative AACs, which acetylate aminoglycosides with a 2′ amino group, such as gentamicin, tobramycin, and KM. ORF *MAB_4395* is annotated as a putative AG 2′-N-acetyltransferase [*aac(2′)*], and *aac(2′)* deletion mutants increased *Mab*'s susceptibility to KM-B, tobramycin, dibekacin, and gentamicin C (Rominski et al., 2017b). Furthermore, *MAB_2385*, which serves as the main determinant of resistance to the first-discovered aminoglycoside, streptomycin, functions as a 3″-O-phosphotransferase. Deletion of *MAB_2385* in *Mab* increases susceptibility to streptomycin, while introducing *MAB_2385* in *M. smegmatis* (*Msm*) confers resistance to streptomycin (Dal Molin et al., 2017). In addition to *MAB_4395* and *MAB_2385*, *Mab* possesses additional AG-modifying enzymes named Eis (enhanced intracellular survival), including *MAB_4124* (also known as *eis1*; sharing 33% identity with *Mtb Rv2416c*) and *MAB_4532c* (*eis2*), which are involved in AG resistance. *MAB_4532c* significantly enhances *Mab*'s intracellular survival and has been shown to modify KM, hygromycin, and AMK *in vitro* (Ung et al., 2019). Deletion of *MAB_4532c* strains increased *Mab*'s susceptibility to AGs and capreomycin (Rominski et al., 2017b; Johansen et al., 2020b). Furthermore, MAB_4532c is responsible for the lack of bactericidal activity of AMK *in vitro* and affected AMK activity *in vivo* (Lorè et al., 2022; Selchow et al., 2022).

Clinically acquired pan-AG resistance is linked to mutations in ribosomal RNA genes, specifically *rrs*, which encode the 16S rRNA molecule as acquired resistance (Rominski et al., 2017b). The prolonged use of AGs can lead to genetic modifications in *rrs* (Wallace et al., 1996; Prammananan et al., 1998; Maurer et al., 2012). It's worth noting that the substitution of adenine with guanine at position 1408 (A1408G) in *rrs* significantly increases resistance to KM, AMK, and tobramycin (Nessar et al., 2011). Recently, two novel *rrs* mutations, C1496T and T1498A, were also identified from *Mab*-pulmonary disease patients (Young et al., 2021). Additionally, mutations at locations T1406A, C1409T, and G1491T in *rrs* could potentially confer a high level of resistance to KM, AMK, and gentamicin (Nessar et al., 2011).

Apramycin (AP; also known as Nebramycin II) is presently authorized by the Veterinary Medicines Directorate in the UK for use in pigs, cattle, rabbits, and chickens. It is available either as (i) a premix for medicated feedstuff (200 g/kg, 100,000 IU/g, 100 g/kg) or (ii) a

soluble powder for oral solution, with a concentration of 10% or less (Moore et al., 2018). AP has a distinctive AG structure and demonstrates potent activity against *Mab* (Selchow et al., 2022). Furthermore, it displays minimal cross-resistance to other aminoglycosides and exhibits favorable therapeutic lung exposure and a low toxicity profile (Matt et al., 2012; Ishikawa et al., 2019; Juhas et al., 2019; Becker et al., 2021; Selchow et al., 2022). Recently, Selchow et al., reported that AP is not modified by Eis2 or Aac(2′) and is not affected by the multidrug resistance regulator WhiB7. This favorable feature of apramycin is reflected in a mouse model of pulmonary *Mab* infection, which demonstrates superior activity, compared with amikacin (Selchow et al., 2022). At present, there are no established antibiotic breakpoints for AP against *Mab* provided by organizations like EUCAST (The European Committee on Antimicrobial Susceptibility Testing) or CLSI (Clinical & Laboratory Standards Institute). Pharmacokinetic/pharmacodynamics studies are essential to address this gap for AP in treating chronic *Mab* infections in humans. This evaluation process holds significant importance for approval by the FDA and the European Medicines Agency (EMA) (Moore et al., 2018). Albeit, AP is currently promising agent as Mab treatment option together with other candidates such as RFB and omadacycline (OMC).

2.2.2 β-Lactam

Beta-lactams are a class of antibiotics characterized by a four-atom beta-lactam ring (De Rosa et al., 2021). They are among the most widely prescribed antibiotics due to their broad spectrum of activity against bacteria (De Rosa et al., 2021). Beta-lactam antibiotics are bactericidal because they inhibit the cross-linking or transpeptidation of the peptidoglycan layer in bacterial cell walls by covalently binding to penicillin-binding proteins (PBPs). Bacterial enzymes that hydrolyze peptidoglycan cross-links continue to function even when PBPs are inactivated by beta-lactam antibiotics, leading to further degradation of the cell wall. The buildup of peptidoglycan precursors activates cell wall hydrolases, ultimately causing the cells to burst (Bush and Bradford, 2016). To counteract the effects of beta-lactam antibiotics, *Mab* possesses a beta-lactamase-encoding gene, namely *blaMab*, which serves to break down beta-lactam antibiotics, rendering them ineffective (Dubée et al., 2015a) (Supplementary Figure S3). BlaMab efficiently degrades multiple β-lactams, surpassing the activity of BlaC, the principal β-lactamase of *Mtb*. Deletion of *blaMab* in a recombinant *Mab* strain increased its susceptibility to β-lactams, making it responsive to antibiotics like amoxicillin and ceftaroline (Lefebvre et al., 2016). Moreover, BlaMab exhibits reduced susceptibility to common β-lactamase inhibitors, such as clavulanate, tazobactam, and sulbactam, unlike inhibitors of BlaC in *Mtb* (Soroka et al., 2017). Additionally, *M. massiliense* harbors an additional β-lactamase, BlaMmas (Ramírez et al., 2017).

However, recent combination studies have shown that non-β-lactam-based β-lactamase inhibitors known as diazabicyclooctane (DBO) inhibitors, including avibactam, effectively inhibit BlaMab. This inhibition leads to a reduction in the minimum inhibitory concentration (MIC) of carbapenems and cephalosporins against *Mab* to clinically achievable levels. Currently, avibactam is exclusively marketed in combination with the cephalosporin ceftazidime under the name Avycaz in the United States (Dubée et al., 2015a; Lefebvre et al., 2017; Meir et al., 2018; Le Run et al., 2019; Kaushik et al., 2019b; Dousa et al., 2022). Furthermore, Dousa et al. have demonstrated the effectiveness of two new non-β-lactam-based β-lactamase DBO inhibitors, relebactam and vaborbactam, when evaluated in combination with various commercially available β-lactams against clinical isolates of *Mab*. In their study, both relebactam and vaborbactam significantly enhanced the anti-*Mab* activity of several carbapenems (IMP and meropenem) and cephalosporins (cefepime, ceftaroline, and cefuroxime) (Dubée et al., 2015b). Currently, the IMP-relebactam combination is undergoing phase III trials, and the meropenem-vaborbactam combination is already available in the market. This established and effective combination opens the door to using potent β-lactams for the treatment of *Mab* infections (Kaushik et al., 2019b). Furthermore, more recent DBO class β-lactamase inhibitors, including nacubactam, zidebactam, and durlobactam, have been suggested as potent β-lactamase inhibitors that can restore susceptibility to β-lactams against *Mab in vitro* (Dubée et al., 2015a; Lefebvre et al., 2017; Meir et al., 2018; Le Run et al., 2019; Kaushik et al., 2019b; Dousa et al., 2022).

2.2.3 Rifampicin

Rifampicin (RFP) stands as the first-line treatment for *Mtb*, primarily due to its ability to halt transcription by binding to the beta-subunit of RNA polymerase encoded by *rpoB*. This enzyme is pivotal for bacterial transcription (Piccaro et al., 2014). This interaction prevents the bacterium from transcribing essential genetic material, ultimately leading to its demise. However, RFP is notably ineffective against *Mab*. In *Mab*, RFP's efficacy is nullified due to the presence of the Arr gene (*MAB_0591*) (Rominski et al., 2017a). This gene produces an RFP ADP-ribosyltransferase homolog, which inactivates rifamycins by catalyzing ADP-ribosylation at position C_{23} (Rominski et al., 2017a) (Supplementary Figure S4). ADP-ribosylation confers innate rifamycin resistance in *Mab* (Ganapathy et al., 2019). Deletion of *MAB_0591* in *Mab* has proven to not only decrease the MIC for RFP but also enhance susceptibility to RFP analogs like rifaximin rifabutin (RFB) and rifapentine (Rominski et al., 2017a; Schäfle et al., 2021). For instance, the removal of this gene results in a significant increase in *Mab*'s susceptibility to RFP, rifapentine, and rifaximin, with a 100-fold reduction in RFP's MIC (Johansen et al., 2020b; Zheng and Lupoli, 2021). Moreover, recent research has highlighted the potential of a rifamycin analogue known as RFB following its identification through drug screening. However, although being a substrate of Arr, RFB has demonstrated promising anti-*Mab* effects both *in vitro* and *in vivo*. In these studies, RFB not only inhibited *Mab* growth but also exhibited bactericidal properties against all three *Mab* subspecies. Particularly, RFB displayed comparable activity to clarithromycin (CLR) against *Mab* K21 in NOD.CB17-Prkdcscid/NCrCrl mice. These *in vitro* and *in vivo* findings suggest that RFB may enhance cure rates and shorten treatment duration for the predominantly challenging *Mab* lung disease. Hence, it should be considered a viable clinical candidate for patients with *Mab* infections (Dick et al., 2020; Johansen et al., 2020a).

Recently, 25-O-desacetyl-25-O-nicotinoylrifabutin (RFB-5 m), a new rifabutin analogue, overcomes inherent rifamycin resistance caused by Arr (Ganapathy et al., 2023b). RFB-5 m prevents enzymatic oxidation by maintaining rifabutin's naphthoquinone core (Lan et al., 2022; Ganapathy et al., 2023b). Importantly, RFB-5 m's unique C25 group prevents Arr *Mab* ADP-ribosylation (Lan et al., 2022; Ganapathy et al., 2023b). Compared to rifabutin, RFB-5 m is 50 times more effective against *Mab* (Lan et al., 2022; Ganapathy et al., 2023b).

Moreover, RFB-5 m was observed to display bactericidal properties against the persisters of *Mab* in caseum (Lan et al., 2022). RFB-5 m also had strong enhanced potency against all members of the *Mab* complex, other clinically relevant rapidly and slowly growing NTM, all of which encode Arr and block ADP-ribosylation (Ganapathy et al., 2023b). Recently, Paulowski et al. reported that benzyl piperidine rifamycin derivative known as 5j, which possesses a morpholino substituted C3 position and a naphthoquinone core, does not undergo any modifications when exposed to pure Arr (Paulowski et al., 2022). The thermal characterization of Arr in the presence of 5j, RMP, or RFB reveals that 5j exhibits no binding affinity towards Arr (Paulowski et al., 2022) and 5j also has substantial antibiotic efficacy against *Mab* within human macrophages, and exhibits synergistic effects when combined with AMK and AZM (Paulowski et al., 2022).

Additionally, Hanh et al. recently shed light on the activity of Rifamycin O, a derivative of rifamycin resulting from the oxidation of natural rifamycin B, against *Mab*. In their study, Rifamycin O exhibited promising *in vitro* activity (MIC90 = 4.0–6.2 μM) and demonstrated comparable *in vivo* efficacy to RFB using a zebrafish (*Danio rerio*) infection model (Hanh et al., 2020b). This suggests that certain rifamycin analogs like RFB and Rifamycin O can evade *MAB_0591*-mediated rifamycin resistance mechanisms. Of note, RFB and Rifamycin O exhibit distinct chemical structures at positions C_1 and C_4, setting them apart from other rifamycin analogs such as RFP, rifapentine, rifamycin SV, and rifaximin. These other analogs contain hydroquinone, which can readily oxidize into RFP quinone in the presence of oxygen and divalent cations. In contrast, RFB and Rifamycin O lack hydroquinone, granting them resistance to autoxidation and thereby ensuring their efficacy against *Mab* even under oxidative conditions. Consequently, it is conjectured that the unique structural attributes at C_1 and C_4 of rifamycin analogs are pivotal for their effectiveness against *Mab* (Hanh et al., 2020b; Ganapathy et al., 2021b). Recently, RFB was redesigned strategically to enhance its potency against *Mab*. Modifications at the C-25 position yielded analogs over a hundred times more powerful than RFP and resistant to *Mab* ADP-ribosylation. Molecular studies highlighted additional interactions, contributing to their superior on-target effectiveness. Validated *in vitro*, these compounds effectively countered Arr-mediated resistance, displaying potent *in vivo* efficacy comparable to clarithromycin against *Mab*. The compound 5 m, exemplary candidate in aspect of antibacterial activity, excellent drug disposition, and significantly improved *in vivo* pharmacokinetic traits is ongoing investigations to unveil its *in vivo* efficacy (Lan et al., 2022).

2.3 Target-modifying enzymes and acquired drug resistance

2.3.1 Macrolides

Macrolides represent an antibiotic class that can effectively combat a wide range of bacterial types, including staphylococci, streptococci, mycoplasma, and more. Macrolides are characterized by their structure, comprising amino sugar and/or neutral sugar components linked to a lactone ring, forming macrolides with 12-, 14-, 15-, or 16-membered rings through glycosidic connections. Their mode of action involves binding to the 50S ribosomal subunit in bacteria, which results in the inhibition of protein synthesis (Dinos, 2017). Macrolides remain the core drugs for treating *Mab* infections (Guo et al., 2021). In certain NTMs, exposure to macrolides triggers the production of specific enzymes that modify the drug's target binding site. For example, resistance to clarithromycin (CLR), whether intrinsic or acquired, is associated with *erm(41)* and mutations in the gene *rrl* encoding a 23S peptidyl transferase in the large 23S ribosomal subunit, respectively (Nessar et al., 2012). In *M. abscessus* and *M. bolletii*, inducible macrolide resistance occurs due to a T-C polymorphism in *erm(41)* at position 28 (only isolates with T28 develop resistance) (Nash et al., 2009). Interestingly, *M. massiliense* isolate exhibits susceptibility to macrolides due to a non-functional *erm(41)* caused by a 274-bp deletion. As a result, determining subspecies and macrolide susceptibility is crucial for guiding appropriate treatment. More recently, Guo et al. identified another macrolide-resistant gene in *Mab*. The gene *MAB_2355c* exhibits ATP hydrolysis activity and contributes to macrolide resistance by protecting ribosomes (Guo et al., 2021). Expression of *MAB_2355c* mRNA is significantly upregulated after exposure to macrolides compared to other ribosome-targeting antibiotics. Deletion of *MAB_2355c* in *Mab* strains resulted in increased sensitivity to macrolides, while complemented strains exhibited reduced sensitivity to macrolides (Guo et al., 2021).

Acquired resistance to macrolides in a clinical setting often arises from spontaneous mutations at positions 2058 and 2059 on the *rrl* gene. Additionally, Vester et al. demonstrated that mutations at positions 2057 and 2,611 on *rrl* can lead to low-level resistance although these mutations are located outside the primary site of macrolide interaction (Vester and Douthwaite, 2001).

2.4 Transcriptional regulator WhiB gene family

Mab possesses a family of transcriptional regulators that may play a role in conferring drug resistance, particularly the WhiB gene family (Morris et al., 2005). WhiB7, a transcriptional activator belonging to the WhiB family of transcriptional regulators, is conserved in actinomycetes and regulates critical cellular processes, including cell division, pathogenesis, and oxidative stress responses. The presence of a helix-turn-helix motif indicates its DNA-binding function (Soliveri et al., 2000; Burian et al., 2012; Nessar et al., 2012). In *Mab*, 128 genes, including *erm(41)* and *eis2*, have been identified in the WhiB7 regulon, indicating their induction through a WhiB7-dependent mechanism. Deletion of *Mab whiB7* (*MAB_3508c*) renders the bacteria more susceptible to antibiotics, such as erythromycin, CLR, streptomycin, spectinomycin (SPC), AMK, and tetracycline, although it does not affect resistance to RFP or INH (Hurst-Hess et al., 2017). Significantly, exposing *Mab* to sub-inhibitory concentrations of CLR leads to the activation of *whiB7* gene expression (Pryjma et al., 2017). This activation subsequently results in the development of resistance to AMK and CLR due to increased expression of *erm(41)* and *eis2* genes (Pryjma et al., 2017; Johansen et al., 2020b).

2.5 Tetracycline

Tetracycline molecules feature a linear fused tetracyclic core to which several functional groups are attached. These compounds are known to inhibit bacterial growth by preventing the binding of

charged aminoacyl-tRNA to the ribosomal A site (Chopra and Roberts, 2001). Tigecycline (TGC) became the first glycylcycline antibiotic approved by the US FDA (Stein and Craig, 2006). While tetracyclines have been one of the most successful classes of antibiotics, their widespread use has led to extensive drug resistance, necessitating their discontinuation in treating various bacterial infections (Rudra et al., 2018). Occasionally, tetracyclines become ineffective due to TetX enzymes, also known as tetracycline destructases. In the past, the limited tolerance of *Msm* and *Mtb* to tetracycline was attributed to the WhiB7-dependent TetV/Tap efflux pump. However, *Mab* exhibits a resistance level approximately 500-fold higher than that of *Msm* and *Mtb*. Recently, Rudra and colleagues revealed that this heightened resistance in *Mab* to the tetracycline class is conferred by a WhiB7-independent tetracycline-inactivating monooxygenase, *MAB_1496c* (*MabTetX*). Exposure to sublethal doses of tetracycline and doxycycline leads to a more than 200-fold induction of *MabTetX*. Conversely, an isogenic deletion strain shows high sensitivity to both antibiotics. The authors also demonstrated that *MabTetX*'s expression is suppressed by *MabTetRx*. This finding highlights the potential use of an inhibitor to potentially reinstate the effectiveness of tetracycline and doxycycline (Rudra et al., 2018). As for acquired drug resistance, mutations in the *sigH-rshA* genes, which regulate heat shock and oxidative-stress responses, have also been found to be involved in TGC resistance or decreased sensitivity in *Mab* (Ng and Ngeow, 2022). Overexpression of the *sigH* gene, resulting from the C51R mutation in *rshA*, causes resistance to or decreased susceptibility to TGC (Ng and Ngeow, 2022).

Recently, OMC, which is classified as a tetracycline antibiotic, has exhibited favorable MIC against various *Mab* species (Singh et al., 2023). The activity and efficacy of OMC against *Mab* infection have been proven in both *in vitro* and *in vivo* (Shoen et al., 2019; Watkins and Deresinski, 2019; Kaushik et al., 2019a; Brown-Elliott and Wallace, 2021; Nicklas et al., 2022). OMC, like other tetracycline derivatives via binding to the tetracycline-binding site of the bacterial 16S ribosomal RNA, inhibiting bacterial protein synthesis (Brown-Elliott and Wallace, 2021). In contrast to first-generation tetracyclines, OMC has been intentionally engineered to bypass ribosomal protection and tetracycline efflux mechanisms. In *Mab*, the production of a monooxygenase enzyme may degrade tetracyclines, such as minocycline and doxycycline, but does not affect OMC (Luthra et al., 2018; El Ghali et al., 2023). This feature, in part, revitalizes its activity against recalcitrant MAB and may serve as a deterrent against the development of resistance during treatment. For example, studies by Bax et al. revealed that, except for a 1.5% occurrence at an OMC concentration of 4 mg/L, no instances of drug resistance selection exceeded the spontaneous mutation frequency (Bax et al., 2019).

2.6 Efflux pumps (EPs)

Active efflux mechanisms have been identified as potential contributors to antibiotic resistance in mycobacteria. The primary role of efflux pump (EP) systems is to protect bacteria from harmful substances, maintain cellular homeostasis, and uphold physiological equilibrium by expelling toxins or metabolites into the extracellular environment (Louw et al., 2009; Remm et al., 2022). *Mab* possesses genetic sequences that encode protein constituents belonging to the major facilitator family ABC transporters and mycobacterial membrane protein large (MmpL) families (Ripoll et al., 2009), although the precise contribution of EPs to antibiotic resistance in *Mab* is not fully elucidated. ABC-type multidrug transporters utilize ATP energy to actively remove compounds from the cellular environment. MmpL transporters are multidrug EPs that play a crucial role in transporting various substrates from the periplasmic space to the extracellular environment (Kerr, 2002; Kerr et al., 2005). In further detail, the MmpL transporter family encodes proteins belonging to the resistance, nodulation, and cell division (RND) category. These proteins function as multidrug resistance pumps with the ability to transport a wide range of compounds, including cationic, anionic, and neutral substances, such as drugs, metals, and fatty acids (Domenech et al., 2005).

SPC is an aminocyclitol antibiotic that robustly inhibits bacterial protein synthesis by binding to the 30S subunit of the ribosome. However, its effectiveness against mycobacteria is restricted due to inherent resistance mechanisms (Hurst-Hess K. R. et al., 2023). *Mab* exhibits a notable inherent resistance to SPC, with MIC exceeding 1,000 μg/mL, rendering it unsuitable for therapeutic applications (Hurst-Hess K. R. et al., 2023). The *whiB7* is responsible for *Mab* resistance for SPC because sublethal exposure to SPC strongly induces *whiB7* and its regulon, and a *ΔMab_whiB7* strain shows SPC sensitive (Hurst-Hess K. R. et al., 2023). Furthermore, MAB_2780c, a TetV-like efflux pump, provides high-level SPC resistance in *Mab* (Hurst-Hess K. et al., 2023). For instance, the elimination of *MAB_2780c* resulted in a significant enhancement of susceptibility to SPC, approximately 150 times greater than that observed in the wildtype bacteria (Hurst-Hess K. R. et al., 2023). The inclusion of the efflux pump inhibitor (EPI), verapamil, leads to a reduction in the MIC of SPC by over 100-fold in bacteria that express *MAB_2780c*, bringing it down to levels comparable to those observed for the deletion mutant of *MAB_2780c* (Hurst-Hess K. R. et al., 2023).

2.6.1 Transcriptional regulator TetR and EPs in *Mab*

Recent studies have attributed the drug resistance function of the *Mab* MmpL family. The MmpS-MmpL protein complex provides significant resistance to thiacetazone (TAC) analogs, bedaquiline (BDQ), and CFZ (Gutiérrez et al., 2019). Point mutations occurring in the *MAB_4384* gene of *Mab*, a transcriptional repressor belonging to the TetR family, have been linked to resistance to various drugs. These mutations lead to elevated expression levels of the *MAB_4383c* (*mmpS5*) and *MAB_4382c* (*mmpL5*) genes, ultimately resulting in drug resistance, including resistance to TAC analogs (Halloum et al., 2017; Richard et al., 2018a). In a separate study, Li et al. identified mutations in *MAB_4384* in clinically isolated strains resistant to BDQ (Li et al., 2018). Additionally, Negatu et al. reported an EP's involvement in LZ resistance. They induced high-level LZ resistance in the *Mab* reference strain *in vitro* and identified resistance mutations in *MAB_4384*, resulting in a lower level of antibiotics resistance for drugs such as Sutezolid (STZ), Tedizolid (TDZ), and TBI-223 (Negatu et al., 2023). This *MAB_4384*-associated lower level of antibiotic resistance was also observed with SPR719 and TAC analogs as well (Halloum et al., 2017; Richard et al., 2018a; Aragaw et al., 2022). The repression of transcriptional expression of two MmpS-MmpL EPs is also facilitated by *MAB_2299c*, which mediates the production of MmpT5 (Alexander et al., 2017). MmpT5 is a member of the TetR family that regulates the expression of the adjacent *mmpS-mmpL*

(*MAB_2300–2,301*) genes (Alexander et al., 2017). Mutations in the DNA-binding domain of *MAB_2299c* lead to upregulated EPs, increased drug efflux, and resistance to CFZ and BDQ (Alexander et al., 2017; Richard et al., 2018b). Furthermore, Gutiérrez et al. identified a new target of *MAB_2299c* named *mmpS-mmpL* (*MAB_1135c-MAB_1134c*), which encodes a new MmpS-MmpL EP system involved in intrinsic resistance to CFZ and BDQ (Gutiérrez et al., 2019).

2.6.2 Other EPs in *Mab*

Apart from the above-mentioned EPs, various EP-related genes exist in *Mab*. Two EP-encoding genes, *MAB_1409* and *MAB_3142*, were consistently overexpressed upon exposure to CLR (Vianna et al., 2019). Guo et al. also identified six clinical isolates with CLR resistance among 194 whole-genome sequenced isolates. These resistant isolates, which lacked the common *rrl* 2270/2271 mutation and showed no mutations in the *rrl, rplC, rplD, rplV,* or *erm(41)* genes, exhibited elevated expression of EP genes, specifically *MAB_2355c, MAB_1409c,* and *MAB_1846* (Guo et al., 2020). Additionally, Gorzynski et al. reported the upregulation of *MAB_0937c, MAB_1137c, MAB_4117c,* and *MAB_4237c*, all of which encode EPs and transporter systems when exposed to AMK (Gorzynski et al., 2021). A promising strategy to enhance drug susceptibility involves inhibiting EP activity using EPIs. EPIs are compounds designed to act on EPs and block their efflux function (Song and Wu, 2016; Remm et al., 2022). Several experimental examples demonstrate the use of EPIs to increase the susceptibility of anti-*Mab* agents. In a study by Vianna et al., the crucial role of efflux activity in *Mab* resistance to CLR was highlighted. This was evident in the increased mRNA expression levels of *MAB_1409* and *MAB_3142* in *Mab* after exposure to CLR. Moreover, the researchers discovered that verapamil (VP), an FDA-approved EPI with potential as adjunctive chemotherapy for tuberculosis, significantly enhanced susceptibility to CLR. This effect was observed across *Mab* clinical isolates belonging to the T28 *erm(41)* sequevar., known for inducible resistance to CLR (Vianna et al., 2019). In addition, Guo et al. reported that the presence of EPIs, such as phenylalanine-arginine β-naphthylamide (PAβN), a peptidomimetic compound, carbonyl cyanide m-chlorophenylhydrazone (CCCP), and VP, significantly decreased the MIC of CLR for *Mab* resistant isolates that exhibited no *rrl* 2270/2271 mutation (Guo et al., 2020).

2.7 Genetic polymorphism of target genes

Genetic polymorphisms in highly conserved genes targeted by pharmaceutical medications have been associated with variations in sensitivity to pharmacological effects in *Mab* infections (Nessar et al., 2012).

2.7.1 Ethambutol

Ethambutol and fluoroquinolone resistance serve as examples of genetic polymorphism influencing drug resistance. Ethambutol is chemically derived from ethylenediamine, possessing the stereochemical structure S,S, achieved by substituting a hydrogen atom on each nitrogen atom of ethane-1,2-diamine with a 1-hydroxybutan-2-yl group (Jahangir et al., 2016). Ethambutol functions as a bacteriostatic medication against mycobacterial infections by inhibiting cell wall formation in these microorganisms (Sreevatsan et al., 1997). However, *Mab* exhibits substantial inherent resistance to ethambutol, primarily due to variant nucleotides within the conserved ethambutol resistance-determining region (ERDR) of the *embB* gene (Alcaide et al., 1997). *Mab* shows amino acid substitutions, particularly the replacement of isoleucine by glutamine at position 303 and leucine by methionine at position 304 (referred to as I303Q and L304M, respectively) (Sreevatsan et al., 1997).

2.7.2 Fluoroquinolone

Another example of genetic polymorphism influencing drug resistance involves fluoroquinolones. These antibiotics encompass over 20 medications originating from the identification of nalidixic acid. Derived from the quinolone family, fluoroquinolones are synthetic compounds formed by modifying 1-alkyl-1,8-naphthyridin-4-one-3-carboxylic acid. Fluoroquinolones strongly inhibit bacterial enzymes, DNA gyrase, and topoisomerase, critical for processes like DNA replication (Redgrave et al., 2014). They are secondary therapeutic agents for multi-drug resistant tuberculosis (MDR-TB), working by inhibiting DNA gyrase's supercoiling activity, a specific target of fluoroquinolones (Pantel et al., 2011). NTM resistance to fluoroquinolones is predominantly due to genetic factors, particularly the analysis of conserved sections called quinolone resistance-determining regions (QRDRs) within DNA gyrase subunits GyrA and GyrB, which are the primary targets of quinolone drugs. In *Mab*, resistance results from the presence of alanine at position 83 (Ala-83) in the GyrA QRDR. Furthermore, resistance is conferred by arginine at position 447 (Arg-447) and asparagine at position 464 (Asn-464) within the GyrB QRDR (Matrat et al., 2008).

2.7.3 Telacebec (Q203)

Telacebec (Q203) is a groundbreaking anti-tuberculosis drug designed to inhibit the cytochrome bc_1 complex, affecting cellular energy production in *Mtb*. This inhibition reduces ATP synthesis, halting bacterial growth (Pethe et al., 2013; de Jager et al., 2020). Notably, Q203 lacks inhibitory activity against *Mab*. A recent study by Sorayah et al. revealed that naturally occurring polymorphisms within *Mab* QcrB are responsible for its increased resistance to Q203. To confirm this resistance mechanism, they engineered a *Mycobacterium bovis* BCG strain, integrating the chimeric *Mab qcrCAB* operon, where four amino acids (D311E, L314A, G179S, and C393A on QcrB) were modified to match their counterparts in *Mtb*. This genetic adjustment rendered the chimeric *M. bovis* BCG strain susceptible to Q203, indicating that *Mab*'s resistance to Q203 is attributable to naturally occurring polymorphisms in the drug target, QcrB, rather than other inherent resistance mechanisms such as efflux pumps, cell wall permeability, or target-modifying enzymes (Sorayah et al., 2019).

3 Acquired drug resistance of newly developing compounds against *Mab*

3.1 Epetraborole

In recent years, aminoacyl-tRNA synthetases (AARSs) have become significant targets for new antibacterial interventions. AARSs facilitate the acylation process, linking amino acids and tRNA. Inhibiting AARS activity halts protein synthesis, impeding bacterial growth. Benzoxaboroles, known as boron-heterocyclic

antibiotics, inhibit leucyl-tRNA synthetase (LeuRS) (Rock et al., 2007). These drugs obstruct protein synthesis via the oxaborole tRNA-trapping mechanism, forming adducts with uncharged tRNALeu molecules that bind to the LeuRS editing domain (Rock et al., 2007). Multiple reports discuss the anti-*Mab* effects of LeuRS inhibitors, particularly a new class of LeuRS inhibitors such as epetraborole, DS86760016, EC/11770, MRX-6038, and GSK656 (Kim et al., 2021; Wu et al., 2022; Ganapathy et al., 2023a). High-level epetraborole resistance may be attributed to mutations in *Mab* at locations S303L, T322I, T323P, F321V, G393V, and Y421D within the LeuS gene (Ganapathy et al., 2021a). Among the LeuRS inhibitors, DS86760016 exhibits an improved pharmacokinetic profile, lower plasma clearance, longer plasma half-life, and higher renal excretion than epetraborole in animal models. A recent study by Nguyen et al. demonstrated that DS86760016 displayed similar activity to epetraborole treatment against *Mab in vitro*, intracellularly, and in zebrafish infection models, with a significantly lower mutation frequency. Laboratory-induced DS86760016-resistant strains included D284G, Q345R, Y420C, I426T, V468L, N469Y, and E524K, which were not found on the LeuS gene in epetraborole-resistant mutants (Nguyen et al., 2023).

3.2 MmpL3 inhibitor

Mycolic acids (MA) exist in various forms, including trehalose monomycolates (TMMs), trehalose dimycolates (TDMs), and mycolates covalently linked to arabinogalactan (AG) polysaccharides (McNeil et al., 2020). In the process of MA synthesis, MmpL3 plays a crucial role by transporting MA across the inner membrane, making its contribution to cell wall production indispensable (McNeil et al., 2020). Inhibition of the MmpL3 transporter leads to the accumulation of TMM intracellularly, causing a decrease in mycolyl arabinogalactan peptidoglycan (mAGP) and TDM levels (McNeil et al., 2020). Consequently, MmpL3 represents a versatile drug target, and inhibiting MmpL3 disrupts cell wall biosynthesis (Li et al., 2014). Multiple MmpL3 inhibitors have been recently identified through phenotypic screenings of chemical libraries against *Mab*. Promisingly, PIPD1, a piperidinol-based molecule, has shown potent *in vitro* and *in vivo* activity against clinical *Mab* strains. Treatment of infected zebrafish with PIPD1 increased embryo survival and reduced bacterial burden (Dupont et al., 2016). Major resistance to PIPD1 and other MmpL3 inhibitors, such as EJMCh-6 (2-(2-cyclohexylethyl)-5,6-dimethyl-1H-benzo[d]imidazole) and BMC-2i, is attributed to mutations in the MmpL3 gene (*MAB_4508*) of *Mab* at location A309P. The overexpression of MmpL3, containing the Ala309Pro mutation in *Mab* wild-type bacteria, results in significant drug resistance to MmpL3 inhibitors, confirming MmpL3 as their target (Dupont et al., 2016; Kozikowski et al., 2017).

3.3 Delpazolid (DPZ)

LZ, a representative oxazolidinone, disrupts protein synthesis by inhibiting the peptidyl transferase activity of the 23S rRNA in the 50S ribosomal subunit, leading to ribosome stalling. Unfortunately, most clinical *Mab* isolates exhibit poor susceptibility to LZ (Negatu et al., 2023). However, the effectiveness of LZ against NTMs varies among different derivatives, and its clinical use in patients with NTMs can sometimes result in adverse events, such as peripheral neuropathy and cytopenias. Recently, Kim et al. introduced a novel oxazolidinone with a cyclic amidrazone named DPZ (LCB01-0371). DPZ demonstrated effective inhibition of *Mab* growth, both *in vitro* and in mouse lungs *in vivo* compared to LZ. Furthermore, DPZ exhibited bactericidal activity against all bacterial strains, irrespective of their resistance to AMK, CFX, or CLR. Kim et al. generated laboratory-induced resistant mutants to DPZ and identified mutations in *rplC* (encoding 50S ribosomal protein L3) at T424C and G419A, along with a nucleotide insertion at position 503 through sequencing analysis (Kim et al., 2017).

3.4 SPR719

The aminobenzimidazole SPR719 targets the ATPase located on Gyrase B in *Mtb*. SPR719 also demonstrates activity against NTM and has recently entered clinical trials for lung diseases caused by NTM (Aragaw et al., 2022). Brown-Elliott et al. (2018) demonstrated *in vitro* activity of SPR719 against *M. abscessus, M. massiliense*, and related subspecies, with an observed MIC_{50} (MIC required to inhibit the growth of 50% of *Mab*) value of ~2.0 μg/mL. Additionally, Rubio et al. reported that the phosphate prodrug SPR720 (of SPR719) exhibited favorable *in vivo* efficacy at a dose of 100 mg/kg/day in an SCID mouse model infected with *Mab* (Egorova et al., 2021). To identify the molecular target for *Mab*, Aragaw et al. recently induced two different morphotypes of SPR719-resistant mutants on agar containing 16 x MIC of SPR719, named large and small colonies. Interestingly, the small colony phenotype reflected a lower level of resistance, while large colonies showed high-level SPR719 resistance (>16-fold MIC increase). All strains contained a single amino acid polymorphism, Thr169Asn, in the ATPase domain of Gyrase B, and non-*gyrB* DNA sequence polymorphisms were revealed by whole-genome sequencing. Thr169 in *Mab* DNA gyrase corresponds to Ser169 in *Mtb* GyrB, causing resistance to SPR719 in *Mtb* (Aragaw et al., 2022).

4 Concluding remarks

Mab has emerged as a significant threat to human health, posing challenges in treatment due to its resistance to currently available commercial medications (Quang and Jang, 2021). The rising number of publications on NTM, especially *Mab*, signifies exponential growth. However, the level of attention dedicated to this issue remains insufficient to effectively address the problem. The primary challenge in developing drugs for *Mab* is attributed to its exceptional innate and acquired resistance capabilities (Wu et al., 2018). High drug resistance discourages investments by both pharmaceutical companies and governments in this area, leading to passive involvement. As a result, small- and medium-sized organizations, along with academic institutions, are currently the primary sources of knowledge regarding *Mab* infections and antibiotics. Antibiotic resistance in mycobacterial species can occur through natural or acquired mechanisms (Nessar et al., 2012). Development of natural drug resistance in *Mab* can be attributed to several factors, including a waxy impermeable cell wall acting as both a physical and chemical barrier (Nessar et al., 2012). Additionally, drug export systems, enzymes capable of modifying drugs or target enzymes, and genetic polymorphism in

target genes contribute to this phenomenon (Nessar et al., 2012). Acquired resistance arises from spontaneous mutations at specific genes in response to antibiotics following extended treatment (Johansen et al., 2020b). Such mutations alter the target gene or other related genes, rendering the medication ineffective (Johansen et al., 2020b). Our understanding of natural or acquired antibiotic resistance in *Mab* remains limited, highlighting the importance of further research into resistance mechanisms against current antibiotics and the discovery of new compounds to overcome resistance hurdles and develop novel drugs.

Author contributions

TN: Investigation, Methodology, Validation, Writing – original draft. BH: Investigation, Methodology, Validation, Writing – review & editing. SJ: Investigation, Methodology, Validation, Writing – review & editing. AA: Investigation, Methodology, Validation, Writing – review & editing. HL: Investigation, Methodology, Validation, Writing – review & editing. CM: Investigation, Methodology, Validation, Writing – review & editing. JJ: Conceptualization, Funding acquisition, Methodology, Validation, Writing – original draft, Writing – review & editing.

Funding

The author(s) declare financial support was received for the research, authorship, and/or publication of this article. This work is supported by a grant of the Ministry of Health & Welfare, Republic of Korea (HI22C136100 and 2020ER520601), funded by the grant 2020R1A2C100407714 and RS-2023-00266419 from the National Research Foundation (NRF) of Republic of Korea. This research was also supported by "Regional Innovation Strategy (RIS)" through the NRF funded by the Ministry of Education (MOE) (2021RIS001, 1345370811). TN, BH, SJ, and AA were supported by the BK21 Four Program. AA was sponsored by the Global Korea Scholarship program under the MOE in Korea.

Acknowledgments

The authors would like to thank all scientists who are developing novel anti-*Mab* agents.

Conflict of interest

The authors declare that the research was conducted in the absence of any commercial or financial relationships that could be construed as a potential conflict of interest.

Publisher's note

Supplementary material

The Supplementary material for this article can be found online at: https://www.frontiersin.org/articles/10.3389/fmicb.2024.1331508/full#supplementary-material

References

Abate, G., Hamzabegovic, F., Eickhoff, C. S., and Hoft, D. F. (2019). BCG vaccination Induces M. Avium and *M. abscessus* cross-protective immunity. *Front. Immunol.* 10:234. doi: 10.3389/FIMMU.2019.00234

Alcaide, F., Pfyffer, G. E., and Telenti, A. (1997). Role of embB in natural and acquired resistance to ethambutol in mycobacteria. *Antimicrob. Agents Chemother.* 41, 2270–2273. doi: 10.1128/AAC.41.10.2270

Alexander, D. C., Vasireddy, R., Vasireddy, S., Philley, J. V., Brown-Elliott, B. A., Perry, B. J., et al. (2017). Emergence of mmpT5 variants during bedaquiline treatment of *Mycobacterium intracellulare* lung disease. *J. Clin. Microbiol.* 55, 574–584. doi: 10.1128/JCM.02087-16

Aragaw, W. W., Cotroneo, N., Stokes, S., Pucci, M., Critchley, I., Gengenbacher, M., et al. (2022). In vitro resistance against DNA gyrase inhibitor SPR719 in Mycobacterium avium and *Mycobacterium abscessus*. *Microbiol. Spectr.* 10:e0132121. doi: 10.1128/SPECTRUM.01321-21

Baker, A. W., Lewis, S. S., Alexander, B. D., Chen, L. F., Wallace, R. J., Brown-Elliott, B. A., et al. (2017). Two-phase hospital-associated outbreak of *Mycobacterium abscessus*: investigation and mitigation. *Clin. Infect. Dis.* 64, 902–911. doi: 10.1093/CID/CIW877

Bax, H. I., De Vogel, C. P., Mouton, J. W., and De Steenwinkel, J. E. M. (2019). Omadacycline as a promising new agent for the treatment of infections with *Mycobacterium abscessus*. *J. Antimicrob. Chemother.* 74, 2930–2933. doi: 10.1093/JAC/DKZ267

Becker, K., Aranzana-Climent, V., Cao, S., Nilsson, A., Shariatgorji, R., Haldimann, K., et al. (2021). Efficacy of EBL-1003 (apramycin) against *Acinetobacter baumannii* lung infections in mice. *Clin. Microbiol. Infect.* 27, 1315–1321. doi: 10.1016/J.CMI.2020.12.004

Bernut, A., Dupont, C., Sahuquet, A., Herrmann, J. L., Lutfalla, G., and Kremer, L. (2015). Deciphering and imaging pathogenesis and cording of *Mycobacterium abscessus* in zebrafish embryos. *J. Vis. Exp.* 103:53130. doi: 10.3791/53130

Bernut, A., Le Moigne, V., Lesne, T., Lutfalla, G., Herrmann, J. L., and Kremer, L. (2014). In vivo assessment of drug efficacy against *Mycobacterium abscessus* using the embryonic zebrafish test system. *Antimicrob. Agents Chemother.* 58, 4054–4063. doi: 10.1128/AAC.00142-14

Bernut, A., Nguyen-Chi, M., Halloum, I., Herrmann, J. L., Lutfalla, G., and Kremer, L. (2016). *Mycobacterium abscessus*-induced granuloma formation is strictly dependent on TNF signaling and neutrophil trafficking. *PLoS Pathog.* 12:e1005986. doi: 10.1371/JOURNAL.PPAT.1005986

Bhattacharjee, M. K. (2016). "Antibiotics that inhibit protein synthesis" in *Chemistry of antibiotics and related drugs* (Cham: Springer), 129–151. Available at: https://link.springer.com/book/10.1007/978-3-319-40746-3

Blauwendraat, C., Dixon, G. L. J., Hartley, J. C., Foweraker, J., and Harris, K. A. (2012). The use of a two-gene sequencing approach to accurately distinguish between the species within the *Mycobacterium abscessus* complex and *Mycobacterium chelonae*. *Eur. J. Clin. Microbiol. Infect. Dis.* 31, 1847–1853. doi: 10.1007/S10096-011-1510-9

Brennan, P. J., and Nikaido, H. (1995). The envelope of mycobacteria. *Annu. Rev. Biochem.* 64, 29–63. doi: 10.1146/ANNUREV.BI.64.070195.000333

Brown-Elliott, B. A., Rubio, A., and Wallace, R. J. (2018). In vitro susceptibility testing of a novel Benzimidazole, SPR719, against nontuberculous mycobacteria. *Antimicrob. Agents Chemother.* 62, e01503-18. doi: 10.1128/AAC.01503-18

Brown-Elliott, B. A., and Wallace, R. J. (2021). In vitro susceptibility testing of omadacycline against nontuberculous mycobacteria. *Antimicrob. Agents Chemother.* 65, e01947-20. doi: 10.1128/AAC.01947-20

Bryant, J. M., Grogono, D. M., Rodriguez-Rincon, D., Everall, I., Brown, K. P., Moreno, P., et al. (2016). Emergence and spread of a humantransmissible multidrug-resistant nontuberculous mycobacterium. *Science* 354, 751–757. doi: 10.1126/science.aaf8156

Burian, J., Ramón-García, S., Howes, C. G., and Thompson, C. J. (2012). WhiB7, a transcriptional activator that coordinates physiology with intrinsic drug resistance in *Mycobacterium tuberculosis*. *Expert Rev. Anti-Infect. Ther.* 10, 1037–1047. doi: 10.1586/ERI.12.90

Bush, K., and Bradford, P. A. (2016). β-Lactams and β-lactamase inhibitors: an overview. *Cold Spring Harb. Perspect. Med.* 6:a025247. doi: 10.1101/CSHPERSPECT.A025247

Carvalho, R., de Sonneville, J., Stockhammer, O. W., Savage, N. D. L., Veneman, W. J., Ottenhoff, T. H. M., et al. (2011). A high-throughput screen for tuberculosis progression. *PLoS One* 6:e16779. doi: 10.1371/JOURNAL.PONE.0016779

Chopra, S., Matsuyama, K., Hutson, C., and Madrid, P. (2011). Identification of antimicrobial activity among FDA-approved drugs for combating *Mycobacterium abscessus* and *Mycobacterium chelonae*. *J. Antimicrob. Chemother.* 66, 1533–1536. doi: 10.1093/jac/dkr154

Chopra, I., and Roberts, M. (2001). Tetracycline antibiotics: mode of action, applications, molecular biology, and epidemiology of bacterial resistance. *Microbiol. Mol. Biol. Rev.* 65, 232–260. doi: 10.1128/MMBR.65.2.232-260.2001

Christianson, S., Grierson, W., Kein, D., Tyler, A. D., Wolfe, J., and Sharma, M. K. (2016). Time-to-detection of inducible macrolide resistance in *Mycobacterium abscessus* subspecies and its association with the Erm(41) Sequevar. *PLoS One* 11:e0158723. doi: 10.1371/JOURNAL.PONE.0158723

Chulluncuy, R., Espiche, C., Nakamoto, J. A., Fabbretti, A., and Milón, P. (2016). Conformational response of 30S-bound IF3 to A-site binders streptomycin and kanamycin. *Antibiotics* 5:38. doi: 10.3390/ANTIBIOTICS5040038

Daher, W., Leclercq, L. D., Johansen, M. D., Hamela, C., Karam, J., Trivelli, X., et al. (2022). Glycopeptidolipid glycosylation controls surface properties and pathogenicity in *Mycobacterium abscessus*. *Cell Chem. Biol.* 29, 910–924.e7. doi: 10.1016/J.CHEMBIOL.2022.03.008

Dal Molin, M., Gut, M., Rominski, A., Haldimann, K., Becker, K., and Sander, P. (2017). Molecular mechanisms of intrinsic streptomycin resistance in *Mycobacterium abscessus*. *Antimicrob. Agents Chemother.* 62, e01427-17. doi: 10.1128/AAC.01427-17

de Jager, V. R., Dawson, R., van Niekerk, C., Hutchings, J., Kim, J., Vanker, N., et al. (2020). Telacebec (Q203), a new antituberculosis agent. *N. Engl. J. Med.* 382, 1280–1281. doi: 10.1056/NEJMC1913327

De Rosa, M., Verdino, A., Soriente, A., and Marabotti, A. (2021). The odd couple(s): an overview of Beta-lactam antibiotics bearing more than one pharmacophoric group. *Int. J. Mol. Sci.* 22:617. doi: 10.3390/IJMS22020617

Dedrick, R. M., Abad, L., Storey, N., Kaganovsky, A. M., Smith, B. E., Aull, H. A., et al. (2023). The problem of *Mycobacterium abscessus* complex: multi-drug resistance, bacteriophage susceptibility and potential healthcare transmission. *Clin. Microbiol. Infect.* 29, 1335.e9–1335.e16. doi: 10.1016/J.CMI.2023.06.026

Degiacomi, G., Sammartino, J. C., Chiarelli, L. R., Riabova, O., Makarov, V., and Pasca, M. R. (2019). *Mycobacterium abscessus*, an emerging and worrisome pathogen among cystic fibrosis patients. *Int. J. Mol. Sci.* 20:5868. doi: 10.3390/IJMS20235868

Desai, A. N., and Hurtado, R. M. (2018). Infections and outbreaks of nontuberculous mycobacteria in hospital settings. *Curr. Treat. Options Infect. Dis.* 10, 169–181. doi: 10.1007/S40506-018-0165-9

Dick, T., Shin, S. J., Koh, W. J., Dartois, V., and Gengenbacher, M. (2020). Rifabutin is active against *Mycobacterium abscessus* in mice. *Antimicrob. Agents Chemother.* 64, e01943-19. doi: 10.1128/AAC.01943-19

Dinos, G. P. (2017). The macrolide antibiotic renaissance. *Br. J. Pharmacol.* 174, 2967–2983. doi: 10.1111/BPH.13936

Domenech, P., Reed, M. B., and Barry, C. E. (2005). Contribution of the *Mycobacterium tuberculosis* MmpL protein family to virulence and drug resistance. *Infect. Immun.* 73, 3492–3501. doi: 10.1128/IAI.73.6.3492-3501.2005

Dousa, K. M., Nguyen, D. C., Kurz, S. G., Taracila, M. A., Bethel, C. R., Schinabeck, W., et al. (2022). Inhibiting *Mycobacterium abscessus* cell wall synthesis: using a novel diazabicyclooctane β-lactamase inhibitor to augment β-lactam action. *MBio* 13:e0352921. doi: 10.1128/MBIO.03529-21

Dubée, V., Bernut, A., Cortes, M., Lesne, T., Dorchene, D., Lefebvre, A. L., et al. (2015a). β-Lactamase inhibition by avibactam in *Mycobacterium abscessus*. *J. Antimicrob. Chemother.* 70, 1051–1058. doi: 10.1093/JAC/DKU510

Dubée, V., Soroka, D., Cortes, M., Lefebvre, A. L., Gutmann, L., Hugonnet, J. E., et al. (2015b). Impact of β-lactamase inhibition on the activity of ceftaroline against Mycobacterium tuberculosis and *Mycobacterium abscessus*. *Antimicrob. Agents Chemother.* 59, 2938–2941. doi: 10.1128/AAC.05080-14

Dupont, C., Viljoen, A., Dubar, F., Blaise, M., Bernut, A., Pawlik, A., et al. (2016). A new piperidinol derivative targeting mycolic acid transport in *Mycobacterium abscessus*. *Mol. Microbiol.* 101, 515–529. doi: 10.1111/MMI.13406

Egorova, A., Jackson, M., Gavrilyuk, V., and Makarov, V. (2021). Pipeline of anti-*Mycobacterium abscessus* small molecules: repurposable drugs and promising novel chemical entities. *Med. Res. Rev.* 41, 2350–2387. doi: 10.1002/MED.21798

El Ghali, A., Morrisette, T., Alosaimy, S., Lucas, K., Tupayachi-Ortiz, M. G., Vemula, R., et al. (2023). Long-term evaluation of clinical success and safety of omadacycline in nontuberculous mycobacteria infections: a retrospective, multicenter cohort of real-world health outcomes. *Antimicrob. Agents Chemother.* 67:e0082423. doi: 10.1128/AAC.00824-23

Falkinham, J. O. (2011). Nontuberculous mycobacteria from household plumbing of patients with nontuberculous mycobacteria disease. *Emerg. Infect. Dis.* 17, 419–424. doi: 10.3201/eid1703.101510

Faria, S., Joao, I., and Jordao, L. (2015). General overview on nontuberculous mycobacteria, biofilms, and human infection. *J. Pathog.* 2015, 1–10. doi: 10.1155/2015/809014

Fernandes Garcia de Carvalho, N., Rodrigues Mestrinari, A. C., Brandão, A., Souza Jorge, L., Franco, C., da Silveira Paro Pedro, H., et al. (2018). Hospital bronchoscopy-related pseudo-outbreak caused by a circulating *Mycobacterium abscessus* subsp. massiliense. *J. Hosp. Infect.* 100, e138–e141. doi: 10.1016/J.JHIN.2018.07.043

Ganapathy, U. S., Dartois, V., and Dick, T. (2019). Repositioning rifamycins for *Mycobacterium abscessus* lung disease. *Expert Opin. Drug Discov.* 14, 867–878. doi: 10.1080/17460441.2019.1629414

Ganapathy, U. S., Del Rio, R. G., Cacho-Izquierdo, M., Ortega, F., Lelièvre, J., Barros-Aguirre, D., et al. (2023a). A Leucyl-tRNA synthetase inhibitor with broad-spectrum anti-mycobacterial activity. *Antimicrob. Agents Chemother.* 95, e02420-20. doi: 10.1128/AAC.02420-20

Ganapathy, U. S., and Dick, T. (2022). Why matter matters: fast-tracking *Mycobacterium abscessus* drug discovery. *Molecules* 27:6948. doi: 10.3390/MOLECULES27206948

Ganapathy, U. S., Gengenbacher, M., and Dick, T. (2021a). Epetraborole is active against *Mycobacterium abscessus*. *Antimicrob. Agents Chemother.* 65:e0115621. doi: 10.1128/AAC.01156-21

Ganapathy, U. S., Lan, T., Dartois, V., Aldrich, C. C., and Dick, T. (2023b). Blocking ADP-ribosylation expands the anti-mycobacterial spectrum of rifamycins. *Microbiol. Spectr.* 11:e0190023. doi: 10.1128/SPECTRUM.01900-23

Ganapathy, U. S., Lan, T., Krastel, P., Lindman, M., Zimmerman, M. D., Ho, H. P., et al. (2021b). Blocking bacterial naphthohydroquinone oxidation and ADP-ribosylation improves activity of rifamycins against *Mycobacterium abscessus*. *Antimicrob. Agents Chemother.* 65:e0097821. doi: 10.1128/AAC.00978-21

Gorzynski, M., Week, T., Jaramillo, T., Dzalamidze, E., and Danelishvili, L. (2021). *Mycobacterium abscessus* genetic determinants associated with the intrinsic resistance to antibiotics. *Microorganisms* 9:2527. doi: 10.3390/MICROORGANISMS9122527

Greendyke, R., and Byrd, T. F. (2008). Differential antibiotic susceptibility of *Mycobacterium abscessus* variants in biofilms and macrophages compared to that of planktonic bacteria. *Antimicrob. Agents Chemother.* 52, 2019–2026. doi: 10.1128/AAC.00986-07

Guo, Q., Chen, J., Zhang, S., Zou, Y., Zhang, Y., Huang, D., et al. (2020). Efflux pumps contribute to intrinsic clarithromycin resistance in clinical, *Mycobacterium abscessus* Isolates. *Infect. Drug Resist.* 13, 447–454. doi: 10.2147/IDR.S239850

Guo, Q., Zhang, Y., Fan, J., Zhang, H., Zhang, Z., Li, B., et al. (2021). MAB_2355c confers macrolide resistance in *Mycobacterium abscessus* by ribosome protection. *Antimicrob. Agents Chemother.* 65:e0033021. doi: 10.1128/AAC.00330-21

Gupta, R., Netherton, M., Byrd, T. F., and Rohde, K. H. (2017). Reporter-based assays for high-throughput drug screening against *Mycobacterium abscessus*. *Front. Microbiol.* 8:2204. doi: 10.3389/FMICB.2017.02204

Gutiérrez, A. V., Richard, M., Roquet-Banères, F., Viljoen, A., and Kremer, L. (2019). The TetR family transcription factor MAB_2299c regulates the expression of two distinct MmpS-MmpL efflux pumps involved in cross-resistance to clofazimine and bedaquiline in *Mycobacterium abscessus*. *Antimicrob. Agents Chemother.* 63, e01000-19. doi: 10.1128/AAC.01000-19

Gutiérrez, A. V., Viljoen, A., Ghigo, E., Herrmann, J. L., and Kremer, L. (2018). Glycopeptidolipids, a double-edged sword of the *Mycobacterium abscessus* complex. *Front. Microbiol.* 9:1145. doi: 10.3389/FMICB.2018.01145

Halloum, I., Viljoen, A., Khanna, V., Craig, D., Bouchier, C., Brosch, R., et al. (2017). Resistance to thiacetazone derivatives active against *Mycobacterium abscessus* involves mutations in the MmpL5 transcriptional repressor MAB_4384. *Antimicrob. Agents Chemother.* 61, e02509-16. doi: 10.1128/AAC.02509-16

Hanh, B. T. B., Kim, T. H., Park, J. W., Lee, D. G., Kim, J. S., Du, Y. E., et al. (2020a). Etamycin as a novel *Mycobacterium abscessus* inhibitor. *Int. J. Mol. Sci.* 21:6908. doi: 10.3390/IJMS21186908

Hanh, B. T. B., Park, J. W., Kim, T. H., Kim, J. S., Yang, C. S., Jang, K., et al. (2020b). Rifamycin O, an alternative anti-*Mycobacterium abscessus* agent. *Molecules* 25:1597. doi: 10.3390/MOLECULES25071597

Harada, T., Akiyama, Y., Kurashima, A., Nagai, H., Tsuyuguchi, K., Fujii, T., et al. (2012). Clinical and microbiological differences between Mycobacterium abscessus and *Mycobacterium massiliense* lung diseases. *J. Clin. Microbiol.* 50, 3556–3561. doi: 10.1128/JCM.01175-12

Howard, S. T., Rhoades, E., Recht, J., Pang, X., Alsup, A., Kolter, R., et al. (2006). Spontaneous reversion of Mycobacterium abscessus from a smooth to a rough morphotype is associated with reduced expression of glycopeptidolipid and reacquisition of an invasive phenotype. *Microbiology* 152, 1581–1590. doi: 10.1099/mic.0.28625-0

Hurst-Hess, K., McManaman, C., Yang, Y., Gupta, S., and Ghosh, P. (2023). Hierarchy and interconnected networks in the WhiB7 mediated transcriptional response to antibiotic stress in *Mycobacterium abscessus*. *PLoS Genet.* 19:e1011060. doi: 10.1371/JOURNAL.PGEN.1011060

Hurst-Hess, K. R., Phelps, G. A., Wilt, L. A., Lee, R. E., and Ghosh, P. (2023). Mab2780c, a TetV-like efflux pump, confers high-level spectinomycin resistance in *Mycobacterium abscessus*. *Tuberculosis (Edinb.)* 138:102295. doi: 10.1016/J.TUBE.2022.102295

Hurst-Hess, K., Rudra, P., and Ghosh, P. (2017). *Mycobacterium abscessus* WhiB7 regulates a species-specific repertoire of genes to confer extreme antibiotic resistance. *Antimicrob. Agents Chemother.* 61, e01347-17. doi: 10.1128/AAC.01353-17

Ishikawa, M., García-Mateo, N., Čusak, A., López-Hernández, I., Fernández-Martínez, M., Müller, M., et al. (2019). Lower ototoxicity and absence of hidden hearing loss point to gentamicin C1a and apramycin as promising antibiotics for clinical use. *Sci. Rep.* 9:2410. doi: 10.1038/S41598-019-38634-3

Jahangir, M., Farwa, U., Mazhar, F., Malik, A., and Ahmad, E. (2016). *Pak. J. Pharm. Sci.* 29:Metal II complexes of ethambutol as good enzyme inhibitor and promising antioxidant, 1601–1608.

Jarlier, V., and Nikaido, H. (1994). Mycobacterial cell wall: structure and role in natural resistance to antibiotics. *FEMS Microbiol. Lett.* 123, 11–18. doi: 10.1111/J.1574-6968.1994.TB07194.X

Jeong, S. H., Kim, S. Y., Huh, H. J., Ki, C. S., Lee, N. Y., Kang, C. I., et al. (2017). Mycobacteriological characteristics and treatment outcomes in extrapulmonary *Mycobacterium abscessus* complex infections. *Int. J. Infect. Dis.* 60, 49–56. doi: 10.1016/J.IJID.2017.05.007

Jeong, J., Kim, G., Moon, C., Kim, H. J., Kim, T. H., and Jang, J. (2018). Pathogen box screening for hit identification against *Mycobacterium abscessus*. *PLoS One* 13:e0195595. doi: 10.1371/JOURNAL.PONE.0195595

Johansen, M. D., Daher, W., Roquet-Banères, F., Raynaud, C., Alcaraz, M., Maurer, F. P., et al. (2020a). Rifabutin is bactericidal against intracellular and extracellular forms of *Mycobacterium abscessus*. *Antimicrob. Agents Chemother.* 64, e00363-20. doi: 10.1128/AAC.00363-20

Johansen, M. D., Herrmann, J. L., and Kremer, L. (2020b). Non-tuberculous mycobacteria and the rise of *Mycobacterium abscessus*. *Nat. Rev. Microbiol.* 18, 392–407. doi: 10.1038/S41579-020-0331-1

Jönsson, B. E., Bylund, J., Johansson, B. R., Telemo, E., and Wold, A. E. (2013). Cord-forming mycobacteria induce DNA meshwork formation by human peripheral blood mononuclear cells. *Pathog. Dis.* 67, 54–66. doi: 10.1111/2049-632X.12007

Juhas, M., Widlake, E., Teo, J., Huseby, D. L., Tyrrell, J. M., Polikanov, Y. S., et al. (2019). In vitro activity of apramycin against multidrug-, carbapenem- and aminoglycoside-resistant enterobacteriaceae and *Acinetobacter baumannii*. *J. Antimicrob. Chemother.* 74, 944–952. doi: 10.1093/JAC/DKY546

Kaushik, A., Ammerman, N. C., Martins, O., Parrish, N. M., and Nuermberger, E. L. (2019a). In vitro activity of new tetracycline analogs omadacycline and eravacycline against drug-resistant clinical isolates of *Mycobacterium abscessus*. *Antimicrob. Agents Chemother.* 63, e00470-19. doi: 10.1128/AAC.00470-19

Kaushik, A., Ammerman, N. C., Parrish, N. M., and Nuermberger, E. L. (2019b). New β-lactamase inhibitors nacubactam and zidebactam improve the in vitro activity of β-lactam antibiotics against *Mycobacterium abscessus* complex clinical isolates. *Antimicrob. Agents Chemother.* 63, e00733-19. doi: 10.1128/AAC.00733-19

Kerr, I. D. (2002). Structure and association of ATP-binding cassette transporter nucleotide-binding domains. *Biochim. Biophys. Acta-Biomembr.* 1561, 47–64. doi: 10.1016/S0304-4157(01)00008-9

Kerr, I. D., Reynolds, E. D., and Cove, J. H. (2005). ABC proteins and antibiotic drug resistance: is it all about transport? *Biochem. Soc. Trans.* 33, 1000–1002. doi: 10.1042/BST0331000

Kim, T. H., Bich Hanh, B. T., Kim, G., Lee, D. G., Park, J. W., Lee, S. E., et al. (2019). Thiostrepton: a novel therapeutic drug candidate for *Mycobacterium abscessus* infection. *Molecules* 24:4511. doi: 10.3390/MOLECULES24244511

Kim, T. S., Choe, J. H., Kim, Y. J., Yang, C. S., Kwon, H. J., Jeong, J., et al. (2017). Activity of LCB01-0371, a novel oxazolidinone, against *Mycobacterium abscessus*. *Antimicrob. Agents Chemother.* 61, e02752-16. doi: 10.1128/AAC.02752-16

Kim, T., Hanh, B. T. B., Heo, B., Quang, N., Park, Y., Shin, J., et al. (2021). A screening of the MMV pandemic response box reveals epetraborole as a new potent inhibitor against *Mycobacterium abscessus*. *Int. J. Mol. Sci.* 22:5936. doi: 10.3390/IJMS22115936

Kozikowski, A. P., Onajole, O. K., Stec, J., Dupont, C., Viljoen, A., Richard, M., et al. (2017). Targeting mycolic acid transport by indole-2-carboxamides for the treatment of *Mycobacterium abscessus* infections. *J. Med. Chem.* 60, 5876–5888. doi: 10.1021/ACS.JMEDCHEM.7B00582

Lan, T., Ganapathy, U. S., Sharma, S., Ahn, Y. M., Zimmerman, M., Molodtsov, V., et al. (2022). Redesign of rifamycin antibiotics to overcome ADP-ribosylation-mediated resistance. *Angew. Chem. Int. Ed. Engl.* 61:e202211498. doi: 10.1002/ANIE.202211498

Le Run, E., Arthur, M., and Mainardia, J. L. (2019). In vitro and intracellular activity of imipenem combined with tedizolid, rifabutin, and avibactam against *Mycobacterium abscessus*. *Antimicrob. Agents Chemother.* 63, e01915-18. doi: 10.1128/AAC.01915-18

Lee, M. R., Sheng, W. H., Hung, C. C., Yu, C. J., Lee, L. N., and Hsueh, P. R. (2015). *Mycobacterium abscessus* complex infections in humans. *Emerg. Infect. Dis.* 21, 1638–1646. doi: 10.3201/EID2109.141634

Lefebvre, A. L., Dubée, V., Cortes, M., Dorchêne, D., Arthur, M., and Mainardi, J. L. (2016). Bactericidal and intracellular activity of β-lactams against *Mycobacterium abscessus*. *J. Antimicrob. Chemother.* 71, 1556–1563. doi: 10.1093/JAC/DKW022

Lefebvre, A. L., Le Moigne, V., Bernut, A., Veckerlé, C., Compain, F., Herrmann, J. L., et al. (2017). Inhibition of the β-lactamase BlaMab by avibactam improves the in vitro and in vivo efficacy of imipenem against *Mycobacterium abscessus*. *Antimicrob. Agents Chemother.* 61, e02440-16. doi: 10.1128/AAC.02440-16

Li, W., Upadhyay, A., Fontes, F. L., North, E. J., Wang, Y., Crans, D. C., et al. (2014). Novel insights into the mechanism of inhibition of MmpL3, a target of multiple pharmacophores in *Mycobacterium tuberculosis*. *Antimicrob. Agents Chemother.* 58, 6413–6423. doi: 10.1128/AAC.03229-14

Li, B., Ye, M., Guo, Q., Zhang, Z., Yang, S., Ma, W., et al. (2018). Determination of MIC distribution and mechanisms of decreased susceptibility to bedaquiline among clinical isolates of *Mycobacterium abscessus*. *Antimicrob. Agents Chemother.* 62, e00175-18. doi: 10.1128/AAC.00175-18

Lipman, M., Kunst, H., Loebinger, M. R., Milburn, H. J., and King, M. (2021). Non tuberculous mycobacteria pulmonary disease: patients and clinicians working together to improve the evidence base for care. *Int. J. Infect. Dis.* 113, S73–S77. doi: 10.1016/J.IJID.2021.03.064

Lopeman, R. C., Harrison, J., Desai, M., and Cox, J. A. G. (2019). *Mycobacterium abscessus*: environmental bacterium turned clinical nightmare. *Microorganisms* 7:90. doi: 10.3390/MICROORGANISMS7030090

López-Roa, P., Esteban, J., and Muñoz-Egea, M. C. (2022). Updated review on the mechanisms of pathogenicity in *Mycobacterium abscessus*, a rapidly growing emerging pathogen. *Microorganisms* 11:90. doi: 10.3390/MICROORGANISMS11010090

Lorè, N. I., Saliu, F., Spitaleri, A., Schäfle, D., Nicola, F., Cirillo, D. M., et al. (2022). The aminoglycoside-modifying enzyme Eis2 represents a new potential in vivo target for reducing antimicrobial drug resistance in *Mycobacterium abscessus* complex. *Eur. Respir. J.* 60:2201541. doi: 10.1183/13993003.01541-2022

Louw, G. E., Warren, R. M., Gey Van Pittius, N. C., McEvoy, C. R. E., Van Helden, P. D., and Victor, T. C. (2009). A balancing act: efflux/influx in mycobacterial drug resistance. *Antimicrob. Agents Chemother.* 53, 3181–3189. doi: 10.1128/AAC.01577-08

Luthra, S., Rominski, A., and Sander, P. (2018). The role of antibiotic-target-modifying and antibiotic-modifying enzymes in *Mycobacterium abscessus* drug resistance. *Front. Microbiol.* 9:2179. doi: 10.3389/FMICB.2018.02179

Malin, J. J., Winter, S., Van Gumpel, E., Plum, G., and Rybniker, J. (2019). Extremely low hit rate in a diverse chemical drug screen targeting *Mycobacterium abscessus*. *Antimicrob. Agents Chemother.* 63, e01008-19. doi: 10.1128/AAC.01008-19

Marrakchi, H., Lanéelle, M. A., and Daffé, M. (2014). Mycolic acids: structures, biosynthesis, and beyond. *Chem. Biol.* 21, 67–85. doi: 10.1016/J.CHEMBIOL.2013.11.011

Martin, C., Timm, J., Rauzier, J., Gomez-Lus, R., Davies, J., and Gicquel, B. (1990). Transposition of an antibiotic resistance element in mycobacteria. *Nat* 345, 739–743. doi: 10.1038/345739a0

Matrat, S., Aubry, A., Mayer, C., Jarlier, V., and Cambau, E. (2008). Mutagenesis in the α3α4 GyrA helix and in the toprim domain of GyrB refines the contribution of *Mycobacterium tuberculosis* DNA gyrase to intrinsic resistance to quinolones. *Antimicrob. Agents Chemother.* 52, 2909–2914. doi: 10.1128/AAC.01380-07

Matt, T., Ng, C. L., Lang, K., Sha, S. H., Akbergenov, R., Shcherbakov, D., et al. (2012). Dissociation of antibacterial activity and aminoglycoside ototoxicity in the 4-monosubstituted 2-deoxystreptamine apramycin. *Proc. Natl. Acad. Sci. U. S. A.* 109, 10984–10989. doi: 10.1073/PNAS.1204073109

Maurer, F. P., Castelberg, C., Quiblier, C., Böttger, E. C., and Somoskövi, A. (2014). Erm(41)-dependent inducible resistance to azithromycin and clarithromycin in clinical isolates of *Mycobacterium abscessus*. *J. Antimicrob. Chemother.* 69, 1559–1563. doi: 10.1093/JAC/DKU007

Maurer, F. P., Rüegger, V., Ritter, C., Bloemberg, G. V., and Böttger, E. C. (2012). Acquisition of clarithromycin resistance mutations in the 23S rRNA gene of *Mycobacterium abscessus* in the presence of inducible erm(41). *J. Antimicrob. Chemother.* 67, 2606–2611. doi: 10.1093/JAC/DKS279

McNeil, M. B., O'Malley, T., Dennison, D., Shelton, C. D., Sunde, B., and Parish, T. (2020). Multiple mutations in *Mycobacterium tuberculosis* MmpL3 increase resistance to MmpL3 inhibitors. *mSphere* 5, e00985-20. doi: 10.1128/MSPHERE.00985-20

Meir, M., Bifani, P., and Barkan, D. (2018). The addition of avibactam renders piperacillin an effective treatment for *Mycobacterium abscessus* infection in an in vivo model. *Antimicrob. Resist. Infect. Control* 7:151. doi: 10.1186/S13756-018-0448-4

Mingeot-Leclercq, M. P., Glupczynski, Y., and Tulkens, P. M. (1999). Aminoglycosides: activity and resistance. *Antimicrob. Agents Chemother.* 43, 727–737. doi: 10.1128/AAC.43.4.727

Moguillansky, N., DeSear, K., and Dousa, K. M. (2023). A 40-year-old female with *Mycobacterium abscessus* successfully treated with a dual beta-lactam combination. *Cureus* 15:e40993. doi: 10.7759/CUREUS.40993

Moore, M., and Frerichs, J. B. (1953). An unusual acid-fast infection of the knee with subcutaneous, abscess-like lesions of the gluteal region; report of a case with a study of the organism, *Mycobacterium abscessus*, n. sp. *J. Invest. Dermatol.* 20, 133–169. doi: 10.1038/jid.1953.18

Moore, J. E., Koulianos, G., Hardy, M., Misawa, N., and Millar, B. C. (2018). Antimycobacterial activity of veterinary antibiotics (apramycin and framycetin) against *Mycobacterium abscessus*: implication for patients with cystic fibrosis. *Int. J. Mycobacteriol.* 7, 265–267. doi: 10.4103/IJMY.IJMY_73_18

Morris, R. P., Nguyen, L., Gatfield, J., Visconti, K., Nguyen, K., Schnappinger, D., et al. (2005). Ancestral antibiotic resistance in *Mycobacterium tuberculosis*. *Proc. Natl. Acad. Sci. U. S. A.* 102, 12200–12205. doi: 10.1073/PNAS.0505446102

Nash, K. A., Brown-Elliott, A. B., and Wallace, R. J. (2009). A novel gene, erm(41), confers inducible macrolide resistance to clinical isolates of *Mycobacterium abscessus* but is absent from *Mycobacterium chelonae*. *Antimicrob. Agents Chemother.* 53, 1367–1376. doi: 10.1128/AAC.01275-08

Negatu, D. A., Aragaw, W. W., Dartois, V., and Dick, T. (2023). Characterization of in vitro resistance to linezolid in *Mycobacterium abscessus*. *Microbiol. Spectr.* 11:e0219923. doi: 10.1128/SPECTRUM.02199-23

Nessar, R., Cambau, E., Reyrat, J. M., Murray, A., and Gicquel, B. (2012). *Mycobacterium abscessus*: a new antibiotic nightmare. *J. Antimicrob. Chemother.* 67, 810–818. doi: 10.1093/JAC/DKR578

Nessar, R., Reyrat, J. M., Murray, A., and Gicquel, B. (2011). Genetic analysis of new 16S rRNA mutations conferring aminoglycoside resistance in *Mycobacterium abscessus*. *J. Antimicrob. Chemother.* 66, 1719–1724. doi: 10.1093/JAC/DKR209

Ng, H. F., and Ngeow, Y. F. (2022). Genetic determinants of tigecycline resistance in Mycobacteroides abscessus. *Antibiotics* 11:572. doi: 10.3390/ANTIBIOTICS11050572

Nguyen, T. Q., Heo, B. E., Hanh, B. T. B., Jeon, S., Park, Y., Choudhary, A., et al. (2023). DS86760016, a Leucyl-tRNA synthetase inhibitor, is active against *Mycobacterium abscessus*. *Antimicrob. Agents Chemother.* 67:e0156722. doi: 10.1128/AAC.01567-22

Nguyen, L., and Thompson, C. J. (2006). Foundations of antibiotic resistance in bacterial physiology: the mycobacterial paradigm. *Trends Microbiol.* 14, 304–312. doi: 10.1016/j.tim.2006.05.005

Nicklas, D. A., Maggioncalda, E. C., Story-Roller, E., Eichelman, B., Tabor, C., Serio, A. W., et al. (2022). Potency of omadacycline against Mycobacteroides abscessus clinical isolates in vitro and in a mouse model of pulmonary infection. *Antimicrob. Agents Chemother.* 66:e0170421. doi: 10.1128/AAC.01704-21

NIH ClinicalTrials (2023). Available at: https://classic.clinicaltrials.gov/ct2/results?cond=abscessus&term=&cntry=&state=&city=&dist=.

Pantel, A., Petrella, S., Matrat, S., Brossier, F., Bastian, S., Reitter, D., et al. (2011). DNA gyrase inhibition assays are necessary to demonstrate fluoroquinolone resistance secondary to gyrB mutations in *Mycobacterium tuberculosis*. *Antimicrob. Agents Chemother.* 55, 4524–4529. doi: 10.1128/AAC.00707-11

Paulowski, L., Beckham, K. S. H., Johansen, M. D., Berneking, L., Van, N., Degefu, Y., et al. (2022). C25-modified rifamycin derivatives with improved activity against *Mycobacterium abscessus*. *PNAS Nexus* 1:pgac130. doi: 10.1093/PNASNEXUS/PGAC130

Pethe, K., Bifani, P., Jang, J., Kang, S., Park, S., Ahn, S., et al. (2013). Discovery of Q203, a potent clinical candidate for the treatment of tuberculosis. *Nat. Med.* 19, 1157–1160. doi: 10.1038/NM.3262

Piccaro, G., Pietraforte, D., Giannoni, F., Mustazzolu, A., and Fattorini, L. (2014). Rifampin induces hydroxyl radical formation in *Mycobacterium tuberculosis*. *Antimicrob. Agents Chemother.* 58, 7527–7533. doi: 10.1128/AAC.03169-14

Prammananan, T., Sander, P., Brown, B. A., Frischkorn, K., Onyi, G. O., Zhang, Y., et al. (1998). A single 16S ribosomal RNA substitution is responsible for resistance to amikacin and other 2-deoxystreptamine aminoglycosides in Mycobacterium abscessus and *Mycobacterium chelonae*. *J. Infect. Dis.* 177, 1573–1581. doi: 10.1086/515328

Pryjma, M., Burian, J., Kuchinski, K., and Thompson, C. J. (2017). Antagonism between front-line antibiotics clarithromycin and amikacin in the treatment of *Mycobacterium abscessus* infections is mediated by the whiB7 gene. *Antimicrob. Agents Chemother.* 61, e01353-17. doi: 10.1128/AAC.01347-17

Quang, N. T., and Jang, J. (2021). Current molecular therapeutic agents and drug candidates for *Mycobacterium abscessus*. *Front. Pharmacol.* 12:2117. doi: 10.3389/FPHAR.2021.724725

Ramírez, A., Ruggiero, M., Aranaga, C., Cataldi, A., Gutkind, G., De Waard, J. H., et al. (2017). Biochemical characterization of β-lactamases from *Mycobacterium abscessus* complex and genetic environment of the β-lactamase-encoding gene. *Microb. Drug Resist.* 23, 294–300. doi: 10.1089/MDR.2016.0047

Ratnatunga, C. N., Lutzky, V. P., Kupz, A., Doolan, D. L., Reid, D. W., Field, M., et al. (2020). The rise of non-tuberculosis mycobacterial lung disease. *Front. Immunol.* 11:303. doi: 10.3389/FIMMU.2020.00303

Redgrave, L. S., Sutton, S. B., Webber, M. A., and Piddock, L. J. V. (2014). Fluoroquinolone resistance: mechanisms, impact on bacteria, and role in evolutionary success. *Trends Microbiol.* 22, 438–445. doi: 10.1016/J.TIM.2014.04.007

Remm, S., Earp, J. C., Dick, T., Dartois, V., and Seeger, M. A. (2022). Critical discussion on drug efflux in *Mycobacterium tuberculosis*. *FEMS Microbiol. Rev.* 46:fuab050. doi: 10.1093/FEMSRE/FUAB050

Richard, M., Gutiérrez, A. V., Viljoen, A. J., Ghigo, E., Blaise, M., and Kremer, L. (2018a). Mechanistic and structural insights into the unique TetR-dependent regulation of a drug efflux pump in *Mycobacterium abscessus*. *Front. Microbiol.* 9:649. doi: 10.3389/FMICB.2018.00649

Richard, M., Gutiérrez, A. V., Viljoen, A., Rodriguez-Rincon, D., Roquet-Baneres, F., Blaise, M., et al. (2018b). Mutations in the MAB_2299c TetR regulator confer cross-resistance to clofazimine and bedaquiline in *Mycobacterium abscessus*. *Antimicrob. Agents Chemother.* 63, e01316-18. doi: 10.1128/AAC.01316-18

Richter, A., Strauch, A., Chao, J., Ko, M., and Av-Gay, Y. (2018). Screening of preselected libraries targeting *Mycobacterium abscessus* for drug discovery. *Antimicrob. Agents Chemother.* 62, e00828-18. doi: 10.1128/AAC.00828-18

Ripoll, F., Pasek, S., Schenowitz, C., Dossat, C., Barbe, V., Rottman, M., et al. (2009). Non mycobacterial virulence genes in the genome of the emerging pathogen *Mycobacterium abscessus*. *PLoS One* 4:e5660. doi: 10.1371/JOURNAL.PONE.0005660

Rock, F. L., Mao, W., Yaremchuk, A., Tukalo, M., Crépin, T., Zhou, H., et al. (2007). An antifungal agent inhibits an aminoacyl-tRNA synthetase by trapping tRNA in the editing site. *Science* 316, 1759–1761. doi: 10.1126/science.1142189

Rominski, A., Roditscheff, A., Selchow, P., Böttger, E. C., and Sander, P. (2017a). Intrinsic rifamycin resistance of *Mycobacterium abscessus* is mediated by ADP-ribosyltransferase MAB_0591. *J. Antimicrob. Chemother.* 72, 376–384. doi: 10.1093/JAC/DKW466

Rominski, A., Selchow, P., Becker, K., Brülle, J. K., Dal Molin, M., and Sander, P. (2017b). Elucidation of *Mycobacterium abscessus* aminoglycoside and capreomycin resistance by targeted deletion of three putative resistance genes. *J. Antimicrob. Chemother.* 72, 2191–2200. doi: 10.1093/JAC/DKX125

Roux, A. L., Viljoen, A., Bah, A., Simeone, R., Bernut, A., Laencina, L., et al. (2016). The distinct fate of smooth and rough *Mycobacterium abscessus* variants inside macrophages. *Open Biol.* 6:160185. doi: 10.1098/RSOB.160185

Rubio, M., March, F., Garrigó, M., Moreno, C., Español, M., and Coll, P. (2015). Inducible and acquired clarithromycin resistance in the *Mycobacterium abscessus* complex. *PLoS One* 10:e0140166. doi: 10.1371/JOURNAL.PONE.0140166

Rudra, P., Hurst-Hess, K., Lappierre, P., and Ghosha, P. (2018). High levels of intrinsic tetracycline resistance in *Mycobacterium abscessus* are conferred by a tetracycline-modifying monooxygenase. *Antimicrob. Agents Chemother.* 62, e00119-18. doi: 10.1128/AAC.00119-18

Ruis, C., Bryant, J. M., Bell, S. C., Thomson, R., Davidson, R. M., Hasan, N. A., et al. (2021). Dissemination of *Mycobacterium abscessus* via global transmission networks. *Nat. Microbiol.* 6, 1279–1288. doi: 10.1038/s41564-021-00963-3

Saxena, S., Spaink, H. P., and Forn-Cuní, G. (2021). Drug resistance in nontuberculous mycobacteria: mechanisms and models. *Biology (Basel).* 10, 1–22. doi: 10.3390/BIOLOGY10020096

Schäfle, D., Selchow, P., Borer, B., Meuli, M., Rominski, A., Schulthess, B., et al. (2021). Rifabutin is inactivated by *Mycobacterium abscessus* Arr. *Antimicrob. Agents Chemother.* 65, e02215-20. doi: 10.1128/AAC.02215-20

Selchow, P., Ordway, D. J., Verma, D., Whittel, N., Petrig, A., Hobbie, S. N., et al. (2022). Apramycin overcomes the inherent lack of antimicrobial bactericidal activity in *Mycobacterium abscessus*. *Antimicrob. Agents Chemother.* 66:e0151021. doi: 10.1128/AAC.01510-21

Shin, S. J., Choi, G. E., Cho, S. N., Woo, S. Y., Jeong, B. H., Jeon, K., et al. (2013). Mycobacterial genotypes are associated with clinical manifestation and progression of lung disease caused by Mycobacterium abscessus and *Mycobacterium massiliense*. *Clin. Infect. Dis.* 57, 32–39. doi: 10.1093/CID/CIT172

Shoen, C., Benaroch, D., Sklaney, M., and Cynamon, M. (2019). In vitro activities of Omadacycline against rapidly growing mycobacteria. *Antimicrob. Agents Chemother.* 63, e02522-18. doi: 10.1128/AAC.02522-18

Singh, S., Wang, J. Y., Heysell, S. K., McShane, P. J., Wadle, C., Shankar, P., et al. (2023). Omadacycline pharmacokinetics/pharmacodynamics in the hollow fiber model and clinical validation of efficacy to treat pulmonary *Mycobacterium abscessus* disease. *Int. J. Antimicrob. Agents* 62:106847. doi: 10.1016/J.IJANTIMICAG.2023.106847

Soliveri, J. A., Gomez, J., Bishai, W. R., and Chater, K. F. (2000). Multiple paralogous genes related to the *Streptomyces coelicolor* developmental regulatory gene whiB are present in streptomyces and other actinomycetes. *Microbiology* 146, 333–343. doi: 10.1099/00221287-146-2-333

Song, L., and Wu, X. (2016). Development of efflux pump inhibitors in antituberculosis therapy. *Int. J. Antimicrob. Agents* 47, 421–429. doi: 10.1016/J.IJANTIMICAG.2016.04.007

Sorayah, R., Manimekalai, M. S. S., Shin, S. J., Koh, W. J., Grüber, G., and Pethe, K. (2019). Naturally-occurring polymorphisms in QcrB are responsible for resistance to telacebec in *Mycobacterium abscessus*. *ACS Infect. Dis.* 5, 2055–2060. doi: 10.1021/ACSINFECDIS.9B00322

Soroka, D., Ourghanlian, C., Compain, F., Fichini, M., Dubée, V., Mainardi, J. L., et al. (2017). Inhibition of β-lactamases of mycobacteria by avibactam and clavulanate. *J. Antimicrob. Chemother.* 72, dkw546–dkw1088. doi: 10.1093/JAC/DKW546

Sreevatsan, S., Stockbauer, K. E., Pan, X., Kreiswirth, B. N., Moghazeh, S. L., Jacobs, W. R., et al. (1997). Ethambutol resistance in *Mycobacterium tuberculosis*: critical role of embB mutations. *Antimicrob. Agents Chemother.* 41, 1677–1681. doi: 10.1128/AAC.41.8.1677

Stein, G. E., and Craig, W. A. (2006). Tigecycline: a critical analysis. *Clin. Infect. Dis.* 43, 518–524. doi: 10.1086/505494

Story-Roller, E., Maggioncalda, E. C., Cohen, K. A., and Lamichhane, G. (2018). Mycobacterium abscessus and β-lactams: emerging insights and potential opportunities. *Front. Microbiol.* 9:2273. doi: 10.3389/FMICB.2018.02273

Stout, J. E., and Floto, R. A. (2012). Treatment of *Mycobacterium abscessus*: all macrolides are equal, but perhaps some are more equal than others. *Am. J. Respir. Crit. Care Med.* 186, 822–823. doi: 10.1164/RCCM.201208-1500ED

Swenson, C., Zerbe, C. S., and Fennelly, K. (2018). Host variability in NTM disease: implications for research needs. *Front. Microbiol.* 9:2901. doi: 10.3389/FMICB.2018.02901

Tsai, S. H., Lai, H. C., and Hu, S. T. (2015). Subinhibitory doses of aminoglycoside antibiotics induce changes in the phenotype of *Mycobacterium abscessus*. *Antimicrob. Agents Chemother.* 59, 6161–6169. doi: 10.1128/AAC.01132-15

Ung, K. L., Alsarraf, H. M. A. B., Olieric, V., Kremer, L., and Blaise, M. (2019). Crystal structure of the aminoglycosides N-acetyltransferase Eis2 from *Mycobacterium abscessus*. *FEBS J.* 286, 4342–4355. doi: 10.1111/FEBS.14975

Ventola, C. L. (2015). The antibiotic resistance crisis: part 1: causes and threats. *Pharm. Ther.* 40:277.

Vester, B., and Douthwaite, S. (2001). Macrolide resistance conferred by base substitutions in 23S rRNA. *Antimicrob. Agents Chemother.* 45, 1–12. doi: 10.1128/AAC.45.1.1-12.2001

Vianna, J. S., Machado, D., Ramis, I. B., Silva, F. P., Bierhals, D. V., Abril, M. A., et al. (2019). The contribution of efflux pumps in *Mycobacterium abscessus* complex resistance to clarithromycin. *Antibiotics (Basel, Switzerland)* 8:153. doi: 10.3390/ANTIBIOTICS8030153

Victoria, L., Gupta, A., Gómez, J. L., and Robledo, J. (2021). *Mycobacterium abscessus* complex: a review of recent developments in an emerging pathogen. *Front. Cell. Infect. Microbiol.* 11:659997. doi: 10.3389/FCIMB.2021.659997

Wallace, R. J., Meier, A., Brown, B. A., Zhang, Y., Sander, P., Onyi, G. O., et al. (1996). Genetic basis for clarithromycin resistance among isolates of Mycobacterium chelonae and *Mycobacterium abscessus*. *Antimicrob. Agents Chemother.* 40, 1676–1681. doi: 10.1128/AAC.40.7.1676

Wassilew, N., Hoffmann, H., Andrejak, C., and Lange, C. (2016). Pulmonary disease caused by non-tuberculous mycobacteria. *Respiration* 91, 386–402. doi: 10.1159/000445906

Watkins, R. R., and Deresinski, S. (2019). Omadacycline: a novel tetracycline derivative with oral and intravenous formulations. *Clin. Infect. Dis.* 69, 890–896. doi: 10.1093/CID/CIZ242

Wu, M. L., Aziz, D. B., Dartois, V., and Dick, T. (2018). NTM drug discovery: status, gaps and the way forward. *Drug Discov. Today* 23, 1502–1519. doi: 10.1016/J.DRUDIS.2018.04.001

Wu, W., He, S., Li, A., Guo, Q., Tan, Z., Liu, S., et al. (2022). A novel leucyl-tRNA synthetase inhibitor, MRX-6038, expresses anti-*Mycobacterium abscessus* activity in vitro and in vivo. *Antimicrob. Agents Chemother.* 66:e0060122. doi: 10.1128/AAC.00601-22

Young, S., Kim, D. H., Moon, S. M., Song, J. Y., Huh, H. J., Lee, N. Y., et al. (2021). Association between 16S rRNA gene mutations and susceptibility to amikacin in *Mycobacterium avium* complex and *Mycobacterium abscessus* clinical isolates. *Sci. Rep.* 11:6108. doi: 10.1038/s41598-021-85721-5

Zheng, M., and Lupoli, T. J. (2021). Modulation of a mycobacterial ADP-ribosyltransferase to augment rifamycin antibiotic resistance. *ACS Infect. Dis.* 7, 2604–2611. doi: 10.1021/ACSINFECDIS.1C00297

Zheng, L., Qi, X., Zhang, W., Wang, H., Fu, L., Wang, B., et al. (2023). Efficacy of PBTZ169 and pretomanid against *Mycobacterium avium*, *Mycobacterium abscessus*, Mycobacterium chelonae, and *Mycobacterium fortuitum* in BALB/c mice models. *Front. Cell. Infect. Microbiol.* 13:1115530. doi: 10.3389/FCIMB.2023.1115530

frontiers | Frontiers in Microbiology

TYPE Systematic Review
PUBLISHED 19 February 2024
DOI 10.3389/fmicb.2024.1321273

OPEN ACCESS

EDITED BY
Matt Johansen,
University of Technology Sydney, Australia

REVIEWED BY
Beatriz E. Ferro,
Universidad Icesi, Colombia
Dereje Abate Negatu,
Center for Discovery and Innovation,
Hackensack Meridian Health, United States

*CORRESPONDENCE
Faramarz Masjedian Jazi
✉ Masjedian.f@iums.ac.ir

RECEIVED 03 January 2024
ACCEPTED 02 February 2024
PUBLISHED 19 February 2024

CITATION
Narimisa N, Bostanghadiri N, Goodarzi F, Razavi S and Jazi FM (2024) Prevalence of *Mycobacterium kansasii* in clinical and environmental isolates, a systematic review and meta-analysis.
Front. Microbiol. 15:1321273.
doi: 10.3389/fmicb.2024.1321273

Prevalence of *Mycobacterium kansasii* in clinical and environmental isolates, a systematic review and meta-analysis

Negar Narimisa[1], Narjess Bostanghadiri[1], Forough Goodarzi[2], Shabnam Razavi[1] and Faramarz Masjedian Jazi[1]*

[1]Department of Microbiology, School of Medicine, Iran University of Medical Sciences, Tehran, Iran, [2]Department of Bacteriology, Faculty of Medical Sciences, Tarbiat Modares University, Tehran, Iran

Background: *Mycobacterium kansasii* infection is one of the most common causes of non-tuberculosis mycobacterial (NTM) disease worldwide. However, accurate information on the global prevalence of this bacterium is lacking. Therefore, this study was conducted to investigate the prevalence of *M. kansasii* in clinical and environmental isolates.

Methods: Databases, including PubMed, Scopus, and the Web of Science, were utilized to gather articles on the prevalence of *M. kansasii* in clinical and environmental isolates. The collected data were analyzed using Comprehensive Meta-Analysis software.

Results: A total of 118 and 16 studies met the inclusion criteria and were used to analyze the prevalence of *M. kansasii* in clinical and environmental isolates, respectively. The prevalence of *M. kansasii* in NTM and environmental isolates were 9.4 and 5.8%, respectively. Subsequent analysis showed an increasing prevalence of *M. kansasii* over the years. Additionally, the results indicated a significant difference in the prevalence of this bacteria among different regions.

Conclusion: The relatively high prevalence of *M. kansasii* among NTM isolates suggests the need for further implementation of infection control strategies. It is also important to establish appropriate diagnostic criteria and management guidelines for screening this microorganism in environmental samples in order to prevent its spread, given its high prevalence in environmental isolates.

KEYWORDS

***Mycobacterium kansasii*, meta-analysis, CMA, prevalence, NTM**

Introduction

The genus *Mycobacterium* comprises over 200 species, divided into the *Mycobacterium tuberculosis* (MTB) complex and non-tuberculosis mycobacteria (NTM) (Karami-Zarandi et al., 2019). NTM is a diverse group of opportunistic bacteria that are commonly found in water, soil, and dust. While tuberculosis (TB) is the most prevalent mycobacterial infection in developing countries, the incidence of NTM diseases is rising globally, surpassing tuberculosis in developed nations (Johansen et al., 2020; Pavlik et al., 2022).

Initially, NTMs were considered contaminants rather than pathogens due to their presence in environmental sources (Koh, 2017). However, the incidence of NTM diseases has increased, and the exact cause of this rise remains poorly understood. Factors such as an aging population, reduced immune function, and environmental exposure to mycobacteria have been suggested as possible explanations (Cowman et al., 2019).

Mycobacterium kansasii (*M. kansasii*) is a slow-growing NTM that causes pulmonary and extra-pulmonary infections, in immunocompromised and immunocompetent individuals (Khosravi et al., 2020). The disease caused by *M. kansasii* closely resembles pulmonary tuberculosis in terms of pathogenesis, clinical features, and treatment response, differing significantly from infections caused by other NTM, particularly the *M. avium* complex (Woods and Washington, 1987).

Traditionally, *M. kansasii* has been recognized as an NTM pathogen causing lung disease rather than a contaminant. The isolation of *M. kansasii* from sputum under appropriate conditions may be sufficient evidence to indicate disease and to initiate treatment (Matveychuk et al., 2012; Daley et al., 2020).

Global reports have identified *M. kansasii* as the sixth most commonly isolated NTM from clinical samples. Additionally, it has been reported as the leading cause of pulmonary NTM disease in sub-Saharan Africa and the third most prevalent NTM causing lung disease in Taiwan (Huang et al., 2017; Okoi et al., 2017).

There is a widely held belief that *M. kansasii* can be acquired from the environment and is present in various natural ecosystems, including water, soil, and dust. Numerous studies have documented the recovery of this organism from municipal water distribution systems, with isolates found in the same communities where *M. kansasii* disease patients have been identified (McSwiggan and Collins, 1974; Steadham, 1980). The epidemiology of *M. kansasii* primarily affects urban areas, particularly high-density, low-income communities in highly industrialized regions (Kwenda et al., 2015).

Considering the clinical importance of *M. kansasii* and the lack of a meta-analysis study examining the prevalence of *M. kansasii* in clinical and environmental samples, the aim of this study is to investigate its prevalence in both clinical and environmental samples. The information obtained from this study can contribute to the effective management of this bacterium.

Materials and methods

Search strategy

We conducted a search of journal articles in three databases (PubMed, Scopus, and Web of Science) until February 2023. All of these databases were searched using the following search strategy: "*Mycobacterium kansasii*" OR "*M. kansasii*."

Eligibility criteria

All studies that provided the precise number of *M. kansasii* isolates - either as total isolates or as part of NTM isolates in clinical samples, as well as studies that reported the bacterial count in environmental samples, were included in this study.

All identified articles were collated using Endnote X20 Citation Manager Software, and duplicate articles were removed prior to review. The citations were then uploaded to Rayyan, a citation classification application (Ouzzani et al., 2016). Two independent reviewers screened the titles and abstracts, and removed irrelevant articles. Full texts of potentially relevant articles were independently collected and reviewed by two authors. If there was a disagreement about the inclusion of an article after screening, a third author determined its eligibility for full review.

Review articles, case report studies, short communications, conference papers, letters, book chapters, articles that did not mention the exact number of isolates, and articles written in languages other than English were excluded.

Data extraction

Two authors independently extracted all data from eligible articles. Any disagreements in data points were resolved through consensus and discussion. From each article, we collected information on the first author, publication year, sampling time, study country, continent, and sample size (total number of samples and number of M. *kansasi* in clinical and environmental samples). This study selection process was presented in a Preferred Reporting Item for Systematic Reviews and Meta-Analyses (PRISMA) flowchart (Figure 1).

Study quality assessment

The quality of included studies was evaluated using the Joanna Briggs Institute (JBI) Critical Appraisal Checklist (Munn et al., 2020). This checklist consists of nine questions that assess the quality of studies, focusing on appropriate sampling techniques, research objectives, and adequate data analysis. Each item is rated as "yes," "no," or "unclear." A score of 1 point is given for each "yes" answer, and a score of 0 points is given for each "no" or "unclear" answer. Finally, the mean score of each paper was independently evaluated by two reviewers, and any disagreements were resolved through consensus between the two reviewers or by consulting a third author, if needed.

Data analysis

Data analysis on the prevalence of *M. kansasi* in clinics and the environment was conducted using Comprehensive Meta-analysis (CMA) software. The analysis included prevalence data for *M. kansasi* in NTM, clinical isolates, water isolates, and soil isolates.

Subgroup analyses were performed based on sampling period, country, continent, and method of detection for prevalence of *M. kansasi* in NTM clinical isolates. For water samples, subgroup analyses were conducted based on country, continent, and place of collection.

A random-effects model was utilized to estimate the pooled prevalence of *M. kansasi* in clinical and environmental samples with a 95% confidence interval. The heterogeneity among the studies in the meta-analysis was assessed using the I^2 statistic. An I^2 value of $\leq$25%

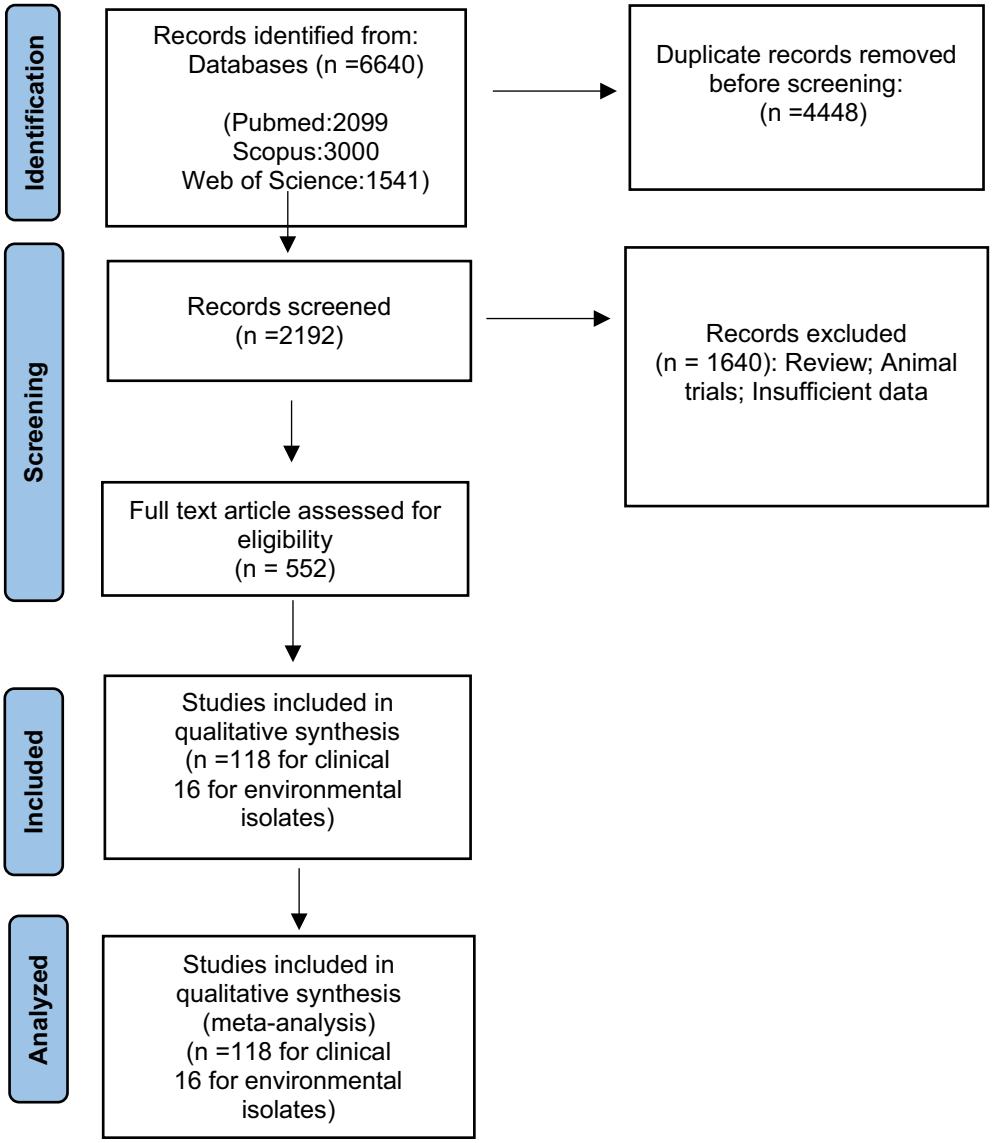

FIGURE 1
The study prisma flow diagram.

indicates low homogeneity, $25\% < I^2 < 75\%$ indicates moderate heterogeneity, and $I^2 > 75\%$ indicates high heterogeneity.

Sensitivity analysis was performed to investigate the impact of individual studies on the prevalence of *M. kansasi* in NTM and environmental isolates. Funnel plots and Begg's test were employed to assess the presence of publication bias. Results were considered to have publication bias if the *p*-value was <0.05.

Results

Search results

A total of 6,640 publications were identified. After removing duplicates using Endnote software, 2,192 articles were screened. Following the screening process, 1,640 studies were excluded, leaving 552 articles for full-text validation. After a thorough review, 118 published studies were used to analyze the prevalence of *M. kansasi* in clinical isolates (Wright et al., 1985; Debrunner et al., 1992; Rastogi and Goh, 1992; Shafer and Sierra, 1992; Parenti et al., 1995; Gamboa et al., 1997; Benjamin et al., 1998; Alcaide et al., 1999; Attorri et al., 2000; Ruiz et al., 2001; Mijs et al., 2002; Scarparo et al., 2002; Alcaide et al., 2003; Kontos et al., 2003; Rodriguez Díaz et al., 2003; Tu et al., 2003; Martin-Casabona et al., 2004; Matos et al., 2004; Morita et al., 2005; Pierre-Audigier et al., 2005; Prammananan et al., 2005; Dailloux et al., 2006; Franco-Álvarez de Luna et al., 2006; Hillemann et al., 2006; Lai et al., 2006; Andréjak et al., 2007; Liao et al., 2007; Bodle et al., 2008; Pedro et al., 2008; Ryoo et al., 2008; al-Mahruqi et al., 2009; Shen et al., 2009; Sorlozano et al., 2009; Amorim et al., 2010; Bicmen et al., 2010; Moore et al., 2010; Shenai et al., 2010; al Houqani et al., 2011; Ani et al., 2011; Bicmen et al., 2011; Chae et al., 2011; del Giudice et al., 2011; Gitti et al., 2011; Hong et al., 2011; Hsiao et al., 2011; Jeong et al., 2011; Lan et al., 2011; Chen et al., 2012; Lucke et al., 2012; Matveychuk et al., 2012; Braun et al., 2013; Cortés-Torres et al., 2013; Hombach et al., 2013; Mirsaeidi et al., 2013; Saifi et al., 2013; Chou et al., 2014; Lin et al.,

2014; Sookan and Coovadia, 2014; Wu et al., 2014; Bainomugisa et al., 2015; Chiang et al., 2015; Kim et al., 2015; Lee et al., 2015; Manika et al., 2015; Ng et al., 2015; Shao et al., 2015; Sheu et al., 2015; Blanc et al., 2016; Kodana et al., 2016; Nasr Esfahani et al., 2016; Ose et al., 2016; Riello et al., 2016; Agizew et al., 2017; Brown-Elliott and Wallace, 2017, 2021; Desikan et al., 2017; Pang et al., 2017; Park et al., 2017; Adzic-Vukicevic et al., 2018; Loizos et al., 2018; Luo et al., 2018; Naito et al., 2018; Nasiri et al., 2018; Tan et al., 2018; Davari et al., 2019; Fang et al., 2019; Gomathy et al., 2019; Marques et al., 2019; Modrá et al., 2019; Mortazavi et al., 2019; Pedrero et al., 2019; Xu et al., 2019; Feysia et al., 2020; Hara et al., 2020; Huang et al., 2020; López-Roa et al., 2020; Takenaka et al., 2020; Thomson et al., 2020; Abate et al., 2021; Ahn et al., 2021; Donohue, 2021; Huang et al., 2021; Kim M. J. et al., 2021; Kim Y. G. et al., 2021; Liu

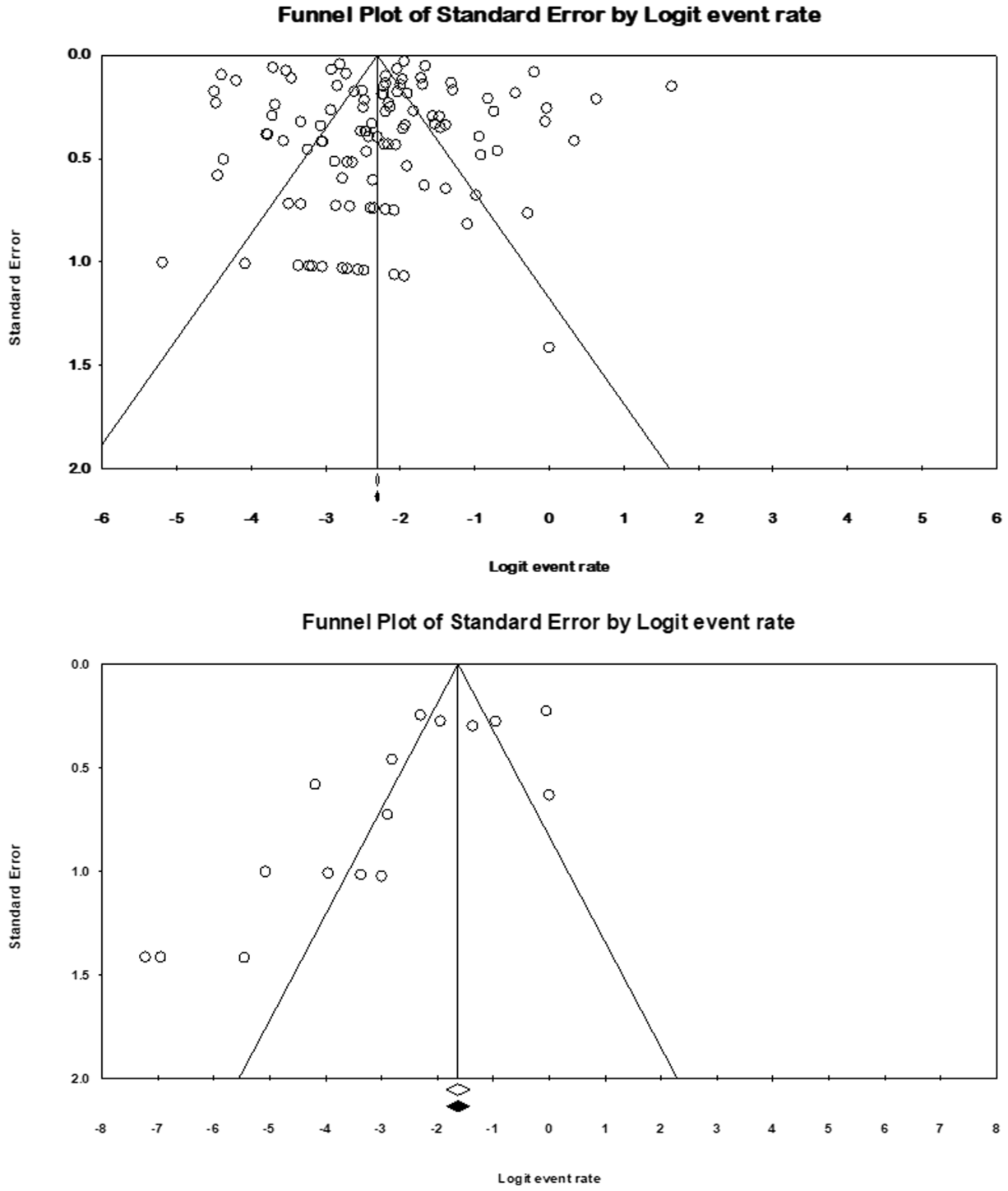

FIGURE 2
Funnel plots for identification of publication bias in clinical and environmental isolates.

et al., 2021; Mahdavi et al., 2021; Ose et al., 2021; Thangavelu et al., 2021; Urabe et al., 2021; Chai et al., 2022; Das et al., 2022; Gaballah et al., 2022; Gao et al., 2022; He et al., 2022; Lee et al., 2022; Lin et al., 2022), while 16 published studies were used to analyze the prevalence of *M. kansasi* in environmental isolates (McSwiggan and Collins, 1974; Engel et al., 1980; Gruft et al., 1981; Wright et al., 1985; Kubalek and Mysak, 1996; Slosárek et al., 1996; Iivanainen et al., 1999; Santos et al., 2005; Ghaemi et al., 2006; Thomas et al., 2006; Sharma et al., 2007; Parashar et al., 2009; Adrados et al., 2011; Kwenda et al., 2015; Moghaddam et al., 2022).

Figure 1 illustrates the review and article selection process based on the Preferred Reporting Items for Systematic Review and Meta-Analyses (PRISMA) statement. Supplementary Table S1 provides the characteristics of the included studies and the quality control analysis score, while Supplementary Table S2 presents the details of the answers to the JBI checklist questions for quality control.

Meta-analysis

Funnel plots (Figure 2) showed publication bias for the prevalence result of *M. kansasi* in NTM clinical isolates and environmental isolates. Begg's test was also used to indicate publication bias for the prevalence results ($p = 0.11$ for prevalence in NTM isolates and $p = 0.079$ for prevalence in environmental isolates).

Sensitivity analysis was conducted, and the results demonstrated that none of the studies influenced the prevalence of *M. kansasi* in NTM clinical isolates and environmental isolates.

This study included 111 articles that reported the prevalence of *M. kansasi* in NTM isolates. The prevalence of *M. kansasi* in these isolates was 9.4% (95% CI: 0.07–0.11%; $I^2 = 97.75\%$; $p < 0.001$).

Additionally, 34 articles provided information on the total number of collected isolates, and the prevalence of *M. kansasi* was found to be 1.5% (95% CI: 0.08–0.028%; $I^2 = 98.44\%$; $p < 0.001$) (Figure 3). Sixteen articles investigated the prevalence of *M. kansasi* in environmental isolates, including water and soil. The prevalence of *M. kansasi* in these isolates was 5.8% (95% CI: 0.028–0.116%; $I^2 = 90.518\%$; $p < 0.001$) (Figure 4). Two articles examined the prevalence of *M. kansasi* in soil, resulting in a prevalence rate of 0.5% (95% CI: 0.000–0.059). Fifteen studies reported the prevalence of *M. kansasi* in water, which was found to be 6.4% (95% CI: 0.031–0.129; $p < 0.001$) (Figure 5).

Subgroup analysis of prevalence of *Mycobacterium kansasii* in NTM isolates

Among the 111 studies that reported the prevalence of *M. kansasi* in NTM isolates, 64 were conducted in Asia, 25 in Europe, 10 in North America, 6 in Africa, 4 in South America, and 2 in Oceania. The

Study name	Event rate	Lower limit	Upper limit	Z-Value	p-Value
FERNANDO ALCAIDE	0.117	0.070	0.187	-7.119	0.000
Fernando Alcaide	0.015	0.010	0.021	-22.882	0.000
Ani AE	0.013	0.002	0.083	-4.342	0.000
Silvia Attorri	0.094	0.078	0.114	-20.887	0.000
Arnold Bainomugisa	0.004	0.001	0.029	-5.469	0.000
W. H. Benjamin Jr	0.010	0.004	0.024	-10.168	0.000
Can Bicmen	0.000	0.000	0.000	-23.249	0.000
Can Bicmen2	0.001	0.000	0.006	-7.111	0.000
Prabha Desikan	0.000	0.000	0.002	-8.316	0.000
HongFang	0.018	0.013	0.026	-21.938	0.000
F. Franco-A ?lvarez de Luna	0.022	0.006	0.084	-5.308	0.000
Ahmed Gaballah	0.100	0.033	0.268	-3.610	0.000
FREDY GAMBOA	0.010	0.001	0.066	-4.602	0.000
Zoe Gitti	0.001	0.000	0.001	-22.548	0.000
Doris Hillemann	0.000	0.000	0.001	-13.969	0.000
Yun Ji Hong	0.008	0.005	0.013	-20.857	0.000
Joseph Jeong	0.002	0.002	0.003	-46.582	0.000
Jian Lin	0.034	0.018	0.065	-9.823	0.000
S.-H. LIN	0.125	0.041	0.324	-3.153	0.002
Katja Lucke†	0.385	0.221	0.579	-1.166	0.244
Mahdavi	0.018	0.002	0.114	-3.990	0.000
Eliana Dias Matos	0.013	0.004	0.039	-7.452	0.000
Alona Matveychuk	0.653	0.554	0.740	2.981	0.003
W. Mijs	0.117	0.094	0.144	-16.464	0.000
-Yuan Chiang	0.012	0.009	0.015	-30.903	0.000
M.J. nasiri	0.027	0.015	0.048	-11.749	0.000
David M. Parenti	0.045	0.026	0.076	-10.739	0.000
Paro Pedro	0.005	0.003	0.011	-13.770	0.000
Therdsak Prammananan	0.068	0.050	0.093	-15.333	0.000
NALIN RASTOG	0.170	0.141	0.204	-13.985	0.000
Sorlozano, Antonio	0.003	0.002	0.008	-13.898	0.000
KalpanaThangavelu	0.001	0.001	0.002	-20.972	0.000
Hui-Zin Tu	0.041	0.032	0.053	-23.138	0.000
Jintian Xu	0.005	0.001	0.020	-7.431	0.000
	0.015	0.008	0.028	-12.565	0.000

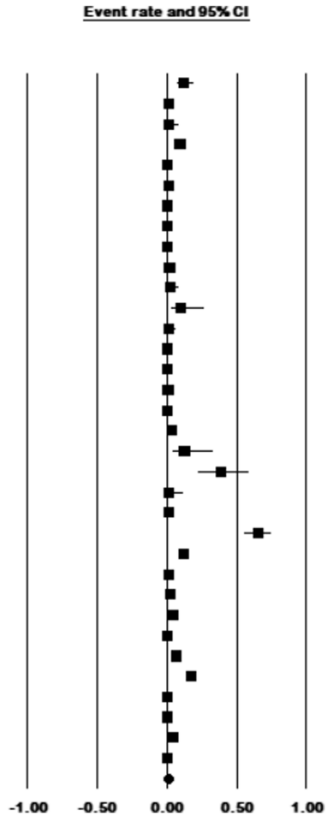

FIGURE 3
Forest plot showing the prevalence of *M. kansasii* in total clinical isolates.

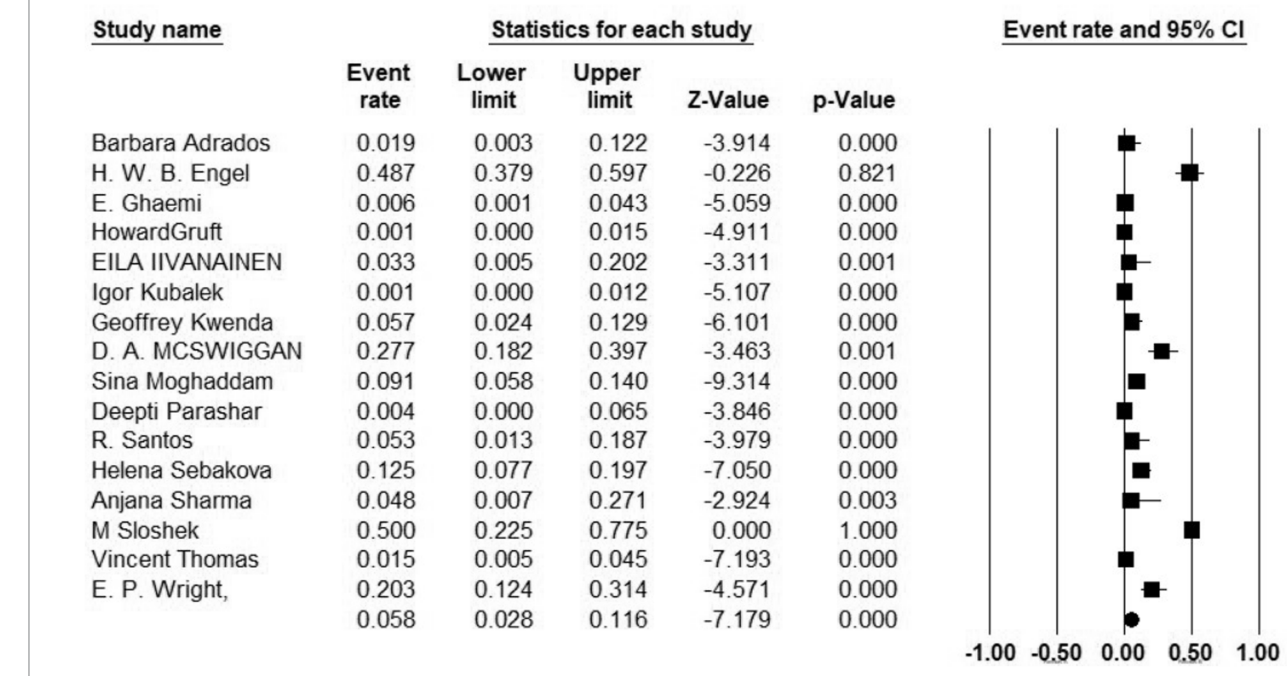

FIGURE 4
Forest plot showing the prevalence of *M. kansasii* in environmental isolates.

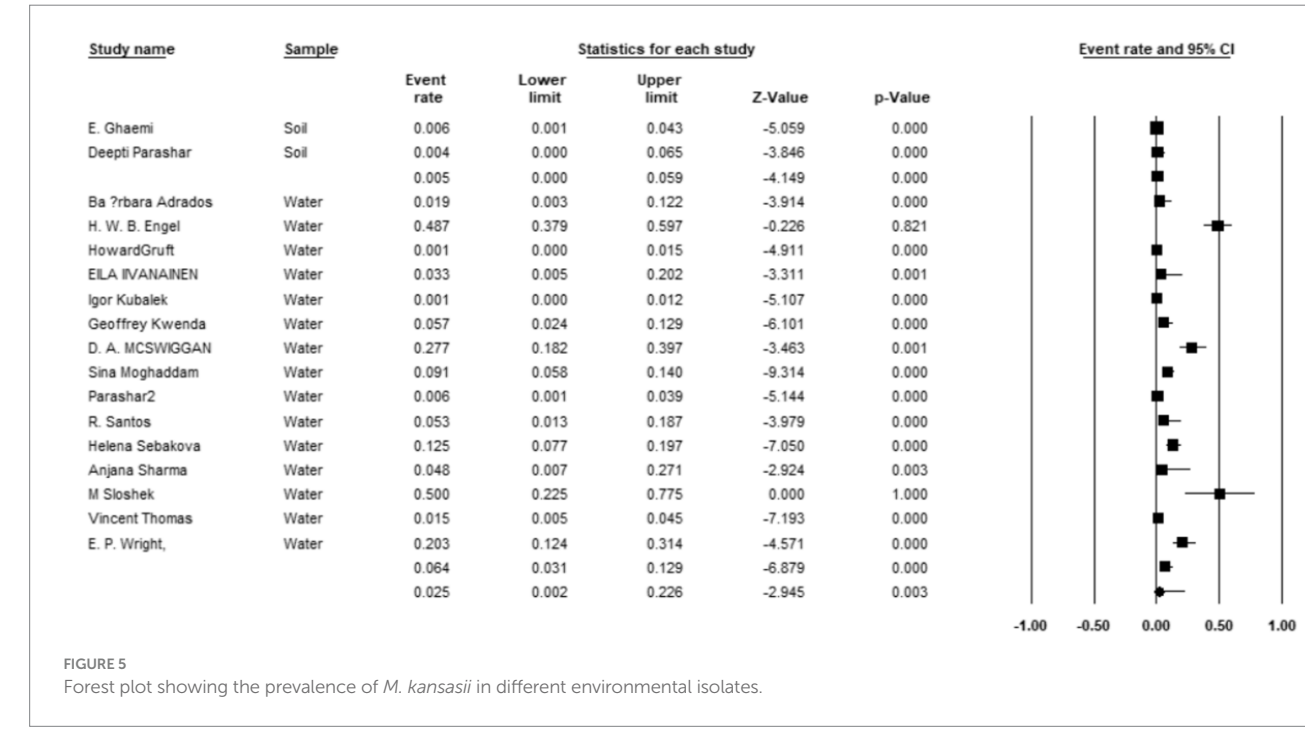

FIGURE 5
Forest plot showing the prevalence of *M. kansasii* in different environmental isolates.

prevalence of *M. kansasi* was highest in Europe with 12.1% (95% CI 0.08–0.17) and lowest in North America with 2.6% (95% CI 0.006–0.0103) ($p < 0.001$) (Figure 6).

The results of the country subgroup meta-analysis showed that Israel had the highest prevalence of *M. kansasi* in NTM with 50% (95% CI 0.162–0.84), while Botswana had the lowest with 0.6% (95% CI 0.00–0.098) ($p < 0.001$) (Figure 7).

We divided the sample collection time into four periods and analyzed studies whose sample collection time matched our grouping. The results showed an increase in prevalence from 4.9% (95% CI 0.01–0.20) in 1990–2000 to 8.9% (95% CI 0.043–0.175) in 2021–2022 ($p < 0.001$) (Figure 8).

In general, we divided *M. kansasi* identification methods into two categories: phenotypic methods including culture characteristics, biochemical methods, MALDI-TOF, and HPLC; and genotypic

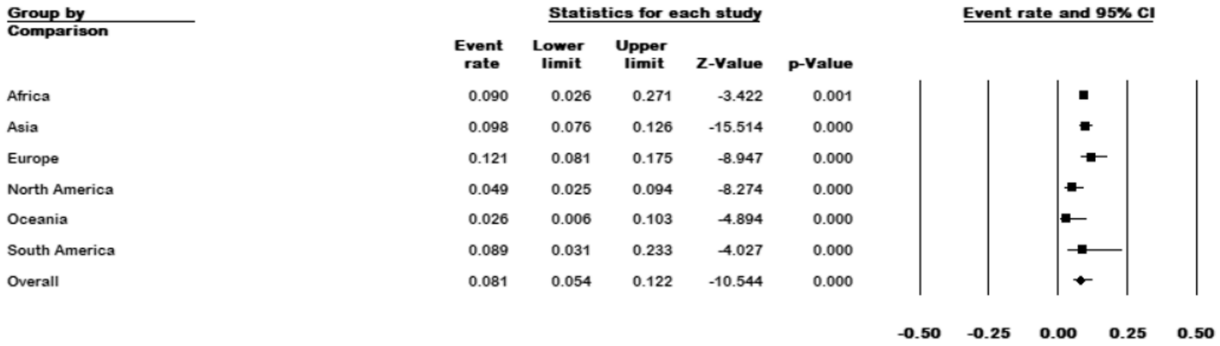

FIGURE 6
Forest plot showing the prevalence of *M. kansasii* in NTM isolates for different continents.

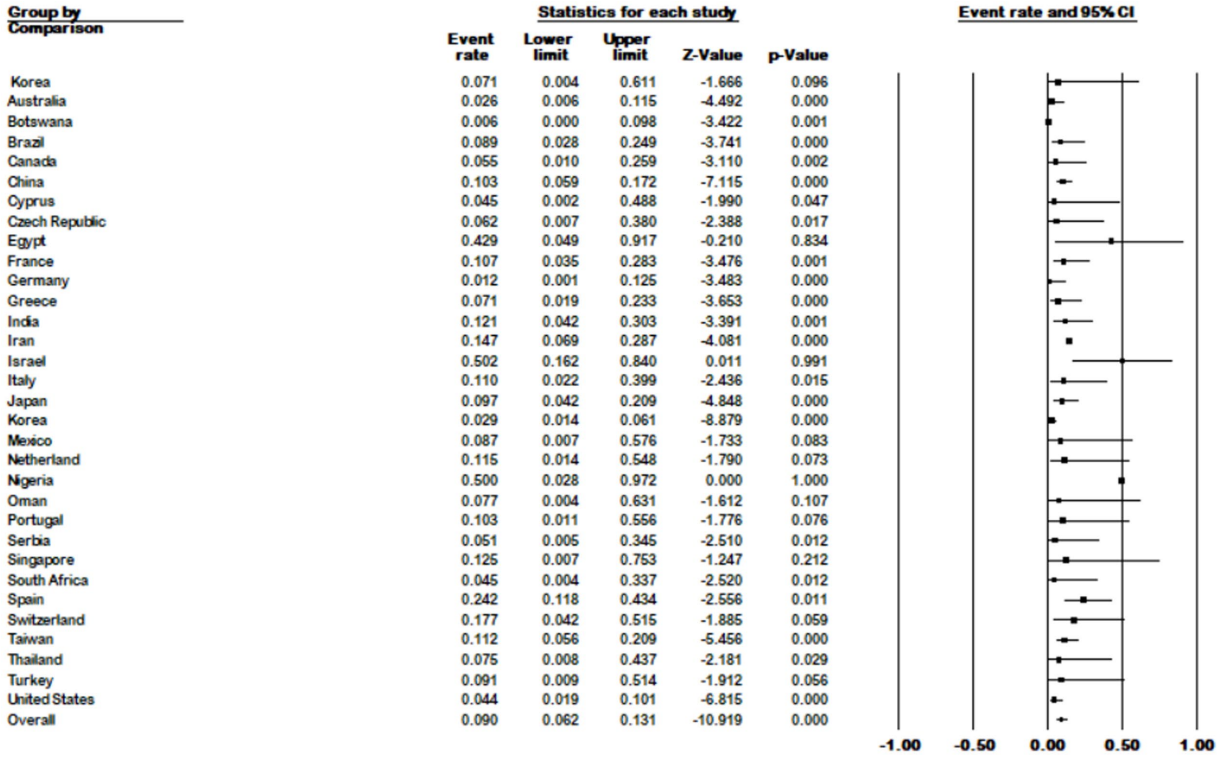

FIGURE 7
Forest plot showing the prevalence of *M. kansasii* in NTM isolates for different countries.

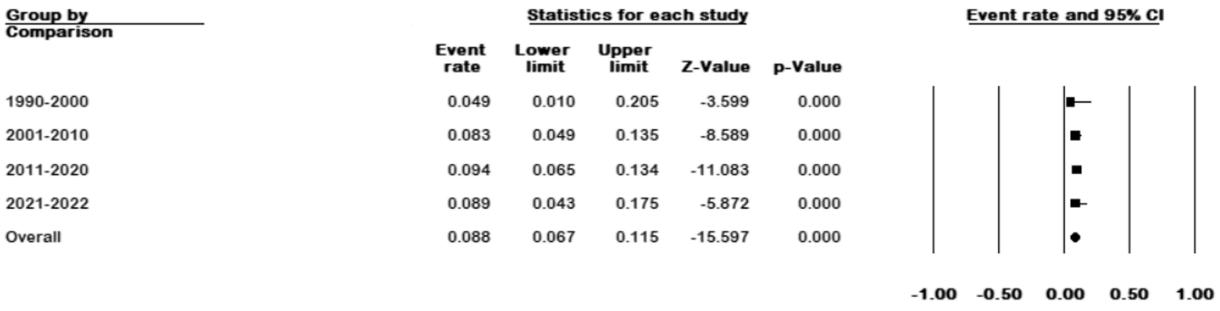

FIGURE 8
Forest plot showing the prevalence of *M. kansasii* in NTM isolates in four periods.

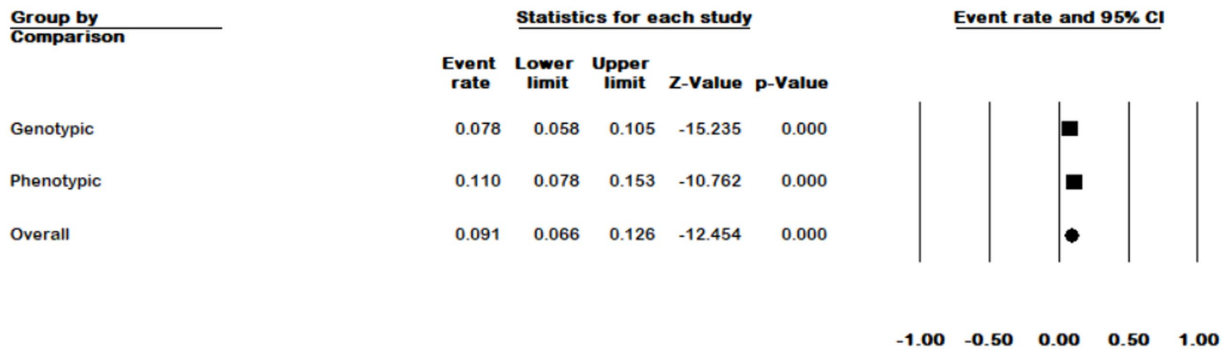

FIGURE 9
Forest plot showing the prevalence of *M. kansasii* in NTM isolates for two detection methods.

methods such as sequencing, hybridization, and using probes. According to genotypic methods, the prevalence of *M. kansasi* in NTM isolates was 7.8% (95% CI 0.058–0.105), and according to phenotypic methods, it was 11% (95% CI 0.078–0.153) ($p = 753$) (Figure 9).

Subgroup analysis of prevalence of *Mycobacterium kansasii* in water

Among the 15 studies reporting the prevalence of *M. kansasi* in water, 3 were conducted in Asia, 10 in Europe, 1 in North America, and 1 in Africa. Europe exhibited the highest prevalence of *M. kansasi* at 9.7% (95% CI 0.042–0.21, $p < 0.001$) (Figure 10).

The results of the country subgroup meta-analysis demonstrated that the Netherlands had the highest prevalence of *M. kansasi* in water, with a rate of 48.7% (95% CI 0.093–0.898, $p < 0.001$) (Figure 11). Furthermore, a subgroup analysis was conducted based on the location of water sample collection. The results indicated a particularly high prevalence of 17.9% (95% CI 0.048–0.484) in mine locations, compared to other sampling sites ($p < 0.001$) (Figure 12).

Discussion

M. kansasii was among the first non-tuberculous mycobacteria (NTM) to be identified as a respiratory pathogen in humans (Akram and Rawla, 2023). It is the sixth most commonly encountered NTM globally, although there is limited information on its prevalence in various sources and countries (Bakuła et al., 2013). This systematic review and meta-analysis sought to investigate the prevalence of *M. kansasii*. Our findings revealed a global prevalence of 9.4% among NTM isolates.

Studies have documented distinct regional differences in the prevalence of *M. kansasii* pulmonary disease, ranging from 3 to 70% worldwide (Guo et al., 2022). Notably, certain regions exhibit a higher prevalence of this bacterium. Our data analysis highlighted that Europe

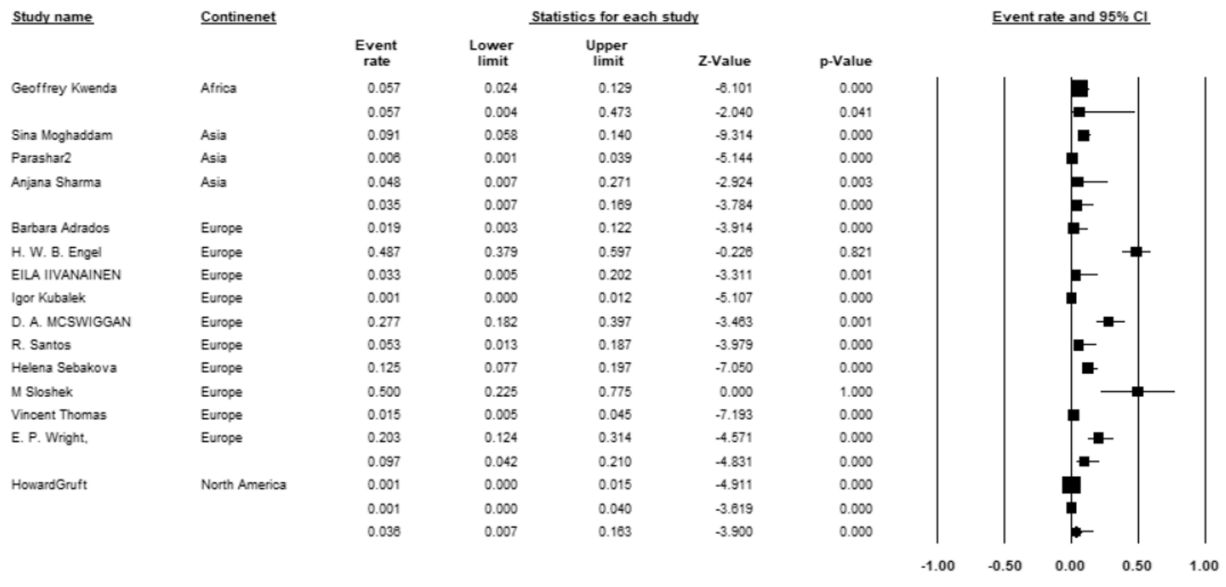

FIGURE 10
Forest plot showing the prevalence of *M. kansasii* in water sample in different continents.

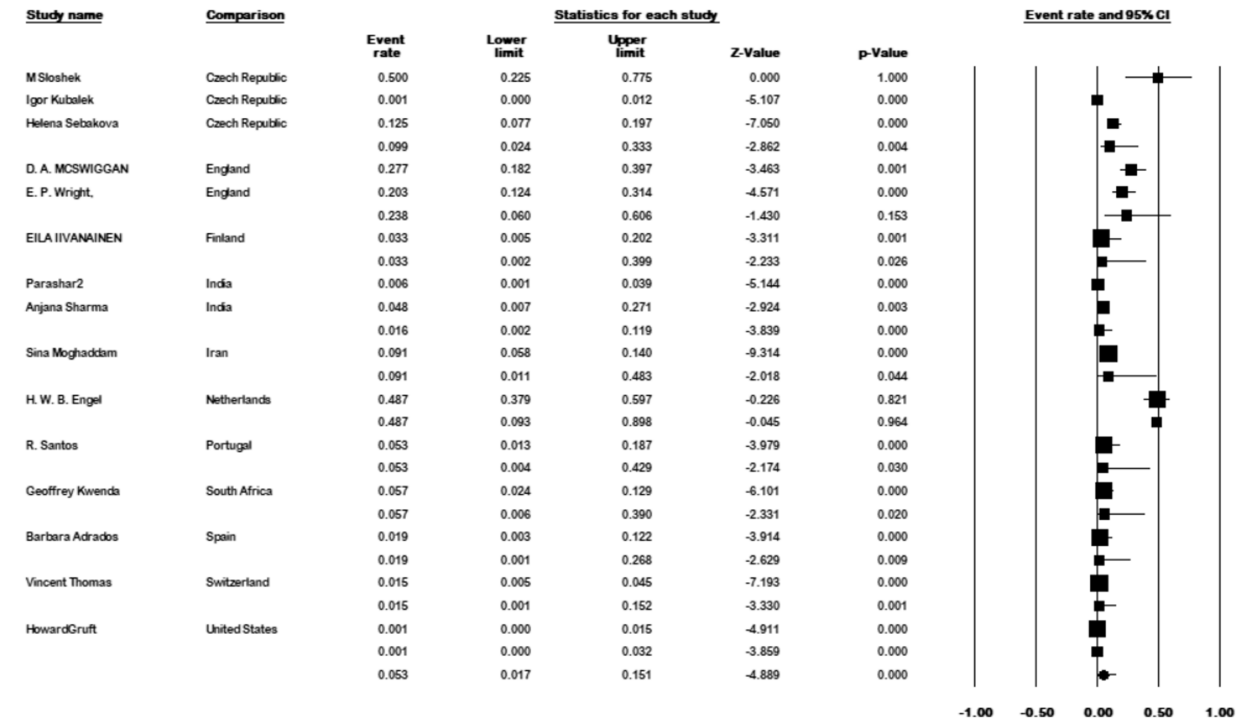

FIGURE 11
Forest plot showing the prevalence of *M. kansasii* in water sample in different countries.

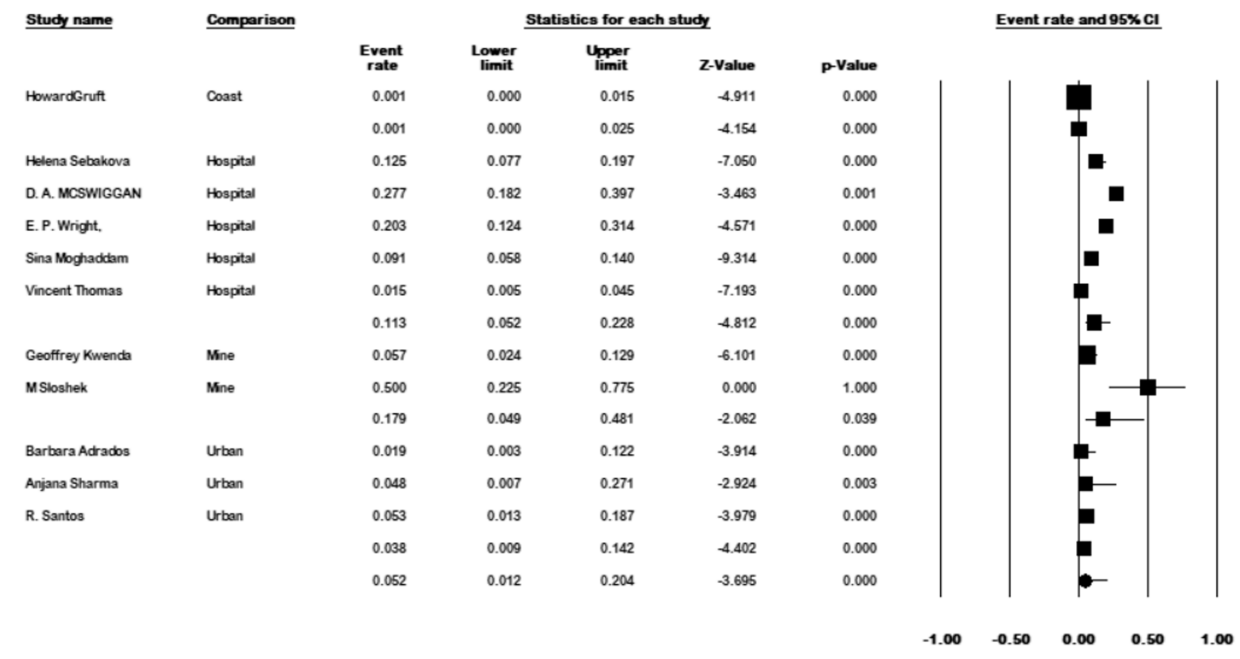

FIGURE 12
Forest plot showing the prevalence of *M. kansasii* in water sample in different locations.

had the highest prevalence at 12.1%, followed by Asia at 9.8%, while Oceania had the lowest prevalence at 2.6% among the continents examined. The reason for the higher prevalence of this bacterium in Europe may be due to the lack of advanced diagnostic facilities in developing countries along with a larger susceptible population due to the aging population in Europe.

Studies have revealed distinct regional differences in the prevalence of *M. kansasii* pulmonary disease, with a relatively high incidence observed in Brazil, Australia, Poland, and the United Kingdom (Zhang et al., 2023). The meta-analysis conducted by Okoi et al. identified *M. kansasii* as the most common cause of pulmonary NTM disease in a sub-Saharan African country (Okoi et al., 2017), with a prevalence rate of 69.2%. Additionally, Khosravi et al. reported frequencies ranging from 13 to 17% for this pathogen among all NTM isolates in Iran (Khosravi et al., 2020). Similarly, Morimoto et al. reported *M. kansasii* as the most prevalent form of NTM in Japan, with a prevalence rate of 43.6% (Morimoto et al., 2017).

Our analysis yielded the highest prevalence rates in Israel, Nigeria, and Egypt, with percentages of 50.2, 50, and 42.9%, respectively. On the other hand, Botswana and Germany exhibited the lowest prevalence rates at 0.06 and 1.2%, respectively.

Overall, NTM diseases are increasingly prevalent worldwide, potentially due to a rising population susceptible to weakened immune systems, organ transplantation, aging, changes in the environment favoring NTM development, and reduced anti-mycobacterial immunity following failed tuberculosis treatment (Chin et al., 2020). To date, there is no comprehensive global study investigating the temporal prevalence of *M. kansasii*. However, existing studies that have examined its prevalence over time have reported a significant increase in the prevalence of this bacterium. We divided the time of sample collection into four periods (1990–2000, 2001–2010, 2011–2020, and 2021–2022). The results of data analysis showed prevalence rates of 49, 83, 94, and 89%, respectively. Overall, our results demonstrated a significant increase in the prevalence of *M. kansasii* over time.

In this study, we analyzed the prevalence of *M. kansasii* in water samples. The prevalence of *M. kansasii* in water samples was found to be 5.8%, while the prevalence in all clinical isolates was 1.5%. This indicates a high prevalence of this microorganism in water samples, suggesting that water serves as a reservoir for this bacterium. Furthermore, the ability of *M. kansasii* to form biofilms may result in the release of this microorganism into water, posing a risk to consumers through drinking or inhalation of aerosols from showers, swimming pools, spas, and other water systems (Muñoz-Egea et al., 2023). Therefore, monitoring water samples is crucial for infection control.

Mining has long been associated with diseases caused by NTM, implying that exposure to mining dust may contribute to NTM transmission (Marras and Daley, 2002). As a result, miners may face a higher risk of exposure to potentially pathogenic environmental mycobacteria compared to workers in other occupations. In our study, water samples isolated from the mine had the highest prevalence rate at 17.9%, underscoring the significance of this location as a potential risk factor for *M. kansasii* transmission.

Although we made efforts to conduct a comprehensive search, it is possible that not all of the relevant existing literature was included. One potential limitation of this meta-analysis is that gray literature was not included in the search strategy. As a result, relevant studies or data that may have been available through gray literature channels, such as conference proceedings or unpublished dissertations, might have been inadvertently overlooked. This limitation could potentially introduce selection bias and limit the comprehensiveness of the findings. The relatively high heterogeneity between studies was another limitation of the present study. To address this, we conducted subgroup analysis to explore the sources of heterogeneity and minimize its impact on the results.

Conclusion

Mycobacterium kansasii is a prevalent causative agent of nontuberculous mycobacterial lung disease globally. Our results have highlighted a substantial prevalence of *M. kansasii* in clinical isolates, emphasizing the urgent need for heightened attention from health authorities, physicians, and microbiologists.

Furthermore, our investigation into the prevalence over time has revealed a significant increase in the occurrence of this bacterium, underscoring the importance of enhanced identification and control measures within infection control strategies to mitigate its further spread. Additionally, our study has demonstrated a higher prevalence of *M. kansasii* in water samples, further accentuating the significance of screening these samples for this microorganism as a preventive measure against the associated disease.

Data availability statement

The original contributions presented in the study are included in the article/Supplementary material, further inquiries can be directed to the corresponding author.

Author contributions

NN: Conceptualization, Formal analysis, Methodology, Software, Writing – original draft, Writing – review & editing. NB: Data curation, Writing – review & editing. FG: Data curation, Writing – review & editing. SR: Investigation, Methodology, Writing – review & editing. FJ: Supervision, Writing – review & editing.

Funding

The authors declare that financial support was received for the research, authorship, and/or publication of this article. This study was financially supported by Iran University of Medical Sciences (Tehran, Iran).

Acknowledgments

The authors thank Iran University of Medical Sciences (Tehran, Iran) for supporting this study.

Conflict of interest

The authors declare that the research was conducted in the absence of any commercial or financial relationships that could be construed as a potential conflict of interest.

Publisher's note

All claims expressed in this article are solely those of the authors and do not necessarily represent those of their affiliated organizations, or those of the publisher, the editors and the reviewers. Any product that may be evaluated in this article, or claim that may be made by its manufacturer, is not guaranteed or endorsed by the publisher.

Supplementary material

The Supplementary material for this article can be found online at: https://www.frontiersin.org/articles/10.3389/fmicb.2024.1321273/full#supplementary-material

References

Abate, G., Stapleton, J. T., Rouphael, N., Creech, B., Stout, J. E., el Sahly, H. M., et al. (2021). Variability in the Management of Adults with Pulmonary Nontuberculous Mycobacterial Disease. *Clin. Infect. Dis.* 72, 1127–1137. doi: 10.1093/cid/ciaa252

Adrados, B., Julián, E., Codony, F., Torrents, E., Luquin, M., and Morató, J. (2011). Prevalence and concentration of non-tuberculous mycobacteria in cooling towers by means of quantitative PCR: a prospective study. *Curr. Microbiol.* 62, 313–319. doi: 10.1007/s00284-010-9706-2

Adzic-Vukicevic, T., Barac, A., Blanka-Protic, A., Laban-Lazovic, M., Lukovic, B., Skodric-Trifunovic, V., et al. (2018). Clinical features of infection caused by non-tuberculous mycobacteria: 7 years' experience. *Infection* 46, 357–363. doi: 10.1007/s15010-018-1128-2

Agizew, T., Basotli, J., Alexander, H., Boyd, R., Letsibogo, G., Auld, A., et al. (2017). Higher-than-expected prevalence of non-tuberculous mycobacteria in HIV setting in Botswana: implications for diagnostic algorithms using Xpert MTB/RIF assay. *PLoS One* 12:e0189981. doi: 10.1371/journal.pone.0189981

Ahn, K., Kim, Y. K., Hwang, G. Y., Cho, H., and Uh, Y. (2021). Continued upward trend in non-tuberculous mycobacteria isolation over 13 years in a tertiary Care Hospital in Korea. *Yonsei Med. J.* 62, 903–910. doi: 10.3349/ymj.2021.62.10.903

Akram, S. M., and Rawla, P., *Mycobacterium kansasii Infection*", in: StatPearls. Treasure Island (FL): StatPearls Publishing. (2023).

al Houqani, M., Jamieson, F., Chedore, P., Mehta, M., May, K., and Marras, T. K. (2011). Isolation prevalence of pulmonary nontuberculous mycobacteria in Ontario in 2007. *Can. Respir. J.* 18, 19–24. doi: 10.1155/2011/865831

Alcaide, F., Benítez, M. A., and Martín, R. (1999). Epidemiology of *Mycobacterium kansasii*. *Ann. Intern. Med.* 131, 310–311. doi: 10.7326/0003-4819-131-4-199908170-00016

Alcaide, F., Galí, N., Domínguez, J., Berlanga, P., Blanco, S., Orús, P., et al. (2003). Usefulness of a new mycobacteriophage-based technique for rapid diagnosis of pulmonary tuberculosis. *J. Clin. Microbiol.* 41, 2867–2871. doi: 10.1128/JCM.41.7.2867-2871.2003

al-Mahruqi, S. H., van Ingen, J., al-Busaidy, S., Boeree, M. J., al-Zadjali, S., Patel, A., et al. (2009). Clinical relevance of nontuberculous mycobacteria, Oman. *Emerg. Infect. Dis.* 15, 292–294. doi: 10.3201/eid1502.080977

Amorim, A., Macedo, R., Lopes, A., Rodrigues, I., and Pereira, E. (2010). Non-tuberculous mycobacteria in HIV-negative patients with pulmonary disease in Lisbon, Portugal. *Scand. J. Infect. Dis.* 42, 626–628. doi: 10.3109/00365541003754485

Andréjak, C., Lescure, F. X., Douadi, Y., Laurans, G., Smail, A., Duhaut, P., et al. (2007). Non-tuberculous mycobacteria pulmonary infection: management and follow-up of 31 infected patients. *J. Infect.* 55, 34–40. doi: 10.1016/j.jinf.2007.01.008

Ani, A. E., Diarra, B., Dahle, U. R., Lekuk, C., Yetunde, F., Somboro, A. M., et al. (2011). Identification of mycobacteria and other acid fast organisms associated with pulmonary disease. *Asian Pac. J. Trop. Dis.* 1, 259–262. doi: 10.1016/S2222-1808(11)60061-3

Attorri, S., Dunbar, S., and Clarridge, J. E. (2000). Assessment of morphology for rapid presumptive identification of Mycobacterium tuberculosis and *Mycobacterium kansasii*. *J. Clin. Microbiol.* 38, 1426–1429. doi: 10.1128/JCM.38.4.1426-1429.2000

Bainomugisa, A., Wampande, E., Muchwa, C., Akol, J., Mubiri, P., Ssenyungule, H., et al. (2015). Use of real time polymerase chain reaction for detection of *M. tuberculosis*, M. Avium and *M. kansasii* from clinical specimens. *BMC Infect. Dis.* 15:181. doi: 10.1186/s12879-015-0921-0

Bakuła, Z., Safianowska, A., Nowacka-Mazurek, M., Bielecki, J., and Jagielski, T. (2013). Subtyping of *Mycobacterium kansasii* by PCR-restriction enzyme analysis of the hsp65 gene. *Biomed. Res. Int.* 2013, 1–4. doi: 10.1155/2013/178725

Benjamin, W. H., Waites, K. B., Beverly, A., Gibbs, L., Waller, M., Nix, S., et al. (1998). Comparison of the MB/BacT system with a revised antibiotic supplement kit to the BACTEC 460 system for detection of mycobacteria in clinical specimens. *J. Clin. Microbiol.* 36, 3234–3238. doi: 10.1128/JCM.36.11.3234-3238.1998

Bicmen, C., Coskun, M., Gunduz, A. T., Senol, G., Cirak, A. K., and Tibet, G. (2010). Nontuberculous mycobacteria isolated from pulmonary specimens between 2004 and 2009: causative agent or not? *New Microbiol.* 33, 399–403.

Bicmen, C., Gunduz, A. T., Coskun, M., Senol, G., Cirak, A. K., and Ozsoz, A. (2011). Molecular detection and identification of *mycobacterium tuberculosis* complex and four clinically important nontuberculous mycobacterial species in smear-negative clinical samples by the genotype mycobacteria direct test. *J. Clin. Microbiol.* 49, 2874–2878. doi: 10.1128/JCM.00612-11

Blanc, P., Dutronc, H., Peuchant, O., Dauchy, F. A., Cazanave, C., Neau, D., et al. (2016). Nontuberculous mycobacterial infections in a French hospital: a 12-year retrospective study. *PLoS One* 11:e0168290. doi: 10.1371/journal.pone.0168290

Bodle, E. E., Cunningham, J. A., Della-Latta, P., Schluger, N. W., and Saiman, L. (2008). Epidemiology of nontuberculous mycobacteria in patients without HIV infection, New York City. *Emerg. Infect. Dis.* 14, 390–396. doi: 10.3201/eid1403.061143

Braun, E., Sprecher, H., Davidson, S., and Kassis, I. (2013). Epidemiology and clinical significance of non-tuberculous mycobacteria isolated from pulmonary specimens. *Int. J. Tuberc. Lung Dis.* 17, 96–99. doi: 10.5588/ijtld.12.0237

Brown-Elliott, B. A., and Wallace, R. J. (2017). In vitro susceptibility testing of Tedizolid against nontuberculous mycobacteria. *J. Clin. Microbiol.* 55, 1747–1754. doi: 10.1128/JCM.00274-17

Brown-Elliott, B. A., and Wallace, R. J. (2021). Comparison of in vitro susceptibility of Delafloxacin with ciprofloxacin, moxifloxacin, and other comparator antimicrobials against isolates of nontuberculous mycobacteria. *Antimicrob. Agents Chemother.* 65:e0007921. doi: 10.1128/AAC.00079-21

Chae, D. R., Kim, Y. I., Kee, S. J., Kim, Y. H., Chi, S. Y., Ban, H. J., et al. (2011). The impact of the 2007 ATS/IDSA diagnostic criteria for nontuberculous mycobacterial disease on the diagnosis of nontuberculous mycobacterial lung disease. *Respiration* 82, 124–129. doi: 10.1159/000320254

Chai, J., Han, X., Mei, Q., Liu, T., Walline, J. H., Xu, J., et al. (2022). Clinical characteristics and mortality of non-tuberculous mycobacterial infection in immunocompromised vs Immunocompetent Hosts. *Front. Med.* 9:884446. doi: 10.3389/fmed.2022.884446

Chen, C. Y., Chen, H. Y., Chou, C. H., Huang, C. T., Lai, C. C., and Hsueh, P. R. (2012). Pulmonary infection caused by nontuberculous mycobacteria in a medical center in Taiwan, 20052008. *Diagn. Microbiol. Infect. Dis.* 72, 47–51. doi: 10.1016/j.diagmicrobio.2011.09.009

Chiang, C. Y., Yu, M. C., Yang, S. L., Yen, M. Y., and Bai, K. J. (2015). Surveillance of tuberculosis in Taipei: the influence of nontuberculous mycobacteria. *PLoS One* 10:e0142324. doi: 10.1371/journal.pone.0142324

Chin, K. L., Sarmiento, M. E., Alvarez-Cabrera, N., Norazmi, M. N., and Acosta, A. (2020). Pulmonary non-tuberculous mycobacterial infections: current state and future management. *Eur. J. Clin. Microbiol. Infect. Dis.* 39, 799–826. doi: 10.1007/s10096-019-03771-0

Chou, M. P., Clements, A. C. A., and Thomson, R. M. (2014). A spatial epidemiological analysis of nontuberculous mycobacterial infections in Queensland, Australia. *BMC Infect. Dis.* 14:14. doi: 10.1186/1471-2334-14-279

Cortés-Torres, N., González-y-Merchand, J. A., González-Bonilla, C., and García-Elorriaga, G. (2013). Molecular analysis of mycobacteria isolated in Mexican patients with different Immunodeficiencies in a tertiary care hospital. *Arch. Med. Res.* 44, 562–569. doi: 10.1016/j.arcmed.2013.09.002

Cowman, S., van Ingen, J., Griffith, D. E., and Loebinger, M. R. (2019). Non-tuberculous mycobacterial pulmonary disease. *Eur. Respir. J.* 54:1900250. doi: 10.1183/13993003.00250-2019

Dailloux, M., Abalain, M. L., Laurain, C., Lebrun, L., Loos-Ayav, C., Lozniewski, A., et al. (2006). Respiratory infections associated with nontuberculous mycobacteria in non-HIV patients. *Eur. Respir. J.* 28, 1211–1215. doi: 10.1183/09031936.00063806

Daley, C. L., Iaccarino, J. M., Lange, C., Cambau, E., Wallace, R. J. Jr., Andrejak, C., et al. (2020). Treatment of nontuberculous mycobacterial pulmonary disease: an official ATS/ERS/ESCMID/IDSA clinical practice guideline. *Clin. Infect. Dis.* 71, 905–913. doi: 10.1093/cid/ciaa1125

Das, S., Mishra, B., Mohapatra, P. R., Preetam, C., and Rath, S. (2022). Clinical presentations of nontuberculous mycobacteria as suspected and drug-resistant tuberculosis: experience from a tertiary care center in eastern India. *Int. J. Mycobacteriol.* 11, 167–174. doi: 10.4103/ijmy.ijmy_68_22

Davari, M., Irandoost, M., Sakhaee, F., Vaziri, F., Sepahi, A. A., Rahimi Jamnani, F., et al. (2019). Genetic diversity and prevalence of nontuberculous mycobacteria isolated from clinical samples in Tehran, Iran. *Microb. Drug Resist.* 25, 264–270. doi: 10.1089/mdr.2018.0150

Debrunner, M., Salfinger, M., Brandli, O., and von Graevenitz, A. (1992). Epidemiology and clinical significance of nontuberculous mycobacteria in patients negative for human immunodeficiency virus in Switzerland. *Clin. Infect. Dis.* 15, 330–345. doi: 10.1093/clinids/15.2.330

del Giudice, G., Iadevaia, C., Santoro, G., Moscariello, E., Smeraglia, R., and Marzo, C. (2011). Nontuberculous mycobacterial lung disease in patients without HIV infection: a retrospective analysis over 3 years. *Clin. Respir. J.* 5, 203–210. doi: 10.1111/j.1752-699X.2010.00220.x

Desikan, P., Tiwari, K., Panwalkar, N., Khaliq, S., Chourey, M., Varathe, R., et al. (2017). Public health relevance of non-tuberculous mycobacteria among AFB positive sputa. *Germs* 7, 10–18. doi: 10.18683/germs.2017.1103

Donohue, M. J. (2021). Epidemiological risk factors and the geographical distribution of eight Mycobacterium species. *BMC Infect. Dis.* 21:258. doi: 10.1186/s12879-021-05925-y

Engel, H., Berwald, L., and Havelaar, A. (1980). The occurrence of *Mycobacterium kansasii* in tapwater. *Tubercle* 61, 21–26. doi: 10.1016/0041-3879(80)90055-0

Fang, H., Shangguan, Y., Wang, H., Ji, Z., Shao, J., Zhao, R., et al. (2019). Multicenter evaluation of the biochip assay for rapid detection of mycobacterial isolates in smear-positive specimens. *Int. J. Infect. Dis.* 81, 46–51. doi: 10.1016/j.ijid.2019.01.036

Feysia, S. G., Hasan-Nejad, M., Amini, S., Hamzelou, G., Kazemian, H., Kardan-Yamchi, J., et al. (2020). Incidence, clinical manifestation, treatment outcome, and drug susceptibility pattern of nontuberculous mycobacteria in HIV patients in Tehran, Iran. *Ethiop. J. Health Sci.* 30, 75–84. doi: 10.4314/ejhs.v30i1.10

Franco-Álvarez de Luna, F., Ruiz, P., Gutiérrez, J., and Casal, M. (2006). Evaluation of the GenoType mycobacteria direct assay for detection of *Mycobacterium tuberculosis* complex and four atypical mycobacterial species in clinical samples. *J. Clin. Microbiol.* 44, 3025–3027. doi: 10.1128/JCM.00068-06

Gaballah, A., Ghazal, A., Almiry, R., Emad, R., Sadek, N., Abdel Rahman, M., et al. (2022). Simultaneous detection of Mycobacterium tuberculosis and atypical mycobacteria by DNA-microarray in Egypt. *Med. Princ. Pract.* 31, 246–253. doi: 10.1159/000524209

Gamboa, F., Manterola, J. M., Lonca, J., Matas, L., Viñado, B., Giménez, M., et al. (1997). Detection and identification of mycobacteria by amplification of RNA and DNA in pretreated blood and bone marrow aspirates by a simple lysis method. *J. Clin. Microbiol.* 35, 2124–2128. doi: 10.1128/jcm.35.8.2124-2128.1997

Gao, C. H., Zhang, Y. A., and Wang, M. S. (2022). Performance of interferon-γ release assays in patients with *Mycobacterium kansasii* infection. *Infect. Drug Resist.* 15, 7727–7732. doi: 10.2147/IDR.S385570

Ghaemi, E., Ghazisaidi, K., Koohsari, H., and Mansoorian, A. (2006). Environmental mycobacteria in areas of high and low tuberculosis prevalence in the Islamic Republic of Iran. *East. Mediterr. Health J.* 12, 280–285.

Gitti, Z., Mantadakis, E., Maraki, S., and Samonis, G. (2011). Clinical significance and antibiotic susceptibilities of nontuberculous mycobacteria from patients in Crete, Greece. *Future Microbiol.* 6, 1099–1109. doi: 10.2217/fmb.11.91

Gomathy, N. S., Padmapriyadarsini, C., Silambuchelvi, K., Nabila, A., Tamizhselvan, M., Banurekha, V. V., et al. (2019). Profile of patients with pulmonary non-tuberculous mycobacterial disease mimicking pulmonary tuberculosis. *Indian J. Tuberc.* 66, 461–467. doi: 10.1016/j.ijtb.2019.04.013

Gruft, H., Falkinham, J. O. III, and Parker, B. C. (1981). Recent experience in the epidemiology of disease caused by atypical mycobacteria. *Rev. Infect. Dis.* 3, 990–996. doi: 10.1093/clinids/3.5.990

Guo, Y., Cao, Y., Liu, H., Yang, J., Wang, W., Wang, B., et al. (2022). Clinical and microbiological characteristics of *Mycobacterium kansasii* pulmonary infections in China. *Microbiol. Spect.* 10, e01475–e01421. doi: 10.1128/spectrum.01475-21

Hara, R., Kitada, S., Iwai, A., Kuge, T., Oshitani, Y., Kagawa, H., et al. (2020). Diagnostic validity of gastric aspirate culture in nontuberculous mycobacterial pulmonary disease. *Ann. Am. Thorac. Soc.* 17, 1536–1541. doi: 10.1513/AnnalsATS.201911-852OC

He, G., Wu, L., Zheng, Q., and Jiang, X. (2022). Antimicrobial susceptibility and minimum inhibitory concentration distribution of common clinically relevant non-tuberculous mycobacterial isolates from the respiratory tract. *Ann. Med.* 54, 2500–2510. doi: 10.1080/07853890.2022.2121984

Hillemann, D., Richter, E., and Rüsch-Gerdes, S. (2006). Use of the BACTEC mycobacteria growth indicator tube 960 automated system for recovery of mycobacteria from 9,558 extrapulmonary specimens, including urine samples. *J. Clin. Microbiol.* 44, 4014–4017. doi: 10.1128/JCM.00829-06

Hombach, M., Somoskövi, A., Hömke, R., Ritter, C., and Böttger, E. C. (2013). Drug susceptibility distributions in slowly growing non-tuberculous mycobacteria using MGIT 960 TB eXiST. *Int. J. Med. Microbiol.* 303, 270–276. doi: 10.1016/j.ijmm.2013.04.003

Hong, Y. J., Chung, Y. H., Kim, T. S., Song, S. H., Park, K. U., Yim, J. J., et al. (2011). Usefulness of three-channel multiplex real-time PCR and melting curve analysis for simultaneous detection and identification of the *Mycobacterium tuberculosis* complex and nontuberculous mycobacteria. *J. Clin. Microbiol.* 49, 3963–3966. doi: 10.1128/JCM.05662-11

Hsiao, C. H., Tsai, T. F., and Hsueh, P. R. (2011). Characteristics of skin and soft tissue infection caused by non-tuberculous mycobacteria in Taiwan. *Int. J. Tuberc. Lung Dis.* 15, 811–817. doi: 10.5588/ijtld.10.0481

Huang, H.-L., Cheng, M. H., Lu, P. L., Shu, C. C., Wang, J. Y., Wang, J. T., et al. (2017). Epidemiology and predictors of NTM pulmonary infection in Taiwan-a retrospective, five-year multicenter study. *Sci. Rep.* 7:16300. doi: 10.1038/s41598-017-16559-z

Huang, J. J., Li, Y. X., Zhao, Y., Yang, W. H., Xiao, M., Kudinha, T., et al. (2020). Prevalence of nontuberculous mycobacteria in a tertiary hospital in Beijing, China, January 2013 to December 2018. *BMC Microbiol.* 20:158. doi: 10.1186/s12866-020-01840-5

Huang, M., Lin, Y., Chen, X., and Wu, D. (2021). The value of gene chip detection of bronchoalveolar lavage fluid in the diagnosis of nontuberculous mycobacterial lung disease. *Ann. Palliat. Med.* 10, 6438–6445. doi: 10.21037/apm-21-1205

Iivanainen, E., Northrup, J., Arbeit, R. D., Ristola, M., Katila, M. L., and von reyn, C. F. (1999). Isolation of mycobacteria from indoor swimming pools in Finland. *APMIS* 107, 193–200. doi: 10.1111/j.1699-0463.1999.tb01544.x

Jeong, J., Kim, S. R., Lee, S. H., Lim, J. H., Choi, J. I., Park, J. S., et al. (2011). The use of high performance liquid chromatography to speciate and characterize the epidemiology of mycobacteria. *Lab. Med.* 42, 612–617. doi: 10.1309/LMDDEHPSYE6ZDM3C

Johansen, M. D., Herrmann, J.-L., and Kremer, L. (2020). Non-tuberculous mycobacteria and the rise of *Mycobacterium abscessus*. *Nat. Rev. Microbiol.* 18, 392–407. doi: 10.1038/s41579-020-0331-1

Karami-Zarandi, M., Bahador, A., Gizaw Feysia, S., Kardan-Yamchi, J., Hasan-Nejad, M., Mosavari, N., et al. (2019). Identification of non-tuberculosis mycobacteria by line probe assay and determination of drug resistance patterns of isolates in Iranian patients. *Arch. Razi Inst.* 74, 375–384. doi: 10.22092/ari.2019.127144.1372

Khosravi, A. D., Asban, B., Hashemzadeh, M., and Nashibi, R. (2020). Molecular identification, and characterization of *Mycobacterium kansasii* strains isolated from four tuberculosis regional reference laboratories in Iran during 2016–2018. *Infect. Drug Resist.* 13, 2171–2180. doi: 10.2147/IDR.S245295

Kim, M. J., Kim, K. M., Shin, J. I., Ha, J. H., Lee, D. H., Choi, J. G., et al. (2021). Identification of nontuberculous mycobacteria in patients with pulmonary diseases in Gyeongnam, Korea, using multiplex PCR and multigene sequence-based analysis. *Can. J. Infect. Dis. Med. Microbiol.* 2021:8844306. doi: 10.1155/2021/8844306

Kim, Y. G., Lee, H. Y., Kwak, N., Park, J. H., Kim, T. S., Kim, M. J., et al. (2021). Determination of clinical characteristics of *Mycobacterium kansasii*-derived species by reanalysis of isolates formerly reported as *M. kansasii*. Ann. *Lab. Med.* 41, 463–468. doi: 10.3343/alm.2021.41.5.463

Kim, J., Seong, M. W., Kim, E. C., Han, S. K., and Yim, J. J. (2015). Frequency and clinical implications of the isolation of rare nontuberculous mycobacteria. *BMC Infect. Dis.* 15:9. doi: 10.1186/s12879-014-0741-7

Kodana, M., Tarumoto, N., Kawamura, T., Saito, T., Ohno, H., Maesaki, S., et al. (2016). Utility of the MALDI-TOF MS method to identify nontuberculous mycobacteria. *J. Infect. Chemother.* 22, 32–35. doi: 10.1016/j.jiac.2015.09.006

Koh, W.-J. (2017). Nontuberculous mycobacteria—overview. *Microbiol. Spect.* 5, 10–128. doi: 10.1128/microbiolspec.TNMI7-0024-2016

Kontos, F., Petinaki, E., Nicolaou, S., Gitti, Z., Anagnostou, S., Maniati, M., et al. (2003). Multicenter evaluation of the fully automated Bactec MGIT 960 system and three molecular methods for the isolation and the identification of mycobacteria from clinical specimens. *Diagn. Microbiol. Infect. Dis.* 46, 299–301. doi: 10.1016/S0732-8893(03)00078-6

Kubalek, I., and Mysak, J. (1996). The prevalence of environmental mycobacteria in drinking water supply systems in a demarcated region in Czech Republic, in the period 1984–1989. *Eur. J. Epidemiol.* 12, 471–474. doi: 10.1007/BF00143998

Kwenda, G., Churchyard, G. J., Thorrold, C., Heron, I., Stevenson, K., Duse, A. G., et al. (2015). Molecular characterisation of clinical and environmental isolates of *Mycobacterium kansasii* isolates from south African gold mines. *J. Water Health* 13, 190–202. doi: 10.2166/wh.2014.161

Lai, C., Lee, L., Ding, L., Yu, C., Hsueh, P., and Yang, P. (2006). Emergence of disseminated infections due to nontuberculous mycobacteria in non-HIV-infected patients, including immunocompetent and immunocompromised patients in a university hospital in Taiwan. *J. Infect.* 53, 77–84. doi: 10.1016/j.jinf.2005.10.009

Lan, R., Yang, C., Lan, L., Ou, J., Qiao, K., Liu, F., et al. (2011). Mycobacterium tuberculosis and non-tuberculous mycobacteria isolates from HIV-infected patients in Guangxi, China. *Int. J. Tuberc. Lung Dis.* 15, 1669–1675. doi: 10.5588/ijtld.11.0036

Lee, E. H., Chin, B. S., Kim, Y. K., Yoo, J. S., Choi, Y. H., Kim, S., et al. (2022). Clinical characteristics of nontuberculous mycobacterial disease in people living with HIV/AIDS

in South Korea: a multi-center, retrospective study. *PLoS One* 17:e0276484. doi: 10.1371/journal.pone.0276484

Lee, M. R., Yang, C. Y., Shu, C. C., Lin, C. K., Wen, Y. F., Lee, S. W., et al. (2015). Factors associated with subsequent nontuberculous mycobacterial lung disease in patients with a single sputum isolate on initial examination. *Clin. Microbiol. Infect.* 21, 250.e1–250.e7. doi: 10.1016/j.cmi.2014.08.025

Liao, C. H., Lai, C. C., Ding, L. W., Hou, S. M., Chiu, H. C., Chang, S. C., et al. (2007). Skin and soft tissue infection caused by non-tuberculous mycobacteria. *Int. J. Tuberc. Lung Dis.* 11, 96–102.

Lin, S. H., Lai, C. C., Huang, S. H., Hung, C. C., and Hsueh, P. R. (2014). Mycobacterial bone marrow infections at a medical Centre in Taiwan, 2001-2009. *Epidemiol. Infect.* 142, 1524–1532. doi: 10.1017/S0950268813002707

Lin, J., Zhao, Y., Wei, S., Dai, Z., and Lin, S. (2022). Evaluation of the MeltPro Myco assay for the identification of non-tuberculous mycobacteria. *Infect. Drug Resist.* 15, 3287–3293. doi: 10.2147/IDR.S369160

Liu, C. F., Song, Y. M., He, W. C., Liu, D. X., He, P., Bao, J. J., et al. (2021). Nontuberculous mycobacteria in China: incidence and antimicrobial resistance spectrum from a nationwide survey. *Infect. Dis. Poverty* 10:59. doi: 10.1186/s40249-021-00844-1

Loizos, A., Soteriades, E. S., Pieridou, D., and Koliou, M. G. (2018). Lymphadenitis by non-tuberculous mycobacteria in children. *Pediatr. Int.* 60, 1062–1067. doi: 10.1111/ped.13708

López-Roa, P., Aznar, E., Cacho, J., Cogollos-Agruña, R., Domingo, D., García-Arata, M. I., et al. (2020). Epidemiology of non-tuberculous mycobacteria isolated from clinical specimens in Madrid, Spain, from 2013 to 2017. *Eur. J. Clin. Microbiol. Infect. Dis.* 39, 1089–1094. doi: 10.1007/s10096-020-03826-7

Lucke, K., Hombach, M., Friedel, U., Ritter, C., and Böttger, E. C. (2012). Automated quantitative drug susceptibility testing of non-tuberculous mycobacteria using MGIT 960/EpiCenter TB eXiST. *J. Antimicrob. Chemother.* 67, 154–158. doi: 10.1093/jac/dkr399

Luo, J., Yu, X., Jiang, G., Fu, Y., Huo, F., Ma, Y., et al. (2018). In vitro activity of Clofazimine against nontuberculous mycobacteria isolated in Beijing, China. *Antimicrob. Agents Chemother.* 62:e00072-18. doi: 10.1128/AAC.00072-18

Mahdavi, N., Gholizadeh, P., Maleki, M. R., Esfahani, A., Chavoshi, S. H., Nikanfar, A., et al. (2021). Isolation and identification of nontuberculous mycobacteria from specimens of lower respiratory tract of transplanted patients based on the evaluation of 16SrRNA gene. *Ann. Ig.* 33, 189–197. doi: 10.7416/ai.2021.2424

Manika, K., Tsikrika, S., Tsaroucha, E., Karabela, S., Karachaliou, I., Bosmi, I., et al. (2015). Distribution of nontuberculous mycobacteria in treated patients with pulmonary disease in Greece - relation to microbiological data. *Future Microbiol.* 10, 1301–1306. doi: 10.2217/FMB.15.50

Marques, L. R. M., Ferrazoli, L., and Chimara, É. (2019). Pulmonary nontuberculous mycobacterial infections: presumptive diagnosis based on the international microbiological criteria adopted in the state of São Paulo, Brazil, 2011-2014. *J. Bras. Pneumol.* 45:e20180278. doi: 10.1590/1806-3713/e20180278

Marras, T. K., and Daley, C. L. (2002). Epidemiology of human pulmonary infection with nontuberculous mycobacteria. *Clin. Chest Med.* 23, 553–567. doi: 10.1016/S0272-5231(02)00019-9

Martin-Casabona, N., Bahrmand, A. R., Bennedsen, J., Østergaard Thomsen, V., Curcio, M., Fauville-Dufaux, M., et al. (2004). Non-tuberculous mycobacteria: patterns of isolation. A multi-country retrospective survey. *Int. J. Tuberc. Lung Dis.* 8, 1186–1193.

Matos, E. D., Santana, M. A., Santana, M. C., Mamede, P., Bezerra, B. L., Panão, E. D., et al. (2004). Nontuberculosis mycobacteria at a multiresistant tuberculosis reference center in Bahia: clinical epidemiological aspects. *Braz. J. Infect. Dis.* 8, 296–304. doi: 10.1590/S1413-86702004000400005

Matveychuk, A., Fuks, L., Priess, R., Hahim, I., and Shitrit, D. (2012). Clinical and radiological features of Mycobacterium kansasii and other NTM infections. *Respir. Med.* 106, 1472–1477. doi: 10.1016/j.rmed.2012.06.023

McSwiggan, D., and Collins, C. (1974). The isolation of M. Kansasii and *M. xenopi* from water systems. *Tubercle* 55, 291–297. doi: 10.1016/0041-3879(74)90038-5

Mijs, W., Vreese, K. D., Devos, A., Pottel, H., Valgaeren, A., Evans, C., et al. (2002). Evaluation of a commercial line probe assay for identification of mycobacterium species from liquid and solid culture. *Eur. J. Clin. Microbiol. Infect. Dis.* 21, 794–802. doi: 10.1007/s10096-002-0825-y

Mirsaeidi, M., Hadid, W., Ericsoussi, B., Rodgers, D., and Sadikot, R. T. (2013). Non-tuberculous mycobacterial disease is common in patients with non-cystic fibrosis bronchiectasis. *Int. J. Infect. Dis.* 17, e1000–e1004. doi: 10.1016/j.ijid.2013.03.018

Modrá, H., Ulmann, V., Caha, J., Hübelová, D., Konečný, O., Svobodová, J., et al. (2019). Socio-economic and environmental factors related to spatial differences in human non-tuberculous mycobacterial diseases in the Czech Republic. *Int. J. Environ. Res. Public Health* 16:3969. doi: 10.3390/ijerph16203969

Moghaddam, S., Nojoomi, F., Dabbagh Moghaddam, A., Mohammadimehr, M., Sakhaee, F., Masoumi, M., et al. (2022). Isolation of nontuberculous mycobacteria species from different water sources: a study of six hospitals in Tehran, Iran. *BMC microbiology* 22:261. doi: 10.1186/s12866-022-02674-z

Moore, J. E., Kruijshaar, M. E., Ormerod, L. P., Drobniewski, F., and Abubakar, I. (2010). Increasing reports of non-tuberculous mycobacteria in England, Wales and Northern Ireland, 1995-2006. *BMC Public Health* 10:612. doi: 10.1186/1471-2458-10-612

Morimoto, K., Hasegawa, N., Izumi, K., Namkoong, H., Uchimura, K., Yoshiyama, T., et al. (2017). A laboratory-based analysis of nontuberculous mycobacterial lung disease in Japan from 2012 to 2013. *Ann. Am. Thorac. Soc.* 14, 49–56. doi: 10.1513/AnnalsATS.201607-573OC

Morita, H., Nakamura, A., Kato, T., Kutsuna, T., Niwa, T., Katou, K., et al. (2005). Isolation of nontuberculous mycobacteria from patients with pneumoconiosis. *J. Infect. Chemother.* 11, 89–92. doi: 10.1007/s10156-004-0368-5

Mortazavi, Z., Bahrmand, A., Sakhaee, F., Hosseini Doust, R., Vaziri, F., Siadat, S. D., et al. (2019). Evaluating the clinical significance of nontuberculous mycobacteria isolated from respiratory samples in Iran: an often overlooked disease. *Infect. Drug Resist.* 12, 1917–1927. doi: 10.2147/IDR.S214181

Munn, Z., Barker, T. H., Moola, S., Tufanaru, C., Stern, C., McArthur, A., et al. (2020). Methodological quality of case series studies: an introduction to the JBI critical appraisal tool. *JBI Evid. Synth.* 18, 2127–2133. doi: 10.11124/JBISRIR-D-19-00099

Muñoz-Egea, M.-C., Akir, A., and Esteban, J. (2023). Mycobacterium biofilms. *Biofilms* 5:100107

Naito, M., Kurahara, Y., Yoshida, S., Ikegami, N., Kobayashi, T., Minomo, S., et al. (2018). Prognosis of chronic pulmonary aspergillosis in patients with pulmonary non-tuberculous mycobacterial disease. *Respir. Investig.* 56, 326–331. doi: 10.1016/j.resinv.2018.04.002

Nasiri, M. J., Dabiri, H., Fooladi, A. A. I., Amini, S., Hamzehloo, G., and Feizabadi, M. M. (2018). High rates of nontuberculous mycobacteria isolation from patients with presumptive tuberculosis in Iran. *New Microbes New Infect.* 21, 12–17. doi: 10.1016/j.nmni.2017.08.008

Nasr Esfahani, B., Moghim, S., Ghasemian Safaei, H., Moghoofei, M., Sedighi, M., and Hadifar, S. (2016). Phylogenetic analysis of prevalent tuberculosis and non-tuberculosis mycobacteria in Isfahan, Iran, based on a 360 bp sequence of the rpoB gene. *Jundishapur J. Microbiol.* 9:e30763. doi: 10.5812/jjm.30763

Ng, S. S. Y., Tay, Y. K., Koh, M. J. A., Thoon, K. C., and Sng, L. H. (2015). Pediatric cutaneous nontuberculous Mycobacterium infections in Singapore. *Pediatr. Dermatol.* 32, 488–494. doi: 10.1111/pde.12575

Okoi, C., Anderson, S. T. B., Antonio, M., Mulwa, S. N., Gehre, F., and Adetifa, I. M. O. (2017). Non-tuberculous mycobacteria isolated from pulmonary samples in sub-Saharan Africa-a systematic review and meta analyses. *Sci. Rep.* 7:12002. doi: 10.1038/s41598-017-12175-z

Ose, N., Maeda, H., Takeuchi, Y., Susaki, Y., Kobori, Y., Taniguchi, S., et al. (2016). Solitary pulmonary nodules due to non-tuberculous mycobacteriosis among 28 resected cases. *Int. J. Tuberc. Lung Dis.* 20, 1125–1129. doi: 10.5588/ijtld.15.0819

Ose, N., Takeuchi, Y., Kitahara, N., Matumura, A., Kodama, K., Shiono, H., et al. (2021). Analysis of pulmonary nodules caused by nontuberculous mycobacteriosis in 101 resected cases: multi-center retrospective study. *J. Thorac. Dis.* 13, 977–985. doi: 10.21037/jtd-20-3108

Ouzzani, M., Hammady, H., Fedorowicz, Z., and Elmagarmid, A. (2016). Rayyan—a web and mobile app for systematic reviews. *Syst. Rev.* 5, 1–10. doi: 10.1186/s13643-016-0384-4

Pang, Y., Zheng, H., Tan, Y., Song, Y., and Zhao, Y. (2017). In vitro activity of Bedaquiline against nontuberculous mycobacteria in China. *Antimicrob. Agents Chemother.* 61:e02627-16. doi: 10.1128/AAC.02627-16

Parashar, D., das, R., Chauhan, D. S., Sharma, V. D., Lavania, M., Yadav, V. S., et al. (2009). Identification of environmental mycobacteria isolated from Agra, North India by conventional & molecular approaches. *Indian J. Med. Res.* 129, 424–431.

Parenti, D. M., Symington, J. S., Keiser, J., and Simon, G. L. (1995). *Mycobacterium kansasii* bacteremia in patients infected with human immunodeficiency virus. *Clin. Infect. Dis.* 21, 1001–1003. doi: 10.1093/clinids/21.4.1001

Park, S., Jo, K. W., Lee, S. D., Kim, W. S., and Shim, T. S. (2017). Clinical characteristics and treatment outcomes of pleural effusions in patients with nontuberculous mycobacterial disease. *Respir. Med.* 133, 36–41. doi: 10.1016/j.rmed.2017.11.005

Pavlik, I., Ulmann, V., Hubelova, D., and Weston, R. T. (2022). Nontuberculous mycobacteria as sapronoses: a review. *Microorganisms* 10:1345. doi: 10.3390/microorganisms10071345

Pedrero, S., Tabernero, E., Arana-Arri, E., Urra, E., Larrea, M., and Zalacain, R. (2019). Changing epidemiology of nontuberculous mycobacterial lung disease over the last two decades in a region of the Basque country. *ERJ Open Res.* 5, 00110–02018. doi: 10.1183/23120541.00110-2018

Pedro, H. D. S. P., Pereira, M. I. F., Goloni, M. R. A., Ueki, S. Y. M., and Chimara, E. (2008). Nontuberculous mycobacteria isolated in São José do Rio Preto, Brazil between 1996 and 2005. *J. Bras. Pneumol.* 34, 950–955. doi: 10.1590/S1806-37132008001100010

Pierre-Audigier, C., Ferroni, A., Sermet-Gaudelus, I., le Bourgeois, M., Offredo, C., Vu-Thien, H., et al. (2005). Age-related prevalence and distribution of nontuberculous mycobacterial species among patients with cystic fibrosis. *J. Clin. Microbiol.* 43, 3467–3470. doi: 10.1128/JCM.43.7.3467-3470.2005

Prammananan, T., Cheunoy, W., Na-Ubol, P., Tingtoy, N., Srimuang, S., and Chaiprasert, A. (2005). Evaluation of polymerase chain reaction and restriction enzyme analysis for routine identification of mycobacteria: accuracy, rapidity, and cost analysis. *Southeast Asian J. Trop. Med. Public Health* 36, 1252–1260.

Rastogi, N., and Goh, K. S. (1992). Effect of pH on radiometric MICs of clarithromycin against 18 species of mycobacteria. *Antimicrob. Agents Chemother.* 36, 2841–2842. doi: 10.1128/AAC.36.12.2841

Riello, F. N., Brígido, R. T. S., Araújo, S., Moreira, T. A., Goulart, L. R., and Goulart, I. M. B. (2016). Diagnosis of mycobacterial infections based on acid-fast bacilli test and bacterial growth time and implications on treatment and disease outcome. *BMC Infect. Dis.* 16:142. doi: 10.1186/s12879-016-1474-6

Rodriguez Díaz, J. C., López, M., Ruiz, M., and Royo, G. (2003). In vitro activity of new fluoroquinolones and linezolid against non-tuberculous mycobacteria. *Int. J. Antimicrob. Agents* 21, 585–588. doi: 10.1016/S0924-8579(03)00048-7

Ruiz, M., Rodriguez, J. C., Escribano, I., Garcia-Martinez, J., Rodriguez-Valera, F., and Royo, G. (2001). Application of molecular biology techniques to the diagnosis of nontuberculous mycobacterial infections. *APMIS* 109, 857–864. doi: 10.1034/j.1600-0463.2001.091208.x

Ryoo, S. W., Shin, S., Shim, M. S., Park, Y. S., Lew, W. J., Park, S. N., et al. (2008). Spread of nontuberculous mycobacteria from 1993 to 2006 in Koreans. *J. Clin. Lab. Anal.* 22, 415–420. doi: 10.1002/jcla.20278

Saifi, M., Jabbarzadeh, E., Bahrmand, A. R., Karimi, A., Pourazar, S., Fateh, A., et al. (2013). HSP65-PRA identification of non-tuberculosis mycobacteria from 4892 samples suspicious for mycobacterial infections. *Clin. Microbiol. Infect.* 19, 723–728. doi: 10.1111/j.1469-0691.2012.04005.x

Santos, R., Oliveira, F., Fernandes, J., Gonçalves, S., Macieira, F., and Cadete, M. (2005). Detection and identification of mycobacteria in the Lisbon water distribution system. *Water Sci. Technol.* 52, 177–180. doi: 10.2166/wst.2005.0258

Scarparo, C., Piccoli, P., Rigon, A., Ruggiero, G., Ricordi, P., and Piersimoni, C. (2002). Evaluation of the BACTEC MGIT 960 in comparison with BACTEC 460 TB for detection and recovery of mycobacteria from clinical specimens. *Diagn. Microbiol. Infect. Dis.* 44, 157–161. doi: 10.1016/S0732-8893(02)00437-6

Shafer, R. W., and Sierra, M. F. (1992). *Mycobacterium xenopi*, *Mycobacterium fortuitum*, Mycobacterium kansasii, and other nontuberculous mycobacteria in an area of endemicity for AIDS. *Clin. Infect. Dis.* 15, 161–162. doi: 10.1093/clinids/15.1.161

Shao, Y., Chen, C., Song, H., Li, G., Liu, Q., Li, Y., et al. (2015). The epidemiology and geographic distribution of nontuberculous mycobacteria clinical isolates from sputum samples in the eastern region of China. *PLoS Negl. Trop. Dis.* 9:e0003623. doi: 10.1371/journal.pntd.0003623

Sharma, A., Chandraker, S. K., and Bharti, M. (2007). Nontubercular mycobacteria in drinking water of some educational institutes in Jabalpur (MP), India. *Indian J. Microbiol.* 47, 233–240. doi: 10.1007/s12088-007-0044-4

Shen, G. H., Hung, C. H., Hu, S. T., Wu, B. D., Lin, C. F., Chen, C. H., et al. (2009). Combining polymerase chain reaction restriction enzyme analysis with phenotypic characters for mycobacteria identification in Taiwan. *Int. J. Tuberc. Lung Dis.* 13, 472–479.

Shenai, S., Rodrigues, C., and Mehta, A. (2010). Time to identify and define non-tuberculous mycobacteria in a tuberculosis-endemic region. *Int. J. Tuberc. Lung Dis.* 14, 1001–1008.

Sheu, L. C., Tran, T. M., Jarlsberg, L. G., Marras, T. K., Daley, C. L., and Nahid, P. (2015). Non-tuberculous mycobacterial infections at San Francisco general hospital. *Clin. Respir. J.* 9, 436–442. doi: 10.1111/crj.12159

Slosárek, M., Alugupalli, S., Kaustová, J., and Larsson, L. (1996). Rapid detection of *Mycobacterium kansasii* in water by gas chromatography/mass spectrometry. *J. Microbiol. Methods* 27, 229–232. doi: 10.1016/S0167-7012(96)00954-2

Sookan, L., and Coovadia, Y. M. (2014). A laboratory-based study to identify and speciate non-tuberculous mycobacteria isolated from specimens submitted to a central tuberculosis laboratory from throughout KwaZulu-Natal Province, South Africa. *S. Afr. Med. J.* 104, 766–768. doi: 10.7196/SAMJ.8017

Sorlozano, A., Soria, I., Roman, J., Huertas, P., Soto, M. J., Piedrola, G., et al. (2009). Comparative evaluation of three culture methods for the isolation of mycobacteria from clinical samples. *J. Microbiol. Biotechnol.* 19, 1259–1264. doi: 10.4014/jmb.0901.0059

Steadham, J. E. (1980). High-catalase strains of *Mycobacterium kansasii* isolated from water in Texas. *J. Clin. Microbiol.* 11, 496–498. doi: 10.1128/jcm.11.5.496-498.1980

Takenaka, S., Ogura, T., Oshima, H., Izumi, K., Hirata, A., Ito, H., et al. (2020). Development and exacerbation of pulmonary nontuberculous mycobacterial infection in patients with systemic autoimmune rheumatic diseases. *Mod. Rheumatol.* 30, 558–563. doi: 10.1080/14397595.2019.1619220

Tan, Y., Su, B., Shu, W., Cai, X., Kuang, S., Kuang, H., et al. (2018). Epidemiology of pulmonary disease due to nontuberculous mycobacteria in southern China, 2013-2016. *BMC Pulm. Med.* 18:168. doi: 10.1186/s12890-018-0728-z

Thangavelu, K., Krishnakumariamma, K., Pallam, G., Dharm Prakash, D., Chandrashekar, L., Kalaiarasan, E., et al. (2021). Prevalence and speciation of non-tuberculous mycobacteria among pulmonary and extrapulmonary tuberculosis suspects in South India. *J. Infect. Public Health* 14, 320–323. doi: 10.1016/j.jiph.2020.12.027

Thomas, V., Herrera-Rimann, K., Blanc, D. S., and Greub, G. (2006). Biodiversity of amoebae and amoeba-resisting bacteria in a hospital water network. *Appl. Environ. Microbiol.* 72, 2428–2438. doi: 10.1128/AEM.72.4.2428-2438.2006

Thomson, R. M., Furuya-Kanamori, L., Coffey, C., Bell, S. C., Knibbs, L. D., and Lau, C. L. (2020). Influence of climate variables on the rising incidence of nontuberculous mycobacterial (NTM) infections in Queensland, Australia 2001-2016. *Sci. Total Environ.* 740:139796. doi: 10.1016/j.scitotenv.2020.139796

Tu, H. Z., Chang, S. H., Huaug, T. S., Huaug, W. K., Liu, Y. C., and Lee, S. S. (2003). Microscopic morphology in smears prepared from MGIT broth medium for rapid presumptive identification of *Mycobacterium tuberculosis* complex, *Mycobacterium avium* complex and *Mycobacterium kansasii*. *Ann. Clin. Lab. Sci.* 33, 179–183.

Urabe, N., Sakamoto, S., Ito, A., Sekiguchi, R., Shimanuki, Y., Kanokogi, T., et al. (2021). Bronchial brushing and diagnosis of pulmonary nontuberculous mycobacteria infection. *Respiration* 100, 877–885. doi: 10.1159/000515605

Woods, G. L., and Washington, J. A. (1987). Mycobacteria other than *Mycobacterium tuberculosis*: review of microbiologic and clinical aspects. *Rev. Infect. Dis.* 9, 275–294. doi: 10.1093/clinids/9.2.275

Wright, E. P., Collins, C. H., and Yates, M. D. (1985). Mycobacterium xenopi and *Mycobacterium kansasii* in a hospital water supply. *J. Hosp. Infect.* 6, 175–178. doi: 10.1016/S0195-6701(85)80095-5

Wu, J., Zhang, Y., Li, J., Lin, S., Wang, L., Jiang, Y., et al. (2014). Increase in nontuberculous mycobacteria isolated in Shanghai, China: results from a population-based study. *PLoS One* 9:e109736. doi: 10.1371/journal.pone.0109736

Xu, J., Li, P., Zheng, S., Shu, W., and Pang, Y. (2019). Prevalence and risk factors of pulmonary nontuberculous mycobacterial infections in the Zhejiang Province of China. *Epidemiol. Infect.* 147:e269. doi: 10.1017/S0950268819001626

Zhang, Y., Yu, C., Jiang, Y., Zheng, X., Wang, L., Li, J., et al. (2023). Drug resistance profile of *Mycobacterium kansasii* clinical isolates before and after 2-month empirical antimycobacterial treatment. *Clin. Microbiol. Infect.* 29, 353–359. doi: 10.1016/j.cmi.2022.10.002

frontiers | Frontiers in Microbiology

TYPE Review
PUBLISHED 16 April 2024
DOI 10.3389/fmicb.2024.1392606

OPEN ACCESS

EDITED BY
Matt Johansen,
University of Technology Sydney, Australia

REVIEWED BY
Dereje Abate Negatu,
Hackensack Meridian Health, United States
Juan Manuel Belardinelli,
Colorado State University, United States
Giulia Degiacomi,
University of Pavia, Italy

*CORRESPONDENCE
Hannelore Iris Bax
✉ h.bax@erasmusmc.nl

RECEIVED 27 February 2024
ACCEPTED 03 April 2024
PUBLISHED 16 April 2024

CITATION
Meliefste HM, Mudde SE, Ammerman NC, de Steenwinkel JEM and Bax HI (2024) A laboratory perspective on *Mycobacterium abscessus* biofilm culture, characterization and drug activity testing.
Front. Microbiol. 15:1392606.
doi: 10.3389/fmicb.2024.1392606

A laboratory perspective on *Mycobacterium abscessus* biofilm culture, characterization and drug activity testing

Henriëtte Margarethe Meliefste[1], Saskia Emily Mudde[1], Nicole Christine Ammerman[1], Jurriaan Evert M. de Steenwinkel[1] and Hannelore Iris Bax[1,2]*

[1]Department of Medical Microbiology and Infectious Diseases, Erasmus University Medical Center, Rotterdam, Netherlands, [2]Department of Internal Medicine, Section of Infectious Diseases, Erasmus University Medical Center, Rotterdam, Netherlands

Mycobacterium abscessus is an emerging opportunistic pathogen causing severe pulmonary infections in patients with underlying lung disease and cystic fibrosis in particular. The rising prevalence of *M. abscessus* infections poses an alarming threat, as the success rates of available treatment options are limited. Central to this challenge is the absence of preclinical *in vitro* models that accurately mimic *in vivo* conditions and that can reliably predict treatment outcomes in patients. *M. abscessus* is notorious for its association with biofilm formation within the lung. Bacteria in biofilms are more recalcitrant to antibiotic treatment compared to planktonic bacteria, which likely contributes to the lack of correlation between preclinical drug activity testing (typically performed on planktonic bacteria) and treatment outcome. In recent years, there has been a growing interest in *M. abscessus* biofilm research. However, the absence of standardized methods for biofilm culture, biofilm characterization and drug activity testing has led to a wide spectrum of, sometimes inconsistent, findings across various studies. Factors such as strain selection, culture medium, and incubation time hugely impact biofilm development, phenotypical characteristics and antibiotic susceptibility. Additionally, a broad range of techniques are used to study *M. abscessus* biofilms, including quantification of colony-forming units, crystal violet staining and fluorescence microscopy. Yet, limitations of these techniques and the selected readouts for analysis affect study outcomes. Currently, research on the activity of conventional antibiotics, such as clarithromycin and amikacin, against *M. abscessus* biofilms yield ambiguous results, underscoring the substantial impact of experimental conditions on drug activity assessment. Beyond traditional drug activity testing, the exploration of novel anti-biofilm compounds and the improvement of *in vitro* biofilm models are ongoing. In this review, we outline the laboratory models, experimental variables and techniques that are used to study *M. abscessus* biofilms. We elaborate on the current insights of *M. abscessus* biofilm characteristics and describe the present understanding of the activity of traditional antibiotics, as well as potential novel compounds, against *M. abscessus* biofilms. Ultimately, this work contributes to the advancement of fundamental knowledge and practical applications of accurate preclinical *M. abscessus* models, thereby facilitating progress towards improved therapies for *M. abscessus* infections.

KEYWORDS

***mycobacterium abscessus*, biofilm, nontuberculous mycobacteria, drug activity testing, *in vitro*, antimicrobial resistance**

1 Introduction

Mycobacterium abscessus, belonging to the rapidly growing non-tuberculous mycobacteria, is an emerging opportunistic pathogen that can cause severe pulmonary infections in patients with underlying lung disease, such as cystic fibrosis. The prevalence of *M. abscessus* infections has been increasing over the past decades (Cristancho-Rojas et al., 2023). This is an alarming threat, as the success rates of available treatment options are limited (Chen et al., 2019). Consequently, there is an urgent need for novel treatment regimens. Central to the challenge of drug development is the lack of preclinical *in vitro* models that accurately mimic *in vivo* conditions and that can reliably predict treatment outcomes in patients.

Mycobacterium abscessus is increasingly recognized for its association with biofilm formation in the alveolar walls and lung cavity of patients, and on medical devices (El Helou et al., 2013; Qvist et al., 2015; Fennelly et al., 2016). It is widely acknowledged that bacteria in biofilms are more recalcitrant to antibiotic treatment compared to planktonic bacteria. For example, the biofilms' extracellular matrix (ECM) forms a barrier that protects the bacteria from antibiotic penetration (Ortíz-Pérez et al., 2011; Singh et al., 2017). Moreover, bacteria within biofilms exhibit a heterogeneity of metabolic states, including a non-replicating state in which bacteria are able to survive low nutrient and oxygen levels, but are less susceptible to antibiotics (Singh et al., 2017). Consequently, guideline-recommended drugs might be insufficient in killing *M. abscessus* within biofilms. Hence, it is plausible that the reliability of preclinical drug activity assays will benefit from incorporating *M. abscessus* biofilm models next to the currently accepted standard assays using planktonic mycobacteria.

In recent years there has been a growing interest in *M. abscessus* biofilm research. However, there is no standardized method for biofilm culture, characterization and drug activity testing, hampering appropriate comparison between different studies. Both the type of biofilm model and experimental conditions used in *M. abscessus* biofilm studies can affect biofilm characteristics and behavior, contributing to the wide spectrum of seemingly inconsistent findings across various *M. abscessus* biofilm studies (Figure 1).

In this context, we provide an overview of the laboratory models and techniques that have been described to study *M. abscessus* biofilms (search strategy is provided in Supplementary material S1). We elaborate on the current insights of *M. abscessus* biofilm characteristics and describe the present understanding of the activity of traditional antibiotics, as well as potential novel compounds, against *M. abscessus* biofilms.

2 Building the biofilm research fundament—laboratory models used for *Mycobacterium abscessus* biofilm culture

2.1 Classical biofilm culture methods

Various static and dynamic culture methods have been used to culture *M. abscessus* biofilms *in vitro,* involving both liquid and solid surface biofilm culture systems. In liquid biofilm cultures, *M. abscessus* has been shown to exhibit various growth patterns, including growth at the bottom of the well, as a pellicle at the liquid-air interface, or even both submerged and as a pellicle (Clary et al., 2018; Hunt-Serracin et al., 2019; Belardinelli et al., 2021; Li et al., 2022). In fact, one study reported that *M. abscessus* formed its biofilm at the liquid-air interface when grown for 20 days in standard medium, while the biofilm submerged within 29 h when exposed to the reducing agent dithiothreitol (Chakraborty et al., 2021). This suggests that environmental factors affect *M. abscessus* biofilm behavior, although the precise factors that contribute to biofilm location remain unknown. Biofilm location is an important aspect for the reproducibility and practicability of experiments. As such, submerged biofilms are more readily separated from the planktonic population, facilitating a reliable assessment of the biofilm population. Importantly, methods to separate pellicle-biofilms from planktonic bacteria are often not described. Moreover, it could be speculated that submerged biofilms might exhibit distinct behavior patterns compared to those at the liquid-air interface due to variations in, for example, oxygen concentration and mechanical forces.

For biofilm culture in liquid medium, the most commonly used method is the static *microtiter plate method*, in which a microtiter plate is inoculated with a *M. abscessus* suspension after which a visible mycobacterial biofilm is formed over time. This relatively simple method enables simultaneous testing of multiple conditions that might affect the formation or degradation of the *M. abscessus* biofilm, facilitating high-throughput screening. However, the limited surface area of microtiter plate wells restricts the amount of biofilm that can be cultured, potentially hampering the reliability and practicability of downstream analyses. Alternatively, larger volumes have been used for biofilm growth, including polystyrene or glass test tubes or tissue culture flasks (Keefe and Bermudez, 2022). While the consequence of using larger volumes is a lower throughput, it is an advantageous method when high biomass is required for in-depth characterisation analyses, such as proteomics. Another well-established method for biofilm culture is the *MBEC (Minimal Biofilm Eradication Concentration) Assay Kit*® (formerly known as the Calgary Biofilm Device) (Ceri et al., 1999). This device consists of a 96-well culture plate with a plastic lid containing 96 pegs. Biofilms form on the pegs, as these pegs are partially submerged in inoculated culture medium. After biofilm formation these pegs can easily be transferred to another 96-wells plate containing a range of antibiotic concentrations, allowing the determination of the minimal biofilm eradication concentration by visual observation or by colony-forming units (CFU) determination, making it a more standardized approach compared to the microtiter plate method. Additionally, *M. abscessus* biofilms can be cultured in *chambered slides* (Muñoz-Egea et al., 2016; Chakraborty et al., 2021; Yue et al., 2022; Kurbatfinski et al., 2023). With this method the biofilm is grown in individual wells on a chamber slide system, allowing for direct visualization of live bacteria using microscopy. As such, chamber slides are suitable for monitoring biofilm maturation and assessing the activity of antimicrobial agents on the biofilm in real-time. Another method described for *M. abscessus* biofilm culture involves the addition of *glass beads* to the culture medium (Falkinham et al., 2012; Oschmann-Kadenbach et al., 2024). The biofilm forms on the glass beads after which the bacteria can be obtained by vortexing.

Besides the above-mentioned static biofilm models, more dynamic models have been developed for biofilm research, in which biofilms can be cultured with a continuous flow of culture medium.

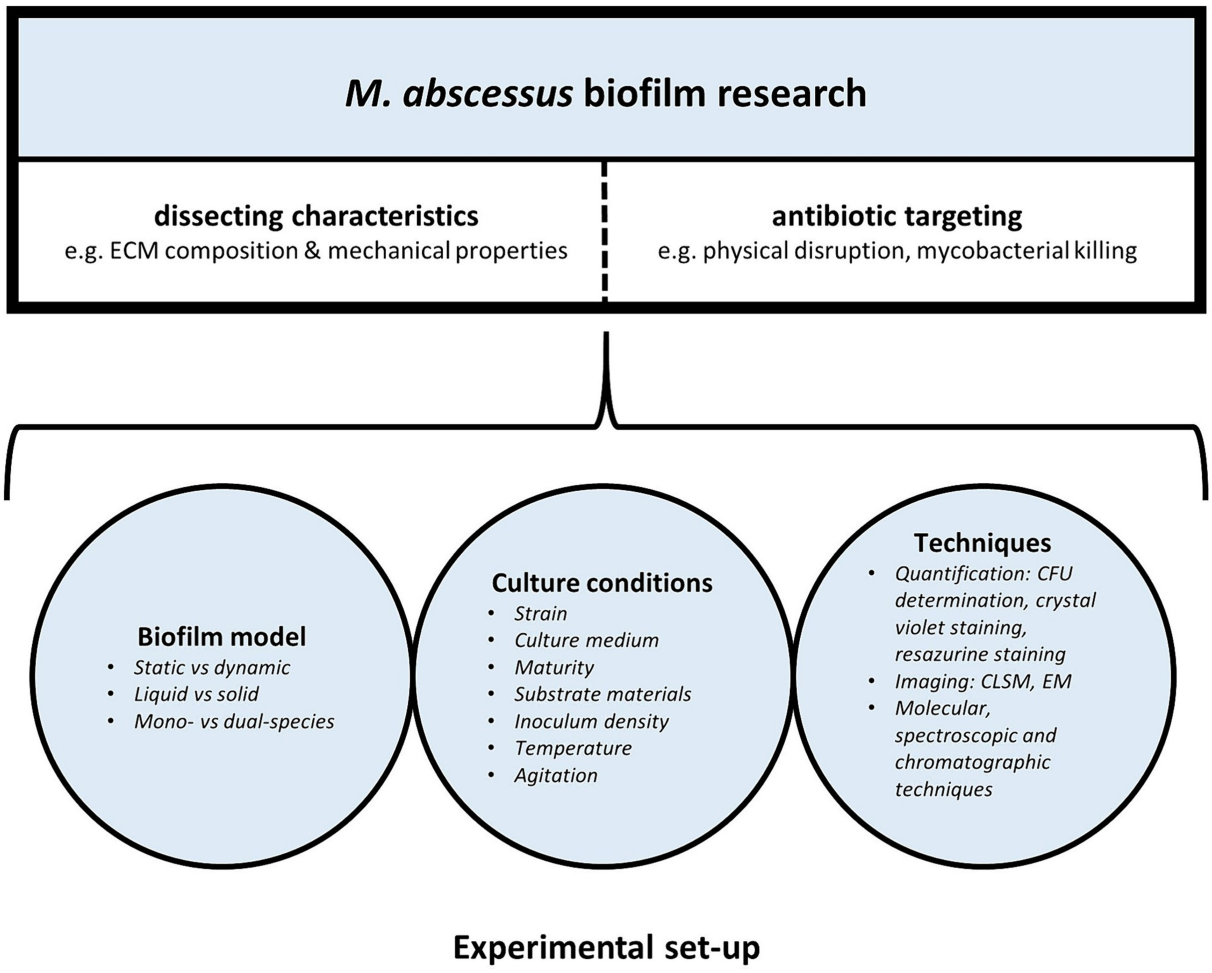

FIGURE 1
Laboratory set-up of *M. abscessus* biofilm research: models, experimental conditions, and techniques influence *M. abscessus* biofilm characteristics and behavior.

Biofilms cultured in a *chamber flow cell* can be easily stained and imaged, allowing for real-time monitoring of the biofilm under dynamic conditions (Malcolm et al., 2013). In addition, the *Centre for Disease Control biofilm reactor,* comprises a vessel equipped with multiple coupons (Goeres et al., 2005). The vessel can be filled with culture medium submerging each coupon, and two pumps facilitate the in- and outflow of medium. The coupons are easily obtained for CFU determination and are available in various materials, allowing the evaluation of various substrate materials on biofilm formation (Mullis and Falkinham, 2013).

An alternative method for growing biofilms in liquid medium is by using *a colony-forming model*, in which the biofilm is grown on a solid surface—typically by placing an inoculated semi-permeable membrane on top of solid agar (Rodríguez-Sevilla et al., 2018a; Gloag et al., 2021; Aguilera-Correa et al., 2023). Biofilms can be detached and collected via sonicating and vortexing the membrane. An important advantage of this model is that biofilm transfer to fresh medium or to medium containing antimicrobials is relatively straightforward. There are no washing steps needed, which is beneficial for fragile biofilms like those formed by *M. abscessus*. Moreover, both sides of the biofilm can be accessed, allowing various analyses, such as the antibiotic permeability assay (Ortíz-Pérez et al., 2011). Colony-forming biofilms share morphological traits of liquid grown biofilms and tend to have more biomass, enabling the study of various aspects, such as its biomechanical properties (Gloag et al., 2021). In addition, the colony-forming biofilm model has been used to study the interaction of *M. abscessus* and *Pseudomonas aeruginosa* in a polymicrobial biofilm, and to analyse the growth of smooth and rough *M. abscessus* biofilms in response to antibiotic exposure (Rodríguez-Sevilla et al., 2018a, 2019; Idosa et al., 2022; Aguilera-Correa et al., 2023).

2.2 Mimicking the *Mycobacterium abscessus* lung niche: more complex biofilm models

During biofilm formation in humans, it has been postulated that *M. abscessus* interacts with host immune factors and other bacterial communities (Park et al., 2021; Idosa et al., 2022). Interestingly, interaction between bacterial species can result in structural and functional changes within the biofilm, leading to increased bacterial

resistance to antibiotics (Burmølle et al., 2014). *M. abscessus* can be co-isolated with *P. aeruginosa*, another major pathogen in cystic fibrosis patients. Therefore, a *dual-species biofilm model* was developed to explore the interaction between *M. abscessus* and *P. aeruginosa* (Adjemian et al., 2018). In this model, a stable colony-forming dual-biofilm is formed within 48–72 h on tryptic soy agar, which is suitable for analyses such as microscopy and CFU determination (Rodríguez-Sevilla et al., 2018a). Later, a similar model was developed using 7H10 Middlebrook agar as culture medium (Idosa et al., 2022). In comparison to *M. abscessus, P. aeruginosa* has a high growth rate, resulting in a greater abundance of *P. aeruginosa* relative to *M. abscessus* within dual-species biofilms (Rodríguez-Sevilla et al., 2018a). Two studies observed that co-culturing *M. abscessus* with *P. aeruginosa* caused a reduction in the number of *M. abscessus* compared to a single-species *M. abscessus* biofilm (Rodríguez-Sevilla et al., 2018a; Idosa et al., 2022). Thus, *P. aeruginosa* could have a competitive advantage over *M. abscessus,* thereby affecting the biofilm structure and characteristics, which could also be the case for other pathogens that are co-isolated in patients with *M. abscessus* infections. Interestingly, *M. abscessus* and *P. aeruginosa* co-aggregate, yet their spatial distribution within the biofilm seems to differ. *M. abscessus* was found to predominantly localize in the inner and lower zone of the biofilm, whereas *P. aeruginosa* also grew in the upper layers (Rodríguez-Sevilla et al., 2018a). The direct dynamics between *M. abscessus* and *P. aeruginosa* within biofilms are still rather unexplored and probably involve a complex interplay. Overall, the dual-species biofilm model provides important additional information compared to the traditional single-species biofilm, as selectively targeting one species can give a competitive advantage to the other, hereby altering the overall biofilm dynamics (Rodríguez-Sevilla et al., 2019).

To more closely mimic host-pathogen interactions, a *3D lung epithelial model* was developed in which *M. abscessus* was able to form a single- and dual-species biofilm with *P. aeruginosa* on lung epithelial cells (Rodríguez-Sevilla et al., 2018b). Moreover, *M. abscessus* biofilm formation was shown in *human airway organoids* (Leon-Icaza et al., 2023). In another model, *neutrophils* were adhered to coverslips in flow cells, after which *M. abscessus* biofilm was formed (Malcolm et al., 2013). Interestingly, biofilm density was enhanced by neutrophils (Malcolm et al., 2013). Ultimately, such models could be used to study the interactions between host cells and bacterial responses to antibiotics.

3 Culture condition complexities—an overview of experimental variables

The absence of standardized biofilm culture methods introduces technical variabilities across studies, including differences in strain selection, culture medium, and biofilm maturity.

3.1 Strain selection

Different *M. abscessus* strains are used in biofilm research. This is important as differences in biofilm formation capability and robustness have been described among different isolates (Martín-de-Hijas et al., 2009; Saptawati et al., 2022). Yet, the factors contributing to this (sub) strain variability and the extent to which this variability affects biofilm formation and behavior remain underexplored. Studies on *M. abscessus* biofilms are most commonly performed using the ATCC 19977 strain, an *M. abscessus* subsp. *abscessus*, due to its widespread availability and its relatively well-established work protocols. Advantageously, the genome of the ATCC 19977 strain is similar to the genomes of other relevant (clinical) isolates (Davidson et al., 2014; Davidson, 2018). Other *M. abscessus* subspecies have only occasionally been used in biofilm research (Table 1). It could be speculated that genetic differences among *M. abscessus* subspecies may affect biofilm formation and characteristics. There are studies on *M. abscessus* biofilms and drug activity testing that include multiple isolates, although their primary focus was not on strain variability. These studies showed no major differences between the isolates in terms of drug susceptibility (Ortíz-Pérez et al., 2011; Rodríguez-Sevilla et al., 2018a; Marini et al., 2019; Rodríguez-Sevilla et al., 2019; Belardinelli et al., 2022a; Feizi et al., 2023). Nevertheless, it may be worthwhile to further unravel strain-specific biofilm behavior, including antibiotic susceptibility, given the paucity of data on this topic.

Another important consideration regarding strain selection is the distinction between the smooth and rough morphotype that *M. abscessus* exhibits. Initially it was thought that only smooth *M. abscessus* morphotypes were capable of forming biofilms (Howard et al., 2006; Greendyke and Byrd, 2008; Bernut et al., 2016). However, subsequent studies demonstrated that the rough morphotype, which differs from the smooth morphotype by absence of glycopeptidolipids in the cell wall, was also able to form biofilms (Howard et al., 2006; Williams et al., 2009; Clary et al., 2018; Gloag et al., 2021; Aguilera-Correa et al., 2023; Veigyabati Devi and Singh, 2023; Oschmann-Kadenbach et al., 2024). This discrepancy is likely due to differences in experimental conditions, experimental duration and strains, further emphasizing the importance of using different experimental variables in *M. abscessus* biofilm research (Clary et al., 2018). The smooth and rough morphotype biofilms have distinct characteristics, including differences in macroscopic and microscopic appearances (Williams et al., 2009; Clary et al., 2018; Gloag et al., 2020; Born et al., 2023). For example, the smooth morphotype colony biofilm has a smooth viscous appearance whilst the rough morphotype has a fractal-like appearance

TABLE 1 Overview of *M. abscessus* isolates and the corresponding number of studies including each isolate for *M. abscessus* biofilm research.

Strain	Number of studies
M. abscessus subsp. *abscessus* ATCC 19977	37
M. abscessus subsp. *abscessus* Bamboo	3
M. abscessus subsp. *bolletii* 101	1
M. abscessus subsp. *bolletii* CIP 108541	1
M. abscessus subsp. *bolletii* NR-44261	1
M. abscessus subsp. *massiliense* GO06	1
M. abscessus subsp. *massiliense* CIP 108297	1
Clinical isolate (no subspecies mentioned)	19
Clinical isolate (subsp. *massiliense*)	3
Clinical isolate (subsp. *abscessus*)	2
Not described	3

on a macroscopic level (Gloag et al., 2021). In liquid culture, the smooth and rough morphotype biofilms were, respectively, described as "oleaginous" and "waxy" (Clary et al., 2018). In addition, smooth and rough morphotype biofilms also differ in their viscoelastic properties (section 5.1.5) (Gloag et al., 2021). Whether the smooth and rough morphotype biofilms also differ in other aspects, such as ECM composition or its interaction with host cells is unknown.

3.2 Culture medium

M. abscessus can form biofilms in different types of culture medium. The most commonly used media are 7H9 Middlebrook medium, Sauton's medium and Synthetic Cystic Fibrosis Medium (SCFM) (Table 2). These media differ in chemical composition, pH, viscosity, and nutrient availability, which could impact biofilm formation. In fact, media dependent differences in macroscopic appearance as well as biochemical composition of *M. abscessus* biofilms have been described (Hunt-Serracin et al., 2019; Keefe and Bermudez, 2022). Of note, some studies specified the omission of Tween 80, a common supplement in 7H9 Middlebrook broth, from their culture medium. Tween 80 inhibits aggregation of *M. abscessus*, and omission of Tween 80 might therefore promote biofilm formation (Kolpen et al., 2020). However, it could be argued that the presence of a detergent such as Tween 80 in culture medium might actually mimic the surface tension reducing function of lung surfactant in the *in vivo* situation. In this context, the exact influence of lung surfactant on *M. abscessus* biofilm formation is unclear. It could be speculated that lung surfactant might inhibit biofilm formation, indicated by the observation that the phospholipid dioleoylphosphatidylcholine (DOPC) slowed down *M. abscessus*' surface attachment *in vitro* (Belardinelli et al., 2021). Whether this also holds true for the *in vivo* situation is currently unknown, especially since not DOPC, but dipalmitoylphosphatidylcholine (DPPC), is the most abundant phosphatidylchole present in lung surfactant (King, 1982). Alternatively, it has been shown for bacteria other than *M. abscessus* that components of lung surfactant were able to induce a stress response in bacteria which facilitated biofilm formation (Willsey et al., 2018). It is however unclear how those findings relate to *M. abscessus*. In addition to culture medium, specific components have been reported to affect biofilm growth. In this context, it was previously suggested that iron plays a role in *M. abscessus* biofilm formation, as a ferritin gene knock out in *M. abscessus* resulted in decreased biofilm formation (Pereira et al., 2023). In addition, omitting FeSO4 from SCFM led to decreased biofilm biomass compared to complete SCFM (Belardinelli et al., 2021). Other specific cations could affect biofilm formation as well. For example, the omission of magnesium from SCFM medium significantly decreased biofilm mass, and RNA sequencing revealed uniquely expressed enzymes in both SCFM- and Hank's Balanced Salt Solutions-grown biofilms that depended on magnesium as a co-factor (Belardinelli et al., 2021; Keefe and Bermudez, 2022). However, since supplementing SCFM with magnesium did not result in increased biofilm mass, its exact role in biofilm formation has yet to be elucidated (Belardinelli et al., 2021). The importance of calcium in biofilm formation is unclear. Although its presence was critical for *M. abscessus* biofilm formation in a colony forming model, other studies using a liquid biofilm model could not confirm these findings (Belardinelli et al., 2021; Keefe and Bermudez, 2022). These inconsistencies might be attributable to the presence of alternative nutrients in the various media that might have acted as calcium substitutes. Of note, to determine the exact effect of medium components on biofilm formation, rather than on mycobacterial growth alone, inclusion of appropriate planktonic controls is required.

Besides considering the medium type and composition, maintaining a static environment versus continuous replenishing of medium is a factor that varies across studies and that could impact biofilm formation. Daily replenishment can provide essential nutrients to support biofilm formation, while maintaining the medium could lead to nutrient depletion, potentially mimicking *in vivo* site-of-infection environments and altering biofilm behavior.

TABLE 2 Overview of culture media and the corresponding number of studies including each medium for *M. abscessus* biofilm research.

	Number of studies
Liquid culture medium	
7H9 Middlebrook broth	11
7H9 Middlebrook broth without Tween 80	5
7H9 Middlebrook broth + OADC	4
7H9 Middlebrook broth +10% OADC +0.5% glycerol	2
Sauton's medium	10
Sauton's medium +10% ADC	1
Synthetic Cystic Fibrosis Medium	6
Mueller-Hinton broth	1
GTSF-2 medium +2.5 mg/L ITS +1.5 g/L sodium bicarbonate +10% FBS*	1
Hartmans-de Bont broth	1
Iscove's medium*	1
Lysogeny broth + glucose	1
M63 salts + glucose + $CaCl_2$ + $MgSO_2$	1
RPMI +10% heat inactivated FBS*	2
Tryptic soy broth	1
Hanks' balanced salt solution	1
Unclear	3
Solid culture medium	
Tryptic soy agar +5% sheep blood	3
7H10 Middlebrook agar + OADC	2
7H11 Middlebrook agar	1
B4 biofilm-promoting solid medium + calcium acetate or EDTA.	1
Mueller-Hinton agar containing antibiotics	1
Solid Synthetic Cystic Fibrosis Medium	1

Cell culture media are indicated with *. OADC, Oleic Albumin Dextrose Catalase; ADC, albumin, dextrose, catalase ITS, Insulin-Transferrin-Selenium; FBS, fetal bovine serum; RPMI, Roswell Park Memorial Institute; EDTA, Ethylenediamine tetraacetic acid.

3.3 Biofilm maturity

The duration of biofilm culture before starting experiments varies widely among studies, ranging from 6 h to 28 days, which might affect

biofilm characteristics (Supplementary Table S1) (Belardinelli et al., 2021; Dokic et al., 2021). Biofilm formation is generally distinguished into 3 phases, including an early, middle and mature stage. Although there is no consensus on the exact duration of each phase for *M. abscessus* biofilm formation, the early phase is typically considered at day 1 to 2, the middle phase at day 3 to 5 and the mature phase at day 6 to 7 (Belardinelli et al., 2021; Dokic et al., 2021; Veigyabati Devi and Singh, 2023). Mature biofilms are often more complex in structure and composition, although prolonged culture duration has been reported to result in decreased biofilm density, decreased bacterial viability, and biofilm dispersal (Belardinelli et al., 2021).

Biofilm maturation has been linked to a shift in gene expression (Belardinelli et al., 2021; Dokic et al., 2021). During the early-stage of surface attachment, an upregulation of genes related to membrane transport and transcription processes was observed compared to planktonic bacteria (Belardinelli et al., 2021). In the middle-stage of biofilm formation, *M. abscessus* upregulated pathways related to translation and transcription processes, along with the upregulation of several chaperones (Belardinelli et al., 2021). In addition, pathways related to fatty acid, glyoxylate and redox metabolism as well as the stress response were upregulated (Dokic et al., 2021). In the final mature stage, substantially more differentially expressed genes have been identified compared to the middle-stage biofilm. Pathways related to cell division, cell wall synthesis, transport, and energy production were reported to be downregulated, with upregulation observed for pathways related to oxidoreductase activity and propanoate metabolism indicating a genetic and metabolic shift towards a dispersal-ready state of the biofilm (Dokic et al., 2021). Overall, a dynamic shift in the expression of genes and metabolic pathways has been described, reflecting the evolving cellular activities during biofilm development. The process of changing gene expression during the different stages of biofilm formation was found to be carefully orchestrated by several transcription regulators, including members from the Tetracycline Resistance Element Repressor and Multiple Antibiotic Resistance Regulator family (both associated with biofilm formation and virulence in other bacteria) (Veigyabati Devi and Singh, 2023). Studying the unique expression of transcripts and transcriptional regulators at specific stages of the biofilm cycle is important as potential therapeutic targets might be identified.

3.4 Others

Several additional experimental variables that might affect *M. abscessus* biofilm formation are important to consider when designing *M. abscessus* biofilm experiments. First, variability in substrate materials has been reported. These substrates might differ in surface texture, hydrophobicity, chemical composition and porosity. While the exact influence of these (subtle) material differences are unclear, it is recognized that biofilm adherence may vary depending on the material. For example, better adherence of *M. abscessus* to glass compared to polyvinyl chloride has been reported (Mullis and Falkinham, 2013). Second, different culture volumes have been reported across studies, which might affect experimental conditions such as nutrient and oxygen availability. Third, the density of the mycobacterial starting inoculum, ranging from 10^5 CFU/mL to 10^9 CFU/mL in *M. abscessus* biofilm studies, might affect biofilm formation since higher inoculum densities might expedite biofilm formation, increase the competition for nutrients, affect inter-microbial interactions, and potentially impact the final density and thickness of a mature biofilm (Stepanović et al., 2003; Rodríguez-Sevilla et al., 2018a; Lichtenberg et al., 2022). In addition, the method of inoculum preparation—either derived from liquid or solid medium—might play a role in biofilm formation, as was observed for bacteria other than *M. abscessus* (Kiers et al., 2001; Stepanović et al., 2007). This might be due to the differential expression of cell-associated molecules related to adhesion, an important process during the initial stages of biofilm development, in solid grown bacteria compared to liquid grown bacteria (Kiers et al., 2001; Stepanović et al., 2007). Fourth, experimental temperature might impact biofilm formation. While the most commonly reported temperature used in *M. abscessus* biofilm experiments was 37°C, reflecting the human body temperature, studies vary in temperature settings from room temperature to 37°C. Yet a fifth factor is culture agitation. Most studies induced biofilm formation without culture agitation. Remarkably, some studies induced biofilm formation under agitating conditions, with a speed ranging from 70 to 150 rpm. This could potentially impact nutrient and oxygen diffusion, as well as affect the mechanical load on the biofilm (Greendyke and Byrd, 2008; Muñoz-Egea et al., 2016; Feizi et al., 2023).

4 Exploring the toolbox—commonly used techniques for studying and analysing *Mycobacterium abscessus* biofilms

A variety of techniques are used for studying *M. abscessus* biofilms, offering insights into the biofilm growth dynamics, structure, mechanical properties, and response to antibiotics.

4.1 Biofilm quantification

CFU determination is the most commonly used method for quantifying the number of viable bacteria within *M. abscessus* biofilms (Supplementary Table S1). In this case, the biofilm is homogenized, after which the biofilm suspension is serially diluted and plated onto agar for subsequent colony counting after several days of incubation. CFU determination is used to assess absolute and relative changes in CFU values over time, and to assess the activity of mycobacterial drugs. Although CFU determination within biofilms is a relatively accessible method, since it does not require specialized equipment, it comes with challenges, as there is a high risk of bacterial clumping due to the presence of an ECM that facilitates bacterial aggregation (Hunt-Serracin et al., 2019). This can lead to an underestimation of the true viable population. Another challenge of CFU determination is that biofilms have different microenvironments, including regions with low nutrient and oxygen availability, in which bacteria may enter a viable but non-culturable state (Li et al., 2014). This can also lead to an underestimation of the viable population. Thus, although CFU determination is a valuable tool, it is essential to be mindful of these considerations influencing accuracy and reliability of the results obtained. As such, combining CFU results with other readouts should provide a more comprehensive understanding of the *M. abscessus* biofilm.

Crystal violet staining is a commonly used method to quantify biofilm biomass. Crystal violet is a cationic dye that penetrates the biofilm structure and binds to negatively charged components of the biofilm. Although it is debatable to what extent crystal violet stains the actual mycobacteria, crystal violet does stain crucial ECM components of the *M. abscessus* biofilm, including polysaccharides, extracellular DNA (eDNA), and proteins. The staining can be quantified by solubilizing the crystal violet with an extraction buffer and measuring the intensity of the absorbed light using a microplate reader. The intensity of the staining correlates with biofilm mass and can be expressed as absolute optical density values or relative biomass. Beyond its role in biofilm quantification, crystal violet staining can also facilitate the macroscopic visualization of the biofilm. Similar to crystal violet, *safranin staining* binds negatively charged molecules and is used for the same purpose as crystal violet, although it is less commonly used. A disadvantage of both staining techniques includes their non-specificity. For example, they do not distinguish between live and dead bacteria.

Another method described for biofilm quantification is the use of *resazurine* or *Tetrazolium chloride (XTT)* (Pettit et al., 2005; Marini et al., 2019). Resazurine is a blue-colored dye that is absorbed by living cells, where it is enzymatically reduced into the fluorescent pink-colored molecule resorufin. Since the fluorescence of resorufin is proportional to the metabolic activity and viability of cells, this stain evaluates the viability of cells within the biofilm. Fluorescence signals obtained by measuring biofilm samples in a microtiter plate reader can be used to estimate the inhibitory activity of compounds against *M. abscessus* residing in biofilms (Belardinelli et al., 2021; Lee et al., 2021, 2022; Feizi et al., 2023). In addition, macroscopic images of the biofilm wells can be obtained allowing rapid colorimetric assessment. Resazurine has the limitation that it specifically identifies metabolically active cells but may not detect non-metabolically active bacteria with intact membranes. Consequently, resazurin serves as a measure of the metabolic activity of the bacterial population rather than as a direct outcome measure for bacterial load. This is particularly important to consider when using resazurine staining in drug activity experiments, as drugs that target protein synthesis can reduce enzyme activity, resulting in less resazurine conversion, without necessarily killing bacteria. Morever, since bacteria in biofilms exhibit a heterogeneity of metabolic states, resazurine staining can result in mixed signals (Sandberg et al., 2009). Another pitfall of this allegedly quantification method is that low bacterial concentrations within the biofilm may results in signals below the lower limit of detection (Sandberg et al., 2009). XTT operates in a manner similar to resazurine, in which yellow salt is reduced by metabolically active bacteria into the orange formazan. Besides XTT, there are other tetrazolium salts available, although these have not yet been utilized for studying *M. abscessus* biofilms.

Finally, in some studies *M. abscessus* is transfected with a *fluorescent protein*, such as mCherry (Clary et al., 2018; Belardinelli et al., 2021, 2022b). This allows the measurement of the relative fluorescence intensity of mycobacteria within biofilms, not only providing insight into the density of bacterial populations, but also into the spatial distribution of the bacteria. Recently, mWasabi transfected *M. abscessus* in a colony-biofilm was photographed using a fluorescence microscope, and the intensity of fluorescence in different areas of the images was measured over time (Aguilera-Correa et al., 2023). Subsequently, the volume of each colony was calculated with a mathematical formula based on the signal intensity and colony size. This approach mirrored the CFU counts, and thus provided a rapid estimation of the number of bacteria in the biofilm (Aguilera-Correa et al., 2023).

4.2 Biofilm imaging

Mycobacterium abscessus biofilm imaging provides insight into biofilm structure, organization, and composition. First, simple bright-field light microscopy can be used in combination with Ziehl-Neelsen acid fast staining, which has been used to show the aggregative nature of *M. abscessus* and to differentiate *M. abscessus* from *P. aeruginosa* in a dual-species biofilm (Rodríguez-Sevilla et al., 2018a; Kolpen et al., 2020). Additional techniques are required for visualizing the ECM of the biofilm, such as *fluorescence microscopy* or *scanning electron microscopy*. Fluorescence microscopy is either performed with a wide field microscope, that yields two-dimensional images, or a confocal laser scanning microscope (CLSM), that yields three-dimensional images with a high resolution allowing the visualization of different layers and regions within the biofilm. This way, CLSM could also be used for biofilm quantification, enabling the assessment of biofilm thickness and biofilm biomass. Various stainings are used for visualizing the ECM, each targeting specific ECM components, including Nile Red (lipids), TOTO-1 iodide (nucleic acids), SYBR Green 1 (nucleic acids), FilmTracer SYPRO (proteins), SYPRO Ruby (proteins), Texas Red Hydrazide (polysaccharides), and Concanavalin A (polysaccharides) (Belardinelli et al., 2021; Chakraborty et al., 2021; Dokic et al., 2021). Furthermore, Syto-9 and propidium iodide are commonly used to stain live and dead bacteria, respectively. Since Syto-9 and propidium iodide stain nucleic acids, not only the DNA of bacteria within the biofilm will be stained, but also eDNA. Propidium iodide has also been used to study the effect of genetic alternations or compounds on the amount of eDNA by adding propidium iodide directly to a biofilm culture followed by quantification of the fluorescence signal using a microplate reader (Rose and Bermudez, 2016). Since the current staining techniques allow for the detection of specific targeted ECM components only, capturing a complete image of the entire ECM might not yet be achievable. Electron microscopy is used to analyse the structure of the biofilm, the abundance of outer matrix, bacterial organization, mycobacterial density and the activity of various mycobacterial drugs or conditions with a higher spatial resolution than CLSM. In this manner, the microstructure of biofilms can be identified (Dokic et al., 2021; Li et al., 2022; Saptawati et al., 2022; Yue et al., 2022; He et al., 2023). Finally, *micro–CT X-ray* has been used to visualize the three-dimensional structures of *M. abscessus* biofilms (Cohen-Cymberknoh et al., 2022).

4.3 Other biofilm profiling techniques

Several metabolic, spectroscopic and chromatographic techniques have been reported for studying *M. abscessus* biofilm characteristics. First, *M. abscessus* gene expression has been evaluated by *RNA sequencing*, which gives a genome-wide overview of gene expression. Alternatively, *qRT-PCR* has been used as a more targeted approach to study the expression of specific transcripts, which can also be applied to validate results found with RNA sequencing. RNA sequencing has

been used to study differentially expressed genes in young and mature *M. abscessus* biofilms compared to a planktonic population (as described in section 3.3) (Belardinelli et al., 2021; Dokic et al., 2021). Moreover, RNA sequencing has been used to study the effect of an antimicrobial peptide on transcripts to obtain a more comprehensive understanding on the peptide's mechanism of action (Li et al., 2022). Additionally, qPCR has been used to specifically study the expression of various transcriptional regions during different specific maturity stages (Veigyabati Devi and Singh, 2023). Second, *Fourier transform infrared spectroscopy* is a non-destructive analytical technique that allows for studying and identifying the chemical composition and structures of molecules. In this context, Fourier transform infrared spectroscopy demonstrated the presence of calcium carbonate minerals and cellulose in the ECM of *M. abscessus* biofilms (Chakraborty et al., 2021; Cohen-Cymberknoh et al., 2022). Third, *mass spectrometry* can be applied to identify and quantify proteins. This technique has been used to compare protein pathways between planktonic *M. abscessus* and *M. abscessus* residing in biofilms (Rojony et al., 2020). Furthermore, proteomics has been used to assess the effect of different media on protein abundance in biofilms (section 3.2) and to examine alterations in protein compositions when biofilms are exposed to antibiotics (Rojony et al., 2020; Keefe and Bermudez, 2022). Lastly, lipids within the ECM can be analysed via *thin-layer chromatography* (see section 5.2.1) (Hunt-Serracin et al., 2019; Belardinelli et al., 2021; Dokic et al., 2021).

5 Integrating biofilm techniques: dissecting the extracellular matrix' composition and mechanical properties

5.1 Composition of the extracellular matrix

Mycobacteria within the biofilm are embedded in an ECM, which consists of multiple components that have a structural as well as a functional role (Karygianni et al., 2020). Studying the ECM is important to gain insights into potential novel therapeutic targets and is usually performed using a combination of several of the techniques described above.

5.1.1 Nucleic acids

Nucleic acids have repeatedly been reported as a fundamental part of biofilms (Karygianni et al., 2020). Multiple functions have been attributed to eDNA in biofilms, including adhesion, structural integrity, aggregation, and nutrient provision (Ibáñez de Aldecoa et al., 2017; Karygianni et al., 2020). Indeed, eDNA is reported as an important constituent of *M. abscessus* biofilms across various culture media and subspecies (Rose et al., 2015; Belardinelli et al., 2021; Chakraborty et al., 2021; Dokic et al., 2021; Oschmann-Kadenbach et al., 2024). An increase in eDNA, likely actively released, has been linked to biofilm maturation (Belardinelli et al., 2021; Ilinov et al., 2021). The increase in eDNA during biofilm maturation was found to be more pronounced compared to other constituents of the ECM, such as sugars and proteins (Belardinelli et al., 2021). eDNA was reported to be dispersed throughout the *M. abscessus* biofilm, mainly in regions with a low bacterial density, suggesting a structural role for eDNA in the *M. abscessus* biofilm by facilitating cellular aggregation. In line, exposure of biofilms to DNase caused dispersion of SCFM-cultured biofilm, although this was not confirmed when biofilms induced by thiol reductive stress were exposed to DNase (Belardinelli et al., 2021; Chakraborty et al., 2021). These contrasting findings may be due to differences in culture medium, exposure duration and biofilm maturation, indicating the role of eDNA in biofilm structure might be context-dependent (Chakraborty et al., 2021). The origin and release process of the DNA in the ECM of *M. abscessus* biofilms is yet an unexplored topic. Understanding this process might provide insights into factors that trigger or control ECM formation. For example, in *M. avium* biofilms genomic DNA is thought to be exported via nonlytic mechanisms. Sodium carbonate has been identified as a trigger for this eDNA release, which is also observed for *M. abscessus* (Rose and Bermudez, 2016). Because of the notable role of eDNA in the *M. abscessus* biofilm, eDNA might be a potential novel drug target (Rose et al., 2015).

5.1.2 Lipids

Lipids in biofilm ECM are believed to contribute to adhesion, cohesion, protection and immune evasion (Karygianni et al., 2020). In *M. abscessus* biofilm, lipids are present on the surface of bacteria as well as in the inter-bacterial space (Belardinelli et al., 2021; Dokic et al., 2021). *M. abscessus* was found to be able to incorporate lipids from the environment into the ECM, in addition to actively producing and secreting endogenous lipids (Belardinelli et al., 2021; Dokic et al., 2021). For example, the phospholipid 1,2-Dioleoyl-sn-glycero-3-phosphocholine, a constituent of SCFM, was most abundantly present in the ECM of SCFM grown biofilms, next to endogenous lipids (e.g., cardiolipin) (Belardinelli et al., 2021). The majority of biofilm ECM lipids are comparable to the lipids found on the surface of planktonic cultures, although there are some lipids that are specific to the ECM of biofilms, including some types of glycerophospholipids, phosphatidylinositol dimannosides, and free mycolic acids (Belardinelli et al., 2021; Dokic et al., 2021). In fact, modifications in the chemical structure of mycolic acids during the transformation from planktonic cultures to *M. abscessus* biofilm structures have been observed in Sauton's medium (Dokic et al., 2021). In addition, more rapidly migrating and longer mycolic acid methyl esters were found to be present in biofilms compared to planktonic cultures, which was associated with upregulation of *M. abscessus* genes related to mycolic acid chain elongation and desaturation (Dokic et al., 2021). In contrast, another study showed that free mycolates were relatively scarce in the ECM of SCFM-grown biofilms and were similar to those found in planktonic cultures (Belardinelli et al., 2021). The amount of trehalose dimycolate was found to be increased in *M. abscessus* biofilms cultured in SCFM, but not in Middlebrook 7H9 or Hartmans-de Bont broth. In contrast, in another study, no increase in trehalose dimycolate levels in SCFM-grown biofilms was observed, indicating that experimental conditions beyond culture medium influence ECM lipid composition (Hunt-Serracin et al., 2019; Belardinelli et al., 2021). Interestingly, exposure of *M. abscessus* biofilms to *phospholipases* dispersed the SCFM-grown biofilm (Belardinelli et al., 2021), whereas *lipase* exposure did not lead to biofilm dispersal in both SCFM-grown and Sauton's medium-grown biofilms (Belardinelli et al., 2021; Chakraborty et al., 2021). Biofilms exposed to amikacin or linezolid were shown to contain higher levels of proteins involved in glycerophospholipid metabolism, possibly affecting the lipid composition of the ECM (Rojony et al., 2020).

5.1.3 Carbohydrates

Carbohydrates have been reported to play a role in biofilm adhesion, scaffolding, stability, and immune evasion (Karygianni et al., 2020). In *M. abscessus* biofilms, carbohydrates not only localize with *M. abscessus* itself, but are also present in the inter-bacterial space, where they may exhibit variations in their structure (Belardinelli et al., 2021; Chakraborty et al., 2021; Dokic et al., 2021). The main carbohydrate present in SCFM cultured biofilms was found to be glucose, which is in fact also a component of the SCFM (Belardinelli et al., 2021). Interestingly, arabinose and galactose were substantially more abundant in biofilm ECM compared to extracellular components of planktonic cultures, indicating an important role for these carbohydrates in biofilms, and suggesting an active release from the bacteria (Belardinelli et al., 2021). Supporting this idea, uniquely expressed proteins in *M. abscessus* biofilm included an enzyme involved in arabinan synthesis (Belardinelli et al., 2021). In *M. abscessus* biofilms cultured in Sauton's medium, cellulose was found to be present (Chakraborty et al., 2021). Exposure of biofilms to an α-mannosidase and cellulose led to a significant dispersal of the biofilm, indicating carbohydrates are indeed a crucial constituent of the *M. abscessus* biofilm (Belardinelli et al., 2021; Chakraborty et al., 2021). In contrast, α-amylase did not lead to biofilm dispersal (Chakraborty et al., 2021).

5.1.4 Proteins

Protein abundance has been reported in *M. abscessus* biofilms, when cultured both in SCFM and Sauton's medium (Belardinelli et al., 2021; Chakraborty et al., 2021; Dokic et al., 2021). These proteins were found to be localized in the deep layers of the biofilm, with limited bacterial co-localization (Belardinelli et al., 2021; Chakraborty et al., 2021; Dokic et al., 2021). Interestingly, the proteases proteinase K and trypsin did not disperse SCFM established *M. abscessus* biofilms, indicating a less prominent role for proteins in biofilm integrity (Belardinelli et al., 2021). Alternatively, proteins might be important during earlier phases of biofilm maturation, such as the initial attachment stage (Fong and Yildiz, 2015). In contrast, proteinase K exposure led to biofilm dispersal in reductive stress-induced Sauton's medium *M. abscessus* biofilm, which suggests a potential role in structure and integrity of biofilms in this particular environment (Chakraborty et al., 2021). This again highlights the variability in outcome when studying the ECM of *M. abscessus* biofilms under different environmental conditions. In SCFM cultured biofilms, proteins that are enriched in the ECM are thought to be mainly involved in central carbon metabolism, respiration, amino acid and lipid metabolism, heat shock responses and hypoxia (Belardinelli et al., 2021).

5.1.5 Mechanical properties

The ECM composition has been reported to affect the mechanical properties of the biofilm (Gloag et al., 2020). Studying the mechanical properties of biofilms is important to understand how biofilms respond to chemical and mechanical forces (Gloag et al., 2020). Roughly two different methods to study biofilm mechanics have been distinguished: indentation, which involves forces that are perpendicular to the surface, and shear stress, which involves forces that are parallel to the surface. In general, biofilms have been described as viscoelastic, probably due to adaptations to withstand mechanical stresses from the environment, in contrast to the stiffer nature of planktonic bacteria (Gloag et al., 2020). The viscoelasticity of biofilms is affected by the ratio of bacteria to ECM content and the relative abundance of specific ECM components.

Techniques to study the mechanical properties of biofilms include bulk rheology and microrheology. In bulk rheology, an entire sample is analysed with a rheometer to study the overall mechanical behavior of biofilm, while microrheology is used to study local mechanical responses and thus can investigate heterogeneities in viscoelastic properties within the biofilm matrix. An overview of all techniques to study biofilm rheology is provided by other reviews (Billings et al., 2015; Gordon et al., 2017).

To our knowledge, only one rheology study has been performed on *M. abscessus* biofilms (Gloag et al., 2021). In this study colony biofilms were exposed to uniaxial indentation and shear forces. In alignment with the general consensus of the mechanical properties of biofilms, *M. abscessus* had viscoelastic properties that were similar between smooth and rough morphotypes. In contrast, the force needed to break down the biofilm was greater for rough morphotype biofilms compared to smooth morphotypes and rough morphotypes could be compressed to a further extent under uniaxial indentation forces (Gloag et al., 2021). Studying the mechanical properties of *M. abscessus* biofilms is potentially relevant, as their stiffness is thought to contribute to its relative resistance to airway clearance (Gloag et al., 2021). Furthermore, biofilms might withstand the stress applied by immune cells, hampering phagocytosis (Gordon et al., 2017). The mechanical properties of a biofilm have been linked to its permeability, which is important in the context of drug susceptibility and to understand the accessibility of bacteria in the deeper layers of the biofilm (Gloag et al., 2020). Interestingly, microsensors have been developed to monitor and profile for example oxygen, pH, CO_2, sulphides, and nitrate throughout the biofilm, providing additional information on the heterogeneity of the biofilm microenvironment (Beyenal and Babauta, 2014).

6 Integrating biofilm techniques: targeting the *Mycobacterium abscessus* biofilm

Drug activity testing against *M. abscessus* biofilms can be approached by studying inhibition of biofilm formation or biofilm destruction. In biofilm inhibition studies, planktonic cultures or young biofilms are generally exposed to subinhibitory antibiotic concentrations. After a predefined time period, the impact on biofilm formation is assessed. In the context of biofilm destruction, compounds are added to pre-established biofilms at higher antibiotic concentrations, allowing the study of physical disruption of established structures as well as the killing of bacteria residing within the biofilm. A summary of studies on drug activity against *M. abscessus* biofilms, along with details on the experimental design of the models used is presented in Supplementary Table S1.

6.1 Common *Mycobacterium abscessus* drugs

6.1.1 Macrolides: clarithromycin and azithromycin

Although one study showed biofilm inhibition in terms of biofilm biomass upon clarithromycin exposure compared to a no drug control, another study found that clarithromycin did not reduce CFU

values in a developing biofilm, indicating that clarithromycin was unable to completely prevent biofilm formation (Flores et al., 2016; Rodríguez-Sevilla et al., 2018b). Clarithromycin, when added to young biofilms cultured for 24 h, arrested mycobacterial growth but was not able to kill *M. abscessus* in these biofilms (Yam et al., 2020; Ganapathy et al., 2021; Negatu et al., 2021; Ganapathy et al., 2023). Studies using 4–5-day old biofilms reported either no or only limited reductions in viable bacteria after clarithromycin exposure, whereas in fully mature biofilms, clarithromycin showed (limited) killing activity, which was suggested to be medium dependent (Greendyke and Byrd, 2008; Ortíz-Pérez et al., 2011; Hunt-Serracin et al., 2019; Lee et al., 2021, 2022; Li et al., 2022; Fan et al., 2024). In addition, a reduction in biofilm biomass was reported, suggesting clarithromycin was also able to disrupt the biofilm structure (Hunt-Serracin et al., 2019). Although less studies were performed with azithromycin, the results are in line with those observed for clarithromycin, indicating the prevention of CFU increase in young biofilms without exhibiting bactericidal activity (Clary et al., 2018; Yam et al., 2020). In addition, azithromycin was not able to prevent an increase in viable bacteria within more mature biofilms, and showed minimal killing activity in fully mature biofilms (Belardinelli et al., 2021; Kaur et al., 2024).

6.1.2 Amikacin

In line with the results for the macrolides, amikacin could not fully prevent biofilm development when amikacin was added at the onset of biofilm formation, although it was able to reduce biofilm biomass (Flores et al., 2016; Rodríguez-Sevilla et al., 2018b). In addition, amikacin did not reduce CFU values in single- and dual species biofilm models during biofilm development (Rodríguez-Sevilla et al., 2018b). Importantly, the latter inhibition assay lasted only 6 h, which could have been too short for this purpose. When added to young biofilms (i.e., 24 h) amikacin has been reported to have both inhibitory as well as killing activity (Clary et al., 2018; Rodríguez-Sevilla et al., 2019; Yam et al., 2020). Multiple studies have assessed amikacin's activity on more mature biofilms, in which different experimental variables were used. In most, but not all, studies, amikacin's activity was reported to (slightly) reduce the mycobacterial load in biofilms compared to no drug controls (Greendyke and Byrd, 2008; Ortíz-Pérez et al., 2011; Marini et al., 2018; Rodríguez-Sevilla et al., 2019; Paulowski et al., 2022). In fully established biofilms amikacin showed no or limited killing activity and did not reduce biofilm biomass (Flores et al., 2016; Hunt-Serracin et al., 2019; Rojony et al., 2020; Li et al., 2022; Fan et al., 2024; Kaur et al., 2024; Oschmann-Kadenbach et al., 2024).

Interestingly, medium dependent differences in amikacin's activity against *M. abscessus* biofilms have been observed, with more pronounced killing activity in 7H9 Middlebrook cultured biofilms compared to biofilms cultured in SCFM (Hunt-Serracin et al., 2019). Moreover, biofilm maturity has been observed to affect amikacin's activity with indications that more mature biofilms have increased resistance to amikacin (Marini et al., 2018; Rodríguez-Sevilla et al., 2019). Another variable reported to affect amikacin's killing capacity is experimental duration, with longer antibiotic exposure linked to increased activity of amikacin (Paulowski et al., 2022). This is interesting, since the majority of studies expose biofilms for 24 or 48 h to amikacin, and thus potentially do not reach a reliable efficacy assessment. Of note, it remains unclear whether there is a difference in amikacins activity against smooth or rough morphotype biofilms. Only one study addressed this issue but found no difference in amikacin susceptibility between the smooth and rough morphotype in young biofilms (Clary et al., 2018).

6.1.3 Imipenem

Imipenem was reported to inhibit biofilm mass accumulation in developing biofilms (Flores et al., 2016). In addition, imipenem showed inhibitory as well as killing activity in young biofilms (Yam et al., 2020), although these effects were not observed in more mature biofilms (Belardinelli et al., 2021). In fully mature biofilms, imipenem had slight bactericidal activity, but did not reduce biofilm biomass (Flores et al., 2016; Li et al., 2022; Fan et al., 2024).

6.1.4 Cefoxitin

Cefoxitin was demonstrated to have inhibitory as well as killing activity against *M. abscessus* in young biofilms (i.e., 24 h) at concentrations 3 to 4 times higher than the minimal inhibitory concentration in planktonic populations (Yam et al., 2020). While exhibiting bacteriostatic activities against *M. abscessus* within 4-day-old biofilms, this effect was observed only at exceptionally high concentrations (Greendyke and Byrd, 2008). In fully mature biofilms, cefoxitin slightly reduced the mycobacterial load after 48 h of exposure (Hunt-Serracin et al., 2019; Li et al., 2022; Fan et al., 2024).

6.1.5 Tigecycline

Tigecycline showed both inhibitory as well as killing activity against *M. abscessus* in young biofilms (i.e., 24 h) Of note, the killing activity was observed at lower concentrations compared to what was needed for the killing of planktonic *M. abscessus* (Yam et al., 2020). In contrast, only minimal killing activity was observed against *M. abscessus* in fully mature biofilms (Oschmann-Kadenbach et al., 2024).

6.1.6 Linezolid

Linezolid was shown to have inhibitory but not bactericidal activity in young *M. abscessus* biofilms (i.e., 24 h), although requiring a concentration three times higher than needed for the growth inhibition of planktonic *M. abscessus* (Yam et al., 2020). Linezolid did not reduce the number of viable bacteria in fully mature biofilms (Rojony et al., 2020; Yam et al., 2020). Despite this, changes in metabolism were reported, indicating linezolid might impact cellular processes (Rojony et al., 2020).

6.1.7 Clofazimine

Clofazimine showed inhibitory as well as killing activity against young biofilms (i.e., 24 h) (Yam et al., 2020). Interestingly, this killing activity was observed at lower concentrations compared to what was needed for the killing of planktonic *M. abscessus* (Yam et al., 2020). In contrast, clofazimine was not able to prevent growth of *M. abscessus* in 4-day old biofilms, suggesting clofazimine predominantly affects early stage biofilms (Belardinelli et al., 2021).

6.1.8 Others

Doxycyline demonstrated inhibitory activity on biofilm formation in terms of biofilm biomass at concentrations lower than the minimal inhibitory concentrations in planktonic bacteria (Flores et al., 2016). However, it only slightly reduced biomass of established biofilms at concentrations exceeding the minimal inhibitory concentration in

planktonic *M. abscessus* (Flores et al., 2016). *Minocycline* did neither inhibit biofilm formation, nor kill *M. abscessus* within young biofilms (Yam et al., 2020). Sub-inhibitory *ciprofloxacin* concentrations were able to inhibit biofilm formation in terms of biofilm biomass, but ciprofloxacin did not affect the biomass of pre-established biofilms (Flores et al., 2016; Belardinelli et al., 2021). Conflicting results have been reported on the effect of ciprofloxacin exposure on the mycobacterial load, ranging from total killing to no inhibitory or killing activity (Ortíz-Pérez et al., 2011; Muñoz-Egea et al., 2015; Blanchard et al., 2018; Belardinelli et al., 2021). *Moxifloxacin* was shown to have inhibitory and killing activity against *M. abscessus* within young biofilms (Yam et al., 2020; Ganapathy et al., 2021). One study showed killing activity of moxifloxacin against *M. abscessus* in fully mature biofilms (Kaur et al., 2024). *Rifamycins* have only sporadically been studied in the context of *M. abscessus* biofilm. *Rifampicin* did not affect *M. abscessus* in 3-day old biofilms, whereas *rifabutin* reduced CFU values in 3-day old biofilms in a time dependent manner, achieving a 3-$\log_{10}$ reduction in percentage of viable bacteria after 96 h of exposure (Paulowski et al., 2022). In line, rifabutin was able to reduce CFU values and colony volume in a colony biofilm (Aguilera-Correa et al., 2023). Notably, the reduction in CFU counts was greater in rough morphotype *M. abscessus* compared to the smooth mophotype (Aguilera-Correa et al., 2023). The sulfanomide *sulfamethoxazole* was able to inhibit biofilm formation at sub-inhibitory concentrations but was not able to destruct established biofilms (Flores et al., 2016). Only limited studies have been conducted on *bedaquiline's* activity against *M. abscessus* biofilm. Bedaquiline did not inhibit biofilm formation when administered at the onset of biofilm formation. Yet, it reduced CFU values in smooth—but not in rough—morphotypes in a 2-day old colony biofilm (Chakraborty et al., 2021; Aguilera-Correa et al., 2023). *Ceftazidime* and *colistin* are not commonly used for treatment of nontuberculous mycobacteria but are more common in the treatment of *P. aeruginosa* infections. Therefore, ceftazidime and colistin were tested in a dual-species biofilm with *P. aeruginosa*. Indeed, ceftazidime and colistin did not reduce CFU values of *M. abscessus* in single- and dual-biofilm (Rodríguez-Sevilla et al., 2018b, 2019). However, selectively targeting *P. aeruginosa* in a dual-species biofilm could lead to increased survival and thus a competitive advantage of *M. abscessus* (Rodríguez-Sevilla et al., 2019).

6.2 Novel compounds

Several novel compounds, with diverse modes of action, have been tested against *M. abscessus* biofilms under various experimental conditions (Supplementary Table S2). Notably, these compounds have only been studied once in this context, highlighting the need to further validate their therapeutic potential. EC/11770, EC/11716, IMA6 and SA23, targeting protein synthesis, DNA replication, mycolic acid transport and the electron transport chain, respectively, exhibited both inhibitory as well as killing activity against *M. abscessus* within young biofilms (i.e., 24 h) (Yam et al., 2020; Ganapathy et al., 2021, 2023). In addition, essential oils derived from *Cymbopogon Flexuos* species and the essential oil constituent carvacrol reduced biofilm biomass of developing as well as pre-established biofilms (Rossi et al., 2017; Marini et al., 2019). The aminoimidazole AB-2–29, several sulfonamides complexed with metals, and several inhibitors of the dormancy survival regulon DosRS (which is essential for *M. abscessus* to persist under hypoxic conditions) inhibited biofilm biomass during biofilm development, but did not reduce the biomass of pre-established biofilms (Bonez et al., 2021; Belardinelli et al., 2022a,b). Moreover, multiple 2-aminoimidazoles, the antibacterial protein RP557, *Panax quinquefolius*, *Coptic chinensis* and its main constituent berberine were able to inhibit biofilm development in terms of biomass, yet their activity on pre-established biofilms was not assessed (Tseng et al., 2020; Li et al., 2022; Belardinelli et al., 2022a; He et al., 2023). For RP557 and *Panax quinquefolius* bacterial inhibition in terms of mycobacterial load and metabolic activity was observed as well. Moreover, RP557 enhanced the killing activity of clarithromycin, amikacin, imipenem and cefoxitin in fully mature biofilms (Li et al., 2022). Clomiphene citrate, which is hypothesized to disrupt the mycobacterial membrane, and 10-DEBC, an inhibitor of the Akt pathway, inhibited the growth of 5-days old biofilms during a 4-day exposure (total assay duration of 9 days), but their killing activity was not assessed (Lee et al., 2021, 2022). 5-aminovulinic acid—photodynamic therapy, HuTipMab (targeting DNA binding proteins) and curcumin reduced biomass in established biofilms (Marini et al., 2018; Yue et al., 2022; Kurbatfinski et al., 2023). In addition, curcumin enhanced the biofilm destructing capacity of amikacin in 4- and 8-day old biofilms (Marini et al., 2018). Colloidal silver, the dendritic amphiphile 3Cam19, the thiopeptide antibiotic NF1001 and the rifamycin derivate 5j reduced mycobacterial viability in established biofilms (Falkinham et al., 2012; Paulowski et al., 2022; Feizi et al., 2023; Kaur et al., 2024). Finally, the antimicrobial peptide D-hLF-1–11, a derivate of lactoferrin, seemed to not affect *M. abscessus* biofilm biomass (Intorasoot et al., 2022).

7 Concluding remarks

M. abscessus biofilm formation is a complex process, which might contribute to the high treatment failure rates observed in clinical settings. Standard preclinical drug activity assays focus on planktonic bacteria, leaving the response of *M. abscessus* within biofilms relatively unexplored. This might contribute to the lack of correlation between *in vitro* susceptibility and clinical performance of the drug. Setting up biofilm experiments can be challenging given the number of models and variables that might affect biofilm characteristics and its susceptibility to antibiotics. The choice of *M. abscessus* strain, culture medium, and biofilm age affect important biofilm characteristics such as its macroscopic structure, ECM composition, and/or physiology. However, in most cases the exact influence of different experimental variables remains unclear, adding complexity to the experimental set-up and interpretation of results. As such, absence of experimental details in published studies can hinder the reproducibility and interpretability of studies. Despite the challenges associated with technical variations, *M. abscessus* consistently forms biofilm under these various conditions, highlighting the significance of this trait. Beyond selecting appropriate laboratory models for biofilm culture (i.e., models with translational value), adopting a multi-technique approach to study biofilms is crucial for thorough and accurate analysis, as each individual technique has its own analytical perspectives and limitations.

As to drug activity assessment, there is only limited data available on the activity of traditional antibiotics against *M. abscessus* biofilms,

with indications that traditional drugs are often not as active against *M. abscessus* residing in biofilm compared to planktonic *M. abscessus*. Thus, including *M. abscessus* biofilm models for comprehensive preclinical drug activity testing could be important to improve the translational value of *in vitro* drug development as well as in order to select the optimal combination of drugs to target both planktonic mycobacteria and those residing in biofilms. However, for proper assessment of the data gained from these biofilm models, certain experimental aspects should be considered. Careful consideration of adequate readouts is important in interpreting data on drug activity. For example, CFU determination and crystal violet staining are the most commonly used methods for biofilm quantification, each providing information on other parameters of the biofilm: viability and biomass, respectively. Using both techniques simultaneously contribute to the understanding whether a compound affects the biofilm structure or the bacteria itself, which is important to try and select the optimal combination of antibiotics against infections with this difficult-to-treat and biofilm forming *M. abscessus*. In addition to using different read-outs, careful consideration of culture medium, exposure time, and biofilm age is needed. Early-stage biofilms are often more susceptible to antibiotics, and longer drug exposure times might lead to more drug activity in biofilms. In most studies, the exposure time was 24 to 48 h only, while prolonged exposure times might have led to more pronounced biofilm destruction (Paulowski et al., 2022). Moreover, differences in biofilm characteristics between the smooth and rough colony morphotype in *M. abscessus* is an underexplored topic which could be an important variable to take into account, especially since differences in morphotype have been linked to clinical outcome (Sanguinetti et al., 2001; Catherinot et al., 2009).

The lack of standardized experimental protocols complicates comparisons between studies. However, selecting the one ideal model for *M. abscessus* biofilm research would be very challenging. In fact, the use of different models offers valuable insights into diverse environments, providing a comprehensive understanding of biofilm characterization and behavior as well as drug activity. It is important to recognize that *M. abscessus* encounters complex environments in patients. Various optimizations have therefore already been implemented into laboratory models, including the use of artificial sputum medium and the creation of dual-species biofilms. Careful consideration of the *M. abscessus* environment in patients and aligning this with a specific research question is crucial to select a model that balances complexity, reproducibility and pragmatism (Coenye et al., 2020).

In conclusion, selected technical tools and variables frame the way we interpret the *M. abscessus* biofilm. In this framing process, we struggle with the challenge of distinguishing between the inherent nature of the biofilm and the impact of our observational tools and selected environmental conditions. Understanding the frame that we use is important in understanding the complex nature of *M. abscessus* biofilm and its behavior upon antibiotic exposure. Moreover, it helps to bridge the gap between *in vitro* models and clinical outcome, thereby increasing the preclinical value of our research.

Author contributions

HM: Writing – original draft, Conceptualization, Writing – review & editing. SM: Conceptualization, Supervision, Writing – review & editing. NA: Writing – review & editing. JS: Writing – review & editing. HB: Conceptualization, Supervision, Writing – review & editing.

Funding

The author (s) declare that no financial support was received for the research, authorship, and/or publication of this article.

Acknowledgments

The authors wish to thank Dr. Maarten Engel from the Erasmus MC Medical Library for developing the search strategies.

Conflict of interest

The authors declare that the research was conducted in the absence of any commercial or financial relationships that could be construed as a potential conflict of interest.

Publisher's note

Supplementary material

The Supplementary material for this article can be found online at: https://www.frontiersin.org/articles/10.3389/fmicb.2024.1392606/full#supplementary-material

References

Adjemian, J., Olivier, K. N., and Prevots, D. R. (2018). Epidemiology of pulmonary Nontuberculous mycobacterial sputum positivity in patients with cystic fibrosis in the United States, 2010-2014. *Ann. Am. Thorac. Soc.* 15, 817–826. doi: 10.1513/AnnalsATS.201709-727OC

Aguilera-Correa, J. J., Boudehen, Y. M., and Kremer, L. (2023). Characterization of *Mycobacterium abscessus* colony-biofilms based on bi-dimensional images. *Antimicrob. Agents Chemother.* 67:e0040223. doi: 10.1128/aac.00402-23

Belardinelli, J. M., Li, W., Avanzi, C., Angala, S. K., Lian, E., Wiersma, C. J., et al. (2021). Unique features of *Mycobacterium abscessus* biofilms formed in synthetic cystic fibrosis medium. *Front. Microbiol.* 12:743126. doi: 10.3389/fmicb.2021.743126

Belardinelli, J. M., Li, W., Martin, K. H., Zeiler, M. J., Lian, E., Avanzi, C., et al. (2022a). 2-Aminoimidazoles inhibit *Mycobacterium abscessus* biofilms in a zinc-dependent manner. *Int. J. Mol. Sci.* 23:2950. doi: 10.3390/ijms23062950

Belardinelli, J. M., Verma, D., Li, W., Avanzi, C., Wiersma, C. J., Williams, J. T., et al. (2022b). Therapeutic efficacy of antimalarial drugs targeting Dos RS signaling in *Mycobacterium abscessus*. *Sci. Transl. Med.* 14:eabj3860. doi: 10.1126/scitranslmed.abj3860

Bernut, A., Viljoen, A., Dupont, C., Sapriel, G., Blaise, M., Bouchier, C., et al. (2016). Insights into the smooth-to-rough transitioning in *Mycobacterium bolletii* unravels a functional Tyr residue conserved in all mycobacterial Mmp L family members. *Mol. Microbiol.* 99, 866–883. doi: 10.1111/mmi.13283

Beyenal, H., and Babauta, J. (2014). Microsensors and microscale gradients in biofilms. *Adv. Biochem. Eng. Biotechnol.* 146, 235–256. doi: 10.1007/10_2013_247

Billings, N., Birjiniuk, A., Samad, T. S., Doyle, P. S., and Ribbeck, K. (2015). Material properties of biofilms-a review of methods for understanding permeability and mechanics. *Rep. Prog. Phys.* 78:036601. doi: 10.1088/0034-4885/78/3/036601

Blanchard, J. D., Elias, V., Cipolla, D., Gonda, I., and Bermudez, L. E. (2018). Effective treatment of *Mycobacterium avium* subsp. hominissuis and *Mycobacterium abscessus* species infections in macrophages, Biofilm, and mice by using liposomal ciprofloxacin. *Antimicrob. Agents Chemother.* 62:e00440-18. doi: 10.1128/AAC.00440-18

Bonez, P. C., Agertt, V. A., Rossi, G. G., Dos Santos Siqueira, F., Siqueira, J. D., Marques, L. L., et al. (2021). Sulfonamides complexed with metals as mycobacterial biofilms inhibitors. *J. Clin. Tuberc. Other Mycobact. Dis.* 23:100217. doi: 10.1016/j.jctube.2021.100217

Born, S. E. M., Reichlen, M. J., Bartek, I. L., Benoit, J. B., Frank, D. N., and Voskuil, M. I. (2023). Population heterogeneity in mycobacterium smegmatis and *Mycobacterium abscessus*. *Microbiology (Reading)* 169:001402. doi: 10.1099/mic.0.001402

Burmølle, M., Ren, D., Bjarnsholt, T., and Sørensen, S. J. (2014). Interactions in multispecies biofilms: do they actually matter? *Trends Microbiol.* 22, 84–91. doi: 10.1016/j.tim.2013.12.004

Catherinot, E., Roux, A. L., Macheras, E., Hubert, D., Matmar, M., Dannhoffer, L., et al. (2009). Acute respiratory failure involving an R variant of *Mycobacterium abscessus*. *J. Clin. Microbiol.* 47, 271–274. doi: 10.1128/JCM.01478-08

Ceri, H., Olson, M. E., Stremick, C., Read, R. R., Morck, D., and Buret, A. (1999). The Calgary Biofilm device: new technology for rapid determination of antibiotic susceptibilities of bacterial biofilms. *J. Clin. Microbiol.* 37, 1771–1776. doi: 10.1128/JCM.37.6.1771-1776.1999

Chakraborty, P., Bajeli, S., Kaushal, D., Radotra, B. D., and Kumar, A. (2021). Biofilm formation in the lung contributes to virulence and drug tolerance of *Mycobacterium tuberculosis*. *Nat. Commun.* 12:1606. doi: 10.1038/s41467-021-21748-6

Chen, J., Zhao, L., Mao, Y., Ye, M., Guo, Q., Zhang, Y., et al. (2019). Clinical efficacy and adverse effects of antibiotics used to treat *Mycobacterium abscessus* pulmonary disease. *Front. Microbiol.* 10:1977. doi: 10.3389/fmicb.2019.01977

Clary, G., Sasindran, S. J., Nesbitt, N., Mason, L., Cole, S., Azad, A., et al. (2018). *Mycobacterium abscessus* smooth and rough Morphotypes form antimicrobial-tolerant Biofilm phenotypes but are killed by acetic acid. *Antimicrob. Agents Chemother.* 62:e01782-17. doi: 10.1128/AAC.01782-17

Coenye, T., Kjellerup, B., Stoodley, P., Bjarnsholt, T., and Biofilm Bash, P. (2020). The future of biofilm research—report on the '2019 Biofilm Bash'. *Biofilms* 2:100012. doi: 10.1016/j.bioflm.2019.100012

Cohen-Cymberknoh, M., Kolodkin-Gal, D., Keren-Paz, A., Peretz, S., Brumfeld, V., Kapishnikov, S., et al. (2022). Calcium carbonate mineralization is essential for biofilm formation and lung colonization. *iScience* 25:104234. doi: 10.1016/j.isci.2022.104234

Cristancho-Rojas, C., Varley, C. D., Lara, S. C., Kherabi, Y., Henkle, E., and Winthrop, K. L. (2023). Epidemiology of *Mycobacterium abscessus*. *Clin. Microbiol. Infect.* doi: 10.1016/j.cmi.2023.08.035

Davidson, R. M. (2018). A closer look at the genomic variation of geographically diverse *Mycobacterium abscessus* clones that cause human infection and disease. *Front. Microbiol.* 9:2988. doi: 10.3389/fmicb.2018.02988

Davidson, R. M., Hasan, N. A., Reynolds, P. R., Totten, S., Garcia, B., Levin, A., et al. (2014). Genome sequencing of *Mycobacterium abscessus* isolates from patients in the United States and comparisons to globally diverse clinical strains. *J. Clin. Microbiol.* 52, 3573–3582. doi: 10.1128/JCM.01144-14

Dokic, A., Peterson, E., Arrieta-Ortiz, M. L., Pan, M., Di Maio, A., Baliga, N., et al. (2021). *Mycobacterium abscessus* biofilms produce an extracellular matrix and have a distinct mycolic acid profile. *Cell Surf.* 7:100051. doi: 10.1016/j.tcsw.2021.100051

El Helou, G., Viola, G. M., Hachem, R., Han, X. Y., and Raad, I. I. (2013). Rapidly growing mycobacterial bloodstream infections. *Lancet Infect. Dis.* 13, 166–174. doi: 10.1016/S1473-3099(12)70316-X

Falkinham, J. O., Macri, R. V., Maisuria, B. B., Actis, M. L., Sugandhi, E. W., Williams, A. A., et al. (2012). Antibacterial activities of dendritic amphiphiles against nontuberculous mycobacteria. *Tuberculosis (Edinb.)* 92, 173–181. doi: 10.1016/j.tube.2011.12.002

Fan, J., Jia, Y., He, S., Tan, Z., Li, A., Li, J., et al. (2024). Gln R activated transcription of nitrogen metabolic pathway genes facilitates biofilm formation by *mycobacterium abscessus*. *Int. J. Antimicrob. Agents* 63:107025. doi: 10.1016/j.ijantimicag.2023.107025

Feizi, S., Cooksley, C. M., Ramezanpour, M., Nepal, R., Psaltis, A. J., Wormald, P. J., et al. (2023). Colloidal silver against macrophage infections and biofilms of atypical mycobacteria. *Biometals* 36, 913–925. doi: 10.1007/s10534-023-00494-w

Fennelly, K. P., Ojano-Dirain, C., Yang, Q., Liu, L., Lu, L., Progulske-Fox, A., et al. (2016). Biofilm formation by *Mycobacterium abscessus* in a lung cavity. *Am. J. Respir. Crit. Care Med.* 193, 692–693. doi: 10.1164/rccm.201508-1586IM

Flores, V. D., Siqueira, F. D., Mizdal, C. R., Bonez, P. C., Agertt, V. A., Stefanello, S. T., et al. (2016). Antibiofilm effect of antimicrobials used in the therapy of mycobacteriosis. *Microb. Pathog.* 99, 229–235. doi: 10.1016/j.micpath.2016.08.017

Fong, J. N. C., and Yildiz, F. H. (2015). Biofilm matrix proteins. *Microbiol. Spectr.* 3, 201–222. doi: 10.1128/microbiolspec.MB-0004-2014

Ganapathy, U. S., Del Río, R. G., Cacho-Izquierdo, M., Ortega, F., Lelièvre, J., Barros-Aguirre, D., et al. (2021). A *Mycobacterium tuberculosis* NBTI DNA Gyrase inhibitor is active against *Mycobacterium abscessus*. *Antimicrob. Agents Chemother.* 65:e0151421. doi: 10.1128/AAC.01514-21

Ganapathy, U. S., Del Rio, R. G., Cacho-Izquierdo, M., Ortega, F., Lelièvre, J., Barros-Aguirre, D., et al. (2023). A Leucyl-tRNA Synthetase inhibitor with broad-Spectrum anti-mycobacterial activity. *Antimicrob. Agents Chemother.* 95:e02420-20. doi: 10.1128/AAC.02420-20

Gloag, E. S., Fabbri, S., Wozniak, D. J., and Stoodley, P. (2020). Biofilm mechanics: implications in infection and survival. *Biofilms* 2:100017. doi: 10.1016/j.bioflm.2019.100017

Gloag, E. S., Wozniak, D. J., Stoodley, P., and Hall-Stoodley, L. (2021). *Mycobacterium abscessus* biofilms have viscoelastic properties which may contribute to their recalcitrance in chronic pulmonary infections. *Sci. Rep.* 11:5020. doi: 10.1038/s41598-021-84525-x

Goeres, D. M., Loetterle, L. R., Hamilton, M. A., Murga, R., Kirby, D. W., and Donlan, R. M. (2005). Statistical assessment of a laboratory method for growing biofilms. *Microbiology (Reading)* 151, 757–762. doi: 10.1099/mic.0.27709-0

Gordon, V. D., Davis-Fields, M., Kovach, K., and Rodesney, C. A. (2017). Biofilms and mechanics: a review of experimental techniques and findings. *J. Phys. D Appl. Phys.* 50:223002. doi: 10.1088/1361-6463/aa6b83

Greendyke, R., and Byrd, T. F. (2008). Differential antibiotic susceptibility of *Mycobacterium abscessus* variants in biofilms and macrophages compared to that of planktonic bacteria. *Antimicrob. Agents Chemother.* 52, 2019–2026. doi: 10.1128/AAC.00986-07

He, Z., Xu, X., Wang, C., Li, Y., Dong, B., Li, S., et al. (2023). Effect of *Panax quinquefolius* extract on *Mycobacterium abscessus* biofilm formation. *Biofouling* 39, 24–35. doi: 10.1080/08927014.2023.2166405

Howard, S. T., Rhoades, E., Recht, J., Pang, X., Alsup, A., Kolter, R., et al. (2006). Spontaneous reversion of *Mycobacterium abscessus* from a smooth to a rough morphotype is associated with reduced expression of glycopeptidolipid and reacquisition of an invasive phenotype. *Microbiology (Reading)* 152, 1581–1590. doi: 10.1099/mic.0.28625-0

Hunt-Serracin, A. C., Parks, B. J., Boll, J., and Boutte, C. C. (2019). *Mycobacterium abscessus* cells have altered antibiotic tolerance and surface glycolipids in artificial cystic fibrosis sputum medium. *Antimicrob. Agents Chemother.* 63:e02488-18. doi: 10.1128/AAC.02488-18

Ibáñez de Aldecoa, A. L., Zafra, O., and González-Pastor, J. E. (2017). Mechanisms and regulation of extracellular DNA release and its biological roles in microbial communities. *Front. Microbiol.* 8:1390. doi: 10.3389/fmicb.2017.01390

Idosa, A. W., Wozniak, D. J., and Hall-Stoodley, L. (2022). Surface dependent inhibition of *Mycobacterium abscessus* by diverse *Pseudomonas aeruginosa* strains. *Microbiol. Spectr.* 10:e0247122. doi: 10.1128/spectrum.02471-22

Ilinov, A., Nishiyama, A., Namba, H., Fukushima, Y., Takihara, H., Nakajima, C., et al. (2021). Extracellular DNA of slow growers of mycobacteria and its contribution to biofilm formation and drug tolerance. *Sci. Rep.* 11:10953. doi: 10.1038/s41598-021-90156-z

Intorasoot, S., Intorasoot, A., Tawteamwong, A., Butr-Indr, B., Phunpae, P., Tharinjaroen, C. S., et al. (2022). In vitro Antimycobacterial activity of human Lactoferrin-derived peptide, D-hLF 1-11, against susceptible and drug-resistant mycobacterium tuberculosis and its synergistic effect with rifampicin. *Antibiotics (Basel)* 11:1785. doi: 10.3390/antibiotics11121785

Karygianni, L., Ren, Z., Koo, H., and Thurnheer, T. (2020). Biofilm Matrixome: extracellular components in structured microbial communities. *Trends Microbiol.* 28, 668–681. doi: 10.1016/j.tim.2020.03.016

Kaur, P., Krishnamurthy, R. V., Shandil, R. K., Mohan, R., and Narayanan, S. (2024). A novel inhibitor against the biofilms of non-Tuberculous mycobacteria. *Pathogens* 13:40. doi: 10.3390/pathogens13010040

Keefe, B. F., and Bermudez, L. E. (2022). Environment in the lung of cystic fibrosis patients stimulates the expression of biofilm phenotype in *Mycobacterium abscessus*. *J. Med. Microbiol.* 71. doi: 10.1099/jmm.0.001467

Kiers, P. J. M., Bos, R., van der Mei, H. C., and Busscher, H. J. (2001). The electrophoretic softness of the surface of *Staphylococcus epidermidis* cells grown in a liquid medium and on a solid agar. *Microbiology (Reading)* 147, 757–762. doi: 10.1099/00221287-147-3-757

King, R. J. (1982). Pulmonary surfactant. *J. Appl. Physiol. Respir. Environ. Exerc. Physiol.* 53, 1–8. doi: 10.1152/jappl.1982.53.1.1

Kolpen, M., Jensen, P., Qvist, T., Kragh, K. N., Ravnholt, C., Fritz, B. G., et al. (2020). Biofilms of *Mycobacterium abscessus* complex can be sensitized to antibiotics by

disaggregation and oxygenation. *Antimicrob. Agents Chemother.* 64:e01212-19. doi: 10.1128/AAC.01212-19

Kurbatfinski, N., Hill, P. J., Tobin, N., Kramer, C. N., Wickham, J., Goodman, S. D., et al. (2023). Disruption of nontuberculous mycobacteria biofilms induces a highly vulnerable to antibiotic killing phenotype. *Biofilms* 6:100166. doi: 10.1016/j.bioflm.2023.100166

Lee, D. G., Hwang, Y. H., Park, E. J., Kim, J. H., and Ryoo, S. W. (2021). Clomiphene citrate shows effective and sustained antimicrobial activity against *Mycobacterium abscessus*. *Int. J. Mol. Sci.* 22:11029. doi: 10.3390/ijms222011029

Lee, D. G., Kim, H. J., Lee, Y., Kim, J. H., Hwang, Y., Ha, J., et al. (2022). 10-DEBC hydrochloride as a promising new agent against infection of *Mycobacterium abscessus*. *Int. J. Mol. Sci.* 23:591. doi: 10.3390/ijms23020591

Leon-Icaza, S. A., Bagayoko, S., Verge, R., Iakobachvili, N., Ferrand, C., Aydogan, T., et al. (2023). Druggable redox pathways against *Mycobacterium abscessus* in cystic fibrosis patient-derived airway organoids. *PLoS Pathog.* 19:e1011559. doi: 10.1371/journal.ppat.1011559

Li, L., Mendis, N., Trigui, H., Oliver, J. D., and Faucher, S. P. (2014). The importance of the viable but non-culturable state in human bacterial pathogens. *Front. Microbiol.* 5:258. doi: 10.3389/fmicb.2014.00258

Li, B., Zhang, Y., Guo, Q., He, S., Fan, J., Xu, L., et al. (2022). Antibacterial peptide RP557 increases the antibiotic sensitivity of *Mycobacterium abscessus* by inhibiting biofilm formation. *Sci. Total Environ.* 807:151855. doi: 10.1016/j.scitotenv.2021.151855

Lichtenberg, M., Kvich, L., Larsen, S. L. B., Jakobsen, T. H., and Bjarnsholt, T. (2022). Inoculum concentration influences *Pseudomonas aeruginosa* phenotype and Biofilm architecture. *Microbiol. Spectr.* 10:e0313122. doi: 10.1128/spectrum.03131-22

Malcolm, K. C., Nichols, E. M., Caceres, S. M., Kret, J. E., Martiniano, S. L., Sagel, S. D., et al. (2013). *Mycobacterium abscessus* induces a limited pattern of neutrophil activation that promotes pathogen survival. *PLoS One* 8:e57402. doi: 10.1371/journal.pone.0057402

Marini, E., Di Giulio, M., Ginestra, G., Magi, G., Di Lodovico, S., Marino, A., et al. (2019). Efficacy of carvacrol against resistant rapidly growing mycobacteria in the planktonic and biofilm growth mode. *PLoS One* 14:e0219038. doi: 10.1371/journal.pone.0219038

Marini, E., Di Giulio, M., Magi, G., Di Lodovico, S., Cimarelli, M. E., Brenciani, A., et al. (2018). Curcumin, an antibiotic resistance breaker against a multiresistant clinical isolate of *Mycobacterium abscessus*. *Phytother. Res.* 32, 488–495. doi: 10.1002/ptr.5994

Martín-de-Hijas, N. Z., García-Almeida, D., Ayala, G., Fernández-Roblas, R., Gadea, I., Celdrán, A., et al. (2009). Biofilm development by clinical strains of non-pigmented rapidly growing mycobacteria. *Clin. Microbiol. Infect.* 15, 931–936. doi: 10.1111/j.1469-0691.2009.02882.x

Mullis, S. N., and Falkinham, J. O. (2013). Adherence and biofilm formation of *Mycobacterium avium*, Mycobacterium intracellulare and *Mycobacterium abscessus* to household plumbing materials. *J. Appl. Microbiol.* 115, 908–914. doi: 10.1111/jam.12272

Muñoz-Egea, M. C., García-Pedrazuela, M., Mahillo, I., and Esteban, J. (2015). Effect of ciprofloxacin in the ultrastructure and development of biofilms formed by rapidly growing mycobacteria. *BMC Microbiol.* 15:18. doi: 10.1186/s12866-015-0359-y

Muñoz-Egea, M. C., García-Pedrazuela, M., Mahillo-Fernandez, I., and Esteban, J. (2016). Effect of antibiotics and Antibiofilm agents in the ultrastructure and development of biofilms developed by nonpigmented rapidly growing mycobacteria. *Microb. Drug Resist.* 22, 1–6. doi: 10.1089/mdr.2015.0124

Negatu, D. A., Beuchel, A., Madani, A., Alvarez, N., Chen, C., Aragaw, W. W., et al. (2021). Piperidine-4-Carboxamides target DNA Gyrase in *Mycobacterium abscessus*. *Antimicrob. Agents Chemother.* 65:e0067621. doi: 10.1128/aac.00676-21

Ortíz-Pérez, A., Martín-de-Hijas, N., Alonso-Rodríguez, N., Molina-Manso, D., Fernández-Roblas, R., and Esteban, J. (2011). Importance of antibiotic penetration in the antimicrobial resistance of biofilm formed by non-pigmented rapidly growing mycobacteria against amikacin, ciprofloxacin and clarithromycin. *Enferm. Infecc. Microbiol. Clin.* 29, 79–84. doi: 10.1016/j.eimc.2010.08.016

Oschmann-Kadenbach, A. M., Schaudinn, C., Borst, L., Schwarz, C., Konrat, K., Arvand, M., et al. (2024). Impact of Mycobacteroides abscessus colony morphology on biofilm formation and antimicrobial resistance. *Int. J. Med. Microbiol.* 314:151603. doi: 10.1016/j.ijmm.2024.151603

Park, E. J., Silwal, P., and Jo, E. K. (2021). Host-pathogen interactions operative during Mycobacteroides abscessus infection. *Immune Netw.* 21:e40. doi: 10.4110/in.2021.21.e40

Paulowski, L., Beckham, K. S. H., Johansen, M. D., Berneking, L., Van, N., Degefu, Y., et al. (2022). C25-modified rifamycin derivatives with improved activity against *Mycobacterium abscessus*. *PNAS Nexus* 1:pgac 130. doi: 10.1093/pnasnexus/pgac130

Pereira, M. M. R., de Oliveira, F. M., da Costa, A. C., Junqueira-Kipnis, A. P., and Kipnis, A. (2023). Ferritin from *Mycobacterium abscessus* is involved in resistance to antibiotics and oxidative stress. *Appl. Microbiol. Biotechnol.* 107, 2577–2595. doi: 10.1007/s00253-023-12420-8

Pettit, R. K., Weber, C. A., Kean, M. J., Hoffmann, H., Pettit, G. R., Tan, R., et al. (2005). Microplate Alamar blue assay for *Staphylococcus epidermidis* biofilm susceptibility testing. *Antimicrob. Agents Chemother.* 49, 2612–2617. doi: 10.1128/AAC.49.7.2612-2617.2005

Qvist, T., Eickhardt, S., Kragh, K. N., Andersen, C. B., Iversen, M., Høiby, N., et al. (2015). Chronic pulmonary disease with *Mycobacterium abscessus* complex is a biofilm infection. *Eur. Respir. J.* 46, 1823–1826. doi: 10.1183/13993003.01102-2015

Rodríguez-Sevilla, G., Crabbé, A., García-Coca, M., Aguilera-Correa, J. J., Esteban, J., and Pérez-Jorge, C. (2019). Antimicrobial treatment provides a competitive advantage to *Mycobacterium abscessus* in a dual-species Biofilm with *Pseudomonas aeruginosa*. *Antimicrob. Agents Chemother.* 63:e01547-19. doi: 10.1128/AAC.01547-19

Rodríguez-Sevilla, G., García-Coca, M., Romera-García, D., Aguilera-Correa, J. J., Mahíllo-Fernández, I., Esteban, J., et al. (2018a). Non-Tuberculous mycobacteria multispecies biofilms in cystic fibrosis: development of an in vitro mycobacterium abscessus and *Pseudomonas aeruginosa* dual species biofilm model. *Int. J. Med. Microbiol.* 308, 413–423. doi: 10.1016/j.ijmm.2018.03.003

Rodríguez-Sevilla, G., Rigauts, C., Vandeplassche, E., Ostyn, L., Mahíllo-Fernández, I., Esteban, J., et al. (2018b). Influence of three-dimensional lung epithelial cells and interspecies interactions on antibiotic efficacy against mycobacterium abscessus and *Pseudomonas aeruginosa*. *Pathog. Dis.* 76:fty034. doi: 10.1093/femspd/fty034

Rojony, R., Danelishvili, L., Campeau, A., Wozniak, J. M., Gonzalez, D. J., and Bermudez, L. E. (2020). Exposure of *Mycobacterium abscessus* to environmental stress and clinically used antibiotics reveals common proteome response among pathogenic mycobacteria. *Microorganisms* 8:698. doi: 10.3390/microorganisms8050698

Rose, S. J., Babrak, L. M., and Bermudez, L. E. (2015). *Mycobacterium avium* possesses extracellular DNA that contributes to Biofilm formation, structural integrity, and tolerance to antibiotics. *PLoS One* 10:e0128772. doi: 10.1371/journal.pone.0128772

Rose, S. J., and Bermudez, L. E. (2016). Identification of bicarbonate as a trigger and genes involved with extracellular DNA export in mycobacterial biofilms. *MBio* 7:e01597-16. doi: 10.1128/mBio.01597-16

Rossi, G. G., Guterres, K. B., Bonez, P. C., da Silva Gundel, S., Aggertt, V. A., Siqueira, F. S., et al. (2017). Antibiofilm activity of nanoemulsions of *Cymbopogon flexuosus* against rapidly growing mycobacteria. *Microb. Pathog.* 113, 335–341. doi: 10.1016/j.micpath.2017.11.002

Sandberg, M. E., Schellmann, D., Brunhofer, G., Erker, T., Busygin, I., Leino, R., et al. (2009). Pros and cons of using resazurin staining for quantification of viable *Staphylococcus aureus* biofilms in a screening assay. *J. Microbiol. Methods* 78, 104–106. doi: 10.1016/j.mimet.2009.04.014

Sanguinetti, M., Ardito, F., Fiscarelli, E., La Sorda, M., D'Argenio, P., Ricciotti, G., et al. (2001). Fatal pulmonary infection due to multidrug-resistant *Mycobacterium abscessus* in a patient with cystic fibrosis. *J. Clin. Microbiol.* 39, 816–819. doi: 10.1128/JCM.39.2.816-819.2001

Saptawati, L., Primaningtyas, W., Dirgahayu, P., Sutanto, Y. S., Wasita, B., Suryawati, B., et al. (2022). Characteristics of clinical isolates of nontuberculous mycobacteria in Java-Indonesia: a multicenter study. *PLoS Negl. Trop. Dis.* 16:e0011007. doi: 10.1371/journal.pntd.0011007

Singh, S., Singh, S. K., Chowdhury, I., and Singh, R. (2017). Understanding the mechanism of bacterial biofilms resistance to antimicrobial agents. *Open Microbiol. J.* 11, 53–62. doi: 10.2174/1874285801711010053

Stepanović, S., Djukić, N., Opavski, N., and Djukić, S. (2003). Significance of inoculum size in biofilm formation by staphylococci. *New Microbiol.* 26, 129–132.

Stepanović, S., Vuković, D., Hola, V., Di Bonaventura, G., Djukić, S., Cirković, I., et al. (2007). Quantification of biofilm in microtiter plates: overview of testing conditions and practical recommendations for assessment of biofilm production by staphylococci. *APMIS* 115, 891–899. doi: 10.1111/j.1600-0463.2007.apm_630.x

Tseng, C. Y., Sun, M. F., Li, T. C., and Lin, C. T. (2020). Effect of Coptis chinensis on Biofilm formation and antibiotic susceptibility in *Mycobacterium abscessus*. *Evid. Based Complement. Alternat. Med.* 2020, 1–9. doi: 10.1155/2020/9754357

Veigyabati Devi, M., and Singh, A. K. (2023). Delineation of transcriptional regulators involve in biofilm formation cycle of *Mycobacterium abscessus*. *Gene* 882:147644. doi: 10.1016/j.gene.2023.147644

Williams, M. M., Yakrus, M. A., Arduino, M. J., Cooksey, R. C., Crane, C. B., Banerjee, S. N., et al. (2009). Structural analysis of biofilm formation by rapidly and slowly growing nontuberculous mycobacteria. *Appl. Environ. Microbiol.* 75, 2091–2098. doi: 10.1128/AEM.00166-09

Willsey, G. G., Ventrone, S., Schutz, K. C., Wallace, A. M., Ribis, J. W., Suratt, B. T., et al. (2018). Pulmonary surfactant promotes virulence gene expression and Biofilm formation in *Klebsiella pneumoniae*. *Infect. Immun.* 86:e00135-18. doi: 10.1128/IAI.00135-18

Yam, Y. K., Alvarez, N., Go, M. L., and Dick, T. (2020). Extreme drug tolerance of *Mycobacterium abscessus* "Persisters". *Front. Microbiol.* 11:359. doi: 10.3389/fmicb.2020.00359

Yue, C., Wang, L., Wang, X., Cen, R., Chen, J., Li, L., et al. (2022). In vitro study of the effect of ALA-PDT on mycobacterium abscessus and its antibiotic susceptibility. *Photodiagn. Photodyn. Ther.* 38:102802. doi: 10.1016/j.pdpdt.2022.102802

frontiers | Frontiers in Microbiology

TYPE Original Research
PUBLISHED 25 April 2024
DOI 10.3389/fmicb.2024.1382665

OPEN ACCESS

EDITED BY
Vishwanath Venketaraman,
Western University of Health Sciences,
United States

REVIEWED BY
Hongyan Jia,
Capital Medical University, China
Ying Luo,
UT Southwestern Medical Center,
United States

*CORRESPONDENCE
Sandip Patil
✉ sandippatil1309@yahoo.com

RECEIVED 06 February 2024
ACCEPTED 15 April 2024
PUBLISHED 25 April 2024

CITATION
Yu Z, Shang Z, Huang Q, Wen F and Patil S (2024) Integrating systemic immune-inflammation index, fibrinogen, and T-SPOT.TB for precision distinction of active pulmonary tuberculosis in the era of mycobacterial disease research. *Front. Microbiol.* 15:1382665. doi: 10.3389/fmicb.2024.1382665

Integrating systemic immune-inflammation index, fibrinogen, and T-SPOT.TB for precision distinction of active pulmonary tuberculosis in the era of mycobacterial disease research

Zhikang Yu[1,2], Zifang Shang[1,2], Qingyan Huang[1,2], Feiqiu Wen[3] and Sandip Patil[3,4]*

[1]Research Experiment Center, Meizhou People's Hospital, Meizhou Academy of Medical Sciences, Meizhou, China, [2]Guangdong Engineering Technological Research Center of Clinical Molecular Diagnosis and Antibody Drugs, Meizhou, China, [3]Department of Haematology and Oncology, Shenzhen Children's Hospital, Shenzhen, China, [4]Paediatric Research Institute, Shenzhen Children's Hospital, Shenzhen, China

Background: The clinical challenge of differentiating suspected tuberculosis with positive T-SPOT.TB results persist. This study aims to investigate the utility of the Systemic Immune-Inflammation Index (SII), Fibrinogen, and T-SPOT.TB in distinguishing between active pulmonary tuberculosis (PTB) and non-tuberculous lung diseases.

Methods: A retrospective analysis included 1,327 cases of active PTB with positive T-SPOT.TB results and 703 cases of non-tuberculous lung diseases from May 2016 to December 2020 at Meizhou People's Hospital. These were designated as the case group and the control group, respectively. The detection indicators of T-SPOT.TB: Early Secreted Antigenic Target 6 (ESAT-6), Culture Filtrate Protein 10 (CFP-10), as well as SII and Fibrinogen levels—were compared and analyzed for association and joint diagnostic value between the two groups.

Results: The case group showed higher values of ESAT-6, CFP-10, SII, and Fibrinogen compared to the control group (all $p < 0.001$). In the case group, SII and Fibrinogen did not correlate with ESAT-6 and CFP-10 (|rs| all < 0.3) but were positively correlated with C-reactive protein (CRP; rs all > 0.3). SII and Fibrinogen values in smear-positive pulmonary tuberculosis were higher than in smear-negative cases (all $p < 0.05$). The optimal diagnostic thresholds for ESAT-6, CFP-10, SII, and Fibrinogen in differentiating between active PTB and non-tuberculous lung diseases were 21.50 SFCs/10^6 PBMC, 22.50 SFCs/10^6 PBMC, 2128.32, and 5.02 g/L, respectively. Regression logistic analysis showed that ESAT-6<21.5 (OR: 1.637, 95% CI: 1.311–2.043, $p < 0.001$), CFP-10<22.5 (OR: 3.918, 95% CI: 3.138–4.892, $p = 0.025$), SII < 2128.32 (OR: 0.763, 95% CI: 0.603–0.967, $p < 0.001$), and FIB < 5.02 (OR: 2.287, 95% CI: 1.865–2.806, $p < 0.001$) were independent risk factors for active PTB. The specificity for ESAT-6+CFP-10, ESAT-6+CFP-10+SII, ESAT-6+CFP-10+FIB, and ESAT-6+CFP-10+SII+FIB was 82.5%, 83.2%, 95.8%, and 80.1%, respectively, while sensitivity was 52.6%, 53.0%, 55.8%, and 44.7%, and positive predictive values were 85.0%, 85.6%, 84.1%, and 89.6%, respectively.

Conclusion: SII and Fibrinogen are positively correlated with the degree of tuberculosis inflammation and the bacterial load of *Mycobacterium tuberculosis*.

The combined detection of SII, Fibrinogen, and T-SPOT.TB is significant in distinguishing between active PTB with positive T-SPOT.TB results and non-tuberculous lung diseases.

KEYWORDS

tuberculosis diagnosis, systemic immune-inflammation index (SII), fibrinogen, T-SPOT.TB, pulmonary disease differentiation

1 Introduction

Tuberculosis, caused by *Mycobacterium tuberculosis* (Mtb) remains globally prevalent and high mortality rate, ranking second only to COVID-19 (Kaufmann, 2023). Prompt diagnosis and treatment, especially for pulmonary tuberculosis, are critical for patient care and curbing transmission (Pang et al., 2019). In China, only approximately 30% of pulmonary tuberculosis cases undergo confirmation through pathogen testing, posing challenges in differentiating active pulmonary tuberculosis (ATB) from non-tuberculous pulmonary diseases with similar radiographic features (Yang and Gao, 2018). Traditional diagnostic methods, relying on smear microscopy and culture, suffer from prolonged duration and low detection rates for negative cases. Nucleic acid detection techniques, while sensitive and rapid, present challenges such as high cost and complex operation, leading to prolonged evaluation times and increased financial burdens (Sun et al., 2022). The World Health Organization (WHO) encourages the development of non-sputum specimen diagnostic techniques, with a growing trend toward combining multiple markers (Verma et al., 2024). Early secreted antigen target 6 (ESAT-6), a protein specific to *Mycobacterium tuberculosis*, and the culture filtrate protein 10 (CFP-10) are indicative of tuberculosis infection, detectable through the tuberculosis infection T-cell spot test (T-SPOT.TB; Hamada et al., 2021; Ortiz-Brizuela et al., 2023). The WHO recommends T-SPOT.TB is primarily for the diagnosis of latent tuberculosis infection (LTBI). In immunocompetent individuals, T-SPOT.TB can differentiate between active and non-active tuberculosis, but a higher detection threshold is often required to identify active pulmonary tuberculosis (APTB; Yang et al., 2020). Hence, there remains a necessity for refined protocols in the utilization of T-SPOT.TB for the differential diagnosis of active tuberculosis. The Systemic Immune-Inflammation Index (SII), gauging immunity and inflammation based on platelet, neutrophil, and lymphocyte counts, serves as a comprehensive biomarker widely used in predicting cancer incidence and assessing inflammatory states (Nøst et al., 2021; Hamad et al., 2022). It reflects the individual's immune status against pathogen infections and the severity of the disease, with minimal influence from mixed conditions (Li et al., 2023), rendering it a novel immune-inflammatory marker that has garnered considerable attention. Previous studies have indicated an association between elevated SII and tuberculosis, with a correlation observed with anxiety (Liu et al., 2022). Fibrinogen, a coagulation system activator, shows heightened levels in tuberculosis infections (Kager et al., 2015; Pinelo et al., 2023). Their roles in the differential diagnosis of suspected tuberculosis remain underexplored. The relationship between SII and Fibrinogen with Mtb infection has been initially comprehended, yet their involvement in the differential diagnosis of suspected tuberculosis has been rarely reported. Hence, this study retrospectively analyzes the T-SPOT.TB, SII, and Fibrinogen test values in 1,327 patients with active pulmonary tuberculosis (APTB) presenting positive T-SPOT.TB results, along with 703 patients exhibiting common clinical non-tuberculosis pulmonary diseases (non-TB). The aim is to explore their collective diagnostic value in the diagnosis and treatment of pulmonary tuberculosis.

2 Materials and methods

This study was conducted in accordance with the guidelines of the Declaration of Helsinki and approved by the Institutional Ethics Committee of our hospital, Meizhou People's Hospital reference number: (2021-C-120) which complies with international ethical standards. Written consent was waived as the research did not use personal information, including names, for research purposes, and data were treated confidentially in line with the principles of the Declaration of Helsinki.

2.1 Subjects

A total of 1,327 patients were diagnosed with active pulmonary tuberculosis (APTB) at Meizhou People's Hospital from May 2016 to December 2020. During the same period, 703 non-TB patients were selected as the control group. APTB patients were identified based on the criteria outlined in the "WS 288-2017 Diagnosis of Pulmonary Tuberculosis," According to this guideline, tuberculosis lesions occur in the lungs, trachea, bronchi, and pleura, these cases including 645 confirmed cases with positive sputum smears, cultures, or *Mycobacterium tuberculosis* nucleic acid tests, and 682 clinically diagnosed cases with evidence of clinical symptoms, signs, imaging findings, and effective tuberculosis treatment. Cases of extrapulmonary tuberculosis without pulmonary tuberculosis and old pulmonary tuberculosis were excluded. The definition of old tuberculosis is as follows: Firstly, patients with a history of tuberculosis must have recovered; secondly, despite the presence of pathological changes revealed by radiological diagnosis, no symptoms of tuberculous poisoning are observed; and thirdly, the results of etiology and pathology tests must be negative. Non-TB patients were those who were diagnosed with pulmonary diseases, excluding PTB, and had evidence such as pneumonia (Supplementary Figure S1). Both groups of patients were aged ≥ 16 years. After T-SPOT.TB testing and blood cell analysis, cases with negative or indeterminate T-SPOT.TB test results were excluded, as well as cases with obvious immune deficiency diseases such as acquired immune deficiency syndrome (HIV) etc. (Figure 1).

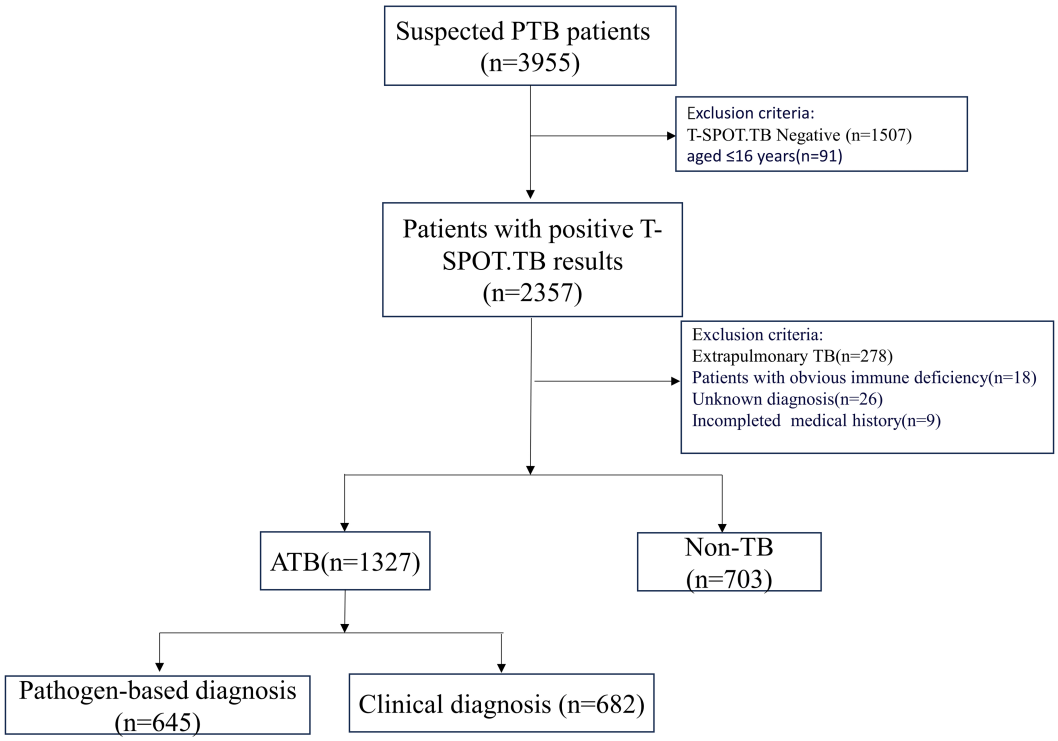

FIGURE 1
Flowchart of study data.

2.2 T-SPOT.TB detection

The T-SPOT.TB test kit (Oxford Immunotech, United Kingdom) was utilized according to the following steps: (1) Peripheral venous blood collection; (2) Isolation, collection, and counting of peripheral blood mononuclear cells (PBMCs); (3) Incubation of PBMCs with antigens (ESAT-6 as antigen A and CFP-10 as antigen B) for 16–20 h; (4) Spot counting; and (5) Result interpretation (Meier et al., 2005). The results are analyzed according to the following criteria: The detection result was positive when the number of spots in the blank control hole was 0 to 5 and (the number of spots in antigen A or antigen B hole—the number of blank control hole) ≥6, or the number of spots in blank control hole was 6 to 10 and (the number of spots in antigen A or antigen B hole) ≥2 × (the number of spots in blank control hole); If the above criteria are not met and the positive control hole is normal, the test result is negative.

2.3 Collection and examination of blood samples

After an overnight fast of 8–12 h, blood samples were collected from the anterior cubital vein using venipuncture. The collection tubes contained EDTA-K2 anticoagulant (2 mL), sodium citrate anticoagulant (2 mL), and gel progel (5 mL). Standard operating procedures on LBY-XC40B, AU5400, ACLTOP700, and SYSMEX XE-2100 blood analyzers were employed to examine erythrocyte sedimentation rate (ESR), C-reactive protein (CRP), four blood coagulation indexes, and blood cell composition, respectively. These included white blood cell count (WBC), neutrophils, lymphocytes, monocytes, platelets, red blood cell count (RBC), lymphocyte hemoglobin (HGB), prothrombin time (PT), activated partial thromboplastin time (APTT), thrombin time (TT), and fibrinogen (FIB).

2.4 Data processing and statistical analysis

With APTB as the target disease and non-tuberculous pulmonary disease as the control, the following indicators were used to evaluate its clinical diagnostic efficacy: sensitivity = True positive cases/(true positive cases + false negative cases), specificity = true negative cases/(true negative cases + false positive cases), positive predictive value = True positive cases/(true positive cases + false positive cases), negative predictive value = true negative cases/(true negative cases + false negative). SPSS 21.0 and GraphPad Prism 8.0 were used for data analysis and mapping, and continuous data were compared using the T-test or Mann–Whitney *U*-test. The categorical variables were expressed numerically (%) and compared using the Chi-square test or Fisher exact test. Pearson and Spearman correlation analysis analyzed the relationship between the correlation test indicators, with the correlation coefficient being denoted by rs. Binary Logistic regression analysis was employed to assess the clinical indicators that influence the occurrence of active pulmonary tuberculosis. The relative risk was quantified using the Odds Ratio (OR) along with its corresponding 95% Confidence Interval (CI). Furthermore, the new value for each combination was derived from the pertinent binary logistic regression analysis equation. A Delong test was employed to assess the statistical significance among the AUCs. ROC curve analysis was conducted to determine the optimal cutoff values of ESAT-6, CFP-10, SII, FIB,

ESAT-6 + CFP-10, ESAT-6 + CFP-10 + SII, ESAT-6 + CFP-10 + FIB, and ESAT-6 + CFP-10 + MLR + PLR for distinguishing APTB from non-TB. The area under the curve (AUC) and cutoff values were determined with the highest sum of sensitivity and specificity. The sensitivities, specificities, and positive and negative predictive values of each threshold were calculated. The 95% confidence intervals (95%CI) were calculated using the Wilson score method. $p < 0.05$ indicated a statistically significant difference.

3 Results

3.1 General information and laboratory parameters

A total of 2,030 cases were enrolled in the Hakka area of South China, including 1,327 cases (1,081 males and 246 females) in the case group, with an average age of (60.48 ± 15.83) years. There were 703 cases (548 males and 155 females) in the control group, with an average age of (61.52 ± 13.23) years, and the age of the case group was lower than that of the control group. The levels of PT, TT, leukocytes, neutrophils, and lymphocytes in the case group were lower than those in the control group ($p < 0.05$). The levels of PLT, FIB, SII, CRP, ESR, ESAT-6, and CFP-10 in the case group were higher than those in the control group ($p < 0.05$). The levels of SIRI, HB, and APPT in the case group were lower than those in the control group, and the monocyte counts and RBC in the case group were higher than those in the control group, but the differences were not statistically significant (Table 1).

3.2 Receiver operating characteristic curve analysis results of each test index used in the differential diagnosis of suspected TB

The optimal critical values of ESAT-6, CFP-10, SII, FIB, ESAT-6 + CFP-10, ESAT-6 + CFP-10 + SII, ESAT-6 + CFP-10 + FIB, and ESAT-6 + CFP-10 + SII + FIB is 21.5 SFCs/10^6 PBMC (spot-forming cells, SFCs; Peripheral Blood Mononuclear Cell, PBMC), 22.5 SFCs/10^6 PBMC, 2128.32, 5.02 g/L, 0.65, 0.68, 0.66, and 0.75, respectively, by receiver operating characteristic (ROC) curve analysis. Furthermore, the calculation of the new values for these combinations was based on the following formulae: $y_{[ESAT\text{-}6+\ CFP\text{-}10]} = 0.217 + 0.007*ESAT\text{-}6 + 0.023*CFP\text{-}10$, $y_{[ESAT\text{-}6+\ CFP\text{-}10+SII]} = -0.661 + 0.008*ESAT\text{-}6 + 0.024*CFP\text{-}10 + 0.001*SII$, $y_{[ESAT\text{-}6+\ CFP\text{-}10+FIB]} = -1.339 + 0.006*ESAT\text{-}6 + 0.023*CFP\text{-}10 + 0.211*FIB$, and $y_{[ESAT\text{-}6+\ CFP\text{-}10+\ SII+FIB]} = -1.521 + 0.008*ESAT\text{-}6 + 0.024*CFP\text{-}10 + 0.001*SII + 0.175*FIB$. When the optimal thresholds are set, the ROC analysis shows ESAT-6, CFP-10, SII, FIB, ESAT-6 + CFP-10, ESAT-6 + CFP-10 + SII, ESAT-6 + CFP-10 + FIB, ESAT-6 + CFP-10 + SII + FIB (area under curve, AUC) were 0.61, 0.71, 0.62, 0.61, 0.72, 0.74, 0.74, 0.76, respectively. Taking the AUC of T-SPOT.TB detection [ESAT-6+ CFP-10] as a reference,

TABLE 1 Characteristics and laboratory parameters of patients with pulmonary tuberculosis and non-tuberculous pulmonary disease.

Parameter	Non-tuberculosis (n = 703)	Pulmonary tuberculosis (n = 1,327)	t/U	p-values
Sex				
Male	548(78.0%)	1,081 (81.5%)		
Female	155(22.0%)	246 (18.5%)		
Age(year)	61.52 ± 13.23	60.48 ± 15.83	$t = -1.489$	0.137
WBC($\times10^{12}$/L)	11.97(7.20,14.10)	9.70(6.60,11.60)	U = −6.95	<0.001
Neutrophil ($\times10^9$/L)	8.85(4.90,11.20)	7.54(4.60,9.00)	$U = -5.478$	<0.001
Lymphocyte($\times10^9$/L)	2.00(0.90,2.00)	1.28(0.80,1.60)	$U = -7.018$	<0.001
Monocytes ($\times10^9$/L)	0.97(0.40,1.00)	0.74(0.50,0.90)	U = −0.196	0.845
RBC($\times10^{12}$/L)	4.25 ± 1.07	4.31 ± 0.79	$t = -1.316$	0.188
HB(g/L)	121.92 ± 29.46	121.46 ± 22.55	$t = 1.237$	0.216
PLT($\times10^9$/L)	223.33(148.00,274.00)	298.83(210.00,367.00)	U = −13.848	<0.001
SII	1697.2(559.09,2185.84)	2440.11(935.72,2789.44)	U = −8.571	<0.001
SIRI	6.44(1.62,7.50)	6.35(1.98,6.90)	U = −1.308	0.191
PT(S)	13.44 ± 4.36	12.96 ± 2.76	$t = 2.699$	0.008
TT(S)	15.04 ± 4.37	14.66 ± 2.59	$t = 2.122$	0.034
APTT(S)	34.04 ± 8.47	33.95 ± 5.78	$t = 0.225$	0.822
FIB(g/L)	5.01 ± 1.89	5.66 ± 1.75	$t = -7.583$	<0.001
ESR(mm/h)	40.26(11.0,60.0)	48.48(19.0,75.0)	$U = -6.938$	<0.001
CRP(mg/L)	51.62(8.76,84.29)	54.20(11.55,84.37)	U = −1.977	0.048
ESAT-6	18.64(7.0,22.0)	38.06(7.0,46.0)	U = −8.727	<0.001
CFP-10	17.70(5.0,21.0)	60.04(10.0,73.0)	$U = -16.120$	<0.001

SII = neutrophil*platelet to lymphocyte ratio, SIRI = neutrophil*monocyte to lymphocyte ratio.

the comparisons of the AUCs of diverse combinations against this reference revealed significant differences, with P_a equaling 0.001, P_b equaling 0.001, and *Pc* being less than 0.0001 (Figure 2).

3.3 Correlation between SII, FIB, and other detection indexes and relationship with tuberculosis disease degree

Based on Figure 3, it can be observed that the Systemic Inflammation Index (SII, SII = neutrophil*platelet to lymphocyte ratio) and Fibrinogen (FIB) values of active pulmonary tuberculosis (APTB) patients are not correlated with ESAT-6 (rs = −0.102, −0.075) and CFP-10 (rs = −0.014, −0.065), with all |rs| values being <0.3. However, there is a positive correlation with C-reactive protein (CRP; rs = 0.390, 0.465), where all rs values are >0.3. As depicted in Figure 4, the levels of SII, FIB, ESAT-6, and CFP-10 in smear-positive pulmonary tuberculosis are significantly higher than those in smear-negative pulmonary tuberculosis ($p < 0.0001$, $p < 0.05$, $p < 0.05$, $p < 0.001$, respectively). Additionally, the SII, FIB, ESAT-6, and CFP-10 levels in the APTB group are significantly higher than those in the non-TB group.

3.4 Logistic regression analysis of risk factors of active pulmonary tuberculosis

Univariate analysis and multivariate logistic regression analysis were performed to measure the relationship between detection indicators and active pulmonary tuberculosis. The results of univariate analysis showed that ESAT-6 < 21.5 (OR: 2.500, 95% CI: 2.048–3.052, $p < 0.001$), CFP-10 < 22.5 (OR: 4.443, 95% CI: 3.609–5.468, $p < 0.001$), SII < 2128.32 (OR: 0.834, 95% CI: 0.674–1.032, $p = 0.095$), and FIB<5.02 (OR: 2.243, 95% CI: 1.861–2.703, $p < 0.001$) were significantly associated with active pulmonary tuberculosis. Multivariate regression logistic analysis showed that ESAT-6 < 21.5 (OR: 1.637, 95% CI: 1.311–2.043, $p < 0.001$), CFP-10 < 22.5 (OR: 3.918, 95% CI: 3.138–4.892, $p = 0.025$), SII < 2128.32 (OR: 0.763, 95% CI: 0.603–0.967, $p < 0.001$), and FIB<5.02 (OR: 2.287, 95% CI: 1.865–2.806, $p < 0.001$) were independent risk factors for active pulmonary tuberculosis (Table 2). ESAT-6 < 21.5, CFP-10 < 22.5, SII < 2128.32, and FIB < 5.02 can be used to diagnosis of active pulmonary tuberculosis.

3.5 The value of different indexes and their combined detection in the differential diagnosis of suspected TB

As shown in Table 3, When the optimal thresholds are set, the specificity of ESAT-6, CFP-10, SII, FIB, ESAT-6 + CFP-10 + SII, ESAT-6 + CFP-10 + FIB, ESAT-6 + CFP-10 + SII + FIB in the differential diagnosis of APTB and non-tuberculosis pulmonary disease was 73.7%(95%CI 70.4–76.9), 77.5%(95%CI 74.4–80.6), 54.3%(95%CI 51.4–58.8), 82.5%(95%CI 79.7–85.3), 83.2%(95%CI 80.4–85.9), 80.1%(95%CI 77.1–83.0), 90.2%(95%CI 87.9–92.4), respectively. The positive predictive values was77.2% (95%CI 74.3–80.1), 82.5% (95%CI 80.0–85.0), 72.4% (95%CI 68.8–75.7), 72.9% (95%CI 71.1–76.1), 85.0% (95%CI 82.5–87.5), 85.6% (95%CI 83.2–88.0), 84.1% (95%CI 81.7–86.5), 89.6% (95%CI 87.2–91.9), respectively.

4 Discussion

The clinical characteristics and imaging results of active pulmonary tuberculosis (APTB) and non-tuberculous lung diseases are similar, making it challenging to distinguish between the two. Early diagnosis of tuberculosis is difficult, leading to many undiagnosed cases, contributing to the sustained transmission of tuberculosis and an increased disease burden (Calderwood et al., 2023; Verma et al., 2024). With the widespread application of T-SPOT.TB testing, various approaches have been provided for its auxiliary diagnosis of active tuberculosis. Studies indicate that raising the T-SPOT.TB detection threshold has diagnostic value for active tuberculosis (Calderwood et al., 2023; Verma et al., 2024). Combining T-SPOT.TB with other meaningful indicators can differentiate suspected pulmonary tuberculosis patients (Liu et al., 2021). *Mycobacterium tuberculosis* infection can induce changes in hematopoietic stem cell proliferation and immune responses, leading to alterations in lymphocyte, platelet, and other cell proportions (Kirwan et al., 2021; Chen et al., 2022). SII is a comprehensive new immunoinflammatory biomarker based on platelet, neutrophil, and lymphocyte counts. Changes in the proportions of peripheral blood cells it represents can accurately reflect local immune responses and systemic inflammatory status (Zhao et al., 2023). Elevated fibrinogen levels may be associated with lung damage caused by tuberculosis infection (Dong et al., 2018). Known immune and coagulation-related indicators SII and FIB are associated with tuberculosis, but their role in distinguishing between APTB and non-TB diagnoses is unclear. This study explores their role in the differential diagnosis between the two and finds that the SII and FIB levels in the APTB group are significantly higher than those in the non-TB group. Moreover, they are positively correlated with the degree of tuberculosis inflammation and related to the tuberculosis bacterial load. Through both univariate and multifactor regression analyses, they, having exceeded the cut-off level, have been identified as risk factors for active pulmonary tuberculosis. Simultaneously, the combination of SII and FIB with T-SPOT.TB testing demonstrates good diagnostic efficacy in differentiating between pulmonary tuberculosis and non-tuberculous lung diseases. T-SPOT.TB testing has diagnostic value for distinguishing between active pulmonary tuberculosis (APTB) and non-tuberculous lung diseases (non-TB; Zhang et al., 2017; Luo et al., 2020; Sun et al., 2022). Our research results indicate that the levels of ESAT-6, CFP-10, Systemic Immune-Inflammation Index (SII), and Fibrinogen (FIB) in the APTB group are significantly higher than those in the non-TB group. This suggests that after tuberculosis infection, SII and FIB may experience varying degrees of elevation, consistent with some previous research findings (Kager et al., 2015; Liu et al., 2022). Inflammatory and coagulation indices tend to increase to different extents after tuberculosis infection (Ştefanescu et al., 2021; Mustafa et al., 2022). However, in our statistical data, the Systemic Inflammation Response Index (SIRI) and Activated Partial Thromboplastin Time (APTT) did not show significant differences between the two groups, possibly due to our control group being related to other pulmonary diseases. When optimal cutoff values were

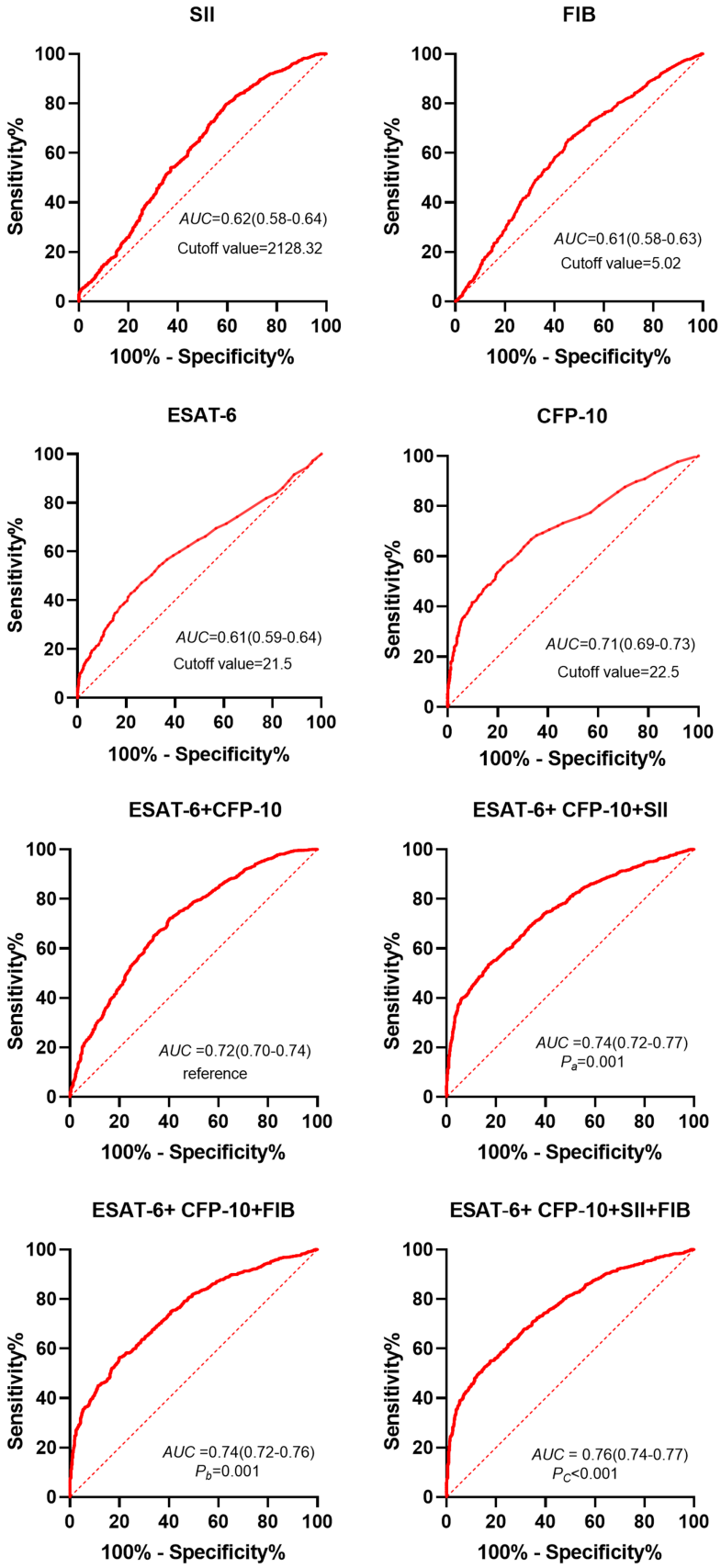

FIGURE 2
ROC analysis results of different indexes in patients with pulmonary tuberculosis and non-tuberculous lung disease with positive T-SPOT results. Dotted line, curvature response sensitivity index of ROC curve; Red line, receiver Operating Characteristic Curve; AUC, Area under ROC Curve; ESAT-6, early secretory antigen target 6; CFP-10, culture filtrate protein 10; SII, systemic immune-inflammation index. P_a: [ESAT-6 + CFP-10 + SII] vs. [ESAT-6 + CFP-10]; P_b: [ESAT-6 + CFP-10 + FIB] vs. [ESAT-6 + CFP-10]; P_c:[ESAT-6 + CFP-10 + FIB+SII] vs. [ESAT-6 + CFP-10].

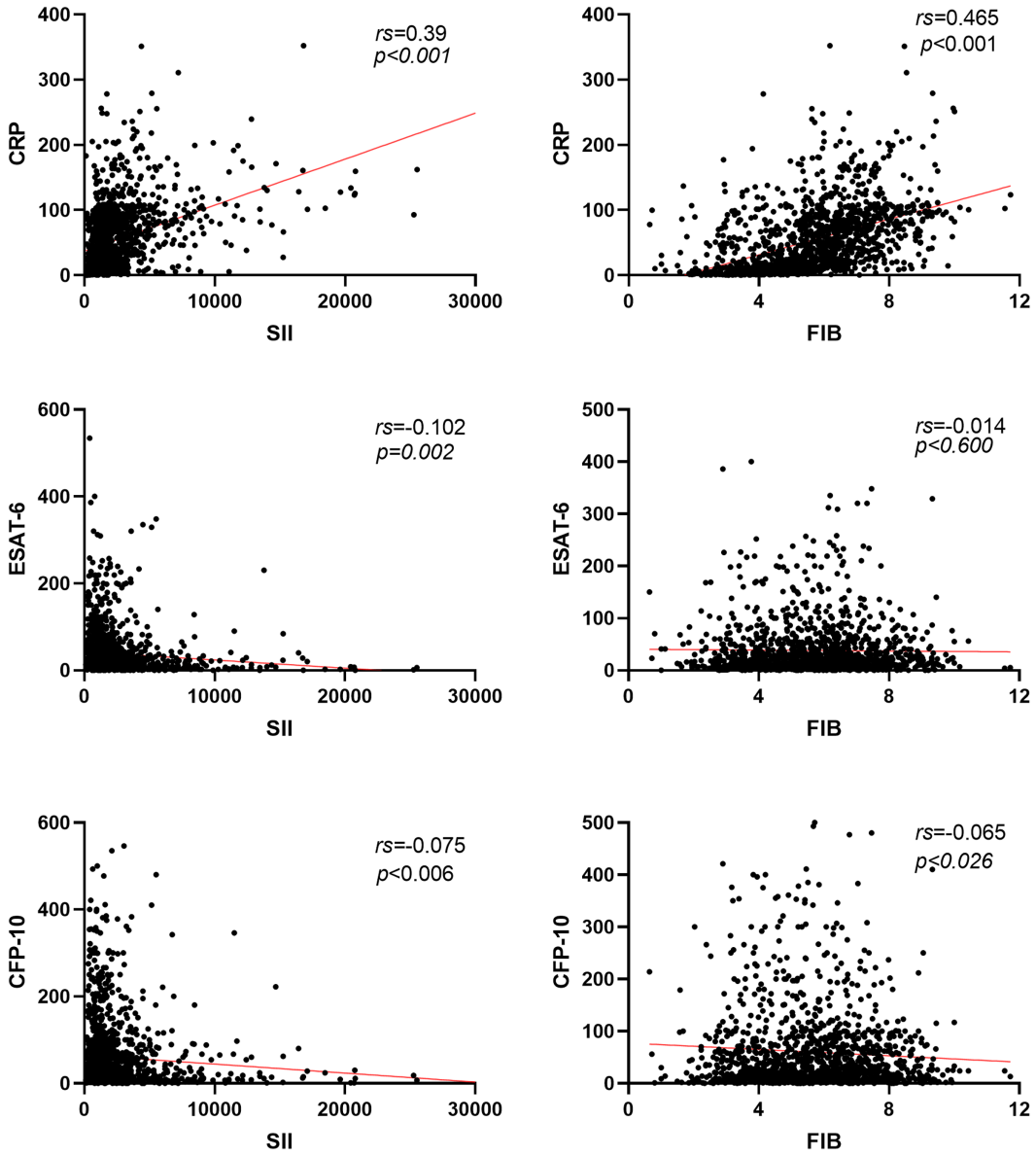

FIGURE 3
Correlation analysis of SII and FIB with ESAT-6, CFP-10, and CRP in patients with pulmonary tuberculosis. Red line, the linear trend line of the two detection indicators; rs, spearman rank correlation coefficient; CRP, C-reactive protein.

applied for ESAT-6, CFP-10, SII, and FIB (Figure 2; Table 3), the Area Under the Curve (AUC), specificity, and positive predictive values for differentiating between APTB and non-TB were good, indicating their utility in the differential diagnosis of suspected tuberculosis. Correlation analysis showed that SII and FIB are not correlated with CFP-10 and ESAT-6, suggesting that SII and FIB are valuable supplements to T-SPOT.TB testing for diagnosing APTB. Both SII and FIB are associated with recognized inflammatory markers, indicating their involvement in the inflammatory process caused by *Mycobacterium tuberculosis* infection. By comparing the levels of SII and FIB in sputum-positive and sputum-negative tuberculosis, as well as non-TB cases, it was found that SII and FIB are positively correlated with the bacterial load of tuberculosis. SII and FIB may be associated with the severity of tuberculosis, potentially serving as predictors of the efficacy of anti-tuberculosis treatment, a topic that will be explored in future research. SII is an indicator of inflammation and immune response, and numerous studies have focused on its effective prognosis in various types of diseases associated with systemic inflammatory reactions (Fest et al., 2018). There are also many studies related to infectious diseases (Mazza et al., 2020). SII levels significantly decrease from a high position after anti-tuberculosis treatment, but the specific reasons and mechanisms are not explained (Ştefanescu et al., 2021). A higher SII is also a predictive factor for depression and anxiety in tuberculosis patients (Liu et al., 2022). SII may be a potential indicator for TB diagnosis. There is currently no research applying it to the auxiliary diagnosis of active pulmonary tuberculosis (APTB). We found that SII when applied to the auxiliary diagnosis of APTB, has good specificity and positive predictive values, especially when used in conjunction with T-SPOT.TB testing, where both specificity and positive predictive values are greater than 83%. Fibrinogen is a

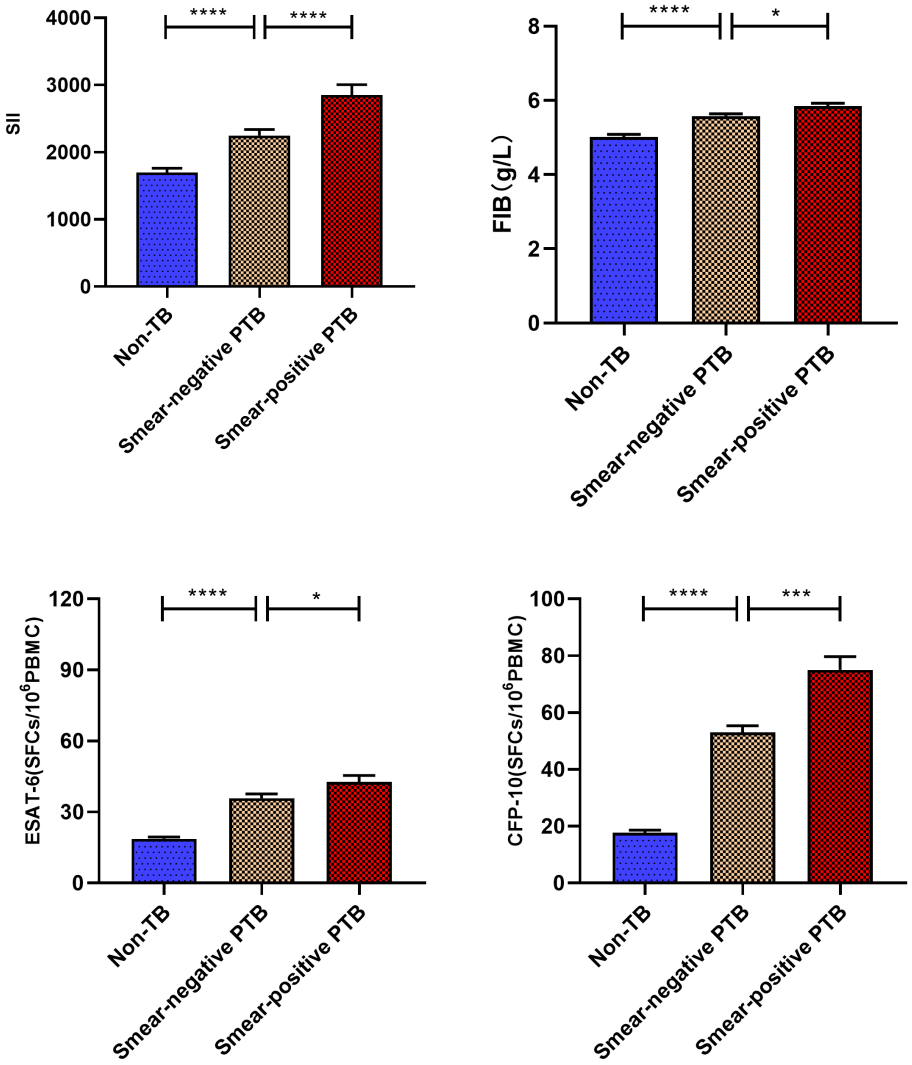

FIGURE 4
Comparative analysis of systemic immune index (SII) and FIB values in various groups. ****$p < 0.0001$, ***$p < 0.001$, *$p < 0.05$. All data are presented as means ± SEMs.

common coagulation marker involved in tissue damage and inflammation (Luyendyk et al., 2019) *Mycobacterium tuberculosis* infection is a process of chronic damage and inflammation, and the acute phase of infection can induce a hypercoagulable state in the body (Kager et al., 2015). Compared to the non-TB group, we found higher levels of Fibrinogen in the APTB group. When applied to the auxiliary diagnosis of APTB, it also exhibits good sensitivity and positive predictive values. When combined with T-SPOT.TB testing, both specificity and positive predictive values are greater than 80%. Finally, we explored the application of combined testing with SII, Fibrinogen, and T-SPOT.TB for the auxiliary diagnosis of APTB, achieving specificity and positive predictive values close to 90%.

Some studies suggest that when the T-SPOT.TB detection threshold exceeds 100 Spot-Forming Cells (SFCs), the specificity for diagnosing APTB exceeds 90%, but clinically, the proportion of people with T-SPOT.TB detection thresholds of less than 100 SFCs are higher. In our approach, the optimal thresholds for ESAT-6 and CFP-10 are 21.5 SFCs and 22.5 SFCs, respectively, addressing the challenge of T-SPOT.TB requires high thresholds to distinguish suspected tuberculosis and provide a new approach for the clinical diagnosis of APTB. There was no statistically significant difference in the positive rates of CFP-10 and ESAT-6 between the disease group and the active TB subgroup, however, there was a statistically significant difference when both ESAT-6 and CFP-10 were positive (Ma et al., 2019). Fox et al. (2007) found that CFP-10 can be used primarily to detect active tuberculosis. The inconsistency of these findings may be due to the heterogeneity of the study population, so more in-depth studies are needed in future work. This study has certain limitations. In the screening and diagnostic protocols for active tuberculosis, the WHO encourages cost-effective solutions, prioritizing non-sputum tests with high sensitivity and specificity. While our approach may have lower sensitivity, the chosen diagnostic indicators are easy to profile, clinically feasible, and represent a non-sputum test with high specificity and positive predictive values. Additionally, this study is single-center research, and due to the incomplete representativeness of the subjects, the results may have bias. Future studies will incorporate multi-center validation for appropriate verification.

TABLE 2 Logistic regression analysis of risk factors of active pulmonary tuberculosis.

Variables	Univariate		Multivariate	
	OR (95% CI)	*p*-value	OR (95% CI)	*p*-value
Gender (female/male)	0.805 (0.642–1.008)	0.059	1.209 (0.979–1.493)	0.079
Age (<60/≥60, years old)	0.844 (0.700–1.018)	0.076	0.797 (0.622–1.023)	0.074
ESAT-6 (<21.5/≥21.5)	2.500 (2.048–3.052)	<0.001	1.637 (1.311–2.043)	<0.001
CFP-10 (<22.5/≥22.5)	4.443 (3.609–5.468)	<0.001	3.918 (3.138–4.892)	<0.025
SII (<2128.32/≥2128.32)	0.834 (0.674–1.032)	<0.095	0.763 (0.603–0.967)	<0.001
FIB (<5.02/≥5.02)	2.243 (1.861–2.703)	<0.001	2.287 (1.865–2.806)	<0.001

OR, odds ratio; CI, confidence interval.

TABLE 3 The diagnostic efficacy of different indexes in patients with pulmonary tuberculosis and non-tuberculosis pulmonary disease with positive T-SPOT.TB results.

Indicators	Sensitivity (95%CI)	Specificity (95%CI)	Positive predictive value(95%CI)	Negative predictive value(95%CI)	AUC(95%CI)
ESAT-6	47.2%(44.5–49.8)	73.7%(70.4–76.9)	77.2%(74.3–80.1)	42.4% (39.7–45.3)	0.61(0.59–0.64)
CFP-10	56.3%(53.6–58.9)	77.5%(74.4–80.6)	82.5%(80.0–85.0)	48.4%(45.5–51.4)	0.71 (0.69–0.73)
SII	35.5%(32.9–38.0)	74.4%(71.1–77.5)	72.4%(68.8–75.7)	37.9%(35.4–40.5)	0.62 (0.58–0.64)
FIB	65.3%(62.7–67.8)	54.3%(51.4–58.8)	72.9%(71.1–76.1)	45.4%(41.9–48.7)	0.61 (0.58–0.63)
ESAT-6 + CFP-10	52.6%(49.9–55.3)	82.5%(79.7–85.3)	85.0%(82.5–87.5)	47.9%(45.2–50.8)	0.72 (0.70–0.74)
ESAT-6 + CFP-10 + SII	53.0%(50.3–55.6)	83.2%(80.4–85.9)	85.6%(83.2–88.0)	48.4%(45.5–51.2)	0.74 (0.72–0.77)
ESAT-6 + CFP-10 + FIB	55.8%(53.1–58.5)	80.1%(77.1–83.0)	84.1%(81.7–86.5)	49.0%(46.1–51.9)	0.74 (0.72–0.76)
ESAT-6 + CFP-10 + SII + FIB	44.7%(42.0–47.4)	90.2%(87.9–92.4)	89.6%(87.2–91.9)	46.3%(43.7–48.9)	0.76 (0.74–0.77)

5 Conclusion

SII and FIB are positively correlated with the degree of tuberculosis inflammation and the bacterial load of *Mycobacterium tuberculosis*. Without raising the T-SPOT.TB detection threshold, the combined detection of SII, FIB, and T-SPOT.TB can effectively distinguish between active pulmonary tuberculosis and non-tuberculous lung diseases when T-SPOT.TB results are all positive. This has significant implications for the differential diagnosis of suspected tuberculosis.

Data availability statement

The original contributions presented in the study are included in the article/Supplementary material, further inquiries can be directed to the corresponding author.

Ethics statement

This study was conducted in accordance with the guidelines of the Declaration of Helsinki and approved by the Institutional Ethics Committee of our hospital, Meizhou People's Hospital reference number: (2021-C-120) which complies with international ethical standards. The studies were conducted in accordance with the local legislation and institutional requirements. Written informed consent for participation was not required from the participants or the participants' legal guardians/next of kin in accordance with the national legislation and institutional requirements.

Author contributions

ZY: Conceptualization, Data curation, Funding acquisition, Investigation, Methodology, Visualization, Writing – original draft, Writing – review & editing. ZS: Conceptualization, Investigation, Project administration, Visualization, Writing – original draft, Writing – review & editing. QH: Conceptualization, Data curation, Validation, Writing – original draft, Writing – review & editing. FW: Formal analysis, Funding acquisition, Supervision, Writing – original draft, Writing – review & editing. SP: Conceptualization, Formal analysis, Methodology, Resources, Writing – original draft, Writing – review & editing.

Funding

The author(s) declare that financial support was received for the research, authorship, and/or publication of this article. This study was supported by the Guangdong Basic and Applied Basic Research Foundation (no. 2021A1515110793), Shenzhen Fund for Guangdong Provincial High-Level Clinical Key Specialties (no. SZGSP012), the Scientific Research Cultivation Project of Meizhou People's Hospital (nos. PY-C2020033 and PY-C2023042), High-level Talent Scientific Research Startup Fund Project of Meizhou People's Hospital (no.

KYQD202303), and Shenzhen Key Medical Discipline Construction Fund (no. SZXK034).

Conflict of interest

The authors declare that the research was conducted in the absence of any commercial or financial relationships that could be construed as a potential conflict of interest.

Publisher's note

All claims expressed in this article are solely those of the authors and do not necessarily represent those of their affiliated organizations, or those of the publisher, the editors and the reviewers. Any product that may be evaluated in this article, or claim that may be made by its manufacturer, is not guaranteed or endorsed by the publisher.

Supplementary material

The Supplementary material for this article can be found online at: https://www.frontiersin.org/articles/10.3389/fmicb.2024.1382665/full#supplementary-material

SUPPLEMENTARY FIGURE S1
Composition of non-TB patients. COPD, chronic obstructive pulmonary disease.

References

Calderwood, C. J., Reeve, B. W., Mann, T., Palmer, Z., Nyawo, G., Mishra, H., et al. (2023). Clinical utility of C-reactive protein-based triage for presumptive pulmonary tuberculosis in south African adults. *J. Infect.* 86, 24–32. doi: 10.1016/j.jinf.2022.10.041

Chen, L., Liu, C., Liang, T., Ye, Z., Huang, S., Chen, J., et al. (2022). Monocyte-to-lymphocyte ratio was an independent factor of the severity of spinal tuberculosis. *Oxid. Med. Cell. Longev.* 2022, 7340330–7340318. doi: 10.1155/2022/7340330

Dong, Z., Shi, J., Dorhoi, A., Zhang, J., Soodeen-Lalloo, A. K., Tan, W., et al. (2018). Hemostasis and lipoprotein indices signify exacerbated lung injury in TB with diabetes comorbidity. *Chest* 153, 1187–1200. doi: 10.1016/j.chest.2017.11.029

Fest, J., Ruiter, R., Ikram, M. A., Voortman, T., van Eijck, C. H. J., and Stricker, B. H. (2018). Reference values for white blood-cell-based inflammatory markers in the Rotterdam study: a population-based prospective cohort study. *Sci. Rep.* 8:10566. doi: 10.1038/s41598-018-28646-w

Fox, A., Jeffries, D. J., Hill, P. C., Hammond, A. S., Lugos, M. D., Jackson-Sillah, D., et al. (2007). ESAT-6 and CFP-10 can be combined to reduce the cost of testing for *Mycobacterium tuberculosis* infection, but CFP-10 responses associate with active disease. *Trans. R. Soc. Trop. Med. Hyg.* 101, 691–698. doi: 10.1016/j.trstmh.2007.03.001

Hamad, D. A., Aly, M. M., Abdelhameid, M. A., Ahmed, S. A., Shaltout, A. S., Abdel-Moniem, A. E., et al. (2022). Combined blood indexes of systemic inflammation as a Mirror to admission to intensive care unit in COVID-19 patients: a multicentric study. *J Epidemiol Glob Health.* 12, 64–73. doi: 10.1007/s44197-021-00021-5

Hamada, Y., Cirillo, D. M., Matteelli, A., Penn-Nicholson, A., Rangaka, M. X., and Ruhwald, M. (2021). Tests for tuberculosis infection: landscape analysis. *Eur. Respir. J.* 58:2100167. doi: 10.1183/13993003.00167-2021

Kager, L. M., Blok, D. C., Lede, I. O., Rahman, W., Afroz, R., Bresser, P., et al. (2015). Pulmonary tuberculosis induces a systemic hypercoagulable state. *J. Infect.* 70, 324–334. doi: 10.1016/j.jinf.2014.10.006

Kaufmann, S. H. E. (2023). Vaccine development against tuberculosis before and after Covid-19. *Front. Immunol.* 14:1273938. doi: 10.3389/fimmu.2023.1273938

Kirwan, D. E., Chong, D. L. W., and Friedland, J. S. (2021). Platelet activation and the immune response to tuberculosis. *Front. Immunol.* 12:631696. doi: 10.3389/fimmu.2021.631696

Li, W., Chen, G., Lin, F., Yang, H., Cui, Y., Lu, R., et al. (2023). A score for predicting invasive pulmonary aspergillosis in immunocompetent critically ill patients. *Eur. J. Clin. Invest.* 53:e13985. doi: 10.1111/eci.13985

Liu, X., Bai, X., Ren, R., Tan, L., Zhang, Y., Lan, H., et al. (2022). Association between depression or anxiety symptoms and immune-inflammatory characteristics in in-patients with tuberculosis: a cross-sectional study. *Front. Psych.* 13:985823. doi: 10.3389/fpsyt.2022.985823

Liu, Y., Yao, L., Wang, F., Sun, Z., Tan, Y., and Sha, W. (2021). The TBAg/PHA ratio in T-SPOT.TB assay has high prospective value in the diagnosis of active tuberculosis: a multicenter study in China. *Respir. Res.* 22:165. doi: 10.1186/s12931-021-01753-5

Luo, Y., Tang, G., Lin, Q., Mao, L., Xue, Y., Yuan, X., et al. (2020). Combination of mean spot sizes of ESAT-6 spot-forming cells and modified tuberculosis-specific antigen/phytohemagglutinin ratio of T-SPOT.TB assay in distinguishing between active tuberculosis and latent tuberculosis infection. *J. Infect.* 81, 81–89. doi: 10.1016/j.jinf.2020.04.038

Luyendyk, J. P., Schoenecker, J. G., and Flick, M. J. (2019). The multifaceted role of fibrinogen in tissue injury and inflammation. *Blood* 133, 511–520. doi: 10.1182/blood-2018-07-818211

Ma, Y., Li, R., Shen, J., He, L., Li, Y., Zhang, N., et al. (2019). Clinical effect of T-SPOT.TB test for the diagnosis of tuberculosis. *BMC Infect. Dis.* 19:993. doi: 10.1186/s12879-019-4597-8

Mazza, M. G., De Lorenzo, R., Conte, C., Poletti, S., Vai, B., Bollettini, I., et al. (2020). Anxiety and depression in COVID-19 survivors: role of inflammatory and clinical predictors. *Brain Behav. Immun.* 89, 594–600. doi: 10.1016/j.bbi.2020.07.037

Meier, T., Eulenbruch, H. P., Wrighton-Smith, P., Enders, G., and Regnath, T. (2005). Sensitivity of a new commercial enzyme-linked immunospot assay (T SPOT-TB) for diagnosis of tuberculosis in clinical practice. *Eur. J. Clin. Microbiol. Infect. Dis.* 24, 529–536. doi: 10.1007/s10096-005-1377-8

Mustafa, A., Abdallah Dafaallah, E. I., Eltayeb Omer, A., Mahmoud Muddathir, A. R., Mangi, A. A., and Bashier Eltayeb, L. (2022). Inflammatory mediators released in pulmonary tuberculosis enhance hyper-Coagulable states: a crucial role of tissue factor. *Pak. J. Biol. Sci.* 25, 725–731. doi: 10.3923/pjbs.2022.725.731

Nøst, T. H., Alcala, K., Urbarova, I., Byrne, K. S., Guida, F., Sandanger, T. M., et al. (2021). Systemic inflammation markers and cancer incidence in the UK biobank. *Eur. J. Epidemiol.* 36, 841–848. doi: 10.1007/s10654-021-00752-6

Ortiz-Brizuela, E., Apriani, L., Mukherjee, T., Lachapelle-Chisholm, S., Miedy, M., Lan, Z., et al. (2023). Assessing the diagnostic performance of new commercial interferon-γ release assays for *Mycobacterium tuberculosis* infection: a systematic review and Meta-analysis. *Clin. Infect. Dis.* 76, 1989–1999. doi: 10.1093/cid/ciad030

Pang, Y., An, J., Shu, W., Huo, F., Chu, N., Gao, M., et al. (2019). Epidemiology of Extrapulmonary tuberculosis among inpatients, China, 2008-2017. *Emerg. Infect. Dis.* 25, 457–464. doi: 10.3201/eid2503.180572

Pinelo, J. E. E., Manandhar, P., Popovic, G., Ray, K., Tasdelen, M. F., Nguyen, Q., et al. (2023). Systematic mapping of the conformational landscape and dynamism of soluble fibrinogen. *J. Thromb. Haemost.* 21, 1529–1543. doi: 10.1016/j.jtha.2023.01.034

Ştefanescu, S., Cocoş, R., Turcu-Stiolica, A., Mahler, B., Meca, A. D., Giura, A. M. C., et al. (2021). Evaluation of prognostic significance of hematological profiles after the intensive phase treatment in pulmonary tuberculosis patients from Romania. *PLoS One* 16:e0249301. doi: 10.1371/journal.pone.0249301

Sun, Y., Yao, X., Ni, Y., Peng, Y., and Shi, G. (2022). Diagnostic efficacy of T-SPOT.TB for active tuberculosis in adult: a retrospective study. *Infect Drug Resist.* 15, 7077–7093. doi: 10.2147/idr.S388568

Verma, R., Ellappan, K., Kempsell, K. E., and Joseph, N. M. (2024). Triage test to diagnose presumptive pulmonary tuberculosis. *Lancet Glob. Health* 12, e175–e176. doi: 10.1016/s2214-109x(23)00604-6

Yang, C., and Gao, Q. (2018). Recent transmission of *Mycobacterium tuberculosis* in China: the implication of molecular epidemiology for tuberculosis control. *Front. Med.* 12, 76–83. doi: 10.1007/s11684-017-0609-5

Yang, Q., Zhang, C., Ruan, Q., Zhang, W., Zhang, H., Li, Y., et al. (2020). Higher T-SPOT.TB threshold may aid in diagnosing active tuberculosis?: a real-world clinical practice in a general hospital. *Clin. Chim. Acta* 509, 60–66. doi: 10.1016/j.cca.2020.06.005

Zhang, L., Cheng, X., Bian, S., Song, Y., Li, Q., Gao, M., et al. (2017). Utility of Th1-cell immune responses for distinguishing active tuberculosis from non-active tuberculosis: a case-control study. *PLoS One* 12:e0177850. doi: 10.1371/journal.pone.0177850

Zhao, Y., Shao, W., Zhu, Q., Zhang, R., Sun, T., Wang, B., et al. (2023). Association between systemic immune-inflammation index and metabolic syndrome and its components: results from the National Health and nutrition examination survey 2011-2016. *J. Transl. Med.* 21:691. doi: 10.1186/s12967-023-04491-y

frontiers | Frontiers in Microbiology

TYPE Original Research
PUBLISHED 31 May 2024
DOI 10.3389/fmicb.2024.1392782

OPEN ACCESS

EDITED BY
Vishwanath Venketaraman,
Western University of Health Sciences, United States

REVIEWED BY
Soraya Mezouar,
Aix-Marseille University, France
Guoliang Zhang,
Shenzhen Third People's Hospital, China
Matt Johansen,
University of Technology Sydney, Australia
Pooja Vir,
Uniformed Services University of the Health Sciences, United States

*CORRESPONDENCE
Joaquín Zúñiga
joazu@yahoo.com;
joaquin.zuniga@iner.gob.mx
Leslie Chávez-Galán
chavezgalan@gmail.com;
lchavez_galan@iner.gob.mx

†These authors have contributed equally to this work and share first authorship

RECEIVED 28 February 2024
ACCEPTED 15 May 2024
PUBLISHED 31 May 2024

CITATION
Choreño-Parra JA, Ramon-Luing LA, Castillejos M, Ortega-Martínez E, Tapia-García AR, Matías-Martínez MB, Cruz-Lagunas A, Ramírez-Martínez G, Gómez-García IA, Ramírez-Noyola JA, Garcia-Padrón B, López-Salinas KG, Jiménez-Juárez F, Guadarrama-Ortiz P, Salinas-Lara C, Bozena-Piekarska K, Muñóz-Torrico M, Chávez-Galán L and Zúñiga J (2024) The rs11684747 and rs55790676 SNPs of ADAM17 influence tuberculosis susceptibility and plasma levels of TNF, TNFR1, and TNFR2.
Front. Microbiol. 15:1392782.
doi: 10.3389/fmicb.2024.1392782

The rs11684747 and rs55790676 SNPs of ADAM17 influence tuberculosis susceptibility and plasma levels of TNF, TNFR1, and TNFR2

José Alberto Choreño-Parra[1,2†], Lucero A. Ramon-Luing[3†], Manuel Castillejos[4], Emmanuel Ortega-Martínez[5,6,7], Alan Rodrigo Tapia-García[2,7], Melvin Barish Matías-Martínez[2,8], Alfredo Cruz-Lagunas[2], Gustavo Ramírez-Martínez[2], Itzel Alejandra Gómez-García[2,8], Jazmín Ariadna Ramírez-Noyola[2,9], Beatriz Garcia-Padrón[2,7], Karen Gabriel López-Salinas[2,8], Fabiola Jiménez-Juárez[2,8], Parménides Guadarrama-Ortiz[10], Citlaltepetl Salinas-Lara[6,7], Karolina Bozena-Piekarska[1], Marcela Muñóz-Torrico[11], Leslie Chávez-Galán[3]* and Joaquín Zúñiga[2,8]*

[1]Dirección de Enseñanza, Instituto Nacional de Enfermedades Respiratorias Ismael Cosio Villegas, Mexico City, Mexico, [2]Laboratory of Immunobiology and Genetics, Instituto Nacional de Enfermedades Respiratorias Ismael Cosío Villegas, Mexico City, Mexico, [3]Laboratory of Integrative Immunology, Instituto Nacional de Enfermedades Respiratorias Ismael Cosío Villegas, Mexico City, Mexico, [4]Departamento de Epidemiología Hospitalaria e Infectología, Instituto Nacional de Enfermedades Respiratorias Ismael Cosío Villegas, Mexico City, Mexico, [5]Posgrado en Ciencias Quimicobiológicas, SEPI, Escuela Nacional de Ciencias Biológicas, Instituto Politécnico Nacional, Mexico City, Mexico, [6]Department of Pathology, Instituto Nacional de Neurología y Neurocirugía Manuel Velasco Suárez, Mexico City, Mexico, [7]Red MEDICI, Facultad de Estudios Superiores Iztacala, Universidad Nacional Autónoma de México, Tlalnepantla de Baz, Mexico, [8]Tecnologico de Monterrey, Escuela de Medicina y Ciencias de la Salud, Mexico City, Mexico, [9]Sección de Posgrado e Investigación, Escuela Superior de Medicina, Instituto Politécnico Nacional, Mexico City, Mexico, [10]Centro Especializado en Neurocirugía y Neurociencias México, Mexico City, Mexico, [11]Clínica de Tuberculosis, Instituto Nacional de Enfermedades Respiratorias Ismael Cosío Villegas, Mexico City, Mexico

Introduction: The proteolytic activity of A Disintegrin and Metalloproteinase 17 (ADAM17) regulates the release of tumor necrosis factor (TNF) and TNF receptors (TNFRs) from cell surfaces. These molecules play important roles in tuberculosis (TB) shaping innate immune reactions and granuloma formation.

Methods: Here, we investigated whether single nucleotide polymorphisms (SNPs) of ADAM17 influence TNF and TNFRs levels in 224 patients with active TB (ATB) and 118 healthy close contacts. Also, we looked for significant associations between SNPs of ADAM17 and ATB status. TNF, TNFR1, and TNFR2 levels were measured in plasma samples by ELISA. Four SNPs of ADAM17 (rs12692386, rs1524668, rs11684747, and rs55790676) were analyzed in DNA isolated from peripheral blood leucocytes. The association between ATB status, genotype, and cytokines was analyzed by multiple regression models.

Results: Our results showed a higher frequency of rs11684747 and rs55790676 in close contacts than ATB patients. Coincidentally, heterozygous to these SNPs of ADAM17 showed higher plasma levels of TNF compared to homozygous to their

respective ancestral alleles. Strikingly, the levels of TNF and TNFRs distinguished participant groups, with ATB patients displaying lower TNF and higher TNFR1/TNFR2 levels compared to their close contacts.

Conclusion: These findings suggest a role for SNPs of ADAM17 in genetic susceptibility to ATB.

KEYWORDS

tuberculosis, ADAM17, TNF-α converting enzyme, tumor necrosis factor, tumor necrosis factor receptors

1 Introduction

Tuberculosis (TB), an infectious disease caused by *Mycobacterium tuberculosis* (Mtb), is a global public health problem which caused 7.5 million new cases and 1.3 million deaths in 2022 (Global Tuberculosis Report 2023, n.d.). Although a primary infection can induce the active form of TB (ATB), most ATB cases derive from latent tuberculosis (LTB) progression, a status of asymptomatic infection without microbiological evidence of bacterial viability but positive readouts of cellular immune memory against Mtb (Tufariello et al., 2003; Mack et al., 2009; Getahun et al., 2015). The last estimation of LTB burden indicated that approximately 1.7 billion individuals were latently infected with Mtb in 2014, representing about a quarter of the global population (Houben and Dodd, 2016). From these, only 5 to 10% will progress to ATB each year with the lung as the main organ affected. Currently, the factors associated with progression to ATB are not completely understood despite its epidemiological relevance. Of course, several genetic, demographic, sociocultural, microbiological, and nutritional characteristics, along with comorbid conditions of cases may affect protective anti-TB immunity. Nonetheless, given the complexity of host-pathogen interactions in TB, a sole immune parameter determinant of protection or pathology has not been found.

For many years, the paradigm of TB immunopathogenesis has established that Mtb infection control greatly relies on memory immune responses of CD4+ T helper cells, which produce interferon-gamma (IFN-γ) to assist macrophages in exploiting their full bactericidal capacity (Shimokata et al., 1986; Flynn et al., 1993; Orme et al., 1993). Unfortunately, the vaccine candidates based on this dogma have failed in providing protection in the real world (Tameris et al., 2013), and IFN-γ-release assays (IGRAs) have no prognostic value to predict ATB progression in individuals with LTB (Diel et al., 2012; Aboudounya and Heads, 2021). Thus, a higher interest in searching for other protective mechanisms has led to striking findings that link previously unrecognized roles of innate immunity and TB protection operating in LTB but not ATB individuals (Khader et al., 2019; Esaulova et al., 2021).

The innate phase of the anti-TB immune response is dominated by alveolar macrophages and recruited monocytes, which participate in granuloma formation, thereby impeding Mtb dissemination (Tsai et al., 2006; Dunlap et al., 2018). Tumor necrosis factor (TNF), a proinflammatory cytokine of innate immunity, plays an essential role in the formation and maintenance of granulomas, macrophage recruitment and nitric oxide production, and the development of giant multinucleated cells (Kindler et al., 1989; Flynn et al., 1995; Roach et al., 2002; Mezouar et al., 2019). Thus, TNF is pivotal in mediating immune protection against Mtb during the early and late stages of infection, as demonstrated by the increased susceptibility to ATB progression among people with LTB receiving anti-TNF immunotherapies (Keane et al., 2001; Gómez-Reino et al., 2003; Mohan et al., 2004; Wallis et al., 2004). Also, diverse reports indicate that single-nucleotide polymorphisms (SNPs) increase the risk of developing TB by decreasing TNF levels or interfering with its signaling (Wu et al., 2019; Adane et al., 2021; Souza de Lima et al., 2021).

TNF is produced by several leucocyte subsets (Dorhoi and Kaufmann, 2014), and it is expressed as a trimeric transmembrane protein (tmTNF) or a soluble form (solTNF). Both TNF forms are bioactive when they attach to TNF receptor 1 (TNFR1), which mediates inflammation and tissue injury, or TNF receptor 2 (TNFR2), which attenuates excessive inflammation during mycobacterial infection (Chavez-Galan et al., 2017, 2019; Ruiz et al., 2021). TNFRs are also expressed on the cell surface as trans-membrane proteins (tmTNFR1 and tmTNFR2) or released from the cell as soluble forms (solTNFR1 and solTNFR2). Whereas tmTNFR1 and tmTNFR2 induce intracellular signaling after the binding with tmTNF or solTNF (Ruiz et al., 2021), soluble TNFRs are anti-inflammatory mediators acting as decoy receptors to neutralize TNF (Kohno et al., 1990). The shedding of TNF and its receptors from the cell membrane is mediated by the proteolytic activity of A Disintegrin and Metalloproteinase 17 (ADAM17), also known as TNF converting enzyme (TACE) (Black et al., 1997; Mohan et al., 2002). Of note, despite the relevance of ADAM17 in regulating TNF and TNFRs levels in diverse diseases (Moss and Minond, 2017; Zunke and Rose-John, 2017), the role of this protease in TB susceptibility has not been assessed.

SNPs of ADAM17 have been implicated in several disorders, including Parkinson's disease, allergy, sepsis, and vascular diseases (Li et al., 2014, 2019; Shao et al., 2016; He et al., 2022; Jung and Hwang, 2022). Hence, this study aimed to characterize the prevalence of SNPs of ADAM17 among people with ATB and their healthy close contacts and the effect of these polymorphisms in the levels of soluble TNF, TNFR1, and TNFR2. Our findings indicate that people with the rs11684747 and rs55790676 SNPs of ADAM17 display higher plasma levels of solTNF but lower concentrations of TNFRs. Remarkably, the frequency of these SNPs of ADAM17 was higher among people without clinical manifestations of the disease despite being in close contact with ATB cases, especially in those with LTB, as defined by positive IGRA results. Finally, logistic regression analyses showed that homozygosity to the ancestral alleles of both variants is associated with a higher risk for ATB as compared to carriers of rs11684747 and rs55790676 SNPs of ADAM17. Our study elucidates a possible role of

ADAM17 in immunity against Mtb and disease susceptibility that deserves further research.

2 Materials and methods

2.1 Study population

Peripheral blood samples were obtained from ATB patients and their household contacts. All participants were enrolled at the TB clinic of the Instituto Nacional de Enfermedades Respiratorias Ismael Cosío Villegas (INER) in Mexico City. The diagnosis of ATB was laboratory-confirmed by positive results in sputum smear microscopy, sputum/bronchoalveolar lavage (BAL) culture, and GeneXpert MTB/RIF test (Cepheid, CA, United States). The LTB group included household contacts, who shared the same enclosed living space for one or more nights per week or extended periods during the day with TB patients three months before enrollment. All these contacts did not show ATB symptoms, and some of them had a positive result in the IGRA QuantiFERON®-TB Gold Plus test (QIAGEN, Hilden, Germany; hereinafter named QTF+). QTF+ participants were considered as having LTB infection and were subjected to clinical evaluation and chest X-ray. The individuals with QTF− were considered as healthy household contacts. QTF+ and QTF− individuals were analyzed as a single group called "No ATB" because they displayed the same behavior in statistical analyses (data indicated in Supplementary material).

Solid-organ transplant recipients and patients with human immunodeficiency virus infection, receiving immunosuppressive treatment, and diagnosed with cancer, or autoimmune diseases were excluded from the study. Clinical and demographic data from participants were obtained by direct clinical interview, physical examination, and review of their medical records.

2.2 Samples

Peripheral blood samples were obtained into BD Vacutainer® EDTA tubes as soon as the diagnosis was made and before treatment initiation for ATB patients, or upon acceptance to participate in the study by healthy-close contacts. Peripheral blood mononuclear cells (PBMCs) were isolated by centrifugation gradient using Ficoll-Paque™ PLUS (GE Healthcare, Life Sciences, PA, United States) for DNA isolation. Plasma aliquots for protein determinations were stored at −70°C until use.

2.3 DNA isolation and genotyping

Genomic DNA was extracted from PBMCs using silica columns (DNeasy® Blood & Tissue Kit, Qiangen™, MD, United States) following the manufacturer's guidelines. Concentration and purity of DNA obtained were determined by measuring the absorbance within the micro-volume spectrophotometer NanoDrop® ND-2000c (ThermoFisher Scientific, Waltham, MA, United States).

For genotyping analysis, the selection of SNPs of the ADAM17 gene was based on a previous study that reported the allele frequency of five SNPs analysis in patients with distinct severity of sepsis (Shao et al., 2016), an infectious disorder where control of inflammation is essential in determining the outcome of affected people, as in TB. Herein, four of these five SNPs of ADAM17 were analyzed using specific TaqMan® genotyping assays commercially available (ThermoFisher Scientific, Waltham, MA, United States; rs12692386, assay number C__31588436_10; rs1524668, assay number C__8348383_30; rs11684747, assay number C__1829895_10; rs55790676, assay number C__25942661_10). The RT-PCR reaction was set up in 96-well plates with a mix of 6 μL TaqMan™ Universal PCR Master Mix (ThermoFisher Scientific, Waltham, MA, United States), 2 μL of free nuclease water, and 3 μL of DNA samples at 5 ng/μL or free nuclease water for negative controls. Thermal cycling was performed at 55°C for 10 min for reverse transcription, followed by 95°C for 10 min, and then 40 cycles of 60°C for 60 s, 60°C for 30 s using a StepOnePlus™ thermocycler (Applied Biosystems, Foster City, CA, United States).

2.4 Cytokine levels

Soluble levels of TNF, TNFR1, TNFR2, and TIM-3 were quantified by Enzyme-linked immunosorbent assay (ELISA) following the manufacturer's protocols (ELISA MAX™ Deluxe Set Human TNF-α, BioLegend, CA, USA; and Human TNFRI/TNFRSF1A, TNFRII/TNFRSF1B Immunoassay Quantikine™, Human TIM-3 DuoSet ELISA; R&D Sytems, MN, USA). The optical density was measured using a microplate reader spectrophotometer (Imark, Bio-Rad, Hercules, United States) set to 450 nm. All proteins were quantified by comparison with the corresponding standard curve.

2.5 Haplotype block construction

This analysis was carried out using Haploview 4.2 software (Barrett et al., 2005), applying the analysis algorithm presented by Gabriel et al. (2002). Linkage disequilibrium (LD) was presented using D′ value. Haplotype-association analysis was performed with Fisher's exact test between cases and controls.

2.6 Ethics statement

The Institutional Review Board of the Instituto Nacional de Enfermedades Respiratorias Ismael Cosío Villegas approved the study protocol code B04-23, approved in February 2023. All participants or their legal guardians provided written informed consent to participate in the investigation in adherence to the Declaration of Helsinki for Human Research. The study was conducted under the Mexican Constitution law NOM-012-SSA3-2012, which establishes the criteria for executing clinical investigations in humans. All the personal data and clinical information were managed according to local legislation.

2.7 Statistical analysis

Descriptive statistics were used to characterize the study cohorts. Frequencies and proportions were calculated for categorical data. Medians, interquartile ranges, and 95% confidence intervals were used

10.3389/fmicb.2024.1392782

for continuous variables. Comparisons between groups were made using a Chi-square test, Fisher's exact test, Mann–Whitney U test, or Kruskal–Wallis with *post hoc* Dunn's test, as appropriate.

A multivariate logistic regression analysis was conducted to identify associations between TB status (ATB) and the soluble levels of TNF, TNFR1 and TNFR2, and SNPs of ADAM17. Thus, multiple logistic regression with three-way interactions was performed with variables that showed statistically significant differences between groups; rs11684747 (AA allele) and rs55790676 (GG allele) SNPs of ADAM17 (which were significantly different in ATB versus no ATB) were defined as dependent variables.

All analyses were performed using GraphPad Prism V 9.0.2 (GraphPad Software, Inc., San Diego, CA, United States) and R statistical software version 4.2.1 (R Foundation for Statistical Computing, Vienna, Austria). p-values $\leqq 0.05$ were considered statistically significant.

3 Results

3.1 Clinical characteristics of participants

This study enrolled a total of 342 participants, 224 with ATB and 118 house close contacts. The second group included 70 individuals with LTB (QTF+) and 48 QTF−. Supplementary Table S1 summarizes the main demographic and clinical characteristics of the study groups. Since QTF+ and QTF− individuals showed similar features, they were consolidated as a single group for some comparisons with ATB patients. Also, given that both groups represent individuals with higher protection against Mtb, analyses of SNPs were made between this consolidated group and ATB. Overall, 60% of participants were women with a median age of 44 years (Table 1). The ATB group significantly differed from close contacts by a higher proportion of males, lower weight, and body mass index (BMI), and higher prevalence of tobacco smoking and diabetes. A similar proportion of ATB and no ATB participants (87 and 89%, respectively) received the Bacillus Calmette-Guerin vaccine (BCG) during childhood.

TABLE 1 Demographic and clinical characteristics of study populations.

Characteristics	Overall $N = 342$	ATB		
		Yes[a] $N = 224$	No[b] $N = 118$	p-value (a vs b)
Group				
QTF−	48 (14%)	0 (0%)	48 (41%)	NA
QTF+	70 (20%)	0 (0%)	70 (59%)	NA
ATB	224 (65%)	224 (100%)	0 (0%)	NA
Male gender	138 (40%)	108 (48%)	30 (25%)	<0.001
Age	44 (31, 56)	44 (31, 57)	44 (30, 54)	0.4
BMI	23 (20, 27)	21 (19, 24)	28 (25, 32)	<0.001
Obesity	48 (14%)	10 (5%)	38 (32%)	<0.001
Low weight	79 (23%)	77 (34%)	2 (2%)	<0.001
Smoking	85 (36%)	57 (47%)	28 (24%)	<0.001
DM	95 (28%)	84 (38%)	11 (9%)	<0.001
SAH	49 (14%)	35 (16%)	14 (12%)	0.3
BCG	249 (88%)	144 (87%)	105 (89%)	0.7

Data are shown as n (%) or median (IQR 25,75). Differences between groups were analyzed using Pearson's Chi-squared test, Kruskal-Wallis rank sum test, or Fisher's exact test, as appropriate. ATB, active pulmonary tuberculosis; BCG, Bacillus Calmette-Guerin vaccine; DM, diabetes mellitus; BMI, body mass index; QTF, QuantiFERON test; SAH, systemic arterial hypertension; NA, not applicable; TB, tuberculosis.

3.2 SNPs of ADAM17 are differentially distributed according to ATB status

To investigate the role of the SNPs of ADAM17 in TB, we analyzed the distribution of rs12692386, rs1524668, rs11684747, and rs55790676 among study groups. First, the possible participation of these SNPs as a cluster of genetic susceptibility was assessed by haplotype blocks. Their genotype distribution among study participants met the Hardy–Weinberg equilibrium ($p > 0.05$) and showed a complete LD (Figure 1). Four blocks of haplotypes were found among cases and controls; however, their frequencies were not different between cases and close contacts (Table 2). Thus, we analyzed each SNP individually.

The allele frequencies of rs12692386 and rs1524668 were not significantly different between participant groups (Table 3; Supplementary Table S2). In contrast, ATB patients showed a higher frequency of homozygosity to ancestral AA rs11684747 and GG rs55790676 alleles, whereas close contacts were heterozygous AG to rs11684747 and GT to rs55790676 with higher frequency than ATB patients (19% vs. 11%, $p = 0.027$; and 19% vs. 10%, $p = 0.021$, respectively). The allelic frequencies were similar between QTF+ and QTF− close contact groups (Supplementary Table S2). Homozygous to these SNPs of ADAM17 (GG to rs11684747 and TT to rs55790676) were not identified in the cohorts.

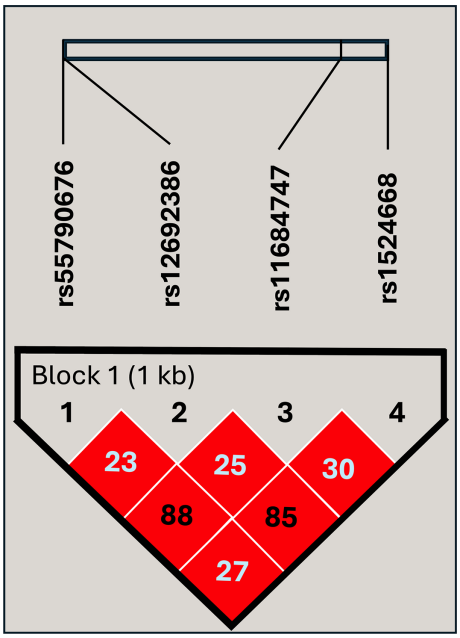

FIGURE 1
Linkage disequilibrium plot of the genetic variants included in the study. The high intensity of the red diamonds indicates a complete linkage disequilibrium (D′ = 100). The values inside the diamonds are the results of the R^2 pairwise measures.

TABLE 2 Haplotype-association analysis of the evaluated *loci* in the genetic susceptibility to ATB.

Haplotype[a]	ATB		*p*-value[b]
	Yes	No	
GAAA	78	77.6	0.8963
GGAC	13.6	11.6	0.3791
TGGC	5	7.5	0.1395
GGAA	3	2.3	0.5708

[a]rs55790676-rs12692386-rs11684747-rs1524668.
[b]Fisher's exact test. The data are displayed as haplotype frequencies in percentages (%).

TABLE 3 Genotypes and allele frequencies in ATB patients and close contacts.

Characteristics	Overall *N* = 342	ATB		
		Yes[a] *N* = 224	No[b] *N* = 118	*p*-value (a vs b)
rs12692386				
AA	206 (61%)	138 (62%)	68 (58%)	0.4
AG	112 (33%)	69 (31%)	43 (36%)	0.3
GG	21 (6%)	14 (6%)	7 (6%)	0.9
A	318 (94%)	207 (94%)	111 (94%)	0.9
G	133 (39%)	83 (38%)	50 (42%)	0.4
rs1524668				
AA	222 (65%)	151 (68%)	71 (60%)	0.15
AC	100 (29%)	58 (26%)	42 (36%)	0.068
CC	18 (5%)	13 (6%)	5 (4%)	0.5
A	322 (95%)	209 (94%)	113 (96%)	0.5
C	118 (35%)	71 (32%)	47 (40%)	0.15
rs11684747				
AA	293 (86%)	198 (89%)	95 (81%)	**0.027**
AG	47 (14%)	24 (11%)	23 (19%)	**0.027**
GG	0 (0%)	0 (0%)	0 (0%)	
A	340 (100%)	222 (100%)	118 (100%)	
G	47 (14%)	24 (11%)	23 (19%)	**0.027**
rs55790676				
GG	297 (87%)	201 (90%)	96 (81%)	**0.021**
GT	44 (13%)	22 (9.9%)	22 (19%)	**0.021**
TT	0 (0%)	0 (0%)	0 (0%)	
G	341 (100%)	223 (100%)	118 (100%)	
T	44 (13%)	22 (9.9%)	22 (19%)	**0.021**

Data are displayed as *n* (%). Differences between groups were analyzed using Pearson's Chi-squared test or Fisher's exact test, as appropriate. *p* value in bold show a statistically significant difference. a = patients with ATB; b = household contact with no ATB wheter QTF+ or QTF-.

3.3 Levels of TNF and TNFRs are influenced by SNPs of ADAM17 and distinguish ATB patients from close contacts

Given the major role of ADAM17 in modulating the release of TNF and TNFRs from cell surfaces, we next investigated an association of SNPs and cytokine levels in TB. These analyses were carried out in the overall study population since all participants were in contact with Mtb, representing biological replicates of the same immunological phenomenon: the production of TNF molecules in response to mycobacteria *in vivo*. First, we measured and compared cytokine levels between study groups, looking for differences that may reflect the distinct grades of protection against Mtb between ATB patients and close contacts. As shown in Figure 2A and Supplementary Table S3, the levels of soluble TNF in plasma were significantly lower in ATB cases than in controls, whereas no differences were observed between QTF+ and QTF− groups (Supplementary Table S4; Supplementary Figure S1). Conversely, TNFR1 and TNFR2 were elevated in ATB patients compared to their close contacts.

Then, a link between SNPs of ADAM17 and TNF, TNFR1, and TNFR2 was evaluated. Notably, homozygous AA to rs11684747 and GG to rs55790676 showed lower plasma levels of TNF than individuals carrying at least one variant allele (Figure 2B). Also, homozygous to ancestral alleles of these SNPs displayed higher levels of TNFR2 that did not reach statistical significance compared to those carrying the variant alleles. No association between rs12692386 and rs1524668 with cytokine levels was found (Figures 2C,D).

3.4 Elevated TIM-3 levels in ATB patients and their association with the rs12692386 SNP of ADAM17

T cell immunoglobulin and mucin-domain-3 (TIM-3 or CD366) is a surface molecule expressed by both CD4+ and CD8+ T cells in mice infected with Mtb and in ATB patients (Wang et al., 2011). Although its precise role in TB remains unclear, TIM-3 is cleaved by ADAM17 (Möller-Hackbarth et al., 2013). Together with galectin 9, TIM-3 has been shown to induce antibacterial activity in infected human macrophages (Sada-Ovalle et al., 2012). In this study, we also measured the levels of TIM-3 across various TB patient groups due to the inability to directly measure ADAM17. Nonetheless, if ADAM17 indeed has a significant influence on ATB and cytokine levels, its effect would be reflected in the regulation of other immune molecules besides TNF and TNFRs, such as TIM-3. As illustrated in Figure 3A, ATB patients exhibited significantly higher soluble TIM-3 levels compared to the household control group. Further analysis investigated the association between SNPs of ADAM17 and TIM-3 levels. Notably, individuals homozygous for the AA genotype at rs12692386 had higher systemic TIM-3 levels than those carrying at least one variant allele (Figure 3B). Other molecules cleaved by ADAM17, such as PD-L1 and IL-8, were also evaluated, but their plasma levels were undetectable (data not shown).

3.5 Multiple logistic regression analysis reveals an association between ATB status, SNPs of ADAM17, TNF, and TNFRs

A multiple logistic regression analysis was performed, looking for variables associated with ATB status, including SNPs of ADAM17, TNF, and TNFR levels. As observed in Supplementary Table S5, male gender, low weight, tobacco smoking, and diabetes were associated with ATB. Importantly, carrying rs11684747 and rs55790676 SNPs of

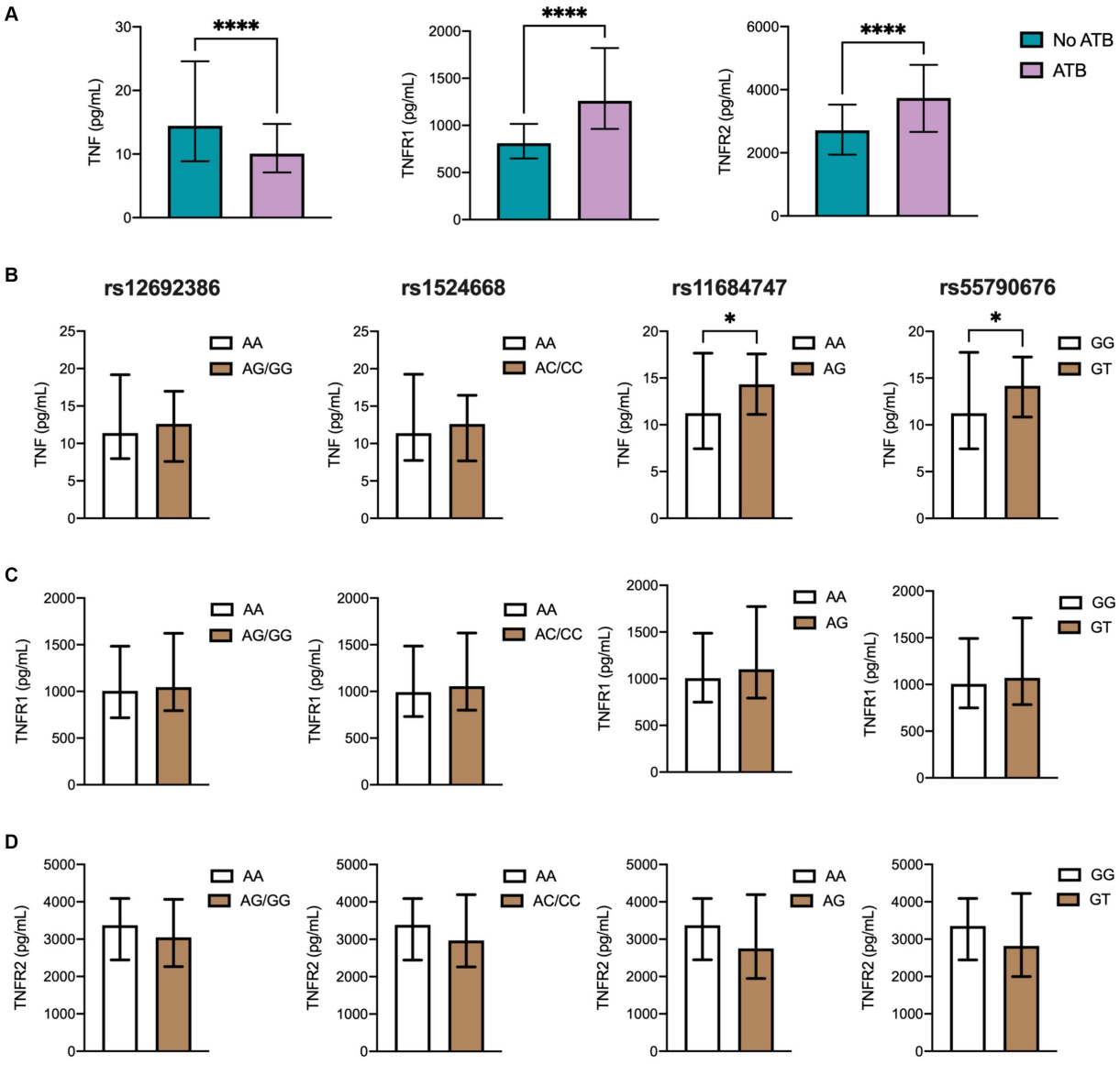

FIGURE 2
TNF and TNFRs plasma levels in the different TB groups. **(A)** Soluble levels of TNF, TNFR1, and TNFR2 were assessed by ELISA. Genotype distribution according to **(B)** TNF, **(C)** TNFR1, and **(D)** TNFR2 levels in the population, including 224 ATB patients and controls comprehending 70 individuals with LTB (QTF+) and 48 with no LTB (QTF−). Data are displayed as median and IQR values. Differences between groups were performed using the Mann–Whitney U test, *$p < 0.05$, and **** $p < 0.0001$.

ADAM17 were inversely correlated with ATB, whereas homozygous to ancestral alleles of these SNPs were positively associated with disease status.

To confirm these findings, we also carried out a multiple regression analysis on rs11684747 and rs55790676 SNPs, considering the TNF, TNFRs, and genotypes. The analytical model was based on the allele with higher frequency in ATB to find a correlation with the disease. This model showed that TNFR1 and TNFR2 correlate with the presence of rs11684747, as well as TNF and TNFR1 individually, TNFR1/TNFR2, and TNF/TNFR1/TNFR2. Moreover, both TNFRs correlate with ATB and AA genotype to rs11684747. The second genotype, homozygous GG to rs55790676 correlated with TNFR1, TNFR2, and both together, but not ATB (Table 4).

4 Discussion

It is well known that genetic factors play a major role in both infection and clinical progression of TB. Many functional and population-based studies have demonstrated that polymorphisms located in genes of immune responses, as well as in genes related with metabolism, are involved in the susceptibility and the multiplexity of TB-host interactions and pathogenesis (Zuiga et al., 2012). TNF is a pivotal mediator in TB immunopathogenesis (Dorhoi and Kaufmann, 2014). As such, several association animal studies have linked low TNF levels with TB progression and morbidity (Kindler et al., 1989; Flynn et al., 1995; Roach et al., 2002; Mezouar et al., 2019), whereas treatment with TNF blockers is known to result in ATB reactivation and dissemination (Keane et al., 2001; Gómez-Reino et al., 2003;

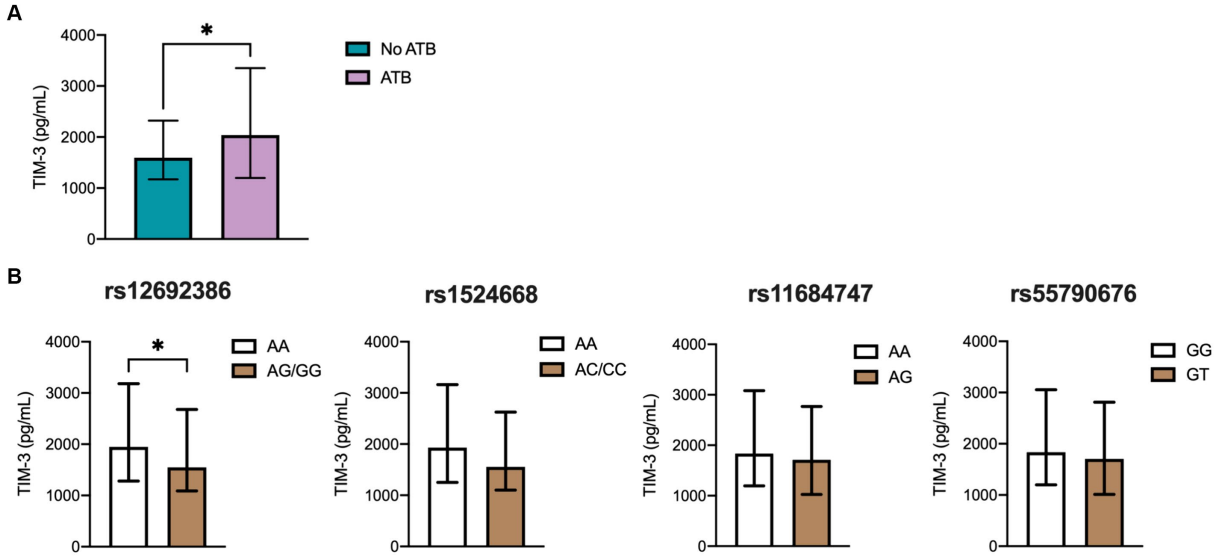

FIGURE 3
TIM-3 plasma levels in the different TB groups. **(A)** Soluble levels of TIM3 were assessed by ELISA. Genotype distribution according to **(B)** TIM-3 levels in the population, including 224 ATB patients and controls comprehending 70 individuals with LTB (QTF+) and 48 with no LTB (QTF–). Data are displayed as median and IQR values. Differences between groups were performed using the Mann–Whitney U test, $*p < 0.05$.

Mohan et al., 2004; Wallis et al., 2004), making TB screening mandatory before anti-TNF therapy (Fernández-Ruiz and Aguado, 2018). The immune effects of TNF are vast and depend on the interactions with either TNFR1 or TNFR2, triggering inflammation, anti-microbial immunity, and cell death. In TB, TNF orchestrates the early induction of chemokines to facilitate leucocyte recruitment and granuloma formation (Roach et al., 2002). Moreover, containment of Mtb infection is attuned to a highly regulated production of this cytokine from different sources, such as myeloid cells and T cells, with several complex mechanisms controlling its abundance and bioavailability to avoid pathogenic functions such as tissue necrosis (Dorhoi and Kaufmann, 2014).

Here, our results showed that TNF levels in ATB patients were lower than in their household contacts. Although previous reports indicated that TB patients have significantly higher TNF levels, those studies used a control group of healthy people with no history of contact with ATB patients, so their immune status against Mtb (QTF or PPD test) is unclear (Mirzaei and Mahmoudi, 2018; Beig et al., 2023). In this sense, our results are in consonance with other studies, where close contacts or healthy controls have higher levels than ATB patients across different age groups (Joshi et al., 2015). Furthermore, TNF expression at the transcriptional level was found to be lower in ATB than in household controls (De Sousa et al., 2023). Our results suggest that TNF might be a readout of loss of protective immunity against Mtb among people exposed to the bacillus, which agrees with a plethora of studies showing that the neutralization of TNF promotes the progression of latent TB infection to ATB (Lin et al., 2010).

One of the processes to optimize TNF expression and function is through the tight control of its interaction with TNFRs. Each of these receptors induces specific immune functions; TNFR1 mediates inflammation and tissue injury (Chavez-Galan et al., 2019), while TNFR2 mediates suppressive activity to reduce excessive inflammation (Chavez-Galan et al., 2017). The transmembrane forms of TNF, TNFR1, and TNFR2 are released into the extracellular space by the protease ADAM17 (Porteu and Nathan, 1990; Black et al., 1997; Mohan et al., 2002; Ruiz et al., 2021), which is essential in establishing a balance between TNF and TNFRs in cell surfaces and tissues. Soluble TNFRs are thought to favor anti-inflammatory functions, acting as decoy receptors of TNF (Kohno et al., 1990). For instance, it has been shown that high TNF levels can induce shedding of TNFR1 by ADAM17, and solTNFR1 then neutralizes circulating TNF, consequently attenuating excessive inflammation (Rowlands et al., 2011).

The metalloprotease function of ADAM17 is not limited to releasing TNF and TNFRs from the cell surface, also shedding more than 80 substrates, including cytokines, growth factors, and cell adhesion molecules receptors, including interleukin (IL)-R1, IL-R6, TGFβ, ACE-2, TIM-3, CD16, among other (Zunke and Rose-John, 2017). Also, it is functionally involved in pathogen recognition and may influence the potential uptake of invading pathogens, inducing the cleavage of PPRs and Toll-like receptors at the macrophages cell surface (Hernandez-Pando et al., 2000). Hence, ADAM17 might be crucial in the immunopathogenesis of several inflammatory disorders and infectious diseases, especially those that depend on TNF signaling and a balanced immune response for protective immunity. Despite this, there is little evidence about the association of ADAM17 with TB, a prototype infectious disease where immune regulation is pivotal in maintaining infection control at the lowest tissue-damage cost during LTB and displaying intense necrosis of granuloma in ATB progressors.

Previous reports suggest that SNPs of ADAM17 are associated with several disorders (Li et al., 2014, 2019; Shao et al., 2016; He et al., 2022; Jung and Hwang, 2022). Importantly, two studies showed that the rs12692386 A > G allele of ADAM17 increased the protease expression and shedding of TNF, IL-6R, and CX3CL1, conferring a higher risk of severe disease and shock in sepsis (Shao et al., 2016; He et al., 2022). Here, we analyzed four SNPs (rs12692386, rs1524668, rs11684747, rs55790676) of ADAM17

TABLE 4 Multiple logistic regression analysis of the association with TB status and levels of TNF and their receptors for the presence of ADAM17 rs11684747 and rs55790676.

Dependent variable	Independent variable	*Z*	*p*-value	OR
rs11684747				
AA				
	TB status (ATB)	0.05844	ns	0.7812
	TNF	1.812	0.0701	0.8293
	TNFR1	2.512	**0.0120**	0.9912
	TNFR2	2.682	**0.0073**	0.9967
	TB status (ATB): TNF	1.430	ns	0.6381
	TB status (ATB): TNFR1	1.305	ns	1.004
	TB status (ATB): TNFR2	0.4261	ns	1.001
	TNF: TNFR1	1.998	**0.0457**	1.000
	TNF: TNFR2	1.689	ns	1.000
	TNFR1: TNFR2	2.834	**0.0046**	1.000
	TB status (ATB): TNF: TNFR1	0.9368	ns	1.000
	TB status (ATB): TNF: TNFR2	1.537	ns	1.000
	TB status (ATB): TNFR1: TNFR2	2.035	**0.0419**	1.000
	TNF: TNFR1: TNFR2	2.028	**0.0426**	1.000
rs55790676				
GG				
	TB status (ATB)	0.5124	ns	0.1337
	TNF	1.299	ns	0.9050
	TNFR1	2.030	**0.0423**	0.9936
	TNFR2	2.455	**0.0141**	0.9970
	TB status (ATB): TNF	0.9732	ns	0.7794
	TB status (ATB): TNFR1	1.141	ns	1.004
	TB status (ATB): TNFR2	0.9367	ns	1.001
	TNF: TNFR1	1.531	ns	1.000
	TNF: TNFR2	1.532	ns	1.000
	TNFR1: TNFR2	2.463	**0.0138**	1.000
	TB status (ATB): TNF: TNFR1	0.9850	ns	1.000
	TB status (ATB): TNF: TNFR2	0.8013	ns	1.000
	TB status (ATB): TNFR1: TNF	1.891	0.0587	1.000
	TNF: TNFR1: TNFR2	1.669	ns	1.000

Statistical comparisons were performed using Multiple logistic regression with three-way interactions for only the two single nucleotide polymorphisms (SNPs) and alleles frequencies that showed a statistically significant difference between ATB and controls (QFT− and QFT+ individuals). The model included each allele, soluble levels in pg/mL of TNF and TNF receptors, and TB status. The absolute value of *Z*: is calculated as the coefficient estimate divided by its standard error. OR: odds ratio; ns: not significant *p*-value. *p* value in bold show a statistically significant difference.

looking for a possible association with TB progression. Although we did not find any relationship between rs12692386 A > G and TB susceptibility, we showed that people with rs11684747 A > G and rs55790676 G > T have higher circulating levels of TNF and are overrepresented among healthy close contacts with LTB compared to ATB patients. Together, both studies favor the assumption that ADAM17 takes a role during infection by modulating the production of inflammatory molecules, mainly TNF, which is required for protective immunity during LTB but could be detrimental when it is produced in excess, as in septic shock. In addition, despite rs12692386 being no different between groups, an association of homozygous AA to rs12692386 was found with patients displaying higher TIM-3 systemic levels, suggesting that the presence of this SNP could be involved in inducing an exhausting status in ATB.

In 2000, Hernández-Pando and colleagues demonstrated that the administration of batimastat, a broad-spectrum metalloproteinase inhibitor acting on ADAM17, reduces TB control in mice infected with Mtb via intratracheal instillation (Hernandez-Pando et al., 2000). In these animals, a delay in granuloma formation, higher disease progression, and increased mortality were associated with lower expression of TNF in lung tissue compared to untreated mice. Although these outcomes could be explained by the disruption of other proteases, the data confirm the protective role of TNF in TB, revealing a possible influence of ADAM17 in the process.

In line with this idea, our findings indicate that in healthy close contacts and LTB, ADAM17 acts principally by shedding TNF to maintain concentrations sufficient to keep infection control below a pathological threshold. Much lower levels might make the individual prone to disease progression. Accordingly, we found higher levels of TNF in close contacts than in ATB cases, mainly in those carrying rs11684747 and rs55790676. Thus, the acquisition of certain genetic variants of ADAM17 associated with higher cytokine production might be beneficial. However, in contrast with our results, other reports showed a link between high serum TNF levels and clinical severity of TB measured by chest X-ray alterations, weight loss, and positive PPD skin test (Júnior et al., 2008; Beig et al., 2023), whereas Kart et al. (2003) found no relationship between increased TNF levels and TB outcomes. Unfortunately, we had no clinical data on the severity of the disease in our ATB cohort. Hence, looking for differences in ATB outcomes according to TNF levels and ADAM17 SNPs is warranted for future investigations.

On the other hand, our data suggest a little effect of ADAM17 on TNFRs during LTB or resistance to infection status since the levels of these receptors were lower in healthy close contacts of ATB cases. Also, we did not find a relationship between SNPs and TNFR1 and TNFR2, although TNFRs levels tended to be lower in people carrying the rs11684747 A > G and rs55790676 G > T SNPs of ADAM17. Of note, the levels of TNFRs, mainly TNFR2, were higher in ATB patients compared to controls. Interestingly, a study in mice infected with aerosolized Mtb found high levels of TNFRs, especially TNFR2, in bronchioalveolar lavage specimens collected one month after inoculation. In this model, the investigators discovered that mannose-capped lipoarabinomannan (ManLAM) was sufficient to promote ADAM17 shedding of TNFR2, and a lower level of TNFR1, hindering the release of tmTNF (Richmond et al., 2012). In agreement with our findings, they also showed higher levels of TNFR2 among ATB patients.

Therefore, we believe that in close contacts resistant to Mtb infection and those with LTB, ADAM17 plays a protective role in keeping TNF levels in adequate concentrations. Nonetheless, when

protective immunity is disrupted by age, diabetes, or immune suppression, proliferation of bacilli increases the amount of ManLAM and other virulence factors, consequently promoting TNFR2 and TNFR1 release, which in turn block TNF signaling, further hindering protective immunity against Mtb. In this process, certain SNPs of ADAM17 might confer protection or susceptibility if they enhance the ability to maintain a favorable balance between TNF and TNFRs. This might extend to other infections like COVID-19, where a disbalance of proinflammatory and anti-inflammatory signals is crucial to determine clinical outcomes. Interestingly, the rs55790676 polymorphism was recently associated with an increased susceptibility to COVID-19 in India (Patil et al., 2021). Also, it is possible that this polymorphism might influence the expression of entry factors important for SARS-CoV-2 infection, as demonstrated by functional studies showing that a lower expression of ADAM17 provokes a reduced release of ACE2 from the cell membrane (Healy and Lilic, 2021), whereas increased protease activity primes the viral S protein favoring susceptibility to SARS-CoV-2 infection (Jocher et al., 2022).

The current study has limitations that must be considered when interpreting the results. Firstly, the small sample size limited our statistical power to examine a small genetic effect, decreasing the accuracy of our genotype–phenotype analyses and hindering the possibility of making more comparisons between certain groups of participants. Due to low allele frequency, we could not identify enough individuals homozygous GG to rs11684747 and TT to rs55790676. Also, the case–control design of this study may bias any true relationship between ADAM17 SNPs and ATB. In addition, the rs11689958 allele was not assessed in our study, which shows a solid pairwise linkage disequilibrium with other SNPs at the ADAM17 promoter region (Shao et al., 2016). Finally, due to technical limitations, we were unable to directly measure ADAM17 in our study. However, we hypothesized that if this protease significantly influences cytokine levels during TB, its effect would be reflected in the regulation of other immune molecules cleaved by ADAM17 that are involved in disease immunopathogenesis. Consequently, we chose to measure TIM-3 levels. TIM-3 is a co-inhibitory molecule that regulates T cell function and may play a role in TB. Recent research indicates that TIM-3 acts as an exhaustion marker in CD4+ and CD8+ T cells during Mtb infection (Jayaraman et al., 2016). Interestingly, we found higher levels of TIM-3 in ATB patients and those homozygous to the rs12692386 SNP of ADAM17, suggesting its involvement in chronic infection, which is in line with previous reports (Chen et al., 2022).

Hence, despite these caveats, our results provide preliminary data that open a novel and unexplored hypothesis of a possible role for ADAM17 in TB; however, the role of these SNPs in latent TB is unknown and requires further investigation in future larger studies. In sum, our main findings were that levels of TNF and TNFRs are influenced by SNPs of ADAM17 and distinguish ATB patients from close contacts. We observed that homozygous AA to rs11684747 and GG to rs55790676 exhibited lower plasma levels of TNF than heterozygous individuals. In contrast, homozygous patients AA to rs11684747 and GG to rs55790676 showed lower levels of TNFR2 when compared to heterozygous individuals. Multiple regression analyses showed a significant association between the levels of TNF, TNFR1, TNFR2, tuberculosis status, and the AA homozygosity on the rs11684747 SNP. This study suggests a role for SNPs of ADAM17 in genetic susceptibility to ATB that warrants further research.

Data availability statement

The datasets presented in this study can be found in online repositories. The names of the repository/repositories and accession number(s) can be found below: https://www.ncbi.nlm.nih.gov/clinvar/, SCV005043058, SCV005043059, SCV005043068, SCV005043069.

Ethics statement

The studies involving humans were approved by the study was approved by the Institutional Review Board of Instituto Nacional de Enfermedades Respiratorias Ismael Cosío Villegas (protocol code B04-23, approved in February 2023). Informed consent was obtained from all subjects involved in the study. The studies were conducted in accordance with the local legislation and institutional requirements. The participants provided their written informed consent to participate in this study.

Author contributions

JC-P: Conceptualization, Methodology, Writing – original draft, Formal analysis, Investigation. LR-L: Conceptualization, Formal analysis, Investigation, Methodology, Writing – original draft, Supervision. MC: Methodology, Writing – review & editing. EO-M: Methodology, Writing – review & editing. AT-G: Methodology, Writing – review & editing. MM-M: Methodology, Writing – review & editing. AC-L: Methodology, Writing – review & editing, Validation. GR-M: Methodology, Writing – review & editing. IG-G: Methodology, Writing – review & editing. JR-N: Writing – review & editing, Investigation. BG-P: Methodology, Writing – review & editing. KL-S: Methodology, Writing – review & editing. FJ-J: Methodology, Writing – review & editing. PG-O: Methodology, Writing – review & editing. CS-L: Methodology, Writing – review & editing. KB-P: Formal analysis, Writing – review & editing. MM-T: Data curation, Writing – review & editing. LC-G: Conceptualization, Methodology, Resources, Supervision, Writing – original draft, Writing – review & editing. JZ: Data curation, Formal analysis, Funding acquisition, Methodology, Project administration, Writing – original draft, Writing – review & editing.

Funding

The author(s) declare financial support was received for the research, authorship, and/or publication of this article. This research was supported by research funds of the Instituto Nacional de Enfermedades Respiratorias Ismael Cosío Villegas (INER), and by the National Council of Humanities, Science and Technology of Mexico (CONAHCYT), grant number FORDECYT/10SE/2020/05/14-06 and FORDECYT/10SE/2020/05/14-07 from the Fondo Institucional de Fomento Regional para el Desarrollo Científico y Tecnológico y de Innovación (FORDECYT) to JZ. JZ also received support from the Secretaría de Ciencia, Tecnología e Innovación de la Ciudad de México (SECTEI CDMX) under the contract SECTEI/050/2020. JC-P is receiving a scholarship from INER to achieve his M.D. degree in pneumology and critical care medicine.

Acknowledgments

The authors thank all participants in this study and Mario Preciado García for the technical assistance.

Conflict of interest

The authors declare that the research was conducted in the absence of any commercial or financial relationships that could be construed as a potential conflict of interest.

The author(s) declared that they were an editorial board member of Frontiers, at the time of submission. This had no impact on the peer review process and the final decision.

Publisher's note

Supplementary material

The Supplementary material for this article can be found online at: https://www.frontiersin.org/articles/10.3389/fmicb.2024.1392782/full#supplementary-material

References

Aboudounya, M. M., and Heads, R. J. (2021). COVID-19 and toll-like receptor 4 (TLR4): SARS-CoV-2 may bind and activate TLR4 to increase ACE2 expression, facilitating entry and causing Hyperinflammation. *Mediat. Inflamm.* 2021, 1–18. doi: 10.1155/2021/8874339

Adane, G., Lemma, M., Geremew, D., Sisay, T., Tessema, M. K., Damtie, D., et al. (2021). Genetic polymorphism of tumor necrosis factor-alpha, interferon-gamma and Interleukin-10 and association with risk of *Mycobacterium Tuberculosis* infection. *J. Evid. Based Integr. Med.* 26:2515690X2110063. doi: 10.1177/2515690X211006344

Barrett, J. C., Fry, B., Maller, J., and Daly, M. J. (2005). Haploview: analysis and visualization of LD and haplotype maps. *Bioinformatics* 21, 263–265. doi: 10.1093/bioinformatics/bth457

Beig, T. Y., Khan, U. H., Ganie, B. A., Tahir, S., Shah, S., and Dhobi, G. N. (2023). Correlation between serum tumor necrosis factor-alpha (TNF-α) and clinical severity of tuberculosis: a hospital-based study. *Cureus* 15:e35626. doi: 10.7759/CUREUS.35626

Black, R. A., Rauch, C. T., Kozlosky, C. J., Peschon, J. J., Slack, J. L., Wolfson, M. F., et al. (1997). A metalloproteinase disintegrin that releases tumour-necrosis factor-∅ from cells. *Nature* 385, 729–733. doi: 10.1038/385729a0

Chavez-Galan, L., Vesin, D., Blaser, G., Uysal, H., Benmerzoug, S., Rose, S., et al. (2019). Myeloid cell TNFR1 signaling dependent liver injury and inflammation upon BCG infection. *Sci. Rep.* 9, 5297–5215. doi: 10.1038/s41598-019-41629-9

Chavez-Galan, L., Vesin, D., Uysal, H., Blaser, G., Benkhoucha, M., Ryffel, B., et al. (2017). Transmembrane tumor necrosis factor controls myeloid-derived suppressor cell activity via TNF receptor 2 and protects from excessive inflammation during BCG-induced pleurisy. *Front. Immunol.* 8:999. doi: 10.3389/fimmu.2017.00999

Chen, H., Zhou, J., Zhao, X., Liu, Q., Shao, L., Zhu, Y., et al. (2022). Characterization of multiple soluble immune checkpoints in individuals with different *Mycobacterium tuberculosis* infection status and dynamic changes during anti-tuberculosis treatment. *BMC Infect. Dis.* 22:543. doi: 10.1186/s12879-022-07506-z

De Sousa, F. D. M., de Paula Souza, I., Amoras, E. D. S. G., Lima, S. S., Cayres-Vallinoto, I. M. V., Ishak, R., et al. (2023). Low levels of TNFA gene expression seem to favor the development of pulmonary tuberculosis in a population from the Brazilian Amazon. *Immunobiology* 228:152333. doi: 10.1016/J.IMBIO.2023.152333

Diel, R., Loddenkemper, R., and Nienhaus, A. (2012). Predictive value of interferon-γ release assays and tuberculin skin testing for progression from latent TB infection to disease state: a meta-analysis. *Chest* 142, 63–75. doi: 10.1378/CHEST.11-3157

Dorhoi, A., and Kaufmann, S. H. E. (2014). Tumor necrosis factor alpha in mycobacterial infection. *Semin. Immunol.* 26, 203–209. doi: 10.1016/j.smim.2014.04.003

Dunlap, M. D., Howard, N., Das, S., Scott, N., Ahmed, M., Prince, O., et al. (2018). A novel role for C-C motif chemokine receptor 2 during infection with hypervirulent *Mycobacterium tuberculosis*. *Mucosal Immunol.* 11, 1727–1742. doi: 10.1038/S41385-018-0071-Y

Esaulova, E., Das, S., Singh, D. K., Choreño-Parra, J. A., Swain, A., Arthur, L., et al. (2021). The immune landscape in tuberculosis reveals populations linked to disease and latency. *Cell Host Microbe* 29, 165–178.e8. doi: 10.1016/J.CHOM.2020.11.013

Fernández-Ruiz, M., and Aguado, J. M. (2018). Risk of infection associated with anti-TNF-α therapy. *Expert Rev. Anti-Infect. Ther.* 16, 939–956. doi: 10.1080/14787210.2018.1544490

Flynn, J. A. L., Chan, J., Triebold, K. J., Dalton, D. K., Stewart, T. A., and Bloom, B. R. (1993). An essential role for interferon gamma in resistance to *Mycobacterium tuberculosis* infection. *J. Exp. Med.* 178, 2249–2254. doi: 10.1084/JEM.178.6.2249

Flynn, J. A. L., Goldstein, M. M., Chan, J., Triebold, K. J., Pfeffer, K., Lowenstein, C. J., et al. (1995). Tumor necrosis factor-alpha is required in the protective immune response against *Mycobacterium tuberculosis* in mice. *Immunity* 2, 561–572. doi: 10.1016/1074-7613(95)90001-2

Gabriel, S. B., Schaffner, S. F., Nguyen, H., Moore, J. M., Roy, J., Blumenstiel, B., et al. (2002). The structure of haplotype blocks in the human genome. *Science* 296, 2225–2229. doi: 10.1126/science.1069424

Getahun, H., Matteelli, A., Chaisson, R. E., and Raviglione, M. (2015). Latent *Mycobacterium tuberculosis* infection. *N. Engl. J. Med.* 372, 2127–2135. doi: 10.1056/NEJMRA1405427

Global Tuberculosis Report 2023 (n.d.). Available at: https://www.who.int/teams/global-tuberculosis-programme/tb-reports/global-tuberculosis-report-2023 (Accessed January 25, 2024).

Gómez-Reino, J. J., Carmona, L., Rodríguez Valverde, V., Mola, E. M., and Montero, M. D. (2003). Treatment of rheumatoid arthritis with tumor necrosis factor inhibitors may predispose to significant increase in tuberculosis risk: a multicenter active-surveillance report. *Arthritis Rheum.* 48, 2122–2127. doi: 10.1002/ART.11137

He, J., Zhao, T., Liu, L., Liao, S., Yang, S., Lu, F., et al. (2022). The −172 A-to-G variation in ADAM17 gene promoter region affects EGR1/ADAM17 pathway and confers susceptibility to septic mortality with sepsis-3.0 criteria. *Int. Immunopharmacol.* 102:108385. doi: 10.1016/J.INTIMP.2021.108385

Healy, E. F., and Lilic, M. (2021). A model for COVID-19-induced dysregulation of ACE2 shedding by ADAM17. *Biochem. Biophys. Res. Commun.* 573, 158–163. doi: 10.1016/J.BBRC.2021.08.040

Hernandez-Pando, R., Orozco, H., Arriaga, K., Pavön, L., and Rook, G. (2000). Treatment with BB-94, a broad spectrum inhibitor of zinc-dependent metalloproteinases, causes deviation of the cytokine profile towards type-2 in experimental pulmonary tuberculosis in Balb/c mice. *Int. J. Exp. Pathol.* 81, 199–209. doi: 10.1046/J.1365-2613.2000.00152.X

Houben, R. M. G. J., and Dodd, P. J. (2016). The global burden of latent tuberculosis infection: a re-estimation using mathematical modelling. *PLoS Med.* 13:e1002152. doi: 10.1371/journal.pmed.1002152

Jayaraman, P., Jacques, M. K., Zhu, C., Steblenko, K. M., Stowell, B. L., Madi, A., et al. (2016). TIM3 mediates T cell exhaustion during *Mycobacterium tuberculosis* infection. *PLoS Pathog.* 12:e1005490. doi: 10.1371/JOURNAL.PPAT.1005490

Jocher, G., Grass, V., Tschirner, S. K., Riepler, L., Breimann, S., Kaya, T., et al. (2022). ADAM10 and ADAM17 promote SARS-CoV-2 cell entry and spike protein-mediated lung cell fusion. *EMBO Rep.* 23:e54305. doi: 10.15252/EMBR.202154305

Joshi, L., Ponnana, M., Sivangala, R., Chelluri, L. K., Nallari, P., Penmetsa, S., et al. (2015). Evaluation of TNF-α, IL-10 and IL-6 cytokine production and their correlation with genotype variants amongst tuberculosis patients and their household contacts. *PLoS One* 10:e0137727. doi: 10.1371/JOURNAL.PONE.0137727

Jung, J., and Hwang, D. (2022). Genetic polymorphism of ADAM17 and decreased bilirubin levels are associated with allergic march in the Korean population. *BMC Med. Genet.* 15:21. doi: 10.1186/s12920-022-01170-7

Júnior, A., De, D. R., Santos, S. A. D., Castro, I., and Andrade, D. R. (2008). Correlation between serum tumor necrosis factor alpha levels and clinical severity of tuberculosis. *Braz. J. Infect. Dis.* 12, 226–233. doi: 10.1590/S1413-86702008000300013

Kart, L., Buyukoglan, H., Tekin, I. O., Altin, R., Senturk, Z., Gulmez, I., et al. (2003). Correlation of serum tumor necrosis factor-α, interleukin-4 and soluble interleukin-2 receptor levels with radiologic and clinical manifestations in active pulmonary tuberculosis. *Mediat. Inflamm.* 12, 9–14. doi: 10.1080/0962935031000096926

Keane, J., Gershon, S., Wise, R. P., Mirabile-Levens, E., Kasznica, J., Schwieterman, W. D., et al. (2001). Tuberculosis associated with infliximab, a tumor necrosis factor alpha-neutralizing agent. *N. Engl. J. Med.* 345, 1098–1104. doi: 10.1056/NEJMOA011110

Khader, S. A., Divangahi, M., Hanekom, W., Hill, P. C., Maeurer, M., Makar, K. W., et al. (2019). Targeting innate immunity for tuberculosis vaccination. *J. Clin. Invest.* 129, 3482–3491. doi: 10.1172/JCI128877

Kindler, V., Sappino, A. P., Grau, G. E., Piguet, P. F., and Vassalli, P. (1989). The inducing role of tumor necrosis factor in the development of bactericidal granulomas during BCG infection. *Cell* 56, 731–740. doi: 10.1016/0092-8674(89)90676-4

Kohno, T., Brewer, M. T., Baker, S. L., Schwartz, P. E., King, M. W., Hale, K. K., et al. (1990). A second tumor necrosis factor receptor gene product can shed a naturally occurring tumor necrosis factor inhibitor. *Proc. Natl. Acad. Sci. USA* 87, 8331–8335. doi: 10.1073/PNAS.87.21.8331

Li, W.-W., Shen, Y.-Y., Chen, D.-W., Li, H.-Y., Shi, Q.-Q., Mei, J., et al. (2019). Genetic association between NGFR, ADAM17 gene polymorphism, and Parkinson's disease in the Chinese Han population. *Neurotox. Res.* 36, 463–471. doi: 10.1007/s12640-019-00031-z

Li, Y., Yang, C., Ma, G., Cui, L., Gu, X., Chen, Y., et al. (2014). Analysis of ADAM17 polymorphisms and susceptibility to sporadic abdominal aortic aneurysm. *Cell. Physiol. Biochem.* 33, 1426–1438. doi: 10.1159/000358708

Lin, P. L., Myers, A., Smith, L., Bigbee, C., Bigbee, M., Fuhrman, C., et al. (2010). Tumor necrosis factor neutralization results in disseminated disease in acute and latent *Mycobacterium tuberculosis* infection with normal granuloma structure in a cynomolgus macaque model. *Arthritis Rheum.* 62, 340–350. doi: 10.1002/ART.27271

Mack, U., Migliori, G. B., Sester, M., Rieder, H. L., Ehlers, S., Goletti, D., et al. (2009). LTBI: latent tuberculosis infection or lasting immune responses to *M. tuberculosis*? A TBNET consensus statement. *Eur. Respir. J.* 33, 956–973. doi: 10.1183/09031936.00120908

Mezouar, S., Diarra, I., Roudier, J., Desnues, B., and Mege, J.-L. (2019). Tumor necrosis factor-alpha antagonist interferes with the formation of granulomatous multinucleated Giant cells: new insights into *Mycobacterium tuberculosis* infection. *Front. Immunol.* 10:1947. doi: 10.3389/fimmu.2019.01947

Mirzaei, A., and Mahmoudi, H. (2018). Evaluation of TNF-α cytokine production in patients with tuberculosis compared to healthy people. *GMS Hyg. Infect. Control.* 13:Doc09. doi: 10.3205/DGKH000315

Mohan, A. K., Coté, T. R., Block, J. A., Manadan, A. M., Siegel, J. N., and Braun, M. M. (2004). Tuberculosis following the use of etanercept, a tumor necrosis factor inhibitor. *Clin. Infect. Dis.* 39, 295–299. doi: 10.1086/421494

Mohan, M. J., Seaton, T., Mitchell, J., Howe, A., Blackburn, K., Burkhart, W., et al. (2002). The Tumor necrosis factor-α converting enzyme (TACE): a unique metalloproteinase with highly defined substrate selectivity. *Biochemistry* 41, 9462–9469. doi: 10.1021/bi0260132

Möller-Hackbarth, K., Dewitz, C., Schweigert, O., Trad, A., Garbers, C., Rose-John, S., et al. (2013). A disintegrin and metalloprotease (ADAM) 10 and ADAM17 are major sheddases of T cell immunoglobulin and mucin domain 3 (Tim-3). *J. Biol. Chem.* 288, 34529–34544. doi: 10.1074/jbc.M113.488478

Moss, M. L., and Minond, D. (2017). Recent advances in ADAM17 research: a promising target for Cancer and inflammation. *Mediat. Inflamm.* 2017, 1–21. doi: 10.1155/2017/9673537

Orme, I. M., Roberts, A. D., Griffin, J. P., and Abrams, J. S. (1993). Cytokine secretion by CD4 T lymphocytes acquired in response to *Mycobacterium tuberculosis* infection. *J. Immunol.* 151, 518–525. doi: 10.4049/JIMMUNOL.151.1.518

Patil, S., Pemmasani, S. K., Chitturi, N., Bhatnagar, I., Acharya, A., and Subash, L. V. (2021). COVID-19 and Indian population: a comparative genetic analysis. *medRxiv* 12:21267816. doi: 10.1101/2021.12.15.21267816

Porteu, F., and Nathan, C. (1990). Shedding of tumor necrosis factor receptors by activated human neutrophils. *J. Exp. Med.* 172, 599–607. doi: 10.1084/jem.172.2.599

Richmond, J. M., Duffy, E. R., Lee, J., Kaboli, K., Remick, D. G., Kornfeld, H., et al. (2012). Mannose-capped Lipoarabinomannan from *Mycobacterium tuberculosis* induces soluble tumor necrosis factor receptor production through tumor necrosis factor alpha-converting enzyme activation. *Infect. Immun.* 80, 3858–3868. doi: 10.1128/iai.00060-12

Roach, D. R., Bean, A. G. D., Demangel, C., France, M. P., Briscoe, H., and Britton, W. J. (2002). TNF regulates chemokine induction essential for cell recruitment, granuloma formation, and clearance of mycobacterial Infection1. *J. Immunol.* 168, 4620–4627. doi: 10.4049/jimmunol.168.9.4620

Rowlands, D. J., Islam, M. N., Das, S. R., Huertas, A., Quadri, S. K., Horiuchi, K., et al. (2011). Activation of TNFR1 ectodomain shedding by mitochondrial Ca2+ determines the severity of inflammation in mouse lung microvessels. *J. Clin. Invest.* 121, 1986–1999. doi: 10.1172/JCI43839

Ruiz, A., Palacios, Y., Garcia, I., and Chavez-Galan, L. (2021). Transmembrane TNF and its receptors TNFR1 and TNFR2 in mycobacterial infections. *Int. J. Mol. Sci.* 22:5461. doi: 10.3390/ijms22115461

Sada-Ovalle, I., Chavez-Galan, L., Torre-Bouscoulet, L., Nava-Gamino, L., Barrera, L., Jayaraman, P., et al. (2012). The Tim3-galectin 9 pathway induces antibacterial activity in human macrophages infected with *Mycobacterium tuberculosis*. *J. Immunol.* 189, 5896–5902. doi: 10.4049/jimmunol.1200990

Shao, Y., He, J., Chen, F., Cai, Y., Zhao, J., Lin, Y., et al. (2016). Association study between promoter polymorphisms of ADAM17 and progression of Sepsis. *Cell. Physiol. Biochem.* 39, 1247–1261. doi: 10.1159/000447830

Shimokata, K., Kishimoto, H., Takagi, E., and Tsunekawa, H. (1986). Determination of the T-cell subset producing gamma-interferon in tuberculous pleural effusion. *Microbiol. Immunol.* 30, 353–361. doi: 10.1111/J.1348-0421.1986.TB00952.X

Souza de Lima, D., Fadoul de Brito, C., Cavalcante Barbosa, A. R., de Andrade, B., Figueira, M., Maciel Bonet, J. C., et al. (2021). A genetic variant in the TRAF1/C5 gene lead susceptibility to active pulmonary tuberculosis by decreased TNF-α levels. *Microb. Pathog.* 159:105117. doi: 10.1016/J.MICPATH.2021.105117

Tameris, M. D., Hatherill, M., Landry, B. S., Scriba, T. J., Snowden, M. A., Lockhart, S., et al. (2013). Safety and efficacy of MVA85A, a new tuberculosis vaccine, in infants previously vaccinated with BCG: a randomised, placebo-controlled phase 2b trial. *Lancet* 381, 1021–1028. doi: 10.1016/S0140-6736(13)60177-4

Tsai, M. C., Chakravarty, S., Zhu, G., Xu, J., Tanaka, K., Koch, C., et al. (2006). Characterization of the tuberculous granuloma in murine and human lungs: cellular composition and relative tissue oxygen tension. *Cell. Microbiol.* 8, 218–232. doi: 10.1111/J.1462-5822.2005.00612.X

Tufariello, J. A. M., Chan, J., and Flynn, J. A. L. (2003). Latent tuberculosis: mechanisms of host and bacillus that contribute to persistent infection. *Lancet Infect. Dis.* 3, 578–590. doi: 10.1016/S1473-3099(03)00741-2

Wallis, R. S., Broder, M. S., Wong, J. Y., Hanson, M. E., and Beenhouwer, D. O. (2004). Granulomatous infectious diseases associated with tumor necrosis factor antagonists. *Clin. Infect. Dis.* 38, 1261–1265. doi: 10.1086/383317

Wang, X., Cao, Z., Jiang, J., Li, Y., Dong, M., Ostrowski, M., et al. (2011). Elevated expression of Tim-3 on CD8 T cells correlates with disease severity of pulmonary tuberculosis. *J. Infect.* 62, 292–300. doi: 10.1016/J.JINF.2011.02.013

Wu, S., Wang, M. G., Wang, Y., and He, J. Q. (2019). Polymorphisms of cytokine genes and tuberculosis in two independent studies. *Sci. Rep.* 9:2507. doi: 10.1038/S41598-019-39249-4

Zuiga, J., Torres-García, D., Santos-Mendoza, T., Rodriguez-Reyna, T. S., Granados, J., and Yunis, E. J. (2012). Cellular and humoral mechanisms involved in the control of tuberculosis. *Clin. Dev. Immunol.* 2012:193923. doi: 10.1155/2012/193923

Zunke, F., and Rose-John, S. (2017). The shedding protease ADAM17: physiology and pathophysiology. *Biochim. Biophys. Acta Mol. Cell Res.* 1864, 2059–2070. doi: 10.1016/j.bbamcr.2017.07.001

frontiers | Frontiers in Microbiology

TYPE Review
PUBLISHED 03 June 2024
DOI 10.3389/fmicb.2024.1394220

OPEN ACCESS

EDITED BY
Selvakumar Subbian,
The State University of New Jersey,
United States

REVIEWED BY
Yadong Zhang,
Harvard Medical School, United States
Thanh Quang Nguyen,
Gyeongsang National University,
Republic of Korea
Lina Davies Forsman,
Karolinska Institutet, Sweden

*CORRESPONDENCE
Bernadette M. Saunders
✉ Bernadette.Saunders@uts.edu.au

RECEIVED 01 March 2024
ACCEPTED 13 May 2024
PUBLISHED 03 June 2024

CITATION
Conyers LE and Saunders BM (2024) Treatment for non-tuberculous mycobacteria: challenges and prospects.
Front. Microbiol. 15:1394220.
doi: 10.3389/fmicb.2024.1394220

Treatment for non-tuberculous mycobacteria: challenges and prospects

Liberty E. Conyers and Bernadette M. Saunders*

School of Life Sciences, University of Technology Sydney, Sydney, NSW, Australia

Non-Tuberculous mycobacteria (NTM) are opportunistic environmental bacteria. Globally, NTM incidence is increasing and modeling suggests that, without new interventions, numbers will continue to rise. Effective treatments for NTM infections remain suboptimal. Standard therapy for *Mycobacterium avium* complex, the most commonly isolated NTM, requires a 3-drug regime taken for approximately 18 months, with rates of culture conversion reported between 45 and 70%, and high rates of relapse or reinfection at up to 60%. New therapeutic options for NTM treatment are urgently required. A survey of ongoing clinical trials for new NTM therapy listed on ClinicalTrials.Gov using the terms '*Mycobacterium avium*', '*Mycobacterium abscessus*', '*Mycobacterium intracellulare*', 'Non tuberculous Mycobacteria' and 'Nontuberculous Mycobacteria' and a selection criterion of interventional studies using antibiotics demonstrates that most trials involve dose and combination therapy of the guideline based therapy or including one or more of; Amikacin, Clofazimine, Azithromycin and the anti-TB drugs Bedaquiline and Linezolid. The propensity of NTMs to form biofilms, their unique cell wall and expression of both acquired and intrinsic resistance, are all hampering the development of new anti-NTM therapy. Increased investment in developing targeted treatments, specifically for NTM infections is urgently required.

KEYWORDS

Non-tuberculous mycobacteria, *Mycobacterium avium*, *Mycobacterium abscessus*, clinical trials, antibiotics, treatment regime

1 Introduction

Non-Tuberculous Mycobacteria (NTM) are environmental bacteria found commonly in soil and water, both natural and municipal sources. This group includes all members of the mycobacteria family excluding *Mycobacterium tuberculosis complex (TB)* and *Mycobacterium leprae*, the causative agents of tuberculosis and leprosy, respectively. NTMs represent a vast group of bacteria with over 190 distinct species (Armstrong et al., 2023). The most common causing disease in humans are the *Mycobacterium avium* complex (MAC), comprised of *Mycobacterium avium* and *Mycobacterium intracellulare*, then *Mycobacterium abscessus* (MAB) (Falkinham, 2013a). Obtaining accurate data on the extent of NTM infection is challenging, as NTMs are not notifiable diseases in many states or countries. Data from Queensland, Australia where NTMs are a notifiable disease, demonstrates that the number of NTM cases more than doubled in the last 10 years from 672 in 2012 (Thomson et al., 2017) to 1,490 cases in 2022 (Queensland Health, 2024). Current projections suggest NTM infections will triple by 2040 (Ratnatunga et al., 2020). Isolation of NTM are now eight times more common in Queensland than *M. tuberculosis*, with 191 cases of TB reported in 2023 versus 1,565 NTM

isolated (Queensland Health, 2024). While isolation of *M. tuberculosis* indicates clinical disease, the clinical relevance of an NTM isolation and the decision to treat is more contentious. Clinical, microbiological, and radiological guidelines developed by the ATS/IDSA are used to clarify the likelihood of NTM pulmonary disease versus colonization (Griffith et al., 2007; Schiff et al., 2019).

Increases in NTM infections have also been identified on multiple continents including North America, Europe, and Asia (Andréjak et al., 2010; Lai et al., 2010; Moore et al., 2010; Park et al., 2010; Taiwo and Glassroth, 2010; Donohue and Wymer, 2016; Diel et al., 2017a). South Korea reported a 5-fold increase in NTM infections between 2007 and 2016 from 6.7 cases per 100,000 to 39.6 per 100,000 with MAC and *M. abscessus* being the most frequently reported (Lee et al., 2019). Japan has also seen a rapid increase in NTM cases 5.7 cases per 100,000 in 2007 to 14.7 cases per 100,000 by 2014, with MAC again, being the most prevalent NTM identified (Namkoong et al., 2016). This incidence rate was higher than the rate of TB in Japan in 2014 at 12.9 cases per 100,000 population (Namkoong et al., 2016).

Multiple theories have been posed to explain the increased numbers of NTMs reported in recent years. Improvements in diagnostic techniques is making accurate diagnosis easier, with faster and more specific tests able to identify NTM infections. The number of individuals who are immunocompromised, and therefore vulnerable to NTM infection is on the rise. A NHIS survey reported an increase from 2.7% in 2013 to 6.6% in 2021 in immunocompromised individuals (Martinson and Lapham, 2024). Individuals with cystic fibrosis (*CF*), who thankfully show an increase in life expectancy are unfortunately, also at increased risk of developing an NTM infection (Ruseckaite et al., 2022).

The changing climate may be another reason for infection rates rising. A retrospective study by Sherrard et al. compared NTM infection rates between those living in tropical and subtropical regions of Queensland (Sherrard et al., 2017). Those living in tropical regions were 2.5 times more likely to be impacted by an NTM infection (Sherrard et al., 2017). Similarly, a large geographic study conducted across the United States found areas with a higher risk of NTM infection had greater levels of precipitation, evapotranspiration and higher average temperatures (Adjemian et al., 2012). In the tropical state of Hawaii, NTM cases *per capita* were four times higher than mainland states (Adjemian et al., 2012) with five novel mycobacterial species recently identified in Hawaiian soils (Hennessee et al., 2009). It is also possible that the tropical climate leads to more outdoor activities, such as hiking and swimming which increase chances of exposure to these bacteria (Koschel et al., 2006). With the changing climate, and expansion of tropical regions, this may increase the risk of NTM infection.

Even with increasing instances of infection, NTMs also have the significant issue of misdiagnosis. Clinically, NTM infections manifest with non-specific symptoms such as chronic cough, weight loss, fatigue and fever (Griffith et al., 2007). Diagnosis requires both clinical and microbiologic confirmation, including pulmonary symptoms, nodular or cavity opacities observed through imaging and positive cultures from sputum, bronchial wash or lavage or lung biopsy with mycobacterial histopathologic features (Griffith et al., 2007). NTMs can be misdiagnosed as TB, especially in areas where TB is endemic (Baldwin et al., 2019). One final and important distinction is that a positive NTM isolation does not always signify infection or disease. This further complicates the choice to begin treatment, or continue monitoring the patient, individual patient risk factors then need to be considered.

The general population is frequently exposed to *M. avium* and other NTMs during everyday activities. A common source of exposure occurs from showerheads, as bacteria found in the municipal water are aerosolized and inhaled (Gebert et al., 2018). NTMs are also found in soils when gardening and can be isolated from hospital equipment (Falkinham, 2013b). Despite the population being frequently exposed to NTM, only a very small percentage develop infection, with immunocompromised individuals at increased risk. NTM infection has been identified in 3.7–24% of *CF* patients with MAC and MAB being the most prevalent (Olivier et al., 2003; Levy et al., 2008; Roux et al., 2009; Hill et al., 2012). NTM infection in *CF* patients results in declined lung functionality and overall reduced life expectancy (Malouf and Glanville, 1999). HIV positive patients are also susceptible to NTM infections (Chai et al., 2022). Bacteria can disseminate from the lungs to anywhere in the body, with bone marrow, liver, spleen and lymph nodes the most common (Horsburgh, 1991; von Reyn et al., 2002). Inexplicably, another group with increased susceptibility to NTM infection, are slender, tall immunocompetent women between the ages of 50–80 (Chan and Iseman, 2010; Takayama et al., 2022). Often referred to as 'Lady Windemere' syndrome, studies have shown that women meeting these criteria are more likely to develop NTM infections. While chronic cough suppression has been hypothesized as a risk factor for their developing MAC disease no direct evidence explaining this increased susceptibility has been established. Some theories include decreased estrogen in post-menopausal women, or abnormalities in fibrillin which result in expression of immunosuppressive TGF-β may lead to greater susceptibility to NTM infections (Chan and Iseman, 2010).

These significant global increases make having an effective treatment for NTM disease increasingly important. Current treatment regimens are not optimal for efficient and sustained clearance of NTM infection. More research to elucidate antibiotics which are effective against NTM is essential. This review aims to highlight the significant challenges related to treatment of NTM infection, with compounding factors such as limited clinical trials, the paucity of NTM drug discovery pipelines and intrinsic and adaptive drug resistance of the pathogen all contributing to this challenge. It will also discuss opportunities of using new therapeutics to tackle this significant and growing problem.

2 Current treatment regime

2.1 Challenges of current treatment options

The current treatment for NTM infection is a minimum of three antibiotics. Most regimes include ethambutol and rifampicin with a macrolide backbone of either clarithromycin or azithromycin(Griffith et al., 2007). Due to the genetic variability of NTMs strains there is not one standardised treatment plan. Treatment is continued 12 months post a negative sputum culture(Griffith et al., 2007). However, studies report between 10 and 60% of patients experience relapse or reinfection within 6–12 months of initial therapy completion (Lee et al., 2015; Koh et al., 2017; Kwon et al., 2019). One possible reason for the poor outcome is the pharmacokinetic interactions between

antibiotics. A study by van Ingen et al. identified that rifampicin significantly reduced peak serum concentrations of macrolides, when used concurrently, clarithromycin and azithromycin concentrations were decreased by up to 68 and 23%, respectively (Van Ingen et al., 2012). If this decrease in serum concentration reduced macrolide killing efficacy in the lung is unknown. Macrolides have strong tissue penetration therefore it is possible therapeutic doses were still being achieved, however, the lack of synergy between these antibiotics may be reducing the efficacy of this treatment regime (Zuckerman et al., 2011).

2.2 Determination of the current treatment regime

The first "American Thoracic Society (ATS) declaration for Nontuberculous Mycobacteria identification and treatment" in 1990 recommended a four drug regimen including 300 mg isoniazid, 600 mg rifampin, and 25 mg/kg ethambutol for the first 2 months followed by 15 mg/kg for the remainder of treatment with streptomycin for the first three to 6 months of therapy (Wallace et al., 1990). This regimen was supported by data from two non-comparative clinical trials (Ahn et al., 1986; Seibert and Bass, 1989). In 1997, the regime was revised to incorporate the macrolides, clarithromycin or azithromycin, now a staple for MAC treatment (American Thoracic Society, 1997).

The ATS/IDSA recommendation for NTM treatment regime was based on data from a number of studies (Table 1) demonstrating that the inclusion of between 250 mg to 750 mg clarithromycin twice daily, to the ethambutol, rifampin and streptomycin regime was highly successful with conversion rates of between 78 and 92%, a low relapse rates of 18% and increased survival (Shafran et al., 1996; Wallace et al., 1996a). Subsequent studies investigating dosing frequency demonstrated a thrice weekly regimen was as effective while reducing toxicity to patients (Griffith et al., 1998, 2000, 2001). Recent studies have seen a shift from rifabutin to rifampin, as rifabutin was associated with higher rates of adverse events (Griffith et al., 2000, 2001). Rifabutin is still recommended as part of the ATS declaration, but is only used in more severe cases of MAC infection.

While the majority of studies demonstrate that the 3-drug regimen induces sputum conversion, the rate of initial conversion, and the rate of relapse, can vary significantly. Studies reported rates of sputum conversion between 47 and 92%, and a relapse rate of 18–39%, with a gradual decrease in rates of conversion evident over time (Table 1). This may be due growing rates of antibiotic resistance, especially against macrolides. Early studies, published in the late 90's were conducted when clarithromycin had been approved for use for less than a decade and resistance was uncommon (Gardner et al., 2005), whereas resistance was reported as an issue by 2003, and this may have contributed to the reduced conversion rates recorded (Kobashi and Matsushima, 2003).

In 2020 an updated report on the guidelines for NTM treatment was published by the ATS, European Respiratory Society (ERS), *European Society of Clinical Microbiology and Infectious Diseases (ESCMID) and the* Infectious Disease Society of America (IDSA). The three-drug regime of ethambutol, rifampicin and a macrolide for treatment of *M. avium* was again endorsed, with the addition of amikacin liposome inhalation suspension (ALIS), approved by the FDA in 2018, for serious infection (U.S. Food and Drug Administration, 2018). If amikacin or streptomycin do not induce negative conversion within 6 months the less toxic ALIS is recommended. While new clinical evidence was used to inform additions to treatment, the report acknowledges the need for 'well designed' clinical trials to justify further alterations to this current, best available, treatment regime.

This same report, also defined the treatment regime for MAB. While it acknowledges that the optimal drugs, regimes and duration of treatment for *M. abscessus* is not known, a combination of at least three drugs including a macrolide, amikacin, imipenem, cefoxitin and tigecycline was recommended (Daley et al., 2020). If the strain is macrolide susceptible at least three drugs should be used, in macrolide resistant strains, treatments should include at least four drugs (Daley et al., 2020). *M. abscessus* is particularly challenging to treat, with success rates ranging between 41 and 46% for all subspecies (Diel et al., 2017b; Kwak et al., 2019). To date, no antibiotic regime based on *in vitro* research has effectively produced long term sputum conversion for patients with *M. abscessus* (Griffith et al., 2007). For all NTMs developing new drugs, with shorter, less toxic, treatment regimens are a research priority.

3 Clinical trials

As indicated, additional clinical trials, to determine the optimum treatment regime for each NTM infection, are urgently required. Although *in vitro* and *in vivo* studies are essential to understand drug and bacterial interactions, translation of promising *in vitro* data into positive clinical correlations has often not been forthcoming (Griffith et al., 2007). Between 85 and 90% of drugs fail the clinical trial phase (Ledford, 2011; Sun et al., 2022). Of those which succeed, only half are approved for clinical use (Ledford, 2011). Unmanageable toxicity accounts for 30% failure, while lack of clinical efficacy is responsible for 40–50% of clinical trial failures (Sun et al., 2022). Factors that influence this lack of efficacy include, variability in metabolic pathways and drug metabolism, complexity and regulation between species and animal models which may not accurately reflect human disease (Pound et al., 2004; Brubaker and Lauffenburger, 2020). For mycobacterial infections most drug discovery research is focused on TB, with few drugs in the NTM development pipeline designed specifically for NTM disease (Wu et al., 2018; Dartois and Dick, 2022). Currently, drugs that show promise in TB are usually then tested on NTM diseases. A focus on progressing drugs that target NTMs to clinical trials is required to effectively address this.

An assessment of registered clinical trials for NTMs on ClinicalTrials.Gov, and searching common NTM using the terms 'Non tuberculous mycobacteria', 'Nontuberculous mycobacteria', '*Mycobacterium. avium*', '*Mycobacterium. intracellulare*' and '*Mycobacterium. abscessus*' and the selection criteria of clinical trial which (1) listed the use of an antibiotic, (2) was an interventional study and (3) listed an NTM under 'condition', identified 58 studies. Of these, 10 are listed as recruiting, 36 were completed with results to be released, and six provided results. One study was terminated, four were active not recruiting, with one with status unknown (Figure 1). The majority of these studies were testing a new antibiotic as monotherapy, or as an addition to the guideline-based therapy (GBT).

The trials with available data fall into two broad categories; studies looking at culture conversion following antibiotic use, or studies assessing pharmacokinetic drug interactions of antibiotics.

Of the trials assessing culture conversion, three utilized liposomal amikacin for inhibition (LAI), combined with standard therapy. The

TABLE 1 Studies guiding the ATS/IDSA recommendations for treatment of *M. avium* disease.

Study Title	Year published	Antibiotic regime	Conversion rate	Reference
Clarithromycin Regimens for Pulmonary *Mycobacterium avium* Complex The First 50 Patients	1996	500 mg clarithromycin twice daily, ethambutol, rifampin or rifabutin and initial streptomycin	Culture conversion 92% (38/39 individuals who completed 5+ months of therapy) Relapse rate 18%	Wallace et al. (1996a)
A Comparison of Two Regimens for the Treatment of *Mycobacterium avium* Complex Bacteremia in AIDS: Rifabutin, Ethambutol, and Clarithromycin versus Rifampin, Ethambutol, Clofazimine, and Ciprofloxacin	1996	Regimen A Rifampin, ethambutol, clofazimine and ciprofloxacin Regimen B Rifabutin (daily), ethambutol (daily), and clarithromycin (twice daily)	Culture conversion Regimen A 29% Regimen B 69%	Shafran et al. (1996)
Initial (6-Month) Results of Three-Times-Weekly Azithromycin in Treatment Regimens for *Mycobacterium avium* Complex Lung Disease in Human Immunodeficiency Virus-Negative Patients	1998	Regimen A TIW azithromycin, daily ethambutol, daily rifabutin and initial twice weekly (BIW) streptomycin Regimen B TIW azithromycin, TIW ethambutol, TIW rifabutin and initial BIW streptomycin	Culture conversion Regimen A 74% Regimen B 62%	Griffith et al. (1998)
Early Results (at 6 Months) with Intermittent Clarithromycin-Including Regimens for Lung Disease Due to *Mycobacterium avium* Complex	2000	Regimens of clarithromycin, rifabutin, and ethambutol TIW	Culture conversion 78%	Griffith et al. (2000)
Azithromycin-Containing Regimens for Treatment of *Mycobacterium avium* Complex Lung Disease	2001	Group A Azithromycin 300 mg-600 mg/day with companion drugs Group B Azithromycin 600 mg TIW with companion drugs daily Group C Azithromycin 600 mg TIW and companion drug TIW Companion drugs rifabutin or rifampin, ethambutol and initial streptomycin	Culture conversion Group A 59% Group B 55% Group C 65%	Griffith et al. (2001)
The Effect of Combined Therapy According to the Guidelines for the Treatment of *Mycobacterium avium* Complex Pulmonary Disease	2003	Clarithromycin, ethambutol, rifampicin and initial streptomycin for 12 months	Culture conversion 57.7% Relapse rate 39%	Kobashi and Matsushima (2003)
A double-blind randomized study of aminoglycoside infusion with combined therapy for pulmonary *Mycobacterium avium* complex disease	2007	Regimen A Rifampicin, ethambutol, clarithromycin and streptomycin Regimen B Rifampicin, ethambutol and clarithromycin	Culture conversion Regimen A 71.1% Regimen B 47.2% Relapse rate Regime A 30.8% Regimen B 35.1%	Kobashi et al. (2007)

addition of LAI to a GBT regime significantly improved culture conversion, rising to 26.7–33.3% within 12 months compared to 9–13.7% for standard therapies (Olivier et al., 2017; Griffith et al., 2018; Winthrop et al., 2021). Although superiority of a LAI containing regime is shown it is notable that these conversion rates of GBT only are lower than the rates referenced above. The inclusion criteria for these studies were patients already receiving at least 6 months of GBT, within the last 12 month. Studies have shown that conversion within 6 months is predictive of treatment success, therefore it is not unexpected that these patients may have decreased conversion rates (Moon et al., 2019). Amikacin is an aminoglycoside primarily used for treatment of NTM infection when macrolide resistant forms are

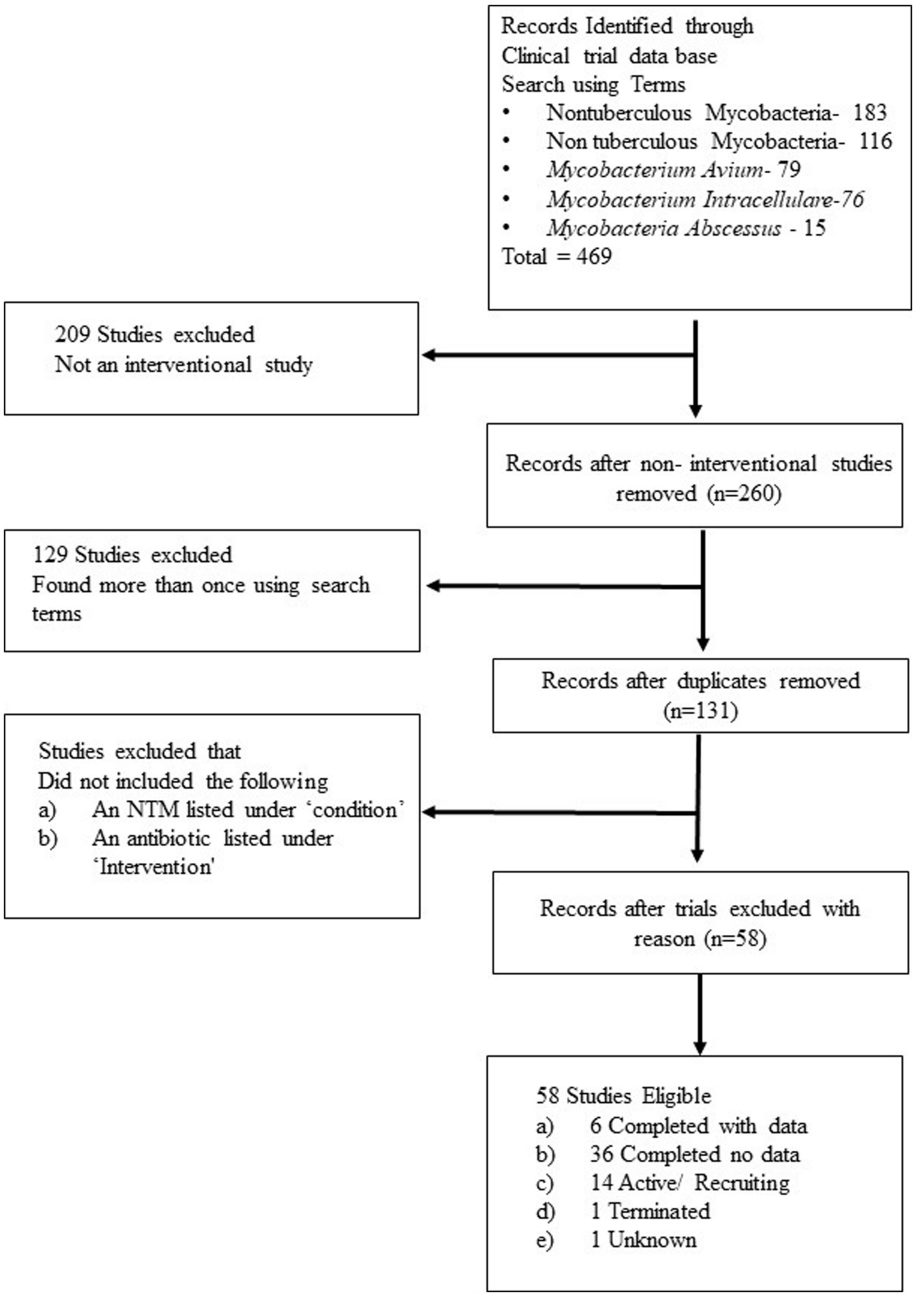

FIGURE 1
Flow diagram of clinical trial selection.

present. Side effects with amikacin are a significant issue, as amikacin treatment can cause irreversible ototoxicity and vestibular toxicity (Griffith et al., 2007). In the studies testing the addition of LAI (Table 2) it was administered as an inhalant. Adverse events, including COPD and bronchiectasis exacerbation, pneumonia, haemoptysis and worsening MAC infection remained high (Olivier et al., 2017; Griffith et al., 2021; Winthrop et al., 2021). LAI treatment was also successful in increasing conversion to culture negative for rapidly growing NTMs, with 50% conversion at 12 months, a 33% relapse rates and few serious adverse events (Siegel et al., 2023). An additional study adding the antibiotic tigecycline to GBT regimes for treatment of patients with *M. abscessus* and *M. chelonae* showed 60% improvement on culture conversion rates (Wallace et al., 2014).

Comorbidities and drug interactions with patients on treatment for other diseases such as *CF* and HIV pose additional challenges for treating NTM infections. The pharmacokinetic study, NCT01894776, revealed an antagonistic relationship between the antiretroviral drug, maraviroc and rifabutin. This antagonistic relationship, result in a suboptimal treatment responses for HIV+ patients (Abel et al., 2008). The relationship with treatments commonly prescribed for comorbidities such as *CF* and HIV in individuals being treated for NTM infection needs to be considered. This was recognized in 2015 by The US Cystic Fibrosis Foundation and the European Cystic Fibrosis Society in their joint statement that NTM disease poses a major threat to patients with *CF* (Floto et al., 2016). All current treatment guideline recommendations are based on data from patients without *CF* or

TABLE 2 Completed clinical trials, assessing liposomal amikacin for inhalation.

NCT number	Study title	# Participants	Groups tested	Culture conversion rates	Adverse Events	Reference
NCT01315236	Liposomal Amikacin for Inhalation (LAI) for Nontuberculous Mycobacteria	90	LAI + GBT, Placebo +GBT	Within 84 days ALIS+GBT 32% GBT 9%	Adverse Events LAI + GBT 93.18% Placebo+ GBT 86.67% Serious Adverse Events LAI + GBT 18.18% Placebo+ GBT 8.89%	Olivier et al. (2017)
NCT02344004	Study to Evaluate Efficacy of LAI When Added to Multi-drug Regimen Compared to Multidrug Regimen Alone	336	LAI + GBT, GBT	Within 6 months ALIS+GBT 29% GBT 9%	Adverse Events LAI + GBT 89.24%, GBT 64.29% Serious Adverse Events LAI + GBT 20.18%, GBT 7.14%	Griffith et al. (2018)
NCT02628600	Open-label Safety Extension Study Assessing Safety and Tolerability of LAI in Patients Who Participated in Study INS-212	163	LAI + GBT Naïve, LAI + GBT prior exposure	Within 6 months ALIS Naïve 26.7% Prior ALIS cohort 9.6% Within 12 months ALIS Naïve 33.3% Prior ALIS cohort 13.7%	Adverse Events LAI + GBT naïve 83.33% LAI + GBT Prior 61.64% Serious Adverse Events LAI + GBT naïve 35.56% LAI + GBT Prior 27.4%	Winthrop et al. (2021)
NCT03038178	Liposomal Amikacin for Inhalation (LAI) in the Treatment of *Mycobacterium abscessus* Lung Disease	33	LAI+ combinations of Azithromycin, Clofazimine, Tigecycline, Imipenem and Linezolid	Within 12 months 50%		Siegel et al. (2023)
NCT00600600	Tigecycline for Treatment of Rapidly Growing Mycobacteria	8	Tigecycline	48.1% following treatment		Wallace et al. (2014)

LAI, liposomal amikacin for inhibition; GBT, guideline-based therapy.

extrapolated from studies with TB (Peloquin, 1997; Griffith et al., 2007). Additional studies for NTM infections to optimize treatment regimens need to consider the potential of antagonistic drug interactions.

3.1 Optimizing treatment regimes

Optimizing the current treatment regime and investigating new or modified antibiotic regimens is critical to increase cure rates and reduce relapse. The FORMat study (NCT04310930) (Table 3), is a multi-arm study 'Finding the Optimal Regimen for *Mycobacterium abscessus* Treatment'. Other ongoing studies are introducing a new drug into the GBT, or studying the efficacy and safety of an isolated drug, which if successful these could lead to marked changes in therapy. The trial NCT05496374, is testing an aminobenzimidazole bacterial DNA gyrase -SPR720, which has demonstrated good activity against mycobacteria (Talley et al., 2021). If successful, SPR720 could be the first novel NTM antibiotic approved for use. The paucity of registered clinical trials for new NTM therapy is a major area of concern.

4 Challenges to developing new therapies

4.1 Antibiotic resistance

Antibiotic resistance is one factor that makes effective treatment of NTM disease challenging. Resistance to NTMs can be either acquired or intrinsic. Unlike most resistance mechanisms which occur from horizontal transfer of mutations, mycobacterial resistance to

TABLE 3 Active NTM clinical trials.

NCT number	Study title	Mycobacteria	Treatment administered	Brief description of study	Phase	Estimated enrolment numbers
NCT03672630	Comparison of Two- Versus Three-antibiotic Therapy for Pulmonary *Mycobacterium avium* Complex Disease	MAC	Azithromycin, Ethambutol, rifampicin	To test whether a 2-drug antibiotic regime can be as effective as a 3-drug regime while maintaining efficacy and increasing tolerability	2&3	500
NCT04677569	Study to Evaluate ALIS (Amikacin Liposome Inhalation Suspension) in Participants With Nontuberculous Mycobacterial Lung Infection Caused by *Mycobacterium avium* Complex	MAC	Azithromycin, Ethambutol, ALIS, ELC (ALIS Placebo)	To evaluate efficacy of ALIS in combination with Azithromycin and Ethambutol compared to Azithromycin and Ethambutol with a placebo empty liposome container on patients respiratory symptoms	3	250
NCT02968212	Clofazimine in the Treatment of Pulmonary *Mycobacterium avium* Complex (MAC)	MAC	Clofazimine, placebo sugar pill	To evaluate the clinical efficacy and safety of clofazimine when used to treat MAC disease	2	102
NCT04287049	A Study of Standard Drugs for *Mycobacterium avium* Complex	MAC	Azithromycin	To assess the early bactericidal activity of Azithromycin over the first 14 days of treatment for MAC disease (monotherapy) followed by treatment with GBT	2	30
NCT03236987	CLArithromycin Versus AZIthromycin in the Treatment of *Mycobacterium avium* Complex (MAC) Lung Infections	MAC	Azithromycin, Clarithromycin, Ethambutol, Rifampicin	To compare efficacy of the macrolides clarithromycin and azithromycin when used in combination with ethambutol and rifampicin	3	424
NCT04630145	A Study of Bedaquiline Administered as Part of a Treatment Regimen with Clarithromycin and Ethambutol in Adult Patients with Treatment-refractory *Mycobacterium avium* Complex lung Disease (MAC-LD)	MAC	Bedaquiline, clarithromycin, ethambutol, rifampicin, rifabutin	To evaluate the efficacy of bedaquiline compared with rifamycin when administered with clarithromycin and ethambutol in participants with MAC disease for 24 weeks	2&3	124

(Continued)

TABLE 3 (Continued)

NCT number	Study title	Mycobacteria	Treatment administered	Brief description of study	Phase	Estimated enrolment numbers
NCT04310930	Finding the Optimal Regimen for *Mycobacterium abscessus* Treatment	MAB	Amikacin, Tigecycline, Imipenem, Cefoxitin, Azithromycin, Clarithromycin, Clofazimine, Ethambutol, Linezolid, Cotrimoxazole	Aims to produce high quality evidence for the best treatment regimens to maximize health outcomes and minimize toxicity and treatment burden to guide decisions for starting treatment and measuring disease severity in patients with MAB	2&3	300
NCT04921943	Hypertonic Saline for MAC	MAC	Hypertonic saline, Azithromycin, Ethambutol, Rifampicin	A study testing whether hypertonic saline helps improve symptoms and clearance of mycobacteria in patients with *M. avium* complex lung infections	4	50
NCT05861258	Pharmacokinetic Study of Minocycline in Patients with Pulmonary Nontuberculous Mycobacterial Disease (Mino-PK)	MAC	Minocycline	Pharmacokinetic study to assess exposure to minocycline in MAC-PD patients with and without concurrent use of rifampicin	2	15
NCT05496374	A Study to Evaluate the Efficacy, Safety, Tolerability, and Pharmacokinetics of SPR720 as Compared with Placebo for the Treatment of Participants with *Mycobacterium avium* Complex (MAC) Pulmonary Disease	NTM	SPR720 (500 mg and 1,000 mg)	To assess the safety, tolerability, pharmacokinetic and microbiological response of NTM patients to various doses of SPR720 compared to a placebo	2	31
NCT04922554	Oral Omadacycline vs. Placebo in Adults with NTM Pulmonary Disease Caused by *Mycobacterium abscessus* Complex (MABc)	MAB	Omadacycline Oral Tablet, Placebo tablet	To evaluate the efficacy, safety and tolerability of oral omadacycline as compared to placebo in adults with MAB	2	75
NCT05327803	Study of Epetraborole in Patients with Treatment-refractory MAC Lung Disease	MAC	Epetraborole + OBR, Placebo + OBR	To test the superiority of epetraborole + OBR compared to placebo + OBR in patients with MAC	2&3	314

(Continued)

TABLE 3 (Continued)

NCT number	Study title	Mycobacteria	Treatment administered	Brief description of study	Phase	Estimated enrolment numbers
NCT06004037	Study to Evaluate the Efficacy of Delpazolid as Add-on Therapy in Refractory *Mycobacterium abscessus* Complex	MAB	Delpazolid	To evaluate the efficacy and safety of delpazolid add-on therapy in Patients with Refractory *Mycobacterium abscessus* Complex Pulmonary disease	2	20
NCT04616924	RHB-204 for the Treatment of Pulmonary *Mycobacterium avium* Complex Disease	MAC	RHB-204 (Oral capsule containing a combination of clarithromycin, rifabutin, and clofazimine), placebo	To evaluate the efficacy and safety of RHB-204 in adult subjects with underlying nodular bronchiectasis and documented MAC lung infection.	3	125
NCT04921943	Hypertonic Saline for MAC	MAC	Hypertonic saline, Azithromycin, Ethambutol, Rifampicin	A study testing whether hypertonic saline helps improve symptoms and clearance of mycobacteria in patients with *M. avium* complex lung infections	4	50

MAC, *Mycobacterium avium* complex; MAB, *Mycobacterium abscessus*; ALIS, amikacin liposome inhalation suspension; ELC, empty liposome control; OBR, Optimized background regime.

antibiotics occurs most commonly through spontaneous mutations on chromosomal genes (Nasiri et al., 2017). Single point mutations on the 23s rRNA gene (rrl) in positions 2058 or 2059 are the most commonly identified source of macrolide resistance (Meier et al., 1996; Wallace et al., 1996b). A mutation in the RNA polymerase beta subunit gene rPOB is responsible for 95% of rifampicin resistance and mutations on the emb CAB operon result in ethambutol resistance (Obata et al., 2006; Lingaraju et al., 2016).

Mutations can arise from a variety of different sources. NTM produce enzymes which can modify or neutralize antibiotics. This is achieved by preventing binding to the drug target or increasing susceptibility to hydrolysis by the bacteria, a classic example of this are beta lactamases (Luthra et al., 2018). Multiple NTM species also contain efflux pumps that contribute to decreased efficacy of antibiotics, by pumping antibiotics out of the cell into the external environment. Prolonged exposure of efflux pumps to NTM antibiotics, facilitated by long treatment times contribute to increased antibiotic resistance (Viveiros et al., 2003). Efflux pump inhibitors, such Verapamil can improve antibiotic success. Verapamil is a Ca^{2+} blocker, that decreases resistance to key NTM and TB drugs including rifampicin, isoniazid, streptomycin and bedaquiline (Song and Wu, 2016; Rodrigues et al., 2017). Finally, mutations in the transcription regulator whiB7, have a significant effect on susceptibility to mycobacterial infection, being associated with both hyper susceptibility and resistance (Warit et al., 2015; The Cryptic Consortium, 2022). Present in both pathogenic and non-pathogenic mycobacteria, whiB7 works on multiple pathways including antibiotic export and modifications of antibiotics and their targets (Burian et al., 2012; Cushman et al., 2021). WhiB7 transcription has been demonstrated to increase in the presence of antibiotics such as aminoglycosides and macrolides and confer various degrees of resistance (Burian et al., 2012). There have also been some reported instances where a frameshift mutation in whiB7 resulted in hyper susceptibility to clarithromycin (Warit et al., 2015). Using combinations of antibiotics lowers the instance of mutations, however, acquired resistance is not the only hurdle to effective treatment. Intrinsic resistance, such as the thick waxy cell wall and the proclivity to form biofilms also pose a significant treatment challenge.

Another challenge to effective treatment against NTMs is the difficulty in correlating *in vitro* drug susceptibility testing with clinical outcomes. Drug sensitivity testing for macrolides and amikacin demonstrate good clinical correlation, whereas minimum inhibitory concentration testing for rifampicin and ethambutol, do not show good correlation with clinical response (Daley, 2017).

4.2 Biofilms

In the environment *M. avium* often form biofilms, such as on PVC plastics in plumbing (Yamazaki et al., 2006b; Falkinham, 2011). Their slow growth rate, ability to adhere to other planktonic bacteria and to

plastics, all facilitate their persistence in waterways (Falkinham, 2018a). Recent murine studies have also shown that *M. avium's* successful persistence *in vivo* is largely dependent on its ability to colonize and establish biofilms within the lung (Yamazaki et al., 2006a). Once established, it is incredibly difficult to kill bacteria in this form. The MBCs of *M. avium* in biofilms are four to six times higher than in planktonic form treated with a single antibiotic (Batista et al., 2023). As the majority of chronic and recurrent bacterial infections are caused by bacteria in biofilm, being able to penetrate, and breakdown, the biofilm will be crucial to the success of new therapeutics (Mah, 2012).

4.3 Colony morphology

The smooth or rough appearance of NTM colony morphology can affect treatment. Although relevant in many species, colony morphology of *M. abscessus* is a key factor in treatment success. A retrospective multicentre cohort study conducted in Sweden between 2009 and 2020 found rough colony morphology was associated with worse treatment outcomes in patients with *M. abscessus*. Only 30% of patients achieved a clinical cure compared to 86% of patients with smooth morphology (Hedin et al., 2023). Mortality was also greater at 50% compared to 7% (Hedin et al., 2023). One key factor affecting colony morphology is the presence of glycopeptidolipids (GPL), with smooth colonies exhibiting higher GPL expression (Hedin et al., 2023). GPL also have a role in biofilm formation, with the smooth morphology *M. abscessus* forming biofilms by spreading out across the entire surface (Oschmann-Kadenbach et al., 2024). The exact mechanism for the poorer clinical outcomes with rough variants is unknown, however rough *M. abscessus* replicate more actively within macrophages and can spread more effectively between cells (Hedin et al., 2023). The rough variants also exhibit more cording, a virulence factor in mycobacterial infections known to inhibit macrophage phagocytosis (Howard et al., 2006; Hedin et al., 2023).

4.4 Cell wall

The unusual cell wall structure of mycobacteria also provides significant intrinsic resistance and a distinct survival advantage, enhancing viability and pathogenesis. Mycobacteria cell walls are highly lipid dense, lipids make up 60% of the cell wall mass (Kurz and Rivas-Santiago, 2020). This includes the outer lipids as well as mycolic acids. Mycolic acids are long chain acids comprising 60–90 carbon chains (Marrakchi et al., 2014; Minnikin and Brennan, 2020). Their structure contributes significantly to the low permeability of the mycobacterial cell wall (Liu et al., 1996). Mycolic acids attach to polysaccharides and then peptidoglycan and provide strength to the wall (Figure 2).

The cell wall is hydrophobic, while the majority of antibiotics are hydrophilic, and therefore cannot penetrate an intact cell wall (Falkinham, 2018b). Beta-lactams (β-lactams) and glycopeptides belong to a class of antibiotics which inhibit cell wall synthesis of both gram negative and positive bacteria (Batt et al., 2020). β-lactams, like penicillin and cephalosporins, work by irreversibly binding to the active sites of penicillin binding proteins and inhibiting 3 → 4 peptide crosslinking, hindering peptidoglycan synthesis of the cell wall (Kurz and Bonomo, 2012; Batt et al., 2020). Unfortunately, mycobacteria, have 3 → 3 peptide crosslinking, so are not inhibited by β-lactams(Kumar et al., 2012; Kurz and Bonomo, 2012). Glycopeptides, like vancomycin and teicoplanin also target peptidoglycan structures, inhibiting cell wall synthesis by binding to the C terminal acyl- D-ala-D-ala residues in peptidoglycan precursors (Reynolds, 1989). The thick waxy exterior of the NTMs hydrophobic outer layer, reduces the capacity of these glycopeptides to access the peptidoglycan layer thereby reducing the overall effectiveness of the antibiotic. Interestingly, mycobacteria have also developed additional strategies to survive cell wall disrupting antibiotics and can replicate in a cell wall deficient state.

5 NTMs and cell wall deficiency

When faced with antibiotic or nutrient stress NTMs are able to alter their morphology, forgoing their normal protective cell wall to grow in a cell wall deficient (CWD) state, previously called L-forms (Claessen and Errington, 2019). Without the cell wall, bacteria display as cocci (Mickiewicz et al., 2019). Cell wall deficiency enables NTMs to survive cell-wall targeting antibiotics and continue to replicate. CWD bacteria were first observed by Klieneberger in *Streptobacillus moniliformis* (Klieneberger, 1935). Initially speculated to be symbiosis between bacterial colonies, this theory was later abandoned by the author (Klieneberger, 1935; Klieneberger-Nobel, 1949). The discovery spurred on significant research into the phenomenon. Subsequent studies demonstrated that bacteria remain viable in these forms and revert back to their cell wall competent forms when the stress is removed (Mickiewicz et al., 2019). Studies in zebrafish have demonstrated that CWD can occur both *in vitro* and *in vivo* (Mickiewicz et al., 2019). The initial switch to a CWD form can occur rapidly in response to environmental factors. Multiple mycobacterial species, including *M. avium* and *M. tuberculosis*, can form viable CWD bacteria under chemical or cryogenic stress (Hines and Styer, 2003; Slavchev et al., 2016). It was initially thought that genetic alteration resulted in this morphological change, however, this was subsequently shown not to be the case, suggesting that changes in morphology were responsible for the increased antibiotic resistance (Slavchev et al., 2016). The potential to exploit the capacity of the bacteria to grow in a CWD state, as a treatment option is worth exploring. While in a CWD state the bacteria are resistant to cell wall inhibiting antibiotics, they may however, become more susceptible to other antibiotics,

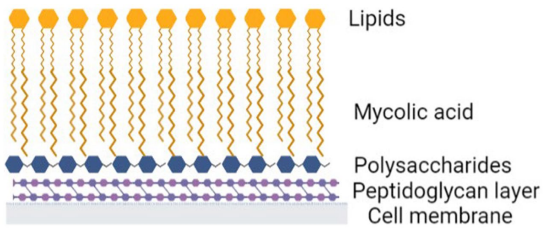

FIGURE 2
Mycobacteria cell wall. Created with Biorender.com

including those that are usually unable to penetrate the cell wall. Targeting synergy with new drugs combinations which induce CWD may provide alternatives to current treatment methods.

6 New options for NTM therapy

Treatment options for NTMs have largely been based on repurposing anti-TB antibiotics. This offers advantages in lower costs and less time to market. Increased instances of multi drug resistant (MDR) and extremely drug resistant (XDR) cases of TB have resulted in a greater focus on new pharmaceuticals with over 35 antibiotic candidates for TB treatment in discovery phase and approximately 30 in clinical trials (Wu et al., 2018). Exploring the options of repurposing antibiotics recently approved for TB, like bedaquiline and linezolid, use may identify new treatment options for NTM infections as well.

6.1 Bedaquiline

Bedaquiline was the first anti-TB drug approved for use by the FDA since rifampicin in 1971, approved against MDR and XDR-TB (World Health Organization, 2013; Nguyen et al., 2016). Bedaquiline acts by inhibiting ATP synthase and stopping mycobacterial F-ATP function, an affect specific to mycobacteria (Kundu et al., 2016). Low MICs have been shown when using this drug with good tolerability. The most significant adverse effect is a prolonging of QT intervals (Shulha et al., 2019) which needs to be monitored in patients. In TB studies, synergy has been shown between bedaquiline and other drugs including cephalosporins, linezolid and pyrazinamide (Khoshnood et al., 2021). While most data from this drug is on use against TB, one study has examined its effect on *M. avium*. This study found that the MIC90 was 0.015 μg/mL with 87% of isolates tested susceptible to bedaquiline at concentrations ≤0.008 μg/mL (Brown-Elliott et al., 2017), similar to the ranges those used for *M. tb* (Ismail et al., 2018). The inclusion of bedaquiline into XDR-TB treatment regimens lowered the risk of death compared to regimes not containing it (Schnippel et al., 2018). At least one listed clinical trial is currently recruiting to assess the effect of bedaquiline against NTM infection (Table 3).

6.2 Linezolid

Another antibiotic recently accepted for therapy against MDR and XRD TB is linezolid (Diekema and Jones, 2000). It acts by binding to 23 s and 50s ribosomal subunits of rRNA to inhibit bacterial protein synthesis at the initiation step (Diekema and Jones, 2000). The downside of linezolid is its high toxicity. A recent systematic review of 367 patients with MDR and XDR TB, found over 55% experienced some form of adverse effect (Zhang et al., 2015). Therapy was discontinued in 35% of these patients, most commonly occurring within the first 2 months (Zhang et al., 2015). Lower doses and shorter durations of antibiotics, by utilizing drugs with synergistic effects, could permit effective use of linezolid at reduced concentrations and thereby reduce toxicity. One study examining refractory NTM infection in 16 patients, demonstrated complete remission in 50% of patients and improvement in a further 25% but adverse reactions remained problematic (Chetchotisakd and Anunnatsiri, 2014). Newer drugs in this class of oxazolidinones are being developed for both TB and NTM infection, with the aim of having an improved safety and toxicity profile (Negatu et al., 2023). The outcome of ongoing studies to assess the effectiveness linezolid and bedaquiline to treat NTM infections are eagerly anticipated (Table 3).

6.3 Phage therapy

Bacteriophages, or phages, are viruses which infect and replicate exclusively within bacterial cells. They are highly diverse and found in abundance in the environment. Phages are host specific and often only infect a specific bacteria species or strain. Phages are absorbed by the bacterial host where they spread their genetic material, replicate and finally lyse the bacteria (Young et al., 2000). The use of phage therapy against NTM infection was first described in 2017 for two patients with *CF* and *M. abscessus* infection (Dedrick et al., 2019). The inclusion of phages, along with continued use of antibiotics, while not leading to complete clearance of the bacteria did generally result in improved clinical responses (Dedrick et al., 2019). A study across a small patient subpopulation receiving this therapy found phages successfully improved conditions in 75% of patients with a rough colony morphology (Dedrick et al., 2023). Several other studies using phages in humans also reported reducing NTM infection (Dedrick et al., 2019, 2021; Nick et al., 2022). Based on current research phages appear to be safe and well tolerated by patients. While resistance to bacteriophages has not been reported, host neutralization of phages may limit their effectiveness. There is also a considerable amount of personalization required for this therapy, making it more difficult to implement as a large-scale solution to NTM infection. Phages may be a useful tool, especially in combination with antibiotics. For large scale implementation, new antibiotics specific to NTM infections, are urgently required.

Expanding research to explore new antibiotics and therapeutic avenues that may demonstrate greater effectiveness against NTM disease is urgently required. Focusing on newly licensed anti-TB antibiotics, such as bedaquiline and linezolid in NTMs is one avenue, but new specific treatments will be required to manage the increasing public health threat posed by NTM disease.

Author contributions

LC: Writing – original draft, Writing – review, editing. BS: Conceptualization, Funding acquisition, Supervision, Writing – original draft, Writing – review, editing.

Funding

The author(s) declare financial support was received for the research, authorship, and/or publication of this article. LC was supported by an Australian Government Research Training Program Stipend.

Conflict of interest

The authors declare that the research was conducted in the absence of any commercial or financial relationships that could be construed as a potential conflict of interest.

Publisher's note

References

Abel, S., Jenkins, T. M., Whitlock, L. A., Ridgway, C. E., and Muirhead, G. J. (2008). Effects of Cyp3A4 inducers with and without Cyp3A4 inhibitors on the pharmacokinetics of maraviroc in healthy volunteers. *Br. J. Clin. Pharmacol.* 65, 38–46. doi: 10.1111/j.1365-2125.2008.03134.x

Adjemian, J., Olivier, K. N., Seitz, A. E., Falkinham, J. O. 3rd, Holland, S. M., and Prevots, D. R. (2012). Spatial clusters of nontuberculous mycobacterial lung disease in the United States. *Am. J. Respir. Crit. Care Med.* 186, 553–558. doi: 10.1164/rccm.201205-0913OC

Ahn, C. H., Ahn, S. S., Anderson, R. A., Murphy, D. T., and Mammo, A. (1986). A four-drug regimen for initial treatment of cavitary disease caused by *Mycobacterium avium* complex. *Am. Rev. Respir. Dis.* 134, 438–441

American Thoracic Society (1997). Diagnosis and treatment of disease caused by nontuberculous mycobacteria. This official statement of the American Thoracic Society was approved by the Board of Directors, march 1997. Medical section of the American Lung Association. *Am. J. Respir. Crit. Care Med.* 156, S1–S25. doi: 10.1164/ajrccm.156.2.atsstatement

Andréjak, C., Thomsen, V., Johansen, I. S., Riis, A., Benfield, T. L., Duhaut, P., et al. (2010). Nontuberculous pulmonary mycobacteriosis in Denmark: incidence and prognostic factors. *Am. J. Respir. Crit. Care Med.* 181, 514–521. doi: 10.1164/rccm.200905-0778OC

Armstrong, D. T., Eisemann, E., and Parrish, N. (2023). A brief update on mycobacterial taxonomy, 2020 to 2022. *J. Clin. Microbiol.* 61:e0033122. doi: 10.1128/jcm.00331-22

Baldwin, S. L., Larsen, S. E., Ordway, D., Cassell, G., and Coler, R. N. (2019). The complexities and challenges of preventing and treating nontuberculous mycobacterial diseases. *PLoS Negl. Trop. Dis.* 13:e0007083. doi: 10.1371/journal.pntd.0007083

Batista, S., Fernandez-Pittol, M., Nicolás, L. S., Martínez, D., Rubio, M., Garrigo, M., et al. (2023). Vitro effect of three-antibiotic combinations plus potential Antibiofilm agents against biofilm-producing Mycobacterium avium and *Mycobacterium intracellulare* clinical isolates. *Antibiotics* 12:1409. doi: 10.3390/antibiotics12091409

Batt, S. M., Burke, C. E., Moorey, A. R., and Besra, G. S. (2020). Antibiotics and resistance: the two-sided coin of the mycobacterial cell wall. *Cell Surf* 6:100044. doi: 10.1016/j.tcsw.2020.100044

Brown-Elliott, B. A., Philley, J. V., Griffith, D. E., Thakkar, F., and Wallace, R. J. (2017). In vitro susceptibility testing of Bedaquiline against *Mycobacterium avium* complex. *Antimicrob. Agents Chemother.* 61:e01798. doi: 10.1128/AAC.01798-16

Brubaker, D. K., and Lauffenburger, D. A. (2020). Translating preclinical models to humans. *Science* 367, 742–743. doi: 10.1126/science.aay8086

Burian, J., Ramón-García, S., Howes, C. G., and Thompson, C. J. (2012). WhiB7, a transcriptional activator that coordinates physiology with intrinsic drug resistance in *Mycobacterium tuberculosis*. *Expert Rev. Anti-Infect. Ther.* 10, 1037–1047. doi: 10.1586/eri.12.90

Chai, J., Han, X., Mei, Q., Liu, T., Walline, J. H., Xu, J., et al. (2022). Clinical characteristics and mortality of non-tuberculous mycobacterial infection in immunocompromised vs. Immunocompetent hosts. *Front. Med. (Lausanne)* 9:884446. doi: 10.3389/fmed.2022.884446

Chan, E. D., and Iseman, M. D. (2010). Slender, older women appear to be more susceptible to nontuberculous mycobacterial lung disease. *Gend. Med.* 7, 5–18. doi: 10.1016/j.genm.2010.01.005

Chetchotisakd, P., and Anunnatsiri, S. (2014). Linezolid in the treatment of disseminated nontuberculous mycobacterial infection in anti-interferon-gamma autoantibody-positive patients. *Southeast Asian J. Trop. Med. Public Health* 45, 1125–1131

Claessen, D., and Errington, J. (2019). Cell Wall deficiency as a coping strategy for stress. *Trends Microbiol.* 27, 1025–1033. doi: 10.1016/j.tim.2019.07.008

Cushman, J., Freeman, E., Mccallister, S., Schumann, A., Hutchison, K. W., and Molloy, S. D. (2021). Increased whiB7 expression and antibiotic resistance in *Mycobacterium chelonae* carrying two prophages. *BMC Microbiol.* 21:176. doi: 10.1186/s12866-021-02224-z

Daley, C. L. (2017). *Mycobacterium avium* complex disease. *Microbiol. Spectr.* 5:2017. doi: 10.1128/microbiolspec.TNMI7-0045-2017

Daley, C. L., Iaccarino, J. M., Lange, C., Cambau, E., Wallace, R. J. Jr., Andrejak, C., et al. (2020). Treatment of nontuberculous mycobacterial pulmonary disease: an official Ats/Ers/Escmid/Idsa clinical practice guideline. *Eur. Respir. J.* 56:2000535. doi: 10.1183/13993003.00535-2020

Dartois, V., and Dick, T. (2022). Drug development challenges in nontuberculous mycobacterial lung disease: Tb to the rescue. *J. Exp. Med.* 219:e20220445. doi: 10.1084/jem.20220445

Dedrick, R. M., Freeman, K. G., Nguyen, J. A., Bahadirli-Talbott, A., Smith, B. E., Wu, A. E., et al. (2021). Potent antibody-mediated neutralization limits bacteriophage treatment of a pulmonary *Mycobacterium abscessus* infection. *Nat. Med.* 27, 1357–1361. doi: 10.1038/s41591-021-01403-9

Dedrick, R. M., Guerrero-Bustamante, C. A., Garlena, R. A., Russell, D. A., Ford, K., Harris, K., et al. (2019). Engineered bacteriophages for treatment of a patient with a disseminated drug-resistant *Mycobacterium abscessus*. *Nat. Med.* 25, 730–733. doi: 10.1038/s41591-019-0437-z

Dedrick, R. M., Smith, B. E., Cristinziano, M., Freeman, K. G., Jacobs-Sera, D., Belessis, Y., et al. (2023). Phage therapy of Mycobacterium infections: compassionate use of phages in 20 patients with drug-resistant mycobacterial disease. *Clin. Infect. Dis.* 76, 103–112. doi: 10.1093/cid/ciac453

Diekema, D. I., and Jones, R. N. (2000). Oxazolidinones: a review. *Drugs* 59, 7–16. doi: 10.2165/00003495-200059010-00002

Diel, R., Jacob, J., Lampenius, N., Loebinger, M., Nienhaus, A., Rabe, K. F., et al. (2017a). Burden of non-tuberculous mycobacterial pulmonary disease in Germany. *Eur. Respir. J.* 49:1602109. doi: 10.1183/13993003.02109-2016

Diel, R., Ringshausen, F., Richter, E., Welker, L., Schmitz, J., and Nienhaus, A. (2017b). Microbiological and clinical outcomes of treating non-*Mycobacterium avium* complex nontuberculous mycobacterial pulmonary disease: a systematic review and Meta-analysis. *Chest* 152, 120–142. doi: 10.1016/j.chest.2017.04.166

Donohue, M. J., and Wymer, L. (2016). Increasing prevalence rate of nontuberculous mycobacteria infections in five states, 2008-2013. *Ann. Am. Thorac. Soc.* 13, 2143–2150. doi: 10.1513/AnnalsATS.201605-353OC

Falkinham, J. O. (2011). Nontuberculous mycobacteria from household plumbing of patients with nontuberculous mycobacteria disease. *Emerg. Infect. Dis.* 17, 419–424. doi: 10.3201/eid1703.101510

Falkinham, J. O. (2013a). Ecology of nontuberculous mycobacteria--where do human infections come from? *Semin. Respir. Crit. Care Med.* 34, 95–102. doi: 10.1055/s-0033-1333568

Falkinham, J. O. (2013b). Reducing human exposure to *Mycobacterium avium*. *Ann. Am. Thorac. Soc.* 10, 378–382. doi: 10.1513/AnnalsATS.201301-013FR

Falkinham, J. O. (2018a). *Mycobacterium avium* complex: adherence as a way of life. *AIMS Microbiol.* 4, 428–438. doi: 10.3934/microbiol.2018.3.428

Falkinham, J. O. (2018b). Challenges of Ntm drug development. *Front. Microbiol.* 9:1613. doi: 10.3389/fmicb.2018.01613

Floto, R. A., Olivier, K. N., Saiman, L., Daley, C. L., Herrmann, J.-L., Nick, J. A., et al. (2016). Us Cystic Fibrosis Foundation and European cystic fibrosis society consensus recommendations for the management of non-tuberculous mycobacteria in individuals with cystic fibrosis. *Thorax* 71, i1–i22. doi: 10.1136/thoraxjnl-2015-207360

Gardner, E. M., Burman, W. J., Degroote, M. A., Hildred, G., and Pace, N. R. (2005). Conventional and molecular epidemiology of macrolide resistance among new *Mycobacterium avium* complex isolates recovered from Hiv-infected patients. *Clin. Infect. Dis.* 41, 1041–1044. doi: 10.1086/433187

Gebert, M. J., Delgado-Baquerizo, M., Oliverio, A. M., Webster, T. M., Nichols, L. M., Honda, J. R., et al. (2018). Ecological analyses of mycobacteria in showerhead biofilms and their relevance to human health. *MBio* 9, e01614–e01618. doi: 10.1128/mBio.01614-18

Griffith, D. E., Aksamit, T., Brown-Elliott, B. A., Catanzaro, A., Daley, C., Gordin, F., et al. (2007). An official Ats/Idsa statement: diagnosis, treatment, and prevention of nontuberculous mycobacterial diseases. *Am. J. Respir. Crit. Care Med.* 175, 367–416. doi: 10.1164/rccm.200604-571ST

Griffith, D. E., Brown, B. A., Cegielski, P., Murphy, D. T., and Wallace, R. J. (2000). Early results (at 6 months) with intermittent clarithromycin-including regimens for lung disease due to *Mycobacterium avium* complex. *Clin. Infect. Dis.* 30, 288–292. doi: 10.1086/313644

Griffith, D. E., Brown, B. A., Girard, W. M., Griffith, B. E., Couch, L. A., and Wallace, R. J. Jr. (2001). Azithromycin-containing regimens for treatment of *Mycobacterium avium* complex lung disease. *Clin. Infect. Dis.* 32, 1547–1553. doi: 10.1086/320512

Griffith, D. E., Brown, B. A., Murphy, D. T., Girard, W. M., Couch, L., and Wallace, R. J. Jr. (1998). Initial (6-month) results of three-times-weekly azithromycin in treatment

regimens for *Mycobacterium avium* complex lung disease in human immunodeficiency virus-negative patients. *J. Infect. Dis.* 178, 121–126. doi: 10.1086/515597

Griffith, D. E., Eagle, G., Thomson, R., Aksamit, T. R., Hasegawa, N., Morimoto, K., et al. (2018). Amikacin liposome inhalation suspension for treatment-refractory lung disease caused by *Mycobacterium avium* complex (Convert). A prospective, open-label, randomized study. *Am. J. Respir. Crit. Care Med.* 198, 1559–1569. doi: 10.1164/rccm.201807-1318OC

Griffith, D. E., Thomson, R., Flume, P. A., Aksamit, T. R., Field, S. K., Addrizzo-Harris, D. J., et al. (2021). Amikacin liposome inhalation suspension for refractory *Mycobacterium avium* complex lung disease: sustainability and durability of culture conversion and safety of long-term exposure. *Chest* 160, 831–842. doi: 10.1016/j.chest.2021.03.070

Hedin, W., Fröberg, G., Fredman, K., Chryssanthou, E., Selmeryd, I., Gillman, A., et al. (2023). A rough Colony morphology of *Mycobacterium abscessus* is associated with Cavitary pulmonary disease and poor clinical outcome. *J. Infect. Dis.* 227, 820–827. doi: 10.1093/infdis/jiad007

Hennessee, C. T., Seo, J. S., Alvarez, A. M., and Li, Q. X. (2009). Polycyclic aromatic hydrocarbon-degrading species isolated from Hawaiian soils: *Mycobacterium crocinum* sp. nov., *Mycobacterium pallens* sp. nov., *Mycobacterium rutilum* sp. nov., *Mycobacterium rufum* sp. nov. and *Mycobacterium aromaticivorans* sp. nov. *Int. J. Syst. Evol. Microbiol.* 59, 378–387. doi: 10.1099/ijs.0.65827-0

Hill, U. G., Floto, R. A., and Haworth, C. S. (2012). Non-tuberculous mycobacteria in cystic fibrosis. *J. R. Soc. Med.* 105 Suppl 2, S14–S18. doi: 10.1258/jrsm.2012.12s003

Hines, M. E., and Styer, E. L. (2003). Preliminary characterization of chemically generated *Mycobacterium avium* subsp. *paratuberculosis* cell wall deficient forms (spheroplasts). *Vet. Microbiol.* 95, 247–258. doi: 10.1016/S0378-1135(03)00185-8

Horsburgh, C. R. (1991). *Mycobacterium avium* complex infection in the acquired immunodeficiency syndrome. *N. Engl. J. Med.* 324, 1332–1338. doi: 10.1056/NEJM199105093241906

Howard, S. T., Rhoades, E., Recht, J., Pang, X., Alsup, A., Kolter, R., et al. (2006). Spontaneous reversion of *Mycobacterium abscessus* from a smooth to a rough morphotype is associated with reduced expression of glycopeptidolipid and reacquisition of an invasive phenotype. *Microbiology (Reading)* 152, 1581–1590. doi: 10.1099/mic.0.28625-0

Ismail, N. A., Omar, S. V., Joseph, L., Govender, N., Blows, L., Ismail, F., et al. (2018). Defining Bedaquiline susceptibility, resistance, cross-resistance and associated genetic determinants: a retrospective cohort study. *EBioMedicine* 28, 136–142. doi: 10.1016/j.ebiom.2018.01.005

Khoshnood, S., Goudarzi, M., Taki, E., Darbandi, A., Kouhsari, E., Heidary, M., et al. (2021). Bedaquiline: Current status and future perspectives. *J. Glob. Antimicrob. Resist.* 25, 48–59. doi: 10.1016/j.jgar.2021.02.017

Klieneberger, E. (1935). The natural occurrence of pleuropneumonia-like organism in apparent symbiosis with *Strrptobacillus moniliformis* and other bacteria. *J. Pathol.* 40, 93–105. doi: 10.1002/path.1700400108

Klieneberger-Nobel, E. (1949). Origin, development and significance of L-forms in bacterial cultures. *Microbiology* 3, 434–443,

Kobashi, Y., and Matsushima, T. (2003). The effect of combined therapy according to the guidelines for the treatment of *Mycobacterium avium* complex pulmonary disease. *Intern. Med.* 42, 670–675. doi: 10.2169/internalmedicine.42.670

Kobashi, Y., Matsushima, T., and Oka, M. (2007). A double-blind randomized study of aminoglycoside infusion with combined therapy for pulmonary *Mycobacterium avium* complex disease. *Respir. Med.* 101, 130–138. doi: 10.1016/j.rmed.2006.04.002

Koh, W. J., Moon, S. M., Kim, S. Y., Woo, M. A., Kim, S., Jhun, B. W., et al. (2017). Outcomes of *Mycobacterium avium* complex lung disease based on clinical phenotype. *Eur. Respir. J.* 50:1602503. doi: 10.1183/13993003.02503-2016

Koschel, D., Pietrzyk, C., Sennekamp, J., and Müller-Wening, D. (2006). Schwimmbadlunge - Exogen-allergische Alveolitis oder Mykobakteriose? *Pneumologie (Stuttgart, Germany)* 60, 285–289. doi: 10.1055/s-2006-932160

Kumar, P., Arora, K., Lloyd, J. R., Lee, I. Y., Nair, V., Fischer, E., et al. (2012). Meropenem inhibitsD,D-carboxypeptidase activity in *Mycobacterium tuberculosis*. *Mol. Microbiol.* 86, 367–381. doi: 10.1111/j.1365-2958.2012.08199.x

Kundu, S., Biukovic, G., Grüber, G., and Dick, T. (2016). Bedaquiline targets the ε subunit of mycobacterial F-Atp synthase. *Antimicrob. Agents Chemother.* 60, 6977–6979. doi: 10.1128/AAC.01291-16

Kurz, S. G., and Bonomo, R. A. (2012). Reappraising the use of β-lactams to treat tuberculosis. *Expert Rev. Anti-Infect. Ther.* 10, 999–1006. doi: 10.1586/eri.12.96

Kurz, S. G., and Rivas-Santiago, B. (2020). Time to expand the picture of mycobacterial lipids: spotlight on nontuberculous mycobacteria. *Am. J. Respir. Cell Mol. Biol.* 62, 275–276. doi: 10.1165/rcmb.2019-0324ED

Kwak, N., Dalcolmo, M. P., Daley, C. L., Eather, G., Gayoso, R., Hasegawa, N., et al. (2019). *Mycobacterium abscessus* pulmonary disease: individual patient data meta-analysis. *Eur. Respir. J.* 54:1801991. doi: 10.1183/13993003.01991-2018

Kwon, B. S., Shim, T. S., and Jo, K. W. (2019). The second recurrence of *Mycobacterium avium* complex lung disease after successful treatment for first recurrence. *Eur. Respir. J.* 53:1801038. doi: 10.1183/13993003.01038-2018

Lai, C. C., Tan, C. K., Chou, C. H., Hsu, H. L., Liao, C. H., Huang, Y. T., et al. (2010). Increasing incidence of nontuberculous mycobacteria, Taiwan, 2000-2008. *Emerg. Infect. Dis.* 16, 294–296. doi: 10.3201/eid1602.090675

Ledford, H. (2011). Translational research: 4 ways to fix the clinical trial. *Nature* 477, 526–528. doi: 10.1038/477526a

Lee, B. Y., Kim, S., Hong, Y., Lee, S. D., Kim, W. S., Kim, D. S., et al. (2015). Risk factors for recurrence after successful treatment of *Mycobacterium avium* complex lung disease. *Antimicrob. Agents Chemother.* 59, 2972–2977. doi: 10.1128/AAC.04577-14

Lee, H., Myung, W., Koh, W. J., Moon, S. M., and Jhun, B. W. (2019). Epidemiology of nontuberculous mycobacterial infection, South Korea, 2007-2016. *Emerg. Infect. Dis.* 25, 569–572. doi: 10.3201/eid2503.181597

Levy, I., Grisaru-Soen, G., Lerner-Geva, L., Kerem, E., Blau, H., Bentur, L., et al. (2008). Multicenter cross-sectional study of nontuberculous mycobacterial infections among cystic fibrosis patients, Israel. *Emerg. Infect. Dis.* 14, 378–384. doi: 10.3201/eid1403.061405

Lingaraju, S., Rigouts, L., Gupta, A., Lee, J., Umubyeyi, A. N., Davidow, A. L., et al. (2016). Geographic differences in the contribution of ubiA mutations to high-level ethambutol resistance in *Mycobacterium tuberculosis*. *Antimicrob. Agents Chemother.* 60, 4101–4105. doi: 10.1128/AAC.03002-15

Liu, J., Barry, C. E., Besra, G. S., and Nikaido, H. (1996). Mycolic acid structure determines the fluidity of the mycobacterial cell wall. *J. Biol. Chem.* 271, 29545–29551. doi: 10.1074/jbc.271.47.29545

Luthra, S., Rominski, A., and Sander, P. (2018). The role of antibiotic-target-modifying and antibiotic-modifying enzymes in *Mycobacterium abscessus* drug resistance. *Front. Microbiol.* 9:2179. doi: 10.3389/fmicb.2018.02179

Mah, T. F. (2012). Biofilm-specific antibiotic resistance. *Future Microbiol.* 7, 1061–1072. doi: 10.2217/fmb.12.76

Malouf, M. A., and Glanville, A. R. (1999). The spectrum of mycobacterial infection after lung transplantation. *Am. J. Respir. Crit. Care Med.* 160, 1611–1616. doi: 10.1164/ajrccm.160.5.9808113

Marrakchi, H., Lanéelle, M. A., and Daffé, M. (2014). Mycolic acids: structures, biosynthesis, and beyond. *Chem. Biol.* 21, 67–85. doi: 10.1016/j.chembiol.2013.11.011

Martinson, M. L., and Lapham, J. (2024). Prevalence of immunosuppression among us adults. *JAMA* 331, 880–882. doi: 10.1001/jama.2023.28019

Meier, A., Heifets, L., Wallace, R. J. Jr., Zhang, Y., Brown, B. A., Sander, P., et al. (1996). Molecular mechanisms of clarithromycin resistance in *Mycobacterium avium*: observation of multiple 23S rdna mutations in a clonal population. *J. Infect. Dis.* 174, 354–360. doi: 10.1093/infdis/174.2.354

Mickiewicz, K. M., Kawai, Y., Drage, L., Gomes, M. C., Davison, F., Pickard, R., et al. (2019). Possible role of L-form switching in recurrent urinary tract infection. *Nat. Commun.* 10:4379. doi: 10.1038/s41467-019-12359-3

Minnikin, D. E., and Brennan, P. J. (2020). "Lipids of clinically significant mycobacteria" in *Health consequences of microbial interactions with hydrocarbons, oils, and lipids*. ed. H. Goldfine (Cham: Springer International Publishing).

Moon, S. M., Jhun, B. W., Baek, S. Y., Kim, S., Jeon, K., Ko, R. E., et al. (2019). Long-term natural history of non-cavitary nodular bronchiectatic nontuberculous mycobacterial pulmonary disease. *Respir. Med.* 151, 1–7. doi: 10.1016/j.rmed.2019.03.014

Moore, J. E., Kruijshaar, M. E., Ormerod, L. P., Drobniewski, F., and Abubakar, I. (2010). Increasing reports of non-tuberculous mycobacteria in England, Wales and Northern Ireland, 1995-2006. *BMC Public Health* 10:612. doi: 10.1186/1471-2458-10-612

Namkoong, H., Kurashima, A., Morimoto, K., Hoshino, Y., Hasegawa, N., Ato, M., et al. (2016). Epidemiology of pulmonary nontuberculous mycobacterial disease, Japan. *Emerg. Infect. Dis.* 22, 1116–1117. doi: 10.3201/eid2206.151086

Nasiri, M. J., Haeili, M., Ghazi, M., Goudarzi, H., Pormohammad, A., Imani Fooladi, A. A., et al. (2017). New insights in to the intrinsic and acquired drug resistance mechanisms in mycobacteria. *Front. Microbiol.* 8:681. doi: 10.3389/fmicb.2017.00681

Negatu, D. A., Aragaw, W. W., Cangialosi, J., Dartois, V., and Dick, T. (2023). Side-by-side profiling of Oxazolidinones to estimate the therapeutic window against mycobacterial infections. *Antimicrob. Agents Chemother.* 67:e0165522. doi: 10.1128/aac.01655-22

Nguyen, T. V., Cao, T. B., Akkerman, O. W., Tiberi, S., Vu, D. H., and Alffenaar, J. W. (2016). Bedaquiline as part of combination therapy in adults with pulmonary multi-drug resistant tuberculosis. *Expert. Rev. Clin. Pharmacol.* 9, 1025–1037. doi: 10.1080/17512433.2016.1200462

Nick, J. A., Dedrick, R. M., Gray, A. L., Vladar, E. K., Smith, B. E., Freeman, K. G., et al. (2022). Host and pathogen response to bacteriophage engineered against *Mycobacterium abscessus* lung infection. *Cell* 185, 1860–1874.e12. doi: 10.1016/j.cell.2022.04.024

Obata, S., Zwolska, Z., Toyota, E., Kudo, K., Nakamura, A., Sawai, T., et al. (2006). Association of rpoB mutations with rifampicin resistance in *Mycobacterium avium*. *Int. J. Antimicrob. Agents* 27, 32–39. doi: 10.1016/j.ijantimicag.2005.09.015

Olivier, K. N., Griffith, D. E., Eagle, G., Mcginnis, J. P., Micioni, L., Liu, K., et al. (2017). Randomized trial of liposomal amikacin for inhalation in nontuberculous mycobacterial lung disease. *Am. J. Respir. Crit. Care Med.* 195, 814–823. doi: 10.1164/rccm.201604-0700OC

Olivier, K. N., Weber, D. J., Wallace, R. J., Faiz, A. R., Lee, J. H., Zhang, Y., et al. (2003). Nontuberculous mycobacteria. I: multicenter prevalence study in cystic fibrosis. *Am. J. Respir. Crit. Care Med.* 167, 828–834. doi: 10.1164/rccm.200207-678OC

Oschmann-Kadenbach, A. M., Schaudinn, C., Borst, L., Schwarz, C., Konrat, K., Arvand, M., et al. (2024). Impact of *Mycobacteroides abscessus* colony morphology on biofilm formation and antimicrobial resistance. *Int. J. Med. Microbiol.* 314:151603. doi: 10.1016/j.ijmm.2024.151603

Park, Y. S., Lee, C. H., Lee, S. M., Yang, S. C., Yoo, C. G., Kim, Y. W., et al. (2010). Rapid increase of non-tuberculous mycobacterial lung diseases at a tertiary referral hospital in South Korea. *Int. J. Tuberc. Lung Dis.* 14, 1069–1071

Peloquin, C. A. (1997). *Mycobacterium avium* complex infection. Pharmacokinetic and pharmacodynamic considerations that may improve clinical outcomes. *Clin. Pharmacokinet.* 32, 132–144. doi: 10.2165/00003088-199732020-00004

Pound, P., Ebrahim, S., Sandercock, P., Bracken, M. B., and Roberts, I. (2004). Where is the evidence that animal research benefits humans? *BMJ* 328, 514–517. doi: 10.1136/bmj.328.7438.514

Queensland Health. (2024). *Notifiable conditions anual reporting*. Queensland Government. Available at: https://www.health.qld.gov.au/clinical-practice/guidelines-procedures/diseases-infection/surveillance/reports/notifiable/annual (Accessed February 27, 2024).

Ratnatunga, C. N., Lutzky, V. P., Kupz, A., Doolan, D. L., Reid, D. W., Field, M., et al. (2020). The rise of non-tuberculosis mycobacterial lung disease. *Front. Immunol.* 11:303. doi: 10.3389/fimmu.2020.00303

Reynolds, P. E. (1989). Structure, biochemistry and mechanism of action of glycopeptide antibiotics. *Eur. J. Clin. Microbiol. Infect. Dis.* 8, 943–950. doi: 10.1007/BF01967563

Rodrigues, L., Parish, T., Balganesh, M., and Ainsa, J. A. (2017). Antituberculosis drugs: reducing efflux=increasing activity. *Drug Discov. Today* 22, 592–599. doi: 10.1016/j.drudis.2017.01.002

Roux, A. L., Catherinot, E., Ripoll, F., Soismier, N., Macheras, E., Ravilly, S., et al. (2009). Multicenter study of prevalence of nontuberculous mycobacteria in patients with cystic fibrosis in France. *J. Clin. Microbiol.* 47, 4124–4128. doi: 10.1128/JCM.01257-09

Ruseckaite, R., Salimi, F., Earnest, A., Bell, S. C., Douglas, T., Frayman, K., et al. (2022). Survival of people with cystic fibrosis in Australia. *Sci. Rep.* 12:19748. doi: 10.1038/s41598-022-24374-4

Schiff, H. F., Jones, S., Achaiah, A., Pereira, A., Stait, G., and Green, B. (2019). Clinical relevance of non-tuberculous mycobacteria isolated from respiratory specimens: seven year experience in a Uk hospital. *Sci. Rep.* 9:1730. doi: 10.1038/s41598-018-37350-8

Schnippel, K., Ndjeka, N., Maartens, G., Meintjes, G., Master, I., Ismail, N., et al. (2018). Effect of bedaquiline on mortality in south African patients with drug-resistant tuberculosis: a retrospective cohort study. *Lancet Respir. Med.* 6, 699–706. doi: 10.1016/S2213-2600(18)30235-2

Seibert, A., and Bass, J. (1989). *Four drug therapy of pulmonary disease due to Mycobacterium avium complex*. Annual Meeting of American Thoracic Society, pp. 14–17.

Shafran, S. D., Singer, J., Zarowny, D. P., Phillips, P., Salit, I., Walmsley, S. L., et al. (1996). A comparison of two regimens for the treatment of *Mycobacterium avium* complex bacteremia in Aids: rifabutin, ethambutol, and clarithromycin versus rifampin, ethambutol, clofazimine, and ciprofloxacin. Canadian Hiv trials network protocol 010 study group. *N. Engl. J. Med.* 335, 377–384. doi: 10.1056/NEJM199608083350602

Sherrard, L. J., Tay, G. T., Butler, C. A., Wood, M. E., Yerkovich, S., Ramsay, K. A., et al. (2017). Tropical Australia is a potential reservoir of non-tuberculous mycobacteria in cystic fibrosis. *Eur. Respir. J.* 49:1700046. doi: 10.1183/13993003.00046-2017

Shulha, J. A., Escalante, P., and Wilson, J. W. (2019). Pharmacotherapy approaches in nontuberculous mycobacteria infections. *Mayo Clin. Proc.* 94, 1567–1581. doi: 10.1016/j.mayocp.2018.12.011

Siegel, S. A. R., Griffith, D. E., Philley, J. V., Brown-Elliott, B. A., Brunton, A. E., Sullivan, P. E., et al. (2023). Open-label trial of amikacin liposome inhalation suspension in *Mycobacterium abscessus* lung disease. *Chest* 164, 846–859. doi: 10.1016/j.chest.2023.05.036

Slavchev, G., Michailova, L., and Markova, N. (2016). L-form transformation phenomenon in *Mycobacterium tuberculosis* associated with drug tolerance to ethambutol. *Int. J. Mycobacteriol.* 5, 454–459. doi: 10.1016/j.ijmyco.2016.06.011

Song, L., and Wu, X. (2016). Development of efflux pump inhibitors in antituberculosis therapy. *Int. J. Antimicrob. Agents* 47, 421–429. doi: 10.1016/j.ijantimicag.2016.04.007

Sun, D., Gao, W., Hu, H., and Zhou, S. (2022). Why 90% of clinical drug development fails and how to improve it? *Acta Pharm. Sin. B* 12, 3049–3062. doi: 10.1016/j.apsb.2022.02.002

Taiwo, B., and Glassroth, J. (2010). Nontuberculous mycobacterial lung diseases. *Infect. Dis. Clin. N. Am.* 24, 769–789. doi: 10.1016/j.idc.2010.04.008

Takayama, Y., Kitajima, T., Honda, N., Sakane, N., Yumen, Y., Fukui, M., et al. (2022). Nutritional status in female patients with nontuberculous mycobacterial lung disease and its association with disease severity. *BMC Pulm. Med.* 22:315. doi: 10.1186/s12890-022-02109-5

Talley, A. K., Thurston, A., Moore, G., Gupta, V. K., Satterfield, M., Manyak, E., et al. (2021). First-in-human evaluation of the safety, tolerability, and pharmacokinetics of Spr720, a novel Oral bacterial Dna gyrase (GyrB) inhibitor for mycobacterial infections. *Antimicrob. Agents Chemother.* 65:e0120821. doi: 10.1128/AAC.01208-21

The Cryptic Consortium (2022). Genome-wide association studies of global *Mycobacterium tuberculosis* resistance to 13 antimicrobials in 10,228 genomes identify new resistance mechanisms. *PLoS Biol.* 20:e3001755. doi: 10.1371/journal.pbio.3001755

Thomson, R., Donnan, E., and Konstantinos, A. (2017). Notification of nontuberculous mycobacteria: an Australian perspective. *Ann. Am. Thorac. Soc.* 14, 318–323. doi: 10.1513/AnnalsATS.201612-994OI

U.S. Food and Drug Administration. (2018). *FDA approves a new antibacterial drug to treat a serious lung disease using a novel pathway to spur innovation*. Available at: https://www.fda.gov/news-events/press-announcements/fda-approves-new-antibacterial-drug-treat-serious-lung-disease-using-novel-pathway-spur-innovation#:~:text=The%20U.S.%20Food%20and%20Drug,not%20respond%20to%20conventional%20treatment%20 (Accessed February 29, 2024).

Van Ingen, J., Egelund, E. F., Levin, A., Totten, S. E., Boeree, M. J., Mouton, J. W., et al. (2012). The pharmacokinetics and pharmacodynamics of pulmonary *Mycobacterium avium* complex disease treatment. *Am. J. Respir. Crit. Care Med.* 186, 559–565. doi: 10.1164/rccm.201204-0682OC

Viveiros, M., Leandro, C., and Amaral, L. (2003). Mycobacterial efflux pumps and chemotherapeutic implications. *Int. J. Antimicrob. Agents* 22, 274–278. doi: 10.1016/S0924-8579(03)00208-5

Von Reyn, C. F., Arbeit, R. D., Horsburgh, C. R., Ristola, M. A., Waddell, R. D., Tvaroha, S. M., et al. (2002). Sources of disseminated *Mycobacterium avium* infection in Aids. *J. Infect.* 44, 166–170. doi: 10.1053/jinf.2001.0950

Wallace, R. J., Brown, B. A., Griffith, D. E., Girard, W. M., and Murphy, D. T. (1996a). Clarithromycin regimens for pulmonary *Mycobacterium avium* complex. The first 50 patients. *Am. J. Respir. Crit. Care Med.* 153, 1766–1772. doi: 10.1164/ajrccm.153.6.8665032

Wallace, R. J., Dukart, G., Brown-Elliott, B. A., Griffith, D. E., Scerpella, E. G., and Marshall, B. (2014). Clinical experience in 52 patients with tigecycline-containing regimens for salvage treatment of Mycobacterium abscessus and *Mycobacterium chelonae* infections. *J. Antimicrob. Chemother.* 69, 1945–1953. doi: 10.1093/jac/dku062

Wallace, R. J., Meier, A., Brown, B. A., Zhang, Y., Sander, P., Onyi, G. O., et al. (1996b). Genetic basis for clarithromycin resistance among isolates of *Mycobacterium chelonae* and *Mycobacterium abscessus*. *Antimicrob. Agents Chemother.* 40, 1676–1681. doi: 10.1128/AAC.40.7.1676

Wallace, R. J., O'Brien, R., Glassroth, J., Raleigh, J., and Dutt, A. (1990). Diagnosis and treatment of disease caused by nontuberculous mycobacteria. *Am. Rev. Respir. Dis.* 142, 940–953. doi: 10.1164/ajrccm/142.4.940

Warit, S., Phunpruch, S., Jityam, C., Jaitrong, S., Billamas, P., Chaiprasert, A., et al. (2015). Genetic characterisation of a whiB7 mutant of a *Mycobacterium tuberculosis* clinical strain. *J. Glob. Antimicrob. Resist.* 3, 262–266. doi: 10.1016/j.jgar.2015.07.004

Winthrop, K. L., Flume, P. A., Thomson, R., Mange, K. C., Yuen, D. W., Ciesielska, M., et al. (2021). Amikacin liposome inhalation suspension for *Mycobacterium avium* complex lung disease: a 12-month open-label extension clinical trial. *Ann. Am. Thorac. Soc.* 18, 1147–1157. doi: 10.1513/AnnalsATS.202008-925OC

World Health Organization (2013). *The use of bedaquiline in the treatment of multidrug-resistant tuberculosis: interim policy guidance*. Berlin: World Health Organization.

Wu, M. L., Aziz, D. B., Dartois, V., and Dick, T. (2018). Ntm drug discovery: status, gaps and the way forward. *Drug Discov. Today* 23, 1502–1519. doi: 10.1016/j.drudis.2018.04.001

Yamazaki, Y., Danelishvili, L., Wu, M., Hidaka, E., Katsuyama, T., Stang, B., et al. (2006a). The ability to form biofilm influences *Mycobacterium avium* invasion and translocation of bronchial epithelial cells. *Cell. Microbiol.* 8, 806–814. doi: 10.1111/j.1462-5822.2005.00667.x

Yamazaki, Y., Danelishvili, L., Wu, M., Macnab, M., and Bermudez, L. E. (2006b). *Mycobacterium avium* genes associated with the ability to form a biofilm. *Appl. Environ. Microbiol.* 72, 819–825. doi: 10.1128/AEM.72.1.819-825.2006

Young, I., Wang, I., and Roof, W. D. (2000). Phages will out: strategies of host cell lysis. *Trends Microbiol.* 8, 120–128. doi: 10.1016/S0966-842X(00)01705-4

Zhang, X., Falagas, M. E., Vardakas, K. Z., Wang, R., Qin, R., Wang, J., et al. (2015). Systematic review and meta-analysis of the efficacy and safety of therapy with linezolid containing regimens in the treatment of multidrug-resistant and extensively drug-resistant tuberculosis. *J. Thorac. Dis.* 7, 603–615. doi: 10.3978/j.issn.2072-1439.2015.03.10

Zuckerman, J. M., Qamar, F., and Bono, B. R. (2011). Review of macrolides (azithromycin, clarithromycin), ketolids (telithromycin) and glycylcyclines (tigecycline). *Med Clin North Am* 95, 761–791. doi: 10.1016/j.mcna.2011.03.012

Frontiers in Microbiology

Explores the habitable world and the potential of microbial life

The largest and most cited microbiology journal which advances our understanding of the role microbes play in addressing global challenges such as healthcare, food security, and climate change.

Discover the latest Research Topics

See more →

Frontiers

Avenue du Tribunal-Fédéral 34
1005 Lausanne, Switzerland
frontiersin.org

Contact us

+41 (0)21 510 17 00
frontiersin.org/about/contact